1980

Dynamic thermal responses of buildings and systems

Desh Paul Mehta
Iowa State University

MEHTA, DESH PAUL

DYNAMIC THERMAL RESPONSES OF BUILDINGS AND SYSTEMS

Iowa State University PH.D. 1980

PLEASE NOTE:

In all cases this material has been filmed in the best possible way from the available copy. Problems encountered with this document have been identified here with a check mark ✓.

1. Glossy photographs ✓
2. Colored illustrations _____
3. Photographs with dark background _____
4. Illustrations are poor copy _____
5. Print shows through as there is text on both sides of page _____
6. Indistinct, broken or small print on several pages _____ throughout _____
7. Tightly bound copy with print lost in spine _____
8. Computer printout pages with indistinct print _____
9. Page(s) _____ lacking when material received, and not available from school or author _____
10. Page(s) _____ seem to be missing in numbering only as text follows _____
11. Poor carbon copy _____
12. Not original copy, several pages with blurred type _____
13. Appendix pages are poor copy _____
14. Original copy with light type _____
15. Curling and wrinkled pages _____
16. Other _____

Dynamic thermal responses of buildings and systems

by

Desh Paul Mehta

A Dissertation Submitted to the

Graduate Faculty in Partial Fulfillment of the

Requirements for the Degree of

DOCTOR OF PHILOSOPHY

Major: Mechanical Engineering

Approved:

Signature was redacted for privacy.

In Charge of Major Work

Signature was redacted for privacy.

For the Major Department

Signature was redacted for privacy.

For the Graduate College

Iowa State University
Ames, Iowa

1980

TABLE OF CONTENTS

LIST OF FIGURES

LIST OF TABLES

NOMENCLATURE

All the variables, symbols and subscripts have been defined at appropriate places in the text. General notation is summarized in the following list.

Variables

A area: (m^2) or (ft^2)

B flux density of magnetic field: (Gauss)

C concentration of methane: (ppm)

specific heat: (J/kg.^oK) or (Btu/lbm.^oF)

thermal capacity: (J/^oK) or (Btu/^oF)

Rate of convective heat loss: (Watts) or (Btu/hr)

D diameter: (meter) or (foot)

E rate of evaporative heat loss: (Watts) or (Btu/hr)

F force: (Newton) or (lbf)

H water head: (m water) or (ft water)

I solar heat gain: (J/hr.m^2) or (Btu/hr.ft^2)

K thermal conductivity: (J/hr.m.^oC) or (Btu/hr.ft.^oF)

L length: (m) or (ft)

M metabolic rate: (watts) or (Btu/hr)

mass: (kg) or (lbm)

P pressure: (N/m^2) or (lbf/ft^2)

Q energy: (J) or (Btu)

R thermal resistance: ($^oC/W$) or (hr.^oF/Btu)

rate of radiant-heat loss (Watts) or (Btu/hr)

S time rate of change in intrinsic body heat: (Watts) or (Btu/hr)

specific heat of water: (J/kg.^{o}K) or (Btu/lbm.^{o}F)

T temperature: (^{o}C) or (^{o}F)

U overall heat transfer coefficient: (J/hr.m^{2}.^{o}C) or (Btu/hr.ft^{2},^{o}F)

V velocity: (m/hour) or (ft/hour)

volume: (m^{3}) or (ft^{3})

W electric power: (Watts)

rate of accomplishing mechanical work: (Watts) or (Btu/hr)

Y displacement: (m) or (ft)

Z displacement: (m) or (ft)

c specific heat: (J/Kg.^{o}K) or (Btu/lbm.^{o}F)

d diameter: (m) or (ft)

e emissivity: (dimensionless)

g acceleration due to gravity: (m/sec^{2}) or ft/sec^{2})

h heat transfer coefficient: (J/m^{2}.hr.^{o}C) or (Btu/ft^{2}.hr.^{o}F)

specific enthalpy: (J/Kg) or (Btu/lbm)

water head: (m water) or (ft water)

k thermal conductivity: (J/hr m^{0}C) or (Btu/hr.ft.^{o}F)

l length: (m) or (ft)

m mass: (Kg) or (lbm)

s specific heat: (J/Kg.^{o}K) or (Btu/lbm.^{o}F)

t time: (hr)

v velocity: (m/hr) or (ft/hr)

Symbols and Subscripts

F floor

G	ground; transfer function
H	transfer function of feedback element
I	internal
K	proportional sensitivity
M	manipulated variable
Nu	Nusselt number
O	outside
Occ	occupant
P	plenum
Pr	Prandtl number
R	roof
Re	Reynold number
S	Laplace Transform variable
V	command signal
W	wall
	watts
X	polynomial in Laplace Transform
Y	polynomial in Laplace Transform
a	air
b	feedback signal
c	controlled variable
Cond.	Conduction
e	actuating signal
f	fluid; furnace
h	hot

i	inlet
inf	infiltration
int	internal; integral
m	manipulated variable
	meter
o	outlet; outside
occ	occupant
os	occupied space
r	reference input signal
s	sensor, supply
	Laplace Transform variable
t	tank
u	disturbance
v	command signal
w	water, well
	entry to plenum

Greek symbols

α	constant
β	constant
Δ	perturbation of a variable
ϵ	surface emissivity (dimensionless)
η	efficiency
θ	Temperature (°C) or (°F)
μ	viscosity: (Kg/m.s) or (lbm/ft.hr)
ν	kinematic viscosity: (m^2/s) or (ft^2/hr)

ρ density: (Kg/m^3) or (lbm/ft^3)

σ Stefan-Boltzman constant: ($W/m^2.K^4$) or ($Btu/hr.ft^2.{}^oR^4$)

τ time constant: (hr)

ACKNOWLEDGMENTS

I wish to express my deepest appreciation to my major professor, Dr. James E. Woods, for his guidance, advice and support. He suggested the topic for this dissertation and during its development I was always inspired by his special talents to apply engineering theory for the benefit of society.

Special thanks are due to my committee members, Professors A. E. Bergles, W. J. Cook, R. C. Fellinger, and G. W. Smith, for their guidance and encouragement at those times when I needed it the most.

Appreciation is also extended to Dr. Donald M. Brueck for his guidance and to Dr. Thomas H. Kuehn for permitting me to coordinate my research schedule with his experiments. I also wish to thank the Iowa Energy Policy Council and the Iowa State University Engineering Research Institute for financial support during this research. I also thank the Iowa State University Research Foundation for letting me use the facilities at the Iowa State University Energy Research House.

Thanks are due to Drs. J. R. Tobias, U. Bonne, and to Mr. J. E. Janssen, all of Honeywell, Inc., for their time to discuss my research plans and for permitting me to use their gas analyzer.

Special thanks are extended to Dr. Max A. Wessler, Chairman, Mechanical Engineering Department at Bradley University, for all the encouragement and support to complete this dissertation. I extend special appreciation and gratitude to Mrs. Alice Woods and to the members of the Woods family for providing me with a quiet environment and their sacrifice

of family time during the long hours of my work with Dr. Woods on weekends at their place. Special thanks are due to my wife and children who had unending patience and support.

Finally, I wish to thank all the members of Building Energy Utilization Laboratory at Iowa State University for their friendship and support during this work.

DEDICATION

Dedicated to my teachers.

1. INTRODUCTION

Projected depletion rates of nonreplenishable fossil fuels demand that we direct our talents and efforts toward development of new sources of energy and reduction of energy use. Of the energy consumed in the U.S., approximately 30% is attributable to the operation of buildings (1).[1] Estimated reductions in energy consumption in new building design range from 10% to 60% (2). Recent estimates indicate that modifications to existing buildings can achieve similar reductions (3). Since the primary source of fuel supply to buildings is in the form of fossil fuels, these estimated reductions should encourage us to develop and use techniques to accomplish these savings. Identification of building energy characteristics and studies of dynamic interactions among the energy characteristics are essential to develop techniques which are effective in reducing energy consumption in buildings.

A building energy characteristic may be defined as a parameter, or a set of factors, that can affect energy consumption in a building (4). Four basic building energy consumption characteristics can be identified: human comfort conditions, climatic variables, building envelope characteristics and heating, ventilating and air conditioning (HVAC) systems. A fifth factor, life style, can also be identified, but is harder to quantify unless identical environments are used as a setting in which life styles are compared.

---

[1] Numbers in parentheses refer to references.

Human comfort has been defined as "that state of mind which expresses satisfaction with the thermal environment" (5). Six different variables, dry bulb air temperature, mean radient temperature (MRT), humidity, relative air velocity, thermal resistance of clothing and activity level, interact with each other to define comfort conditions which can be quantified by a single index called Standard Effective Temperature (SET*) (6).

The most influential climatic variable is the temperature, with insolation and wind as secondary, but important parameters. The effect of insolation and wind, and the penetration of both will be dictated by the envelope characteristics. Therefore, the building envelope is an important factor that determines how temperature differential, insolation and infiltration affect the human comfort and energy consumption in a building.

The building envelope can be defined as the surface which separates the enclosed spaces from the external elements that influence human comfort. Orientation, size and shape, siting and landscaping, fenestration and construction of opaque structures are important characteristics of the envelope which influence energy consumption and comfort inside the envelope.

Finally, performance characteristics, configuration and selection of HVAC components and control systems have a significant influence on the energy consumption and the comfort conditions in a building.

1.1 Problem Statement

All the factors identified above interact with each other dynamically and result in a complex transfer of energy between interior and exterior environments. In the past, design and analysis of buildings have been, and

in general still are, based on steady state considerations. HVAC systems are designed and selected on maximum load requirements and are often oversized, energy intensive and their optimal performance factors are seldom obtained (7).

Primarily because of the present and expected future cost of the energy used by building environmental control systems, it is necessary to understand the dynamic responses of building systems. The problem is that reliable dynamic models to predict the performance of a building system have not been developed so far and the development of the dynamic models is the subject matter of this dissertation.

1.2 Research Objectives

The objectives of the research work reported in this dissertation were:

1. To analyze the physics of dynamic processes involved in operating a building system.
2. To develop dynamic models to predict building performance.
3. To experimentally validate the dynamic models.
4. To determine the effects of control dynamics on energy consumption.
5. To develop a design criterion based upon dynamic performance.

1.3 Background

An extensive literature search was made to review the work done in the past on dynamic performances of building envelopes, HVAC components,

control systems or on dynamic interactions between climate, envelope, HVAC components, internal loads and control systems. Findings are reported here in the same order. Summaries of literature review on the dynamic performance of envelopes, HVAC components and control systems, and of dynamic interactions of building energy characteristics are given in Table 1.1, Table 1.2 and Table 1.3, respectively.

Historically, interest in dynamic thermal performance of materials can be traced back to as early as 1822 when Fourier explained the basic mathematics for transient heat transfer in solids (8). Applications of analytical techniques to predict transient thermal response of building envelopes started in 1944 (9) and research efforts in this area were of academic interest only for the subsequent 25 years (10-13). With the advent of high speed digital computers, efforts were initiated to analyze actual building structures for dynamic performance. In 1967 Mitalas and Stephenson initiated the response factor method (14-15). In 1969 Kasuda extended the calculations of response factors to multi-layer structures of various curvatures (16). Stephenson and Mitalas further developed the response factor method by using Z-transforms for the inversion (17).

Since 1973 many computer programs have been developed which make use of thermal response factor methods, consider systems, internal loads and compare alternative methods for meeting the energy requirements of a building based on economic analysis. However, these programs, such as TRACE (by Trane Co.), E-Cube (by American Gas Association), NECAP (by NASA), AXCESS (by American Air Filter), use algorithms for HVAC systems simulation which were developed from steady state (18).

During the past 35 years, dynamic behavior of building envelopes has also been of interest to control engineers who have been investigating analog passive circuits simulations (19-24). Nelson applied analog computer techniques to simulate a one-story house and its associated heating and air-conditioning plant (25). Models of an on-off thermostat, a first order heating plant and an instantaneous cooling plant were used in his studies. He compared the predicted results with measured data and reported that analog passive circuit simulation of the envelope accurately predicts dynamic conditions in a building. Application of an analog computer has also been reported by Magnussen to simulate an air-conditioning system in a commercial building (26). Kaya converted a thermal circuit of one zone of the multi-zoned commercial building simulated by Magnusses to an equivalent transfer function (27). Analysis using control theory was introduced by him. However, validation of this technique has not been reported.

Few people have directed their research efforts during the past years to establish dynamic responses of HVAC components and their control systems. Zelenski, Lund, Harrison and Sowls investigated a closed-loop system for duct air temperature control loop (28). Room dynamics were excluded from this loop. Dynamics of the heat exchanger, valve, actuator, controller and transducer were lumped together in the forward block and it was concluded that it could be approximated by a dead time and a time constant. It was shown that the system containing one slow and other fast components exhibits a transient response of a first order corresponding to the dominant time constant while the fast elements simply introduce a delay or a dead time. Stoecker et al. have also studied the dynamic

characteristics of an air temperature control loop to find the limiting value of gain of the loop for stability (29). This effort also excluded the room dynamics. Models used for the valve included the effects of hysteresis. An important finding was that a nonlinear model for the controller had to be used to correlate experimental data with theoretical predictions, whereas Stenger et al. (30) showed that a linear model for the controller was quite satisfactory. Another finding by Stoecker et al. was that an extremely simple model for the heating coil was adequate, whereas other cited literature revealed that an extensive research effort was directed during the past 15 years to develop a dynamic model for a heat exchanger (31-46). All these efforts regarding dynamic performances of HVAC components and control systems were concerned mainly with finding the limiting gain of the loop to keep the system stable while achieving minimum steady-state deviation or offset.

With the energy shortages experienced after the oil embargo of 1973, studies of the dynamics of air-temperature control loops began considering energy consumptions. Hamilton, Leonard and Pearson investigated the dynamic responses near full load and part heating load of a discharge air temperature control system (47). This research effort did not include the envelope in the loop. Models for individual elements like controller, heat exchanger and valve were discussed. The project became bogged down in the complexities of valve dynamics. It was concluded that a valve size criterion should take into account the dynamics of the heat exchanger. It was demonstrated that a design criterion based on the dynamics of the com-

ponents of the loop should be developed to aid the designer in selecting components for HVAC systems.

Very few research efforts have been devoted in the past to develop models which describe dynamic interactions of weather, envelope, internal loads, HVAC components and control systems. Harrison et al. applied the techniques of classical control theory to predict room temperature response to sudden heat disturbance inputs (48-49). The emphasis of their effort was to illustrate an approach and as such no data were taken on an actual system. Individual dynamic characteristics of various elements like amplifier, controller, valve, heat exchanger or duct were not taken into consideration. Initially the room was modeled as a first order system assuming perfect air mixing and neglecting capacitance of walls, floor and furniture. Later work by Harrison, Hansen and Zelenski considered the case of no mixing of air and included the capacitance of walls, floor and furniture in the development of a room transfer function (50). They concluded that these considerations did not change the basic first order character of the transfer function for the room though assumptions of no mixing of air inside the room introduce a "dead time" which could be significant if the air changes per hour are low.

Recent increases in depletion rates of natural resources and the corresponding increase in fuel costs have led the American Society of Heating, Refrigeration and Air Conditioning Engineers (ASHRAE) to direct a major portion of its future research efforts toward the study of dynamic responses of building systems. Project RP212 was sponsored in 1976 to study the effect of room and control system dynamics on energy consumption

(51). A workshop on dynamic response applications and research plans was conducted by ASHRAE at Purdue University on March 13-15, 1979. A seminar on the same subject was held during ASHRAE Annual Meeting at Detroit, Michigan on June 24-28, 1979 and a symposium is planned in Los Angeles on February 3-7, 1980. The objectives of the Task Group on Dynamic Responses are to develop within ASHRAE an understanding of the role dynamic characteristics play in the use of energy by the environmental control processes of buildings and to determine the research necessary to make consideration of dynamic characteristics a part of the design and operation of building. A multi-million dollar research program is under formulation by ASHRAE (52). As shown by this literature review, this dissertation is a timely effort through which a cost effective method has been developed for predicting dynamic performances of building systems.

Table 1.1. Summary of literature review on dynamic performance of building envelopes

Year(s)	Author(s)	Comment(s)
Part A: Analytical techniques		
1822	Fourier (8)	Explained basic mathematics for heat transfer in solids.
1944-63	MacKey and Wright (9, 10), Hill (12) and Muncey (13)	Published research papers giving solutions of Heat Conduction equation under different boundary conditions.
1967-71	Mitalas and Stephenson (14,15), Kusuda (16), Stephenson and Mitalas (17)	Developed Thermal Response Factor Method and Weighting Factor Method.
1971-79	Trane Co., AGA, NASA, American Air Filter, etc. Based on Stoecker's simulations (18) and cited by Cuba (53).	Developed computer programs which make use of thermal response factor methods, consider systems, internal loads and compare alternative methods for meeting energy requirements of buildings based on economic analysis. Programs use algorithms for HVAC systems simulation which were developed on steady state operation basis.
Part B: Analog passive circuits simulations		
1942-56	Paschkis (19), Willcox et al. (20), Nottage and Parmelee (21,22), and Buchberg (23,24)	Developed analog passive circuits for dynamic thermal performances of walls, roofs or building envelopes.
1965	Nelson (25)	Simulated one-story house and its associated heating and air-conditioning plant.
1970	Magnussen (26)	Simulated a commercial building and an air conditioning system on an analog computer.
1976	Kaya (27)	Converted a thermal circuit of one zone of the multi-zoned commercial building to an equivalent transfer function.

Table 1.2. Summary of literature review on dynamic performances of HVAC components and control systems

Year(s)	Author(s)	Comment(s)
1939-77	Cohen and Johnson (31), Masubuchi (32), Larsen (33), Hampel (34), Gartner and Harrison (35,36), Gartner and Daane (37), Gartner (38), Pearson and Leonard (39), Tobias (40), Bhargave et al. (41), Pearson et al. (42), Goodman (43), Elmahdy (44), Elmahdy and Mitalas (45,46)	Developed dynamic models for heat exchangers.
1968	Zelenski et al. (28)	Investigated a closed-loop system for duct air temperature excluding room dynamics.
1974	Hamilton et al. (47)	Investigated the dynamic responses near full load and part load of a discharge air temperature control system.
1975	Stenger et al. (30)	Studied the behavior of a discharge air temperature control system excluding room dynamics.
1978	Stoecker et al. (29)	Studied the dynamic characteristics of an air temperature control loop to find the limiting value of gain of loop for stability. Room dynamics were not included.

Table 1.3. Summary of literature review on dynamic interactions of building energy characteristics

Year(s)	Author(s)	Comment(s)
1965-66	Zermuehlen and Harrison (48), Zelenski and Harrison (49)	Predicted dynamic response of room temperature due to sudden heat disturbance.
1968	Harrison et al. (50)	Developed room transfer function model for short term transient response.
1976	ASHRAE (51)	Sponsored Research Project RP212 to study the effect of room and control system dynamics on energy consumption.
1979	Thompson and Chen (51)	Reviewed literature for ASHRAE Research Project RP212.
1979	Chapman (52)	ASHRAE is formulating multi-million dollar research program on dynamic response applications. Workshop at Purdue University, March, 1979. Seminar at Annual Meeting, June, 1979. Symposium at Los Angeles, February, 1980.

2. REVIEW OF COMFORT CRITERIA

Because in most cases reasons for controlling building environments involve people, we are ultimately interested in the human reaction to the controlled variables. Therefore, a review of human comfort criteria is in order before proceeding with analyses of building systems. The quality of a controlled environment in a space intended for human occupancy can be assessed for human comfort in terms of thermal and mass air quality, lighting and noise levels.

2.1 Human Thermal Comfort

During the past 20 years, several studies of temperature regulation and heat exchange between man and the environment were conducted (54). During the sixties, the incentive for this widening interest was the extension of man's living environment to space and undersea and the need to predict human performance in those extreme environments before actual human tests. The stimulus to extend the studies during the seventies has been the necessity to reduce energy consumption in buildings. The objective of the present review is to identify those models which can be used to predict the occupant's thermal and physiological responses to the environments in buildings. These models can be useful in assessing the consequences on occupant acceptability of any energy saving scheme that affects the thermal environment of an occupied space.

In general, the study of heat exchange between man and the environment during temperature regulation falls into two major categories:

A. The Passive System

1) Heat flow from the skin surface to the environment. Of concern is the exchange of heat by the processes of conduction, radiation, and convection.

2) Heat flow from the central core to the skin surface. Of concern is the vascular mechanism within the skin layer periphery that transports heat from the heat producing areas within the body to the skin surface.

B. The Control System

Of concern is the neural control of skin blood flow, sweating, and shivering necessary for maintaining normal body temperature.

Studies of heat exchange between man and the environment during temperature regulation have led to the development and use of various environmental indices which can be used to assess the effect of thermal environment on man. These indices may be classified as: 1, direct; 2, rationally derived; and 3) empirical.

The first single temperature scale, which was used to measure the thermal comfort of the environment, was developed by Houghten and Yaglou (55) for ASH&VE in 1923. By a series of carefully chosen experimental conditions, they were able to predict loci of constant temperature sensation expressed in terms of dry bulb, air movement and humidity. This scale has shown the importance of humidity and dry bulb in judging comfort and has been used as a temperature standard for working conditions in many occupations (56-57). This scale overemphasizes the effect

of humidity in cooler and neutral conditions, underemphasizes its effect in warm conditions, and does not fully account for air velocity under hot-humid conditions.

In the 1950's, ASHRAE decided to reevaluate its Effective Temperature Scale. Studies of Koch et al. (58) in 1960 showed humidity had negligible effect on comfort until 60% rh and 18 C (65 F) dry-bulb were reached. Below these levels, dry bulb temperature alone was the governing factor. In 1966, Nevins et al. (59) extended this study for ASHRAE. Using 720 subjects wearing similar light clothing, they obtained high statistical validity. Their new comfort line as affected by humidity proved to be between the earlier data of Houghten (55) and of Koch et al. (58).

The early success of the Effective Temperature Scale stimulated new research to establish a rational physiological and physical basis for it. Tens of thousands of thermal sensation responses have been obtained from subjects over the years (54-93). These responses have been empirically related to air temperature, thermal radiation, humidity, air movement, activity and clothing insulation. They have also been related to physiological factors. From the experimental results mathematical models have evolved to rationally account for the occupant's responses. These models can be used to thermally simulate people in a wide variety of conditions.

Human simulation models essentially apply an energy balance to a person and, from the energy exchange mechanisms and certain physiological parameters, predict the thermal sensation and comfort response of the person. The general energy balance relating physiological response to a thermal environment can be expressed as (5-6):

$$S = M - W + E + C + R \tag{2.1}$$

where

S = time rate of change in intrinsic body heat

M = metabolic heat production rate

W = rate of accomplishing mechanical work

E = rate of evaporative heat loss from diffusion, respiration and sweating

C = rate of convective heat loss from body surface and respiration

R = rate of radiant heat loss to the surrounding surfaces

A summary of energy exchange mechanisms of equation (2.1) for three of the many human simulations models is given in Table 2.1. The three models are those deemed most useful for comfort applications. They were in the chronological order of their development.

1. The Fanger Comfort Model
2. The Pierce Two Node Model
3. The Kansas State University Two Node Model

2.1.1 Comparison of comfort models

The three comfort models reviewed (Table 2.1) are similar in that they all use the heat balance equation together with some physiological parameters to predict sensation of a person in an environment. The Fanger model used heat transfer deviations from the comfort state. The two node and KSU models coupled the energy balance with an active physiological thermal regulatory model. The Pierce model for sedentary situations converted the actual environment to a standard one that would produce the equivalent physiological strain. The thermal sensation was then predicted from the temperature and humidity of the standard environment with the

Table 2.1. Review of comfort models

Parameter	Fanger's Model	Pierce Two Node Model	KSU Two Node Model
a) M and W	1. Defined external mechanical efficiency $\eta = W/M$. 2. Values of M derived from Bioastronautics Data Book, NASA, 1964 (60).	1. Used Gagge's simple lumped parameter model considering man as two concentric thermal compartments representing the skin and core of body (6). 2. Distinguished between the metabolic rate in the core of the body and part of the metabolic heat transferred at the skin taking into account the changes in core temperature and skin temperature (6).	1. Same as in Pierce two node model.
b) E	1. For diffusion losses, used experimental data from studies by Inouye et al. (61) to determine the permeance coefficient of skin concerning evaporative loss for sedentary subjects under comfort conditions. 2. For respiration losses, correlated pulmonary ventilation rate to the metabolic heat production using data reported by Asmussen and Neilsen (62). Difference in humidity ratio between expired and inspired air	1. Introduced skin wettedness factor as the ratio of heat loss due to sweating to the maximum evaporative heat loss from the skin. 2. Maximum evaporative heat loss from the skin was calculated from relations reported by Gagge et al. (67) and by Ibamato and Nishi (68). Permeation of clothing to water vapor was taken into account (69). 3. Diffusion heat loss was taken to be 6% of maximum evaporative loss from skin	1. Diffusion losses were calculated using Fanger's model. 2. Maximum evaporative losses were calculated using Pierce model. 3. Respiration heat losses were calculated using Fanger's model.

Table 2.1. (Continued)

Parameter	Fanger's Model	Pierce Two Node Model	KSU Two Node Model
	was calculated by the relation developed by McCutchan and Taylor (63). 3. For heat losses due to evaporation of sweat, experimental data were used to correlate evaporative heat loss to the metabolic rate including data available from McNall et al. (64).	and a correction for skin wettedness factor was applied. 4. Respiration heat losses were calculated using Fanger's model.	
c) C and R	1. For free convection, heat transfer coefficients reported by Nielsen and Pedersen (65) from their studies on clothed subjects and a manikin were used. 2. For forced convection heat transfer coefficients reported by Winslow et al. (66) from their studies on clothed subjects were used. 3. The effective radiation area of the clothed body was obtained from DuBois area (the surface area of a nude body) by multiplying it by a correction factor for clothing and	1. Convection and radiation heat transfers are expressed as a function of dry heat transfer coefficient from nude body h = (hc + hr), the Burton clothing efficiency factor Fcl (72), and the difference between the mean skin temperature and the operative temperature ($t_{sk} - t_o$). 2. Operative temperature t_o is the uniform temperature of an imaginary enclosure with which man will exchange the same dry heat by radiation and convection (R + C) as in the actual environment.	1. Same as in Pierce two node model.

Table 2.1. (Continued)

Parameter	Fanger's Model	Pierce Two Node Model	KSU Two Node Model
	by shape factors. Values of shape factors were determined experimentally and correction factors for clothing were taken from work reported by Nielsen and Pedersen (65).		
d) Time	1. Steady-state considerations only.	1. Capable of describing dynamic effects.	1. Quasi-steady-state considerations.
e) Physiological model used	1. The skin temperature and sweat rate are linearly related to a person's activity level.	1. Gagge's two node model was used which considers metabolic rates during shivering, blood flow rates, rates of changes in core temperature and skin temperature.	1. Physiological strain was measured from changes in skin thermal conductance and skin wettedness from those at neutrality (77). 2. Skin thermal conductance is a composite index for tissue conductance and blood flow rate from core to skin and is derived empirically.

Table 2.1. (Continued)

Parameter	Fanger's Model	Pierce Two Node Model	KSU Two Node Model
f) Environmental indices developed and/or used	1. Predicted Mean Vote (PMV). 2. Predicted Percentage of Dissatisfied (PPD).	1. Effective temperature scale (ET*). 2. Standard effective temperature (SET*). 3. Index of skin wettedness. 4. Operative temperature. 5. Mean radiant temperature. 6. Thermal sensations on a seven point scale.	1. Skin thermal conductance. 2. Index of skin wettedness. 3. Mean radiant temperature. 4. Thermal sensations on a nine point scale.
g) Variables in the model	1. Metabolic heat production rate. 2. External mechanical efficiency. 3. Water vapor pressures at ambient temperature and mean temperature of clothing. 4. Mean radiant temperature. 5. Convection heat transfer coefficient for surface of clothing.	1. Standard effective temperature (SET*). 2. Skin temperature. 3. Water vapor pressure at skin temperature, at dewpoint, and at SET*. 4. Dry heat transfer coefficient from nude body. 5. Operative temperature. 6. Convection heat trasnfer coefficient for skin. 7. Burton's clothing efficiency factor.	1. Thermal conductance of skin. 2. Skin wettedness.

correlation based on extensive subject testing in the standard environment. For higher activity levels and transients an adjusted skin temperature was used to predict thermal sensation. The KSU model predicts thermal sensation from changes in thermal conductance between core and skin in cool environments and from skin wettedness in warm environments. As conditions deviate from neutral the more accurate predictions are given by the KSU and the Pierce models. The KSU and Pierce models also have transient capabilities.

There are other considerations as well. The Fanger model predictions can be made from prepared tables and graphs. This model also predicts the percentage of dissatisfied persons in the environment. The KSU and two node models, though, give a rather complete prediction of the thermal physiological response or state of a person, providing sweat rate, skin and core temperatures and skin wettedness. This information is often essential for heat and cold stress environment applications. Two-node model also predicts the discomfort response of an individual. The discomfort and thermal sensation responses are very similar in cold environments but in warm environments the thermal sensation increases faster with temperature than does discomfort.

2.1.2 Temperature and humidity fluctuations

Fluctuations in temperature and humidity can have a decided effect on a person's thermal acceptability by influences on physiological and sensory responses which show differential effects between sexes and age groups. Thermal transients usually occur when a person changes location and moves from one place to another, cooler or warmer (78). In other

cases, a person stays in the same place but air temperature or humidity vary either as ramp increases or decreases over time, or with cyclic changes. A literature review revealed that little work has been done to study the effects of thermal transients with drifts in dry bulb temperature and humidity while the subject's stay at one place, and occupant acceptability of such procedures is unclear (79-83).

Studies by Sprague and McNall (79) showed that allowable fluctuating limits stated in ASHRAE Comfort Standard 55-66 were conservative. In a study by Griffiths and McIntyre (81) subjects were exposed to slow one-directional temperature changes of 0, 0.5 and 1.5°C/hour, centered about 23°C, over 6 hour periods. The clothing was in the 0.7 to 0.9 Clo range. From the mean thermal sensation votes of the subjects, Griffiths and McIntyre determined the corresponding Predicted Percent Dissatisfied (PPD) using the relationship developed by Fanger (5). Based on the predicted percent dissatisfied they have recommended a maximum rate of temperature change of 0.75°C/hr with a maximum deviation from the mean comfort temperature of 2.25°C. Berglund and Gonzalez (85) have reported a study on the effects of thermal transients in which direct subjective judgments of acceptability were evaluated. Dry bulb temperature was changed over a 4.5 hour period in morning experiments at rates of change in space temperature of ±0.5, 1.0 and 1.5°C/hr from a 25°C neutral point, while humidity was constant to 10 Torr. Subjects were unacclimated and wore clothing directly evaluated (86). These studies have shown that for sedentary persons, the slower temperature changes (±0.5°C/hr) from a neutral/comfort point were indistinguishable from the constant temperature conditions. The

neutral point was determined by the clothing levels of the subjects. In these studies a ±0.5°C/hr rate of change from a base temperature of 25°C was acceptable to 80% of the subjects.

Gonzalez and Berglund have used the data available from studies reported by Wyon et al. (87), Griffiths and McIntyre (81), McIntyre and Gonzalez (88) and Nevins et al. (82) to calculate thermal sensitivity (change in warmth sensation per unit change in space temperature) and concluded that the apparent sensitivity is much greater for a falling temperature than for a rising one (89). A second study has been reported by Gonzalez and Berglund in which air temperature was allowed to rise at +0.6°C/hr over a 8-hour working day (89). Summer clothing was worn by the subjects and two levels of elevated, but constant, humidity were employed. It has been reported from this study that there was no sign of decrements in thermal acceptability for low rates of chante ($\leq$ ±0.6°C/hr) as long as air temperature level is less than 28°C or dew point temperature is below 20°C for normal summer clothing. It has also been shown in this 8 hour test study that humidity level was a less important consideration than dry bulb temperature. In another study by Gonzalez et al. (89), direct thermal acceptance was judged by subjects. Four males and 3 females were each exposed randomly to slow humidity changes over a 4.5 hour period (~10% rh per hour) at each of two dry bulb temperatures: 25°C and 27°C. The drift changes corresponded to a dew point change of 2.5°C per hour. Subjects were summer acclimated and wore clothing estimated at 0.4 and 0.8 Clo. Humidity increases at dry bulb temperature levels of 25°C and 27°C and 0.4 Clo did not cause significant decrements in thermal acceptability,

although at higher Clo values there were marked decrements in acceptability. Griffiths and McIntyre have also reported that at 28°C a low humidity was preferred and 50%-75% rh were considered by their subjects as "more oppressive and uncomfortable" (90).

In another study made by Gonzalez (91), humidity was elevated each hour over a 3-hour period at 27°C; thermal sensation and warm discomfort were assessed in 3 groups of individuals: young males, young females, and older females in which half were older than 60 years. No significant differences were evident in thermal sensation values for the groups, or for individual changes within a group, at each humidity level. In some male and female subjects, in which skin temperatures and core temperatures were measured, humidity levels of 40%, 60% and 80% rh at 27°C that did not affect mean skin temperature, which stayed constant within ±0.2°C throughout a 3-hour period. Core temperature was also not elevated more than ±0.1°C. So temperature sensation, as judged by psycho-physically by the subjects, is associated with skin temperature. It, in turn, is governed by ambient temperature and not modified by humidity level, as long as skin temperature is higher than dew point temperature. This response was as expected since relative humidity exerts little effect on the loss of heat by evaporation when the body is in the zone of vasomotor regulation (78).

Other current laboratory and field data (82,91-93) also indicate that in the range of dry bulb temperature of 22.8°C to 25°C, variations in relative humidity from 20 to 60% do not have any appreciable effect on comfort sensations for sedentary, normally clothed individuals. However,

ASHRAE Standard 55-74 guidelines are too broad; they specify that rate of change of rh should not exceed 20% per hour, if peak to peak variation in humidity is 10% rh or greater (84).

Table 2.2 summarizes the various studies discussed on the effects of temperature and humidity fluctuations on comfort.

2.2 Mass Air Quality

Indoor air quality is affected by permeation, infiltration, ventilation and indoor generation. Much work has been reported in literature regarding thermal comfort, but less has been reported regarding the comfort range associated with gaseous and particulate concentrations within indoor environments. The ASHRAE Standard 62-73 specifies minimum and recommended ventilation air quantities for the preservation of human health, safety and well-being in spaces intended for human occupancy (94). This standard also defines "acceptable outside air" as air which meets or exceeds the conditions listed in Table 2.3.

The levels listed are met by ambient outdoor air in many major cities, or will be met by such outdoor air when passed through minimal air treatment systems (containing suitable combinations of heaters, coolers, humidifiers, etc.; and including roughing particulate filters). Conformity of user's local air to these concentrations may be determined by reference to the Storage and Retrieval of Aerometric Data System (SORAD) of the National Air Pollution Control Administration.

Further, air for ventilation is considered unacceptable if it contains any contaminant concentration greater than one-tenth the Threshold

Table 2.2. Effects of drifts in temperature and humidity on comfort, acceptability and health

Year	Investigators	Conditions of test:	Findings:	Reference(s)
Temperature Drifts				
1970	Sprague and McNall	1) 78 males and 78 females (age group (17.8-23.0 years) with Clo values of 0.6 were used in tests on thermal drifts. Test periods were 3 hours each. 2) In another study, 16 different tests on temperature drift of fluctuation periods varying from 1/2-1 hr, amplitudes 0.56-3.33°C, fluctuation rates 1.67-10.94°C/hr.	In practical air conditioned spaces where dry bulb air temperature fluctuates, no serious occupancy complaints should occur due to temperature fluctuations if $(\Delta T^2 x CPH) < 4.63\ \Delta T$ is the peak to peak amplitude of the temperature fluctuation (°C) and CPH is the cycling frequency (cycles/hour).	79
1974	Griffiths and McIntyre	Subjects were exposed to slow one-directional temperature changes of 0, 0.5, and 1.5°C/hour, centered about 23°C, over 6 hour period. The clothing was in the 0.7 to 0.9 Clo range.	A maximum rate of temperature change of 0.75°C/hr with a maximum deviation of 2.25°C from the mean comfort temperature was recommended.	81
1978	Berglund and Gonzalez	Subjects were exposed to space temperature changes of ±0.5, 1.0, and 1.5°C/hr from a 25°C neutral point (determined from Clo values) while humidity was constant at 10 Torr. Test periods were of 4.5 hr duration.	For sedentary persons, a ±0.5°C/hr rate of change from a base temperature of 25°C was acceptable to 80% of the subjects.	85

Table 2.2. (Continued)

Year	Investigators	Conditions of test:	Findings:	Reference(s)
1979	Gonzalez and Berglund	Subjects were exposed to space temperature change of +0.6°C/hr over a 8-hour working day. Summer clothing was worn by the subjects and two levels of elevated but constant humidity were employed.	There was no sign of decrements in thermal acceptability for ±0.6°C/hr as long as air temperature is below 28°C or dew point temperature is below 25°C for normal summer clothing.	89
Humidity Drifts				
1970	Sprague and McNall	1) Number of both males and females in humidity drift test was 48 each (age group 18.4-21.6 years). 2) 9 different tests on humidity drifts of periods 1/2-1 hour, amplitude 3-14% rh, fluctuation rates of 10-42% rh/hour were conducted.	1) In practical air conditioned spaces where relative humidity variations can be expected, no serious occupancy complaints should occur if specifications of ASHRAE Standard 55-66 Section 3.2.2 on fluctuating relative humidity are followed. Fluctuations more severe than those allowed by ASHRAE Standard may not be objectionable but more research efforts were recommended before the standard is relaxed.	79
1973	Griffiths and McIntyre	Subjects were exposed to different rh values at constant dry bulb temperature of 28°C.	At 28°C a low humidity was preferred and 50%-75% rh was considered by the subjects to be "more oppressive and uncomfortable."	90

Table 2.2. (Continued)

Year	Investigators	Conditions of test:	Findings:	Reference(s)
1977	Gonzalez	1) 3 groups of individuals: young males, young females, and older females (50% older than 60 years) were subjected to humidity increases each hour (40%, 60% and 80% rh) for a 3-hour period at 27°C.	1) No significant differences were evident in thermal sensation values for the groups, or for individual changes within a group, at each humidity level. 2) Mean skin temperatures were constant within ±0.2°C and core temperatures were constant ±0.1°C at all humidity levels.	91
1979	Gonzalez and Berglund	Four males and three females were each exposed randomly to slow humidity changes over a 4.5 hour period (~10% rh per hour) at each of two dry bulb temperatures of 25°C and 27°C. The drift was equivalent to a dew point change of 2.5°C per hour. Subjects were summer acclimated and wore 0.4-0.8 Clo.	Humidity increases at dry bulb temperature levels of 25°C and 27°C at 0.4 Clo did not cause significant decrements in thermal acceptability, although at higher Clo values there were marked decrements in acceptability.	89

Table 2.3. Maximum allowable concentrations for ventilation air in ASHRAE Standard 62-73 (94)

Contaminant	Annual average (arithmetic mean) $\mu g/m^3$	Short-term level (not to be exceeded more than once a year) $\mu g/m^3$	Averaging period (h)
Particulates	60[a]	150[a]	24
Sulfur oxides	80	400	24
Carbon monoxide	20,000	30,000	8
Photochemical oxidant	100	500	1
Hydrocarbons (not including methane)	1,800	4,000	3
Nitrogen oxides	200	500	24
Odor	200	Essentially unobjectionable[b]	

[a]Federal criteria for U.S. by 1975.

[b]Judged unobjectionable by 60% of a panel of 10 untrained subjects.

Limit Value (TLV) currently accepted by the American Conference of Government Hygienists (1974) (94). If acceptable outside air is unavailable and/or economics of energy savings likely to be achieved through treatment of indoor air for mass air quality are attractive, filtration or other air treatment methods must be incorporated in HVAC systems.

2.3 Sound Control

Sound control, the maintenance of an acoustical environment compatible with the intended function of a room or space, is an important part of building design. Today it ranks equally with the control of proper thermal and luminous environments.

Noise is unwanted or objectionable sound and can be produced by people, machines, traffic, air conditioning and air distribution equipment. Sound becomes noisy when it is loud, when its frequency is objectionable, or when there is a combination of both effects. Noisy environments prevent satisfactory communication, are fatiguing, distract workers and affect productivity and tolerance. Extreme noise levels can impair hearing through physical damage.

Loudness (level) of sound is measured in terms of decibels (dB). The weakest sound that can be heard by a person with very good hearing, in an extremely quiet location, is assigned the value of 0 dB. At 140 dB, the threshold of pain is reached. In between is the noise level in a large office, usually between 50 and 60 dB.

Frequency (or pitch) is another important, yet subtle, part of noise and hearing. Our ears discriminate naturally against low-frequency sounds. Therefore, we can tolerate more low-frequency noise than high-

frequency noise. When we begin to lose our hearing, our ears usually become less sensitive at first to the higher frequencies.

Sound pressure level cannot be taken at face value as an indication of loudness, because the frequence (in hertz) of a sound has quite a bit to do with how loud it sounds. The frequency effect leads to the concept of weighting network. Weighting networks are the sound-level meter's means of responding more to some frequencies than to others, with a prejudice something like that of the human ear. Acoustical standards have established 3 weighting characteristics, designated A, B, and C. The primary differences among them are that very low frequencies are discriminated against quite severely by the A network, moderately by the B network, and hardly at all by the C network. Therefore, if the measured sound-level of a noise is much higher on C weighting than on A weighting, much of the noise is probably at low frequencies. Curves for the A, B and C weighting networks are shown in Figure 2.1 which is adopted from reference (95).

Although the A-scale provides a simple, single-number rating or screening measurement, it gives no real information on the spectrum content of the sound. A single-number method of providing information on the spectrum content employs Noise Criteria Curves and the resulting NC numbers (96). These curves, Figure 2.2, were constructed from loudness and speech interference data and have been related to acoustical comfort or desired noise levels in various spaces. Design goals have been formulated by ASHRAE (54) and representative values are shown in Table 2.4 (97).

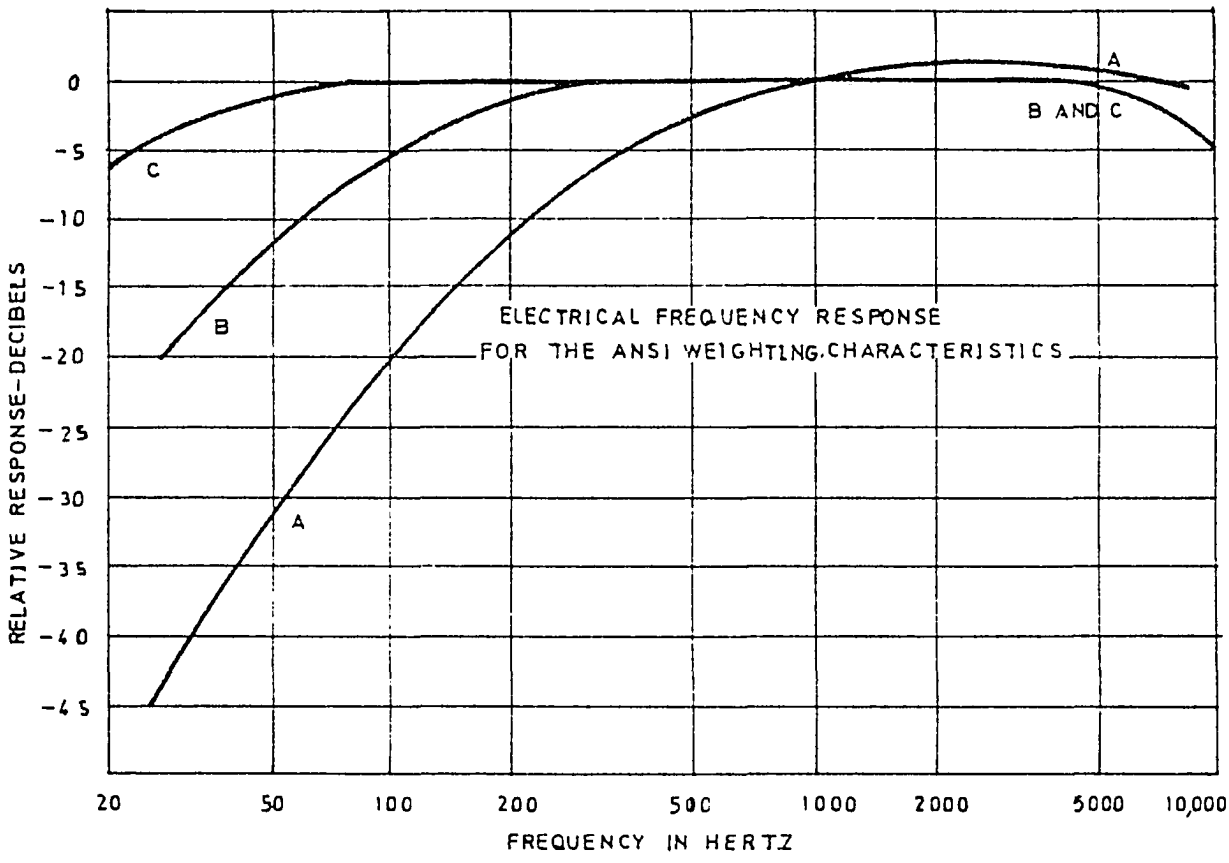

Figure 2.1. Curves for the A, B and C weighting networks (95).

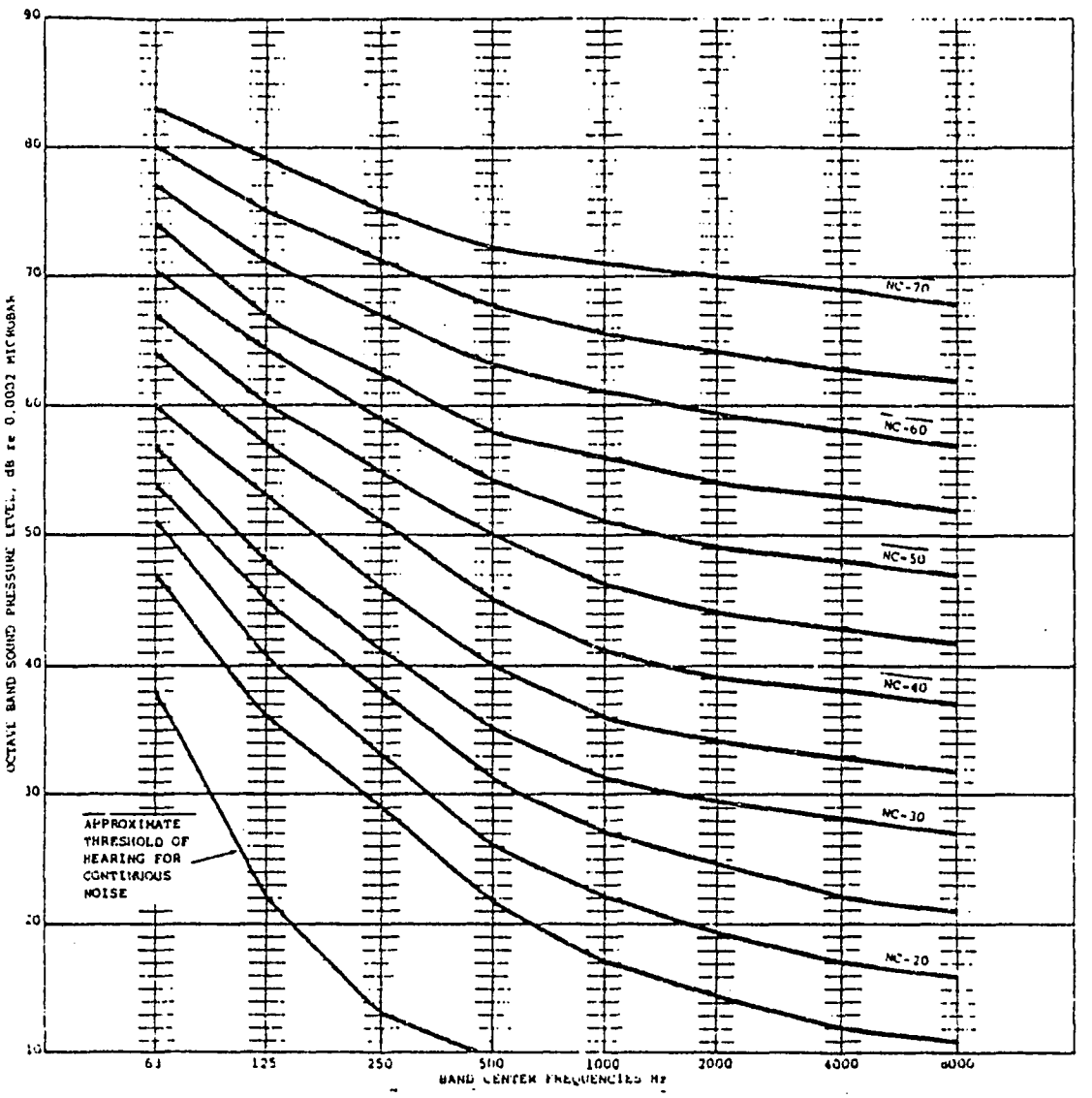

Figure 2.2. Noise criteria curves (97).

Table 2.4. Ranges of indoor design goals for air conditioning system sound control (97)

Area	Ranges of NC curves (dB)
Private homes	25-35
Apartments	30-40
Hotel sleeping rooms	30-40
Lobbies	35-45
Executive offices	30-40
Open offices	35-50
Concert halls	20-25
Libraries	30-40
Classrooms	30-40
Supermarkets	40-55

2.4 Lighting Control

Light impinging upon the eye enters through the pupil, the size of which is controlled by the iris, thereby controling the amount of light entering the eye. The lens focuses the image on the retina from which the optic nerve conveys the visual message by electric impulse to the brain.

There are four basic characteristics of each visual task with which the eye is confronted; size, brightness, contrast, and time exposure of the object or area being viewed. The basic visual tasks are the perception of low contrast, fine detail, and brightness gradient. These abilities are all dependent on the 4 stated basic characteristics.

Visual activity is generally proportional to the physical size of the object being viewed given fixed brightness, contrast, and exposure time.

Since the actual parameter is not physical size but subtended visual angle, visual ability can be increased by bringing the object nearer the eye.

The candela (candle power), Cd, is the unit of luminous intensity (time rate of luminous energy per unit solid angle). It is analogous to pressure in a hydraulic system. An ordinary wax candle has a luminous intensity horizontally of approximately one candela (candlepower) whence the name. A source of one candela intensity produces a total light output in all directions of 4π lumens. The lumen, lm, is the unit of luminous flux (time rate of luminous energy). It is analogous to flow in hydraulic systems and is a measure of the amount of light generated by a luminous source. The footcandle or lux, fc (lx), is the unit used to measure the density of luminous flux and is therefore equal to lumens per square foot (m^2) (time rate of luminous energy per unit area). Tables 2.5 and 2.6 give values of required footcandles for some tasks in occupied spaces and has been adopted from IES Lighting Handbook (98). For good contrast, the brightness of the task should be the same as that of the background, but ratios up to 3 to 1 are acceptable in most circumstances.

Registering a meaningful visual image is not an instantaneous process, but one that requires finite amounts of time. Higher the illumination, shorter is the amount of time.

To conclude, the luminance, contrast, size and exposure are the four basic factors that affect the visual performance. Generally, exposure time and size are not readily controllable parameters, leaving luminance and contrast to be manipulated by the lighting designer in such a way as

Table 2.5. Typical Blackwell illumination data (98)

Task	Required footcandles
School	
1. Sample of ink writing	1.4
4. 6-point text type	3.0
57. Average of 8 samples of spirit duplicated material--(difficult)	684.0
Office	
8. Sample of shorthand copy with #3 pencil	76.5
11. Typed carbon, 5th copy	133.0
13. Thermal reproduced copy, poor quality	589.0
49. White line on blueprint, tracing paper overlay	5,090.0
Garment Industry	
15. White chalk mark on blue serge cloth	10.0
20. Gray stiching on gray silk	
vertical stitching	4,160.0
horizontal stitching	>10,000.0
Store Tasks	
29. Price tag, pencil	241.0
30. Price tag, ink	3.1

to give a comfortable and efficient visual environment. Such an environment must be efficient in the sense that it provides for optimal performance of a given task, and comfortable in the sense that this visual task performance takes place with minimum fatigue, whether conscious of it or not.

Table 2.6. Current footcandle recommendations for specific visual tasks (98)

Seeing task	Primary task plane footcandles[a] (Dekalux)
Dining	15 (16)
Grooming, shaving, make-up	50 (54)
Handcraft	
Ordinary seeing tasks	70 (75)
Difficult seeing tasks	100 (110)
Very difficult seeing tasks	150 (160)
Critical seeing tasks	200 (220)
Ironing (hand and machine)	50 (54)
Kitchen duties	
Food preparation and cleaning (at sink, range and counter)	
Involving difficult seeing tasks	150 (160)
Serving and other noncritical tasks	50 (54)
Laundry tasks	
Preparation, sorting, inspection	50 (54)
Tub area-soaking, tinting hand wash	50 (54)
Washer and dryer areas	30 (32)
Reading and writing	
Handwriting, reproductions, and poor copies	70 (75)
Books, magazines, and newspapers	30 (32)
Reading piano or organ scores	
Advanced (substandard size)	150 (160)
Advanced	70 (75)
Simple	30 (32)
Sewing	
Hand (dark fabrics)	200 (220)
Hand (medium fabrics)	100 (110)
Hand (light fabrics)	50 (54)
Hand (occasional--high contrast)	30 (32)
Sewing	
Machine (dark fabrics)	200 (220)

[a]Minimum on the task plane at any time. These levels are based on young eyes with 20-20 vision. Older eyes, even when properly corrected by glasses, have reduced visual acuity, a longer period of adaptation and decreased resistance to glare. To state it simply, older persons need more light, and special precautions against glare.

Table 2.6. (Continued)

Seeing task	Primary task plane footcandles (Dekalux)
Machine (medium fabrics)	100 (110)
Machine (light fabrics)	50 (54)
Machine (occasional--high contrast)	30 (32)
Study	70 (75)
Table games	30 (32)
Table tennis	20 (22)

3. DYNAMICS OF AN OCCUPIED SPACE

3.1 Dynamic Performance vs. Steady State Performance of a System

A building system is made up of three physical components as shown in Figure 3.1, i.e., envelope, HVAC system, and equipment (boilers, chillers, cooling towers, etc.). These three components interact with each other through controllers. Figure 3.2 shows the major components and the controller (thermostat) for a residential heating system. The response of components in the system to various inputs is of extreme importance in control work. For example, the components of the system shown in Figure 3.2 constantly receive input signals due to variations in climatic variables, and their response to these inputs must be known in order to achieve a satisfactory system. Prediction of the responses of physical components requires the ability to write and solve mathematical models for the components. A summary of the methodologies used for modeling and analysis of physical systems is shown in Figure 3.3.

Complete solution of the mathematical model for the physical component(s) is made up of complementary solution and particular solution. Complementary solution decreases in magnitude with increasing values of time and ultimately vanishes. These functions are transient in nature and describe the dynamic performance of the component(s). The particular solution is not modified by the time, and in addition, yields the ultimate value (time $\rightarrow \infty$) of the complete solution. This part of the solution is given the name steady state solution and describes the steady state performance of the component(s).

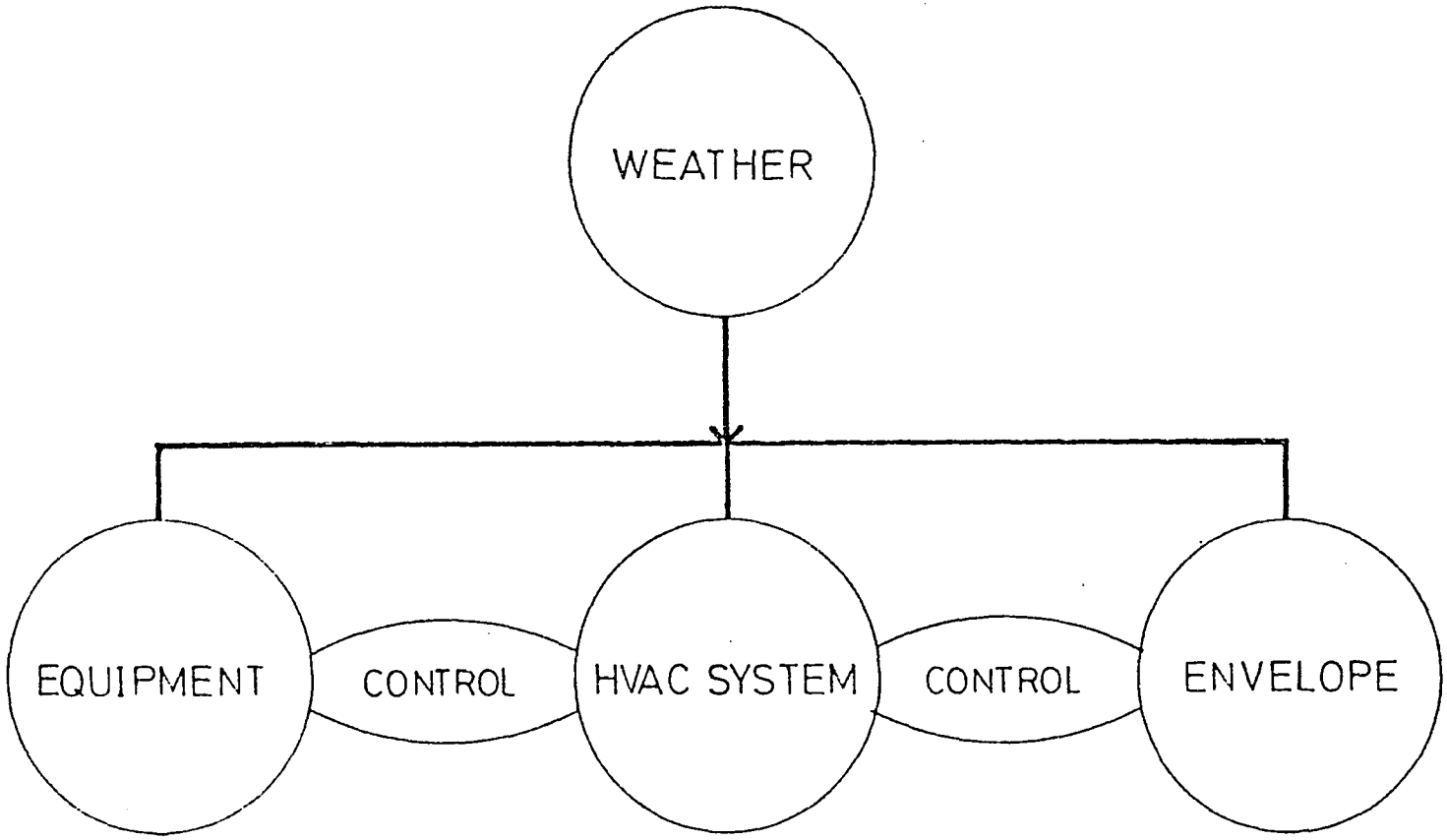

Figure 3.1. Physical components of a building system and weather inputs.

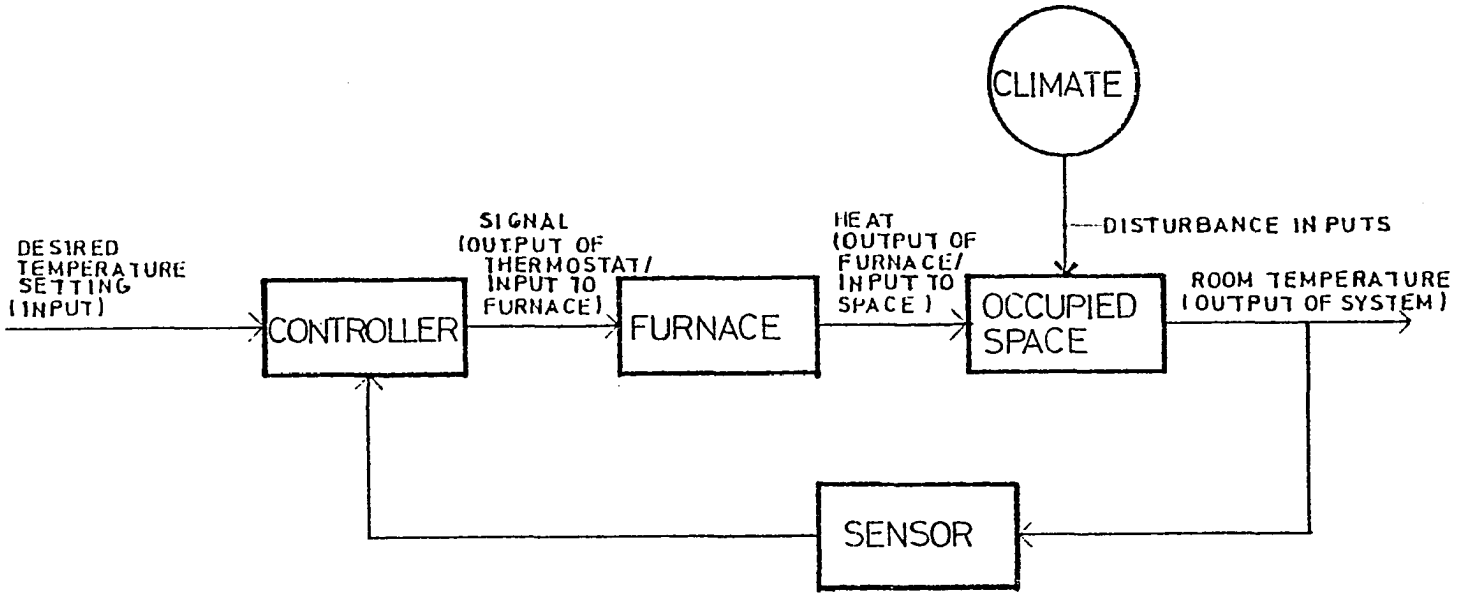

Figure 3.2. A block diagram for the residential heating system.

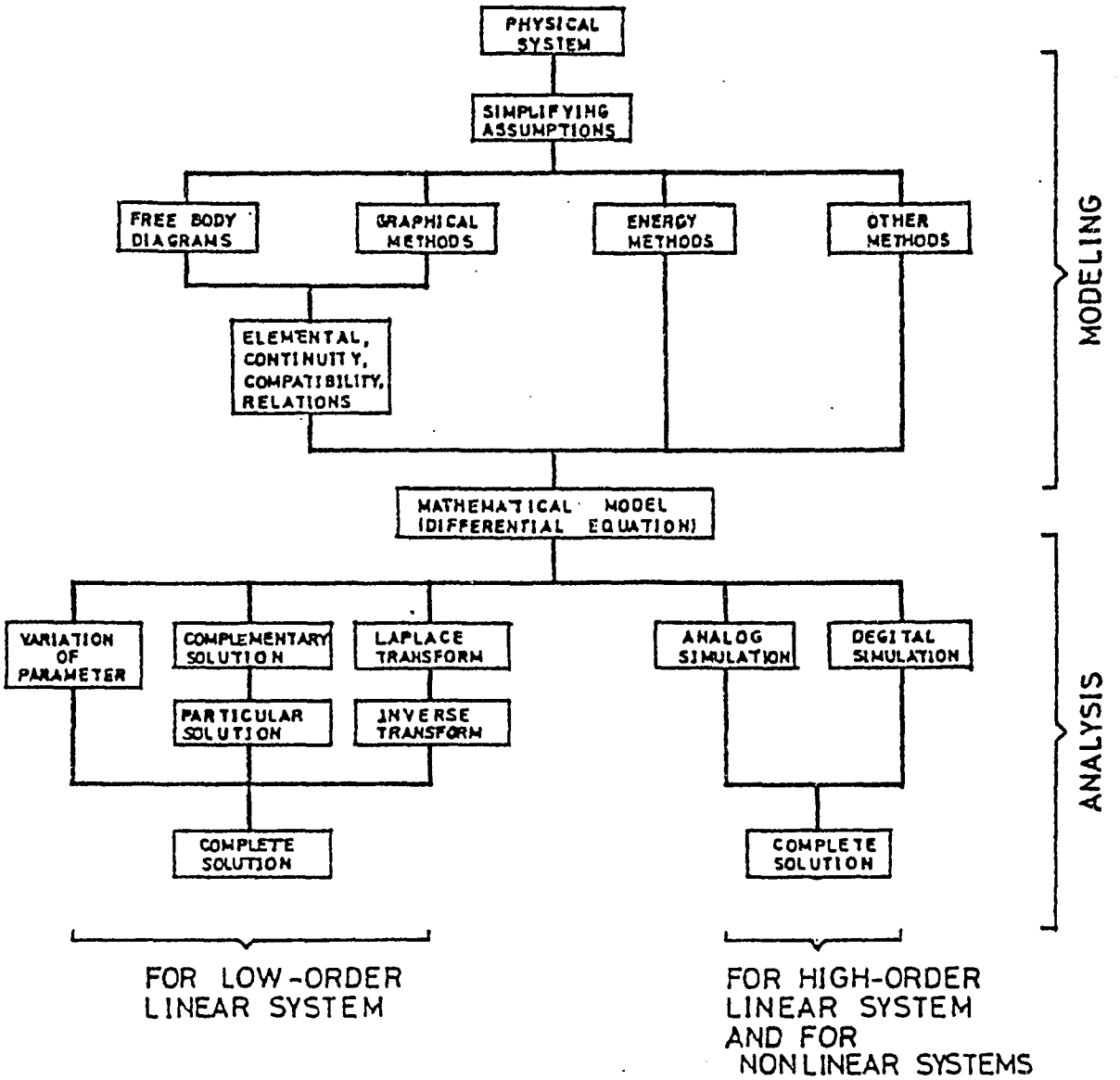

Figure 3.3. Methodologies for systems analysis.

To illustrate the definitions of dynamic and steady state performance of components in a building system, a hot water generator used to supply hot water is analyzed. A sketch of such a heater is shown in Figure 3.4. The tank is insulated to reduce heat loss to the surrounding air. The input variables to the heater are mass flow rate of cold water and the heat transfer from the resistance coil. The output variable is the temperature of hot water. The necessary simplifying assumptions are as follows:

1. Heat storage in the insulation is negligible. This is valid since the specific heat of the insulation is small and the water temperature variation is small.
2. All of the water in the tank is at a uniform temperature. This requires perfect mixing of the water.

Definitions of the system parameters and variations are as follows:

$\dot{Q}$ = rate of energy transfer from resistance coil (for dimensions of these quantities, see List of Nomenclature)

$\dot{Q}_t$ = rate of change of stored energy of water in tank

$\dot{Q}_0$ = rate of energy out due to hot water leaving tank

$\dot{Q}_i$ = rate of energy in due to cold water entering tank

$\dot{Q}_e$ = rate of energy lost through tank insulation

T = temperature of water in tank

T_i = temperature of water entering tank

T_a = temperature of air surrounding tank

C = thermal capacitance of water in tank

R = thermal resistance of insulation

$\dot{m}_w$ = mass flow rate of water from tank

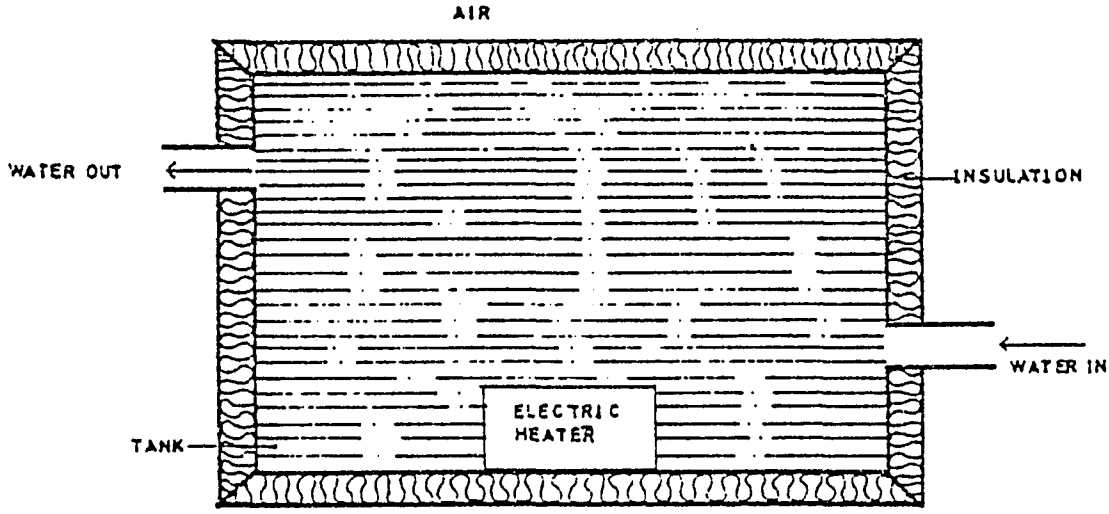

Figure 3.4. Electric water heater.

S = specific heat of water

An energy balance on the hot water generator yields:

$$\dot{Q}_t + \dot{Q}_0 - \dot{Q}_i + \dot{Q}_e = \dot{Q} \tag{3.1}$$

where

$$\dot{Q}_t = C \frac{dT}{dt}$$

$$\dot{Q}_0 = \dot{m}_w S T$$

$$\dot{Q}_i = \dot{m}_w S T_i$$

$$\dot{Q}_e = \frac{T - T_a}{R}$$

Substituting these quantities in equation (3.1) gives

$$C \frac{dT}{dt} + \dot{m}_w S(T - T_i) + \frac{T - T_a}{R} = \dot{Q} \tag{3.2}$$

There are four variables in this equation: T, T_i, T_a, and $\dot{m}_w$. Three of them must be specified in order to solve the problem. For the special case in which $\dot{m}_w$ is a constant and $T_a = T_i$, equation (3.2) can be simplified. In terms of θ, which now is the temperature above the reference T_a, the equation is

$$D\theta + \left(\frac{R\dot{m}_w S + 1}{RC}\right)\theta = \dot{Q}/C \tag{3.3}$$

or

$$D\theta + K\theta = \dot{Q}/C \tag{3.4}$$

where

$$K = \frac{RS\dot{m}_w + 1}{RC}$$

The complementary function θ_c for the solution of equation (3.4) is obtained by solving the associated homogeneous equation

$$D\theta + K\theta = 0 = \theta(p + K)$$

The characteristic equation and its roots are

$$p + K = 0 \text{ and } p = -K$$

Therefore,

$$\theta c = C_1 e^{p\theta} = C_1 e^{-K\theta}$$

If the input is a step function of constant magnitude $\dot{Q}$ at $t \geq 0$, the particular integral can be assumed to be constant; $\theta_p = A$ and the derivative $d\theta_p/dt = 0$. Substituting in equation (3.4):

$$KA = \dot{Q}/C$$

$$A = \dot{Q}/KC$$

The complete solution is

$$\theta = \theta_c + \theta_p = C_1 e^{-Kt} + \dot{Q}/KC$$

For the initial conditions $\theta = 0$ when $t = 0$

$$0 = C_1 + \dot{Q}/KC$$

$$C_1 = -\dot{Q}/KC$$

Therefore

$$\theta = \dot{Q}/KC(1 - e^{-Kt}) \qquad (3.5)$$

A graphical representation of the response of the hot water generator given by equation (3.5) is shown in Figure 3.5. The complementary function

$$-\frac{\dot{Q}e^{-Kt}}{KC}$$

decreases with increasing values of time and ultimately vanishes. This function describes the short term dynamics of the process. The value of time which makes the exponent of e equal to -1 is called the time constant τ. Thus the time constant for the water heater is given by

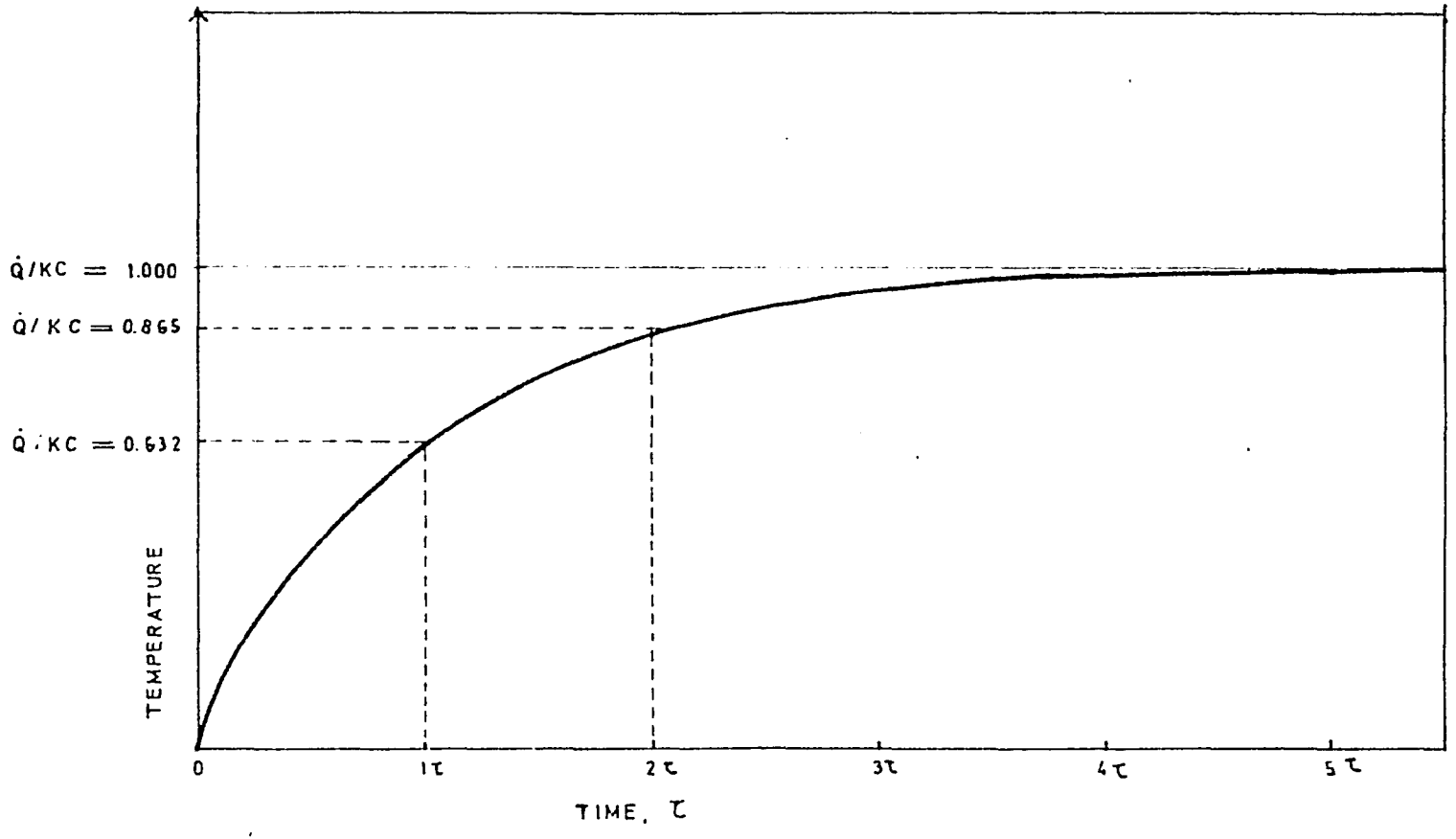

Figure 3.5. Graphical representation of equation (3.5).

$$\tau = \frac{1}{K} = \frac{RC}{RS\dot{m}_w + 1} \tag{3.6}$$

The time constant is dependent upon the parameters of the system and is an important characteristic of the dynamic performance of the system. Particular integral ($\dot{Q}/KC$) is not modified by the time and yields the ultimate value of water temperature as $t \to \infty$. This part of the solution describes the steady state performance of the water heater.

3.2 Mathematical Model of Occupied Space

Now that we have reviewed the end use requirements of controlled variables in occupied spaces in Chapter 2 and distinguished between steady state vs. dynamic responses, models to predict dynamic responses of the occupied space will be developed. Though the review has revealed that comfort depends upon thermal factors, mass air quality, sound levels, and lighting levels, the scope of the present work is restricted to models to predict short term dynamics of temperature inside buildings.

Applications of analog computer techniques which simulate the dynamic conditions (temperature) inside a building have been reported by Nelson (25) and Magnussen (26). Analog computer methods were preferred over analytical methods because of the complexity of analytical techniques. However, the analog computer methods restricted the use of analytical optimization techniques. Realizing the deficiencies of analog computer methods, Kaya has reported the development of analytical models based upon analog passive circuits (27). However, the validity of analytical models developed from analog passive circuits has not been

examined so far. Hence one of the efforts of this dissertation was to test the validity and to evaluate the suitability of analytical models to predict dynamic conditions inside a building.

3.2.1 Analytical closed-loop model from analog passive circuits

Consider the temperature control loop (Figure 3.6) which is similar to those in Figures 5, 6 and 2a of references 25, 26 and 27, respectively. Figure 3.7 shows the thermal circuit of one zone of multizone commercial building which is similar to Figure 1 of references 26 and 27. A block diagram of the thermal circuit is shown in Figure 3.8 which is similar to Figure 2(B) of reference 27. Transfer functions reported for these blocks in reference 27 are shown in Table 3.1 and the mathematical model of the same reference is reproduced in Figure 3.9. Actual controller used in the commercial building simulated by Magnussen was a thermostat switch with on-off operation, so the nonlinear (NL) block in Figure 3.9 is replaced with a transfer function of K = 1 for "on" operation and K = 0 for "off" operation and the simplified block diagram is shown in Figure 3.10. Block diagram algebra is used in Figure 3.10 to derive the following closed loop transfer function

$$T(s) = \frac{(R(s) - D_1(s)KG(s) + D_2(s)G(s)(1 + KH_1(s))}{1 + KH_1(s) - KH(s)G(s)} \tag{3.7}$$

where

$$D_1(S) = \frac{0.567M_2(S)(0.923S+1)(0.909S+1)}{[(0.909S+1) + 0.135(0.192S+1)](0.909S+1)(20S+1)} \tag{3.8}$$

$$D_2(S) = \frac{0.32M_1(S)(4S+1)(2.8S+1)}{(1.35S+1)} \tag{3.9}$$

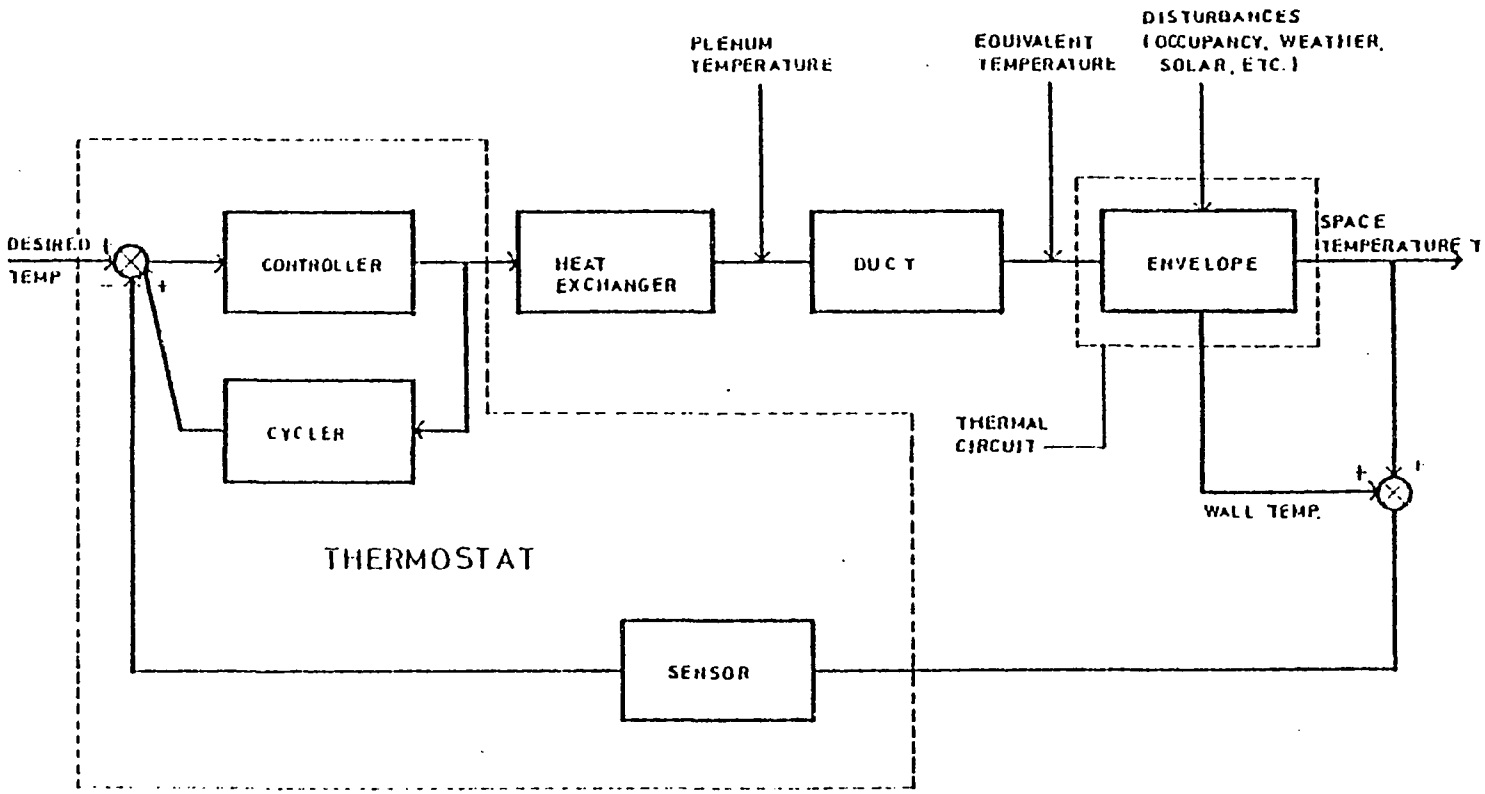

Figure 3.6. Temperature control loop.

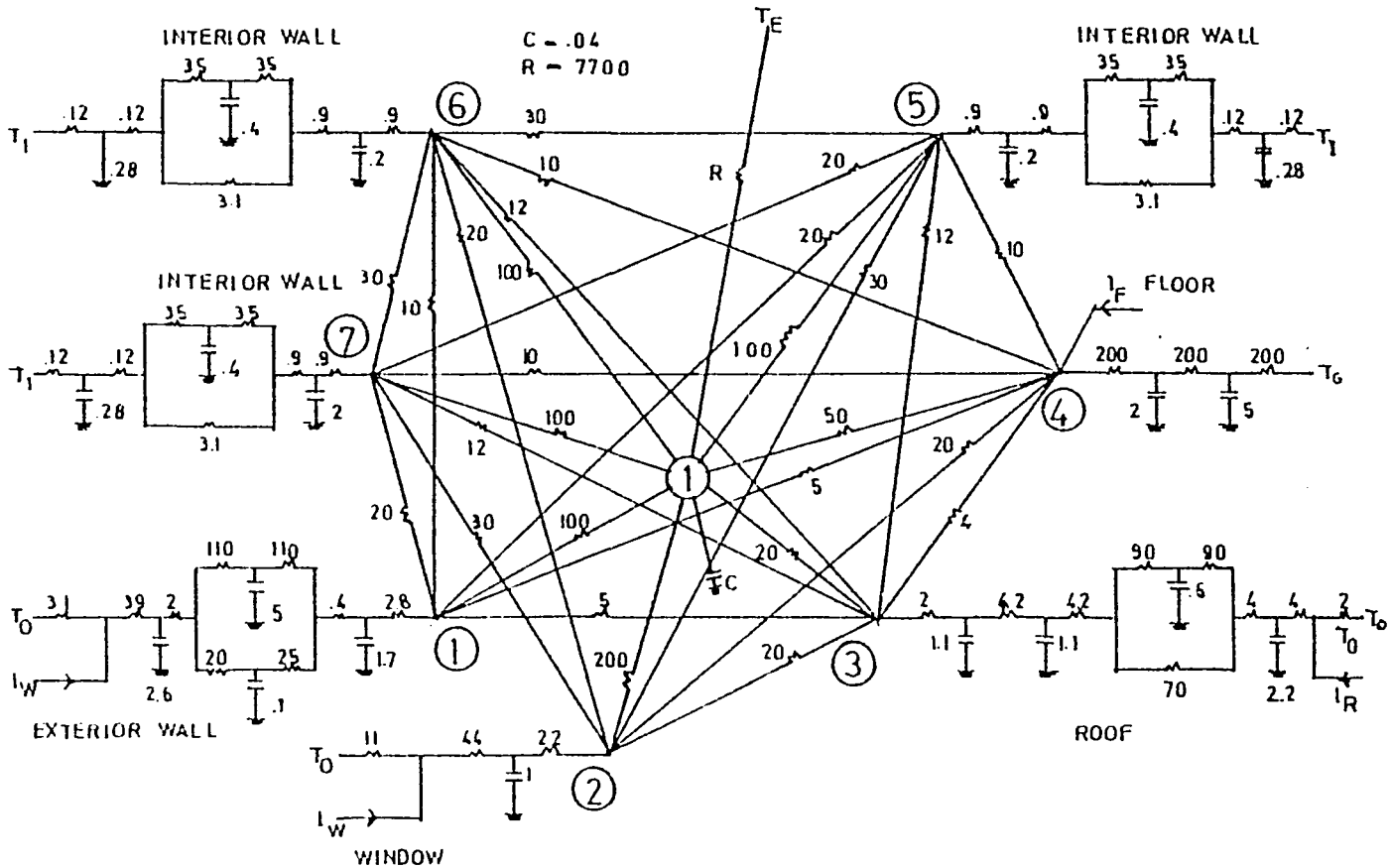

Figure 3.7. Simulated thermal circuit of one zone in a multizone building (same as Figure 1 of reference 27).

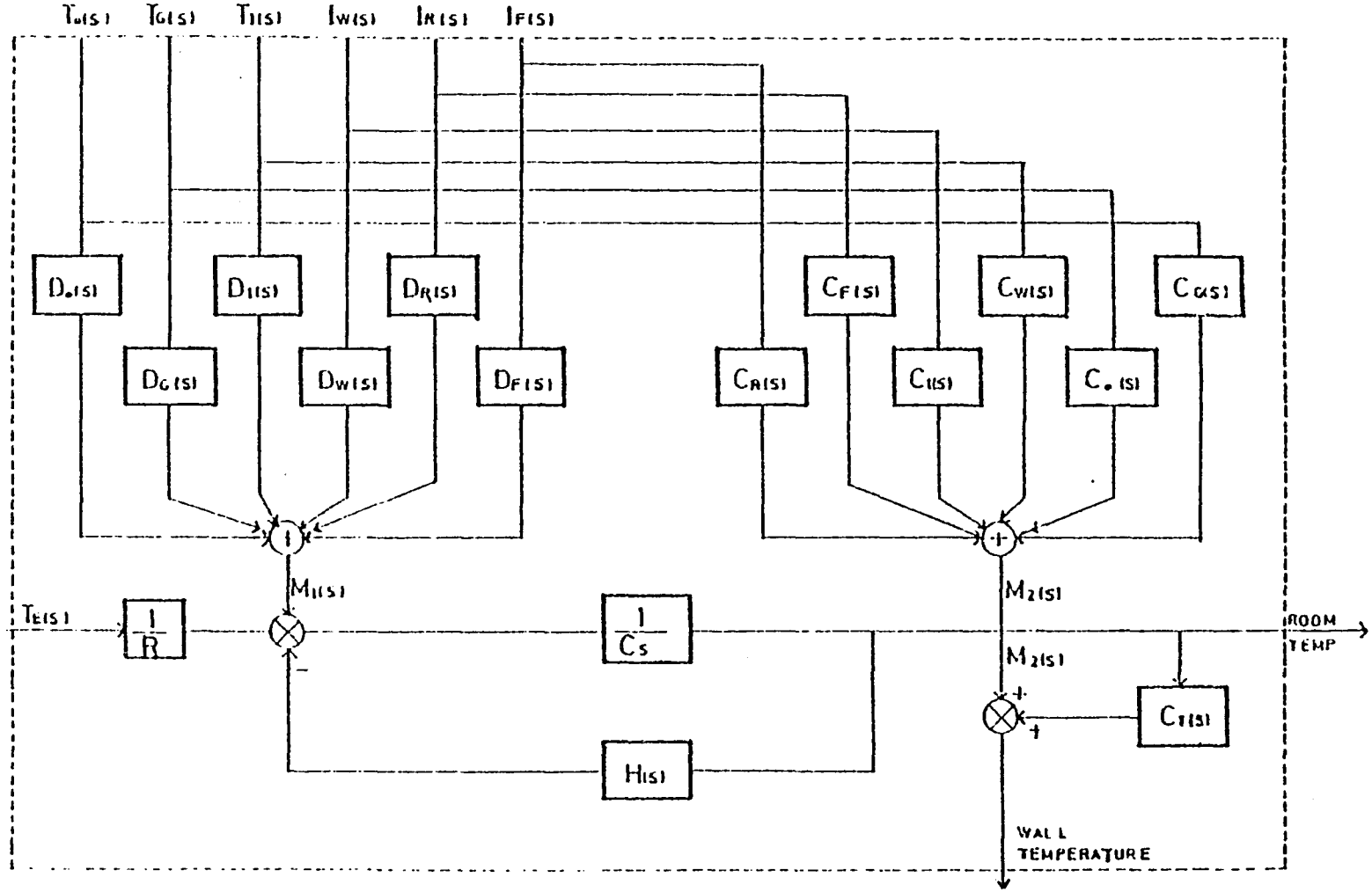

Figure 3.8. Block diagram of thermal circuit (same as Figure 2B of reference 27).

Table 3.1. Transfer functions of blocks of thermal circuit (same as Table 3 of reference 27)

$D_0(s) = \frac{0.0045}{(6.67S+1)}$	$R = 7700$
$D_G(s) = \frac{10^{-6}}{(303S+1)^2}$	$C_o(s) = \frac{0.025(0.1S+1)}{(1.25S+1)(0.333S+1)}$
$D_1(s) = \frac{0.02}{(0.714S+1)(0.028S+1)}$	$C_G(s) = \frac{10^{-5}(0.562)(0.2S+1)}{(285.7S+1)^2(1.389S+1)}$
$D_w(s) = \frac{0.02}{(3.85S+1)}$	$C_I(s) = \frac{0.596}{(0.555S+1)(0.0286S+1)}$
$D_r(s) = \frac{0.005}{(6.25S+1)^3}$	$C_w(s) = \frac{0.126(0.152S+1)}{(0.455S+1)(2.632S+1)}$
$D_F(s) = \frac{0.158(2S+1)}{(0.67S+1)}$	$C_R(s) = \frac{0.025(0.12S+1)}{(31.25S+1)(3.125S+1)^2(0.526S+1)}$
$H(s) = \frac{0.094(5S+1)}{(4.55S+1)}$	$C_F(s) = \frac{0.813(0.167S+1)}{(2.86S+1)}$
$C = 0.04$	$C_T(s) = \frac{0.135(0.192S+1)}{(0.909S+1)}$

Performance of the control system shown in Figure 3.10 can be verified by taking inverse Laplace Transform of the right hand side polynomial of equation (3.7). Figure 3.11 is an oscillograph recording of system variables recorded by Magnussen for the last 2 days of January and the first day of February, 1955. Using variables like outside air temperature and solar radiation from Figure 3.11 as inputs to the analytical closed loop model of equation (3.7), values of space temperature can be predicted. Comparison between the predicted results from the analytical

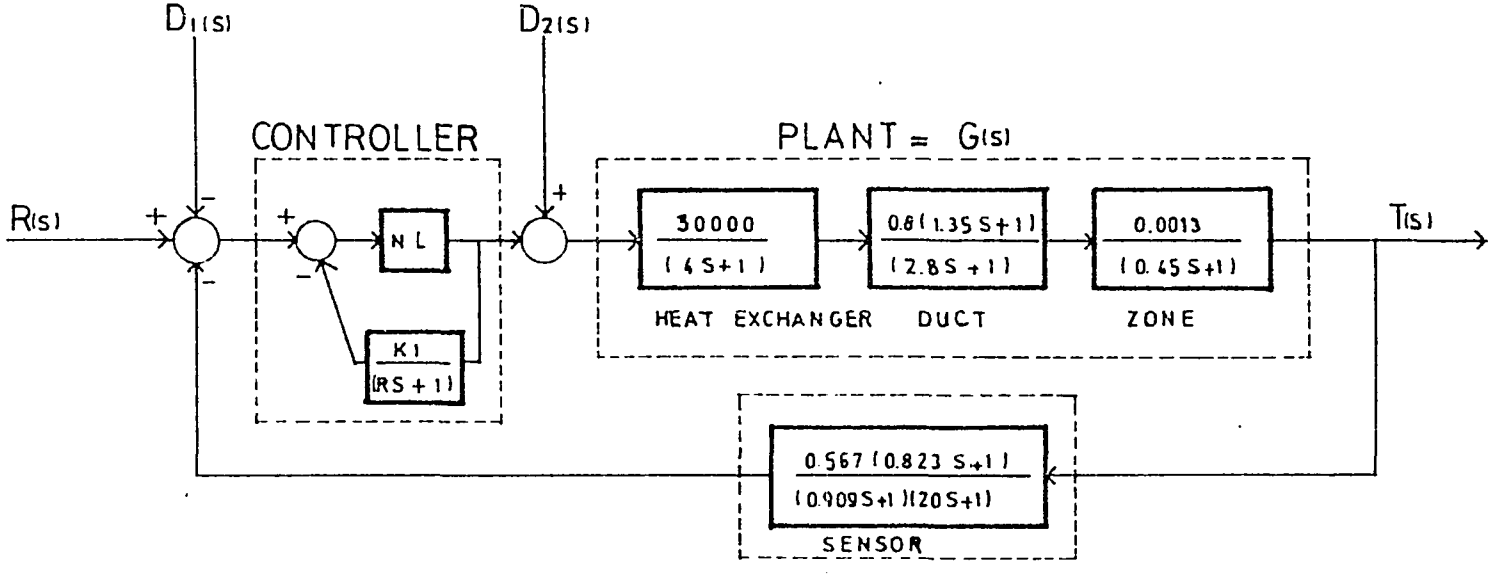

Figure 3.9. Mathematical model of temperature control system of a zone in a multizone system (same as Figure 4A of reference 27).

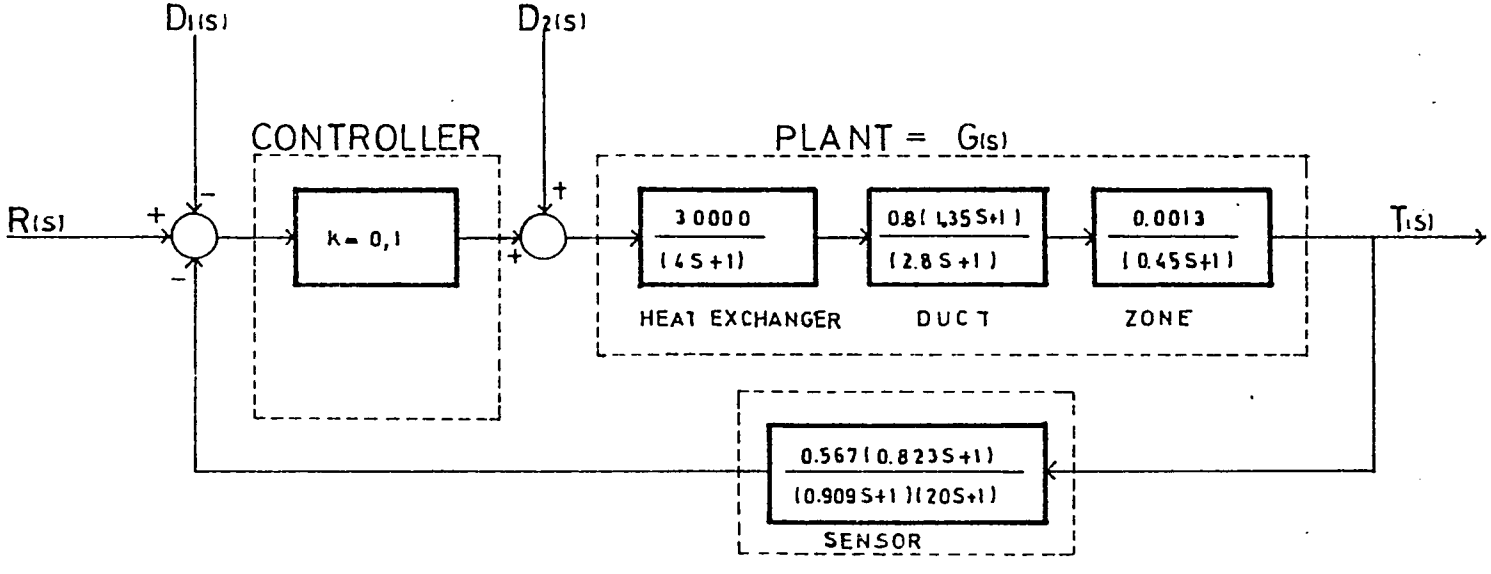

Figure 3.10. Simplified mathematical model of temperature control system shown in Figure 3.9.

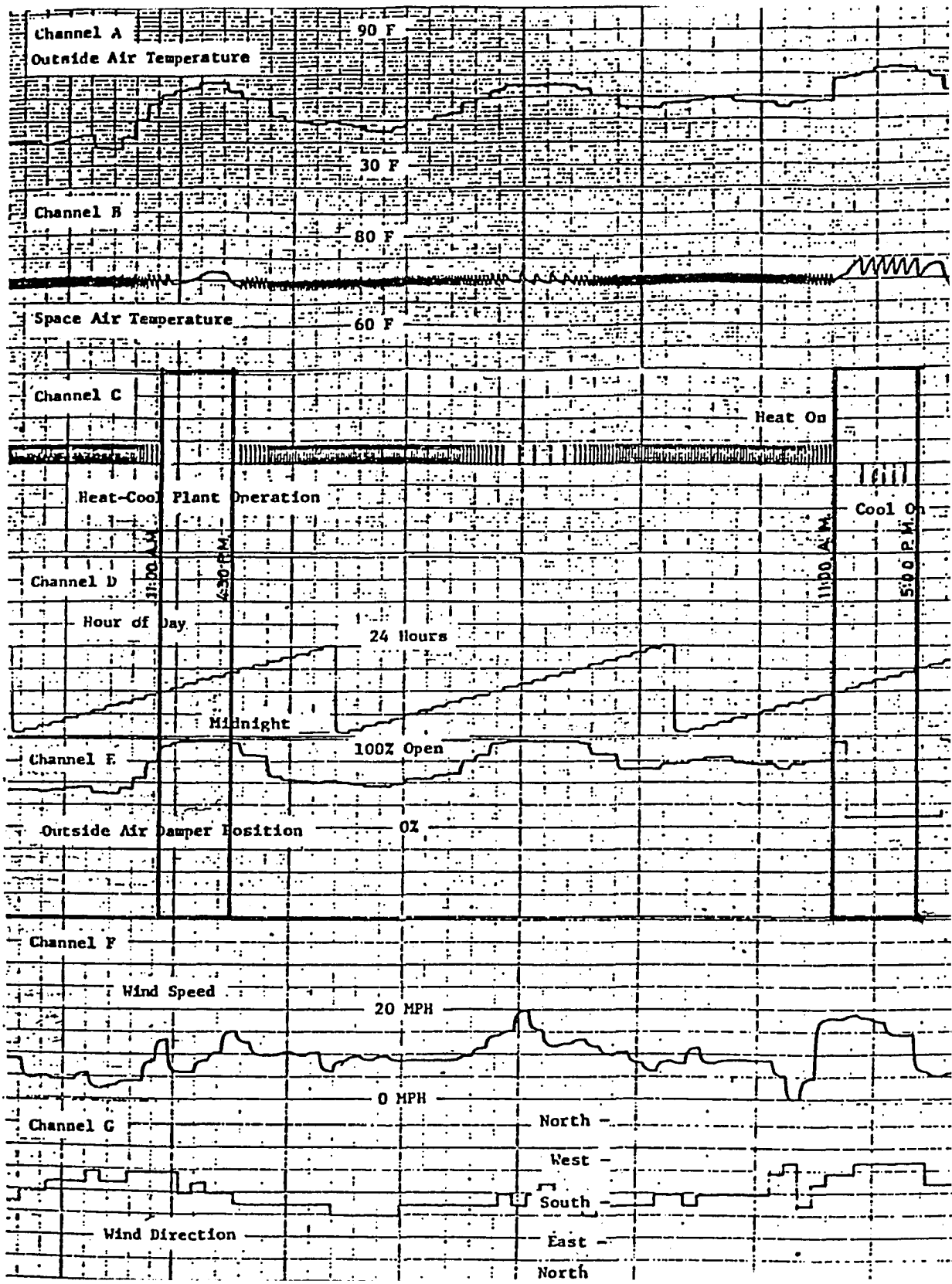

Figure 3.11. Oscillograph recording of system variables by analog com-

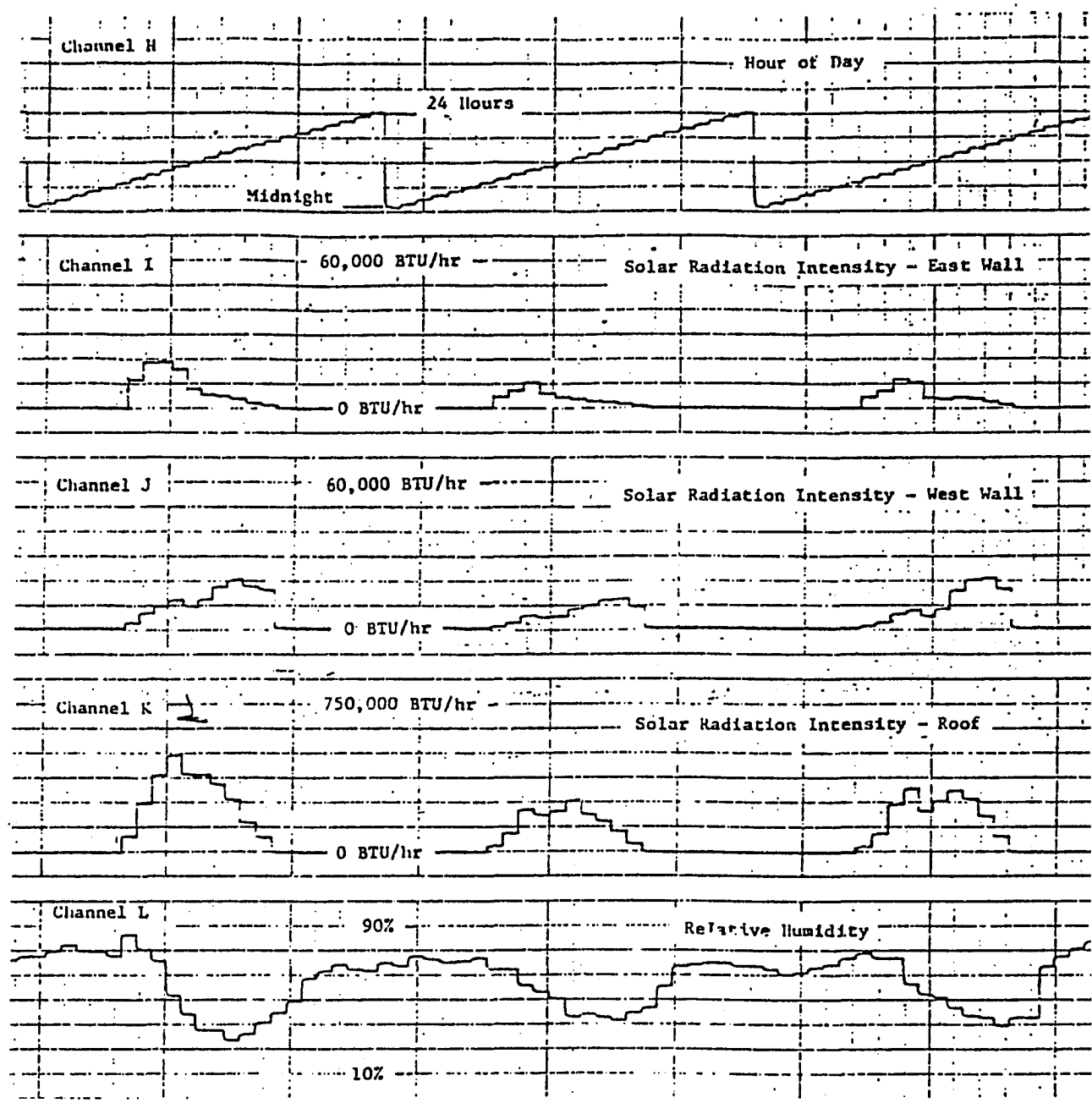

re 3.11. (Continued)

model with those simulated values by analog computer model should lead to conclusions about the validity of analytical model. However, such an analysis of closed loop transfer function is limited due to the following difficulties:

1. The analytical model is based on the thermal circuit of one zone 15' by 15' by 8' in height. The analog computer simulation shown in Figure 3.11 considers the entire building (30' x 90' x 8') to be a single zone. So the zone block in Figure 3.9 is not the same as simulated in Figure 3.11.
2. The analog computer model (Figure 3.11) simulates a single-story single zone building 30' wide by 90' long by 8' in height. The building is assumed to have a one stage heating and one stage cooling system incorporating an air economizer. The analytical model (Figure 3.9) assumes a furnace of suitable capacity for a single zone. Thus the heat exchanger block in Figure 3.9 is not the same as simulated in Figure 3.11.
3. Duct and sensor blocks in Figure 3.9 are also different from those simulated in Figure 3.11 because the two models use different HVAC systems.

Even if the systems had been similar, substituting the transfer function for individual blocks of Figure 3.10 in the closed loop transfer function in equation (3.7), it is shown in Appendix A that the analytical model for closed loop transfer function will involve solving 14 polynomials and some of them are of the 10th order. So even if the analog computer simulation and the analytical model were for one zone employing

the same HVAC system, validation of the analytical model would have involved complex algebraic calculations. If the analytical models were to be developed for all the 12 different zones in the building, the analytical solution would require a difficult mathematical analysis and would not be suitable for engineering purposes.

3.2.2 Analytical model for occupied space from analog passive circuits

It has been shown in section 3.2.1 that the validity of the technique proposed by Kaya (27) cannot be tested on the basis of the data available from the analog computer experiments by Magnussen (26) when the HVAC system is operating. An examination of simulation results reported by Magnussen (26) in Figure 3.11 reveals that on the first day as well as on the third day of simulation, weather conditions for certain periods were such that no heating or cooling was required. For such periods of time when HVAC system is off, difficulties described in section 3.2.1 due to differences in HVAC systems of Figures 3.9 and 3.11 are eliminated. Thus an open loop transfer function derived for the system shown in Figure 3.10 will be based on Kaya's technique (27) and should describe the responses of the zone to the inputs from disturbances $D_2(s)$ due to weather which can be compared with the data shown in Figure 3.11 for periods when HVAC plant is off.

So, substituting K = 0 in equation (3.7) for off period of HVAC system,

$$T(s) = D_2(s)G(s) \tag{3.10}$$

Substituting for $D_2(s)$ and G(s) in equation (3.10)

$$T(s) = \frac{10.01M_1}{(0.45S+1)} \tag{3.11}$$

where

$$M_1(s) = D_o(s)T_o(s) + D_G(s)T_G(s) + D_I(s)T_I(s) + D_w(s)I_w(s) + D_R(s)I_R(s) + D_F(s)I_F(s) \quad (3.12)$$

where

$T_o(s)$ = Laplace Transform of outdoor temperature function

$T_G(s)$ = Laplace Transform of ground temperature function

$T_I(s)$ = Laplace Transform of temperature function of space adjacent to interior walls

$I_w(s)$ = Laplace Transform of solar radiation function incident on external wall

$I_R(s)$ = Laplace Transform of solar radiation function incident on roof

$I_F(s)$ = Laplace Transform of solar radiation passing through window and incident on floor.

All the D's are the transfer functions given in Table 3.1. Substitution of (3.12) into (3.11) yields

$$T(s) = \frac{10.01}{(0.45S+1)} [D_o(s)T_o(s) + D_G(s)T_G(s) + D_I(s)T_I(s) + D_w(s)I_w(s) + D_R(s)I_R(s) + D_F(s)I_F(s)] \quad (3.13)$$

Substituting D's from Table 3.1

$$T(s) = \frac{10.01}{(0.45S+1)} \left[\frac{0.0045T_o}{S(6.67S+1)} + \frac{10^{-6}T_G}{S(303S+1)^2} + \frac{0.02T_I}{S(0.714S+1)(0.028S+1)} + \frac{0.02I_w}{S(3.85S+1)} + \frac{0.005I_R}{S(6.25S+1)^3} + \frac{0.158(2S+1)I_F}{S(0.67S+1)}\right]$$

Or

$$T(s) = \frac{0.015T_0}{S(S+2.2222)(S+0.1499)} + \frac{2.4229 \times 10^{-10}T_G}{S(S+2.2222)(S+.0033)^2} + \frac{22.2533T_I}{S(S+2.2222)(S+1.4006)(S+35.7143)} + \frac{0.1155I_w}{S(S+2.2222)(S+0.2597)}$$

$$+ \frac{0.0005I_R}{S(S+2.2222)(S+0.16)^3} + \frac{10.4914(S+0.5)I_F}{S(S+2.2222)(S+1.4925)}$$

$$= \frac{0.015T_o}{S(S+2.2222)(S+0.1499)} + T_G[\frac{1 \times 10^{-5}}{S} - \frac{2.215 \times 10^{-11}}{(S+2.2222)}$$

$$- \frac{3.3090 \times 10^{-8}}{(S+0.0033)^2} - \frac{1 \times 10^{-5}}{(S+0.0033)}]^1 + T_I[\frac{0.1980}{S} + \frac{0.3638}{(S+2.2222)}$$

$$- \frac{0.5634}{(S+1.4006)} - \frac{54.2157 \times 10^{-5}}{(S+35.7143)}]^2 + I_w[\frac{0.1155}{S(S+2.2222)(S+0.2597)}]$$

$$+ I_R[\frac{5490 \times 10^{-5}}{S} + \frac{2.5650 \times 10^{-5}}{(S+2.2222)} - \frac{150 \times 10^{-5}}{(S+0.16)^3} - \frac{870 \times 10^{-5}}{(S+0.16)^2}$$

$$- \frac{5336 \times 10^{-5}}{(S+0.16)}]^3 + 10.4914I_F[\frac{(S+0.5)}{S(S+2.2222)(S+1.4925)}]$$

Therefore, taking the inverse Laplace transform:

$$T(t) = T_o[0.04503 - 0.04829e^{-0.1499t} + 0.00326e^{-2.2222t}] + T_G[10^{-5}$$

$$- 2.215 \times 10^{-11}e^{-2.2222t} - 3.3089 \times 10^{-8}te^{-0.0033t}$$

$$- 10^{-5}e^{-0.0033t}] + T_I[0.1980 + 0.3638e^{-2.2222t}$$

$$- 0.5634e^{-1.40006t} - 54.2157 \times 10^{-5}e^{-35.7143t}] + I_w[0.20014$$

$$- 0.22662e^{-0.2597t} + 0.02648e^{-2.2222t}] + I_R[5490 \times 10^{-5}$$

$$+ 2.565 \times 10^{-5}e^{-2.2222t} - 75 \times 10^{-5}t^2e^{-0.16t} - 870$$

$$\times 10^{-5}te^{-0.16t} - 5336 \times 10^{-5}e^{-0.16t}] + I_F[1.58163$$

---

[1] See Appendix B for partial fractions of coefficient of T_G.

[2] See Appendix C for partial fractions of coefficient of T_I.

[3] See Appendix D for partial fractions of coefficient if I_R.

$$+ 9.56104e^{-1.4925t} - 11.14268e^{-2.2222t}] \qquad (3.14)$$

Equation (3.14) can be solved for the inputs of T_o, T_G, T_I, I_w, I_R and I_F to get the responses of the occupied space at desired intervals of time t. The responses of the occupied space are calculated in the next section.

3.2.3 Dynamic responses of the analytical model

To determine the dynamic responses of the occupied space of Figure 3.10 from its analytical model described by equation (3.14), values of the input weather data are taken from Figure 3.11 for those periods of time when the HVAC system is off. These data include the adjustments for the dimensions of the zone and are shown in Tables 3.2 and 3.3. Variations in space temperatures ΔT are calculated at intervals of 0.10 hour each using equation (3.14) and weather inputs shown in Tables 3.2 and 3.3. Average values of increments in space temperature for one hour are used to predict the space temperature at the end of each hour. Predicted increments and space temperatures from the analytical model (equation 3.14) are shown in the last two columns of Tables 3.2 and 3.3. Plots of predicted space temperatures and actual outdoor air temperature are shown in Figures 3.12 and 3.13 assuming the heating and cooling system was not operational.

It is seen from Figure 3.12 that the analytical model predicts space temperatures to be higher than the outdoor air temperatures until about 4:30 PM. These predictions are compatible with the analog computer simulations of Magnussen (26) as plotted in Figure 3.11 where the heating system was predicted to be off and the outdoor air damper was predicted to be 100% open until 4:30 PM. In Figure 3.12, analytical model predicts the

Table 3.2. Input and output data for analytical model for a day when free cooling is possible

	Input weather data taken from Figure 3.11												Predicted outputs of analytical model	
Time	T_o °F	T_G °F	T_I °F	I_w B/hr	I_R B/hr	I_F B/hr	ΔT_o °F	ΔT_G °F	ΔT_I °F	ΔI_w B/hr	ΔI_R B/hr	ΔI_F B/hr	ΔT °F	T_{space} °F
10:00 AM	58	61	70	690	26041	0	0	0	0	+330	+5209	0		
11:00 AM	58	61	70	1020	31250	0	+4	+4	0	+210	+2081	0	+16.36	86.36
12:00 noon	62	65	70	1230	33333	0	+2	+2	0	+120	0	0	+8.75	95.11
1:00 PM	64	67	70	1350	33333	0	0	0	0	0	-5000	0	+3.39	98.50
2:00 PM	64	67	70	1350	28333	0	+2	+2	0	-120	-6667	0	-6.77	91.73
3:00 PM	66	69	70	1230	21666	0	0	0	0	-210	-833	0	-12.41	79.32
4:00 PM	66	69	70	1020	20833	0	-4	-4	0	-330	-10000	0	-7.05	72.27
5:00 PM	62	65	70	690	10833	0	-2	-2	0	-450	-10833	0	-22.85	49.42
6:00 PM	60	63	70	240	0	0	-	-	-	-	-	-	-	-

Table 3.3. Input and output data for analytical model for a day when free cooling is not possible

	Input weather data taken from Figure 3.11												Predicted outputs of analytical model	
Time	T_o °F	T_G °F	T_I °F	I_w B/hr	I_R B/hr	I_F B/hr	ΔT_o °F	ΔT_G °F	ΔT_I °F	ΔI_w B/hr	ΔI_R B/hr	ΔI_F B/hr	ΔT °F	T_{space} °F
10:00 AM	58	61	70	690	8333	0	0	0	0	+330	+8333	0	-	-
11:00 AM	58	61	70	1020	16666	0	+10	+10	0	+210	+10417	0	+20.90	90.60
12:00 noon	68	71	70	1230	27083	0	+2	+2	0	+120	-6250	0	+21.00	111.60
1:00 PM	70	73	70	1350	20833	0	+1	+1	0	0	+4167	0	-5.08	106.52
2:00 PM	71	74	70	1350	25000	0	+2	+2	0	-120	0	0	+5.64	112.16
3:00 PM	73	76	70	1230	25000	0	0	0	0	-210	-2084	0	-3.39	108.77
4:00 PM	73	76	70	1020	22916	0	-2	-2	0	-330	-8333	0	-8.75	100.02
5:00 PM	71	74	70	690	14583	0	-1	-1	0	-450	-8333	0	-20.60	79.42
6:00 PM	70	73	70	240	6250	0	-	-	-	-	-	-	-	-

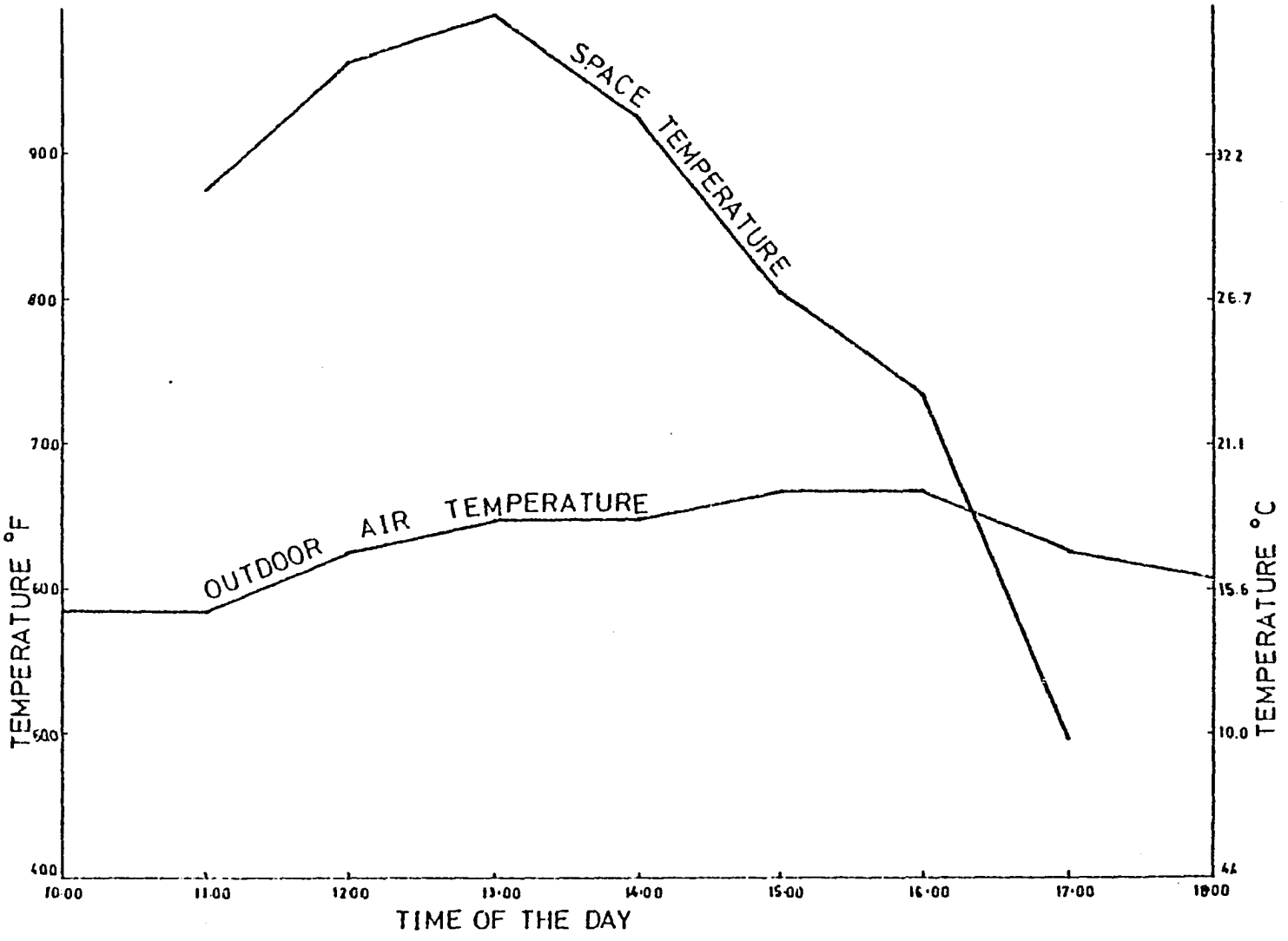

Figure 3.12. Analytically predicted space temperatures for the outdoor temperatures shown in Figure 3.11 for the first day.

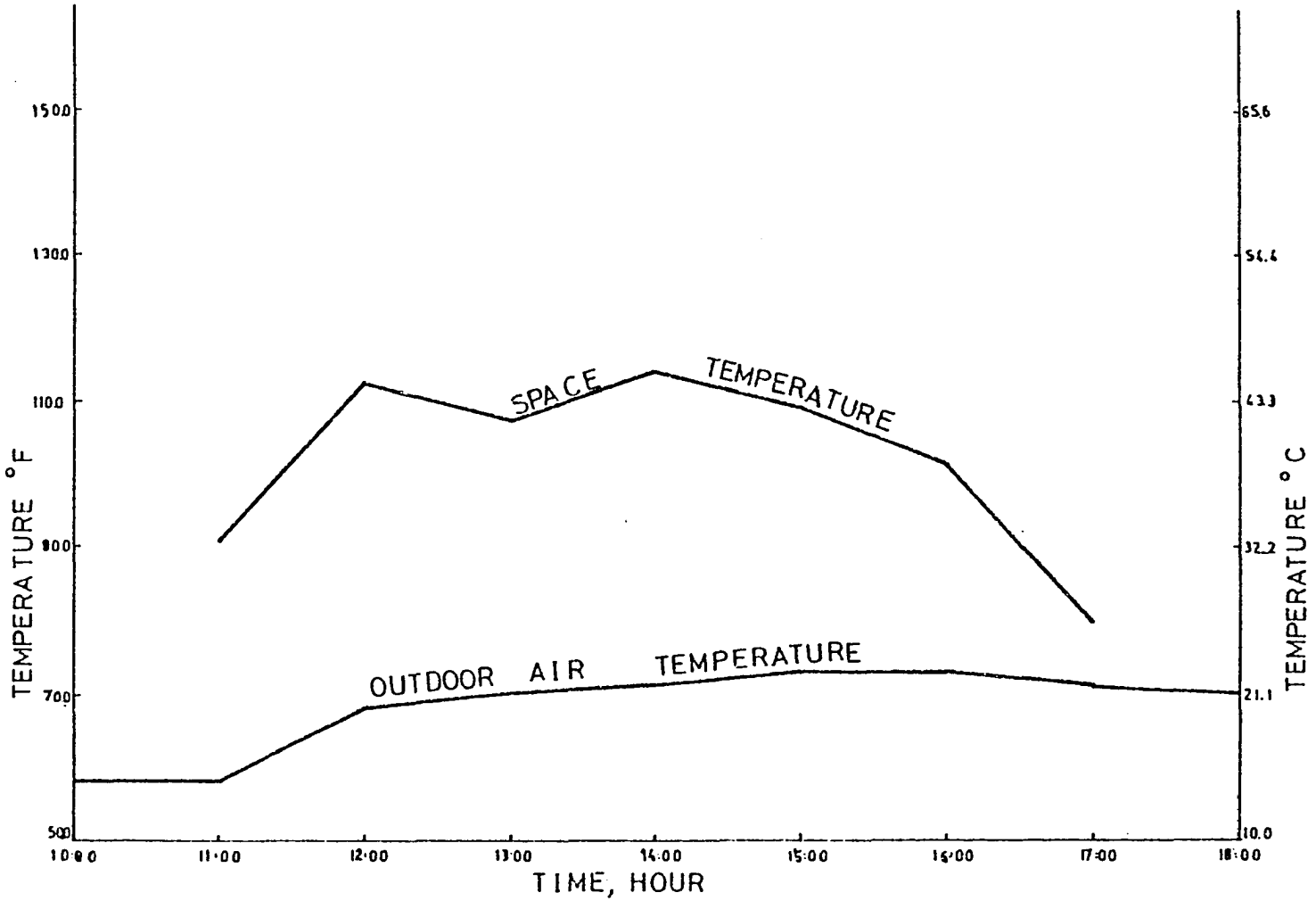

Figure 3.13. Analytically predicted space temperatures for the outdoor temperatures shown in Figure 3.11 for the third day.

space temperature to be higher than 21.1°C in between 11:00 AM and 4:00 PM whereas the outdoor air temperature during this period is lower than 21.1°C which can be used for free cooling and hence the outdoor air damper should be 100% open as predicted by Magnussen (26). Crossover point for the analytically predicted space temperature and the outdoor air temperature occurs at about 4:30 PM in Figure 3.12 which agrees with the predictions by Magnussen that at 4:30 PM the heat was turned on. It is seen from Figure 3.13 that the analytical model predicted space temperatures on the third day to be higher than the outdoor air temperatures throughout the day (11:00 AM to 5:00 PM). These predictions are again in agreement with the analog computer simulations of Magnussen (Figure 3.11) which predict the outdoor air damper to be in the minimum ventilation position and the cooling system in operation during this time. In Figure 3.13, it is seen that the space temperatures predicted from the analytical model during 11:00 AM to 5:00 PM are higher than 26.7°C whereas the outdoor air temperatures were higher than the desired indoor temperature (21.1°C). Hence outdoor could not be used for free cooling and the cooling plant was operating during this period as predicted by Magnussen (26).

The validation of analytical model which was derived from transfer functions of Table 3.1 (27) would have been more powerful, if measured data on floating temperatures of the space were available. Moreover, the development of an analytical model from the transfer functions revealed that for an environmental control system, this technique will lead to a very high order model leading to complex mathematical analysis (Appendix A). Therefore, for practical use, simple low order analytical models

should be developed and validated on the basis of actual measured data in a test facility.

3.3. Rational[1] Model from Energy Balance

The thermal processes involved in heating an occupied space exist in time and space and as such should be described in terms of dynamically distributed parameters. Mathematical models of these processes lead to partial differential equations involving time and space coordinates as independent variables. Exact simultaneous solutions of these equations under different boundary conditions make the model quite complex. Shaviv and Shaviv (99) have reported that computer time for one simulation run was approximately 4 hours for a typical house. This simulation was for four consecutive days and nights only. Moreover, it is clear from the analysis in Section 3.2 that a model of reduced complexity is needed for design analysis. To meet this need, a rational model of reduced complexity has been derived from energy and mass balance considerations (100). The thermal processes required to control the thermal environment within an occupied space of Figure 3.14 are shown in Figure 3.15. The following assumptions are made:

1. The properties of the thermal process involved in heating the occupied space are "lumped" at the location at which the occupants experience the controlled conditions. This assumption permits us to describe the process with ordinary linear differential equations instead of partial differential equations.

---

[1]The word "rational" is used to distinguish the analytical models from empirical models.

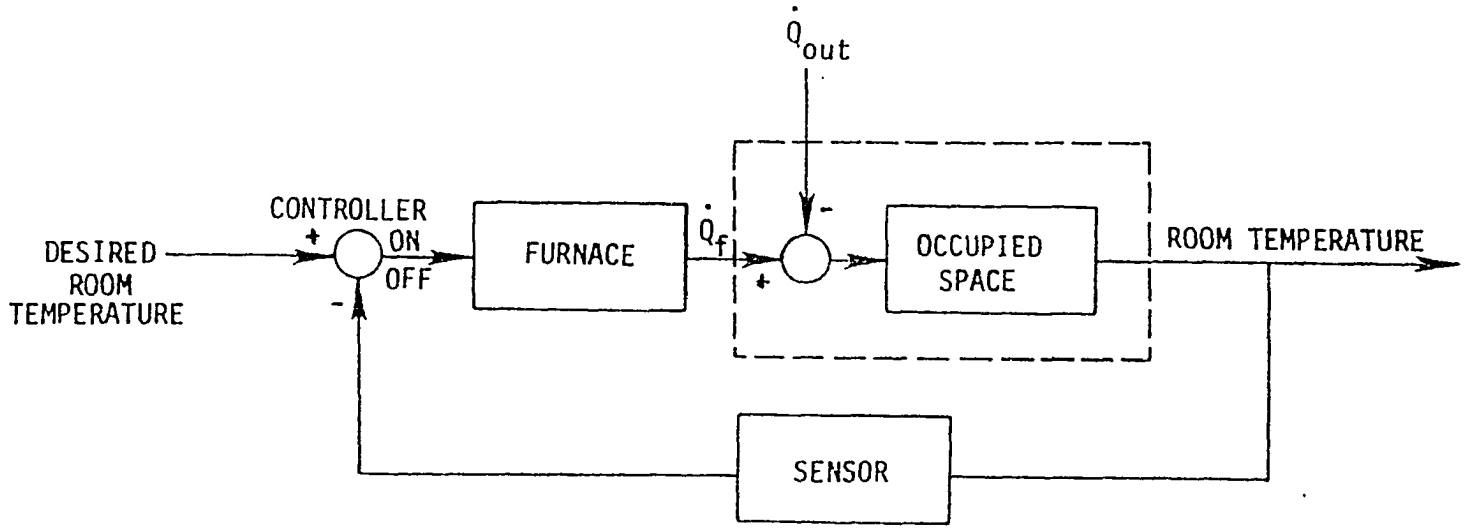

Figure 3.14. Block diagram for a two position residential heating system.

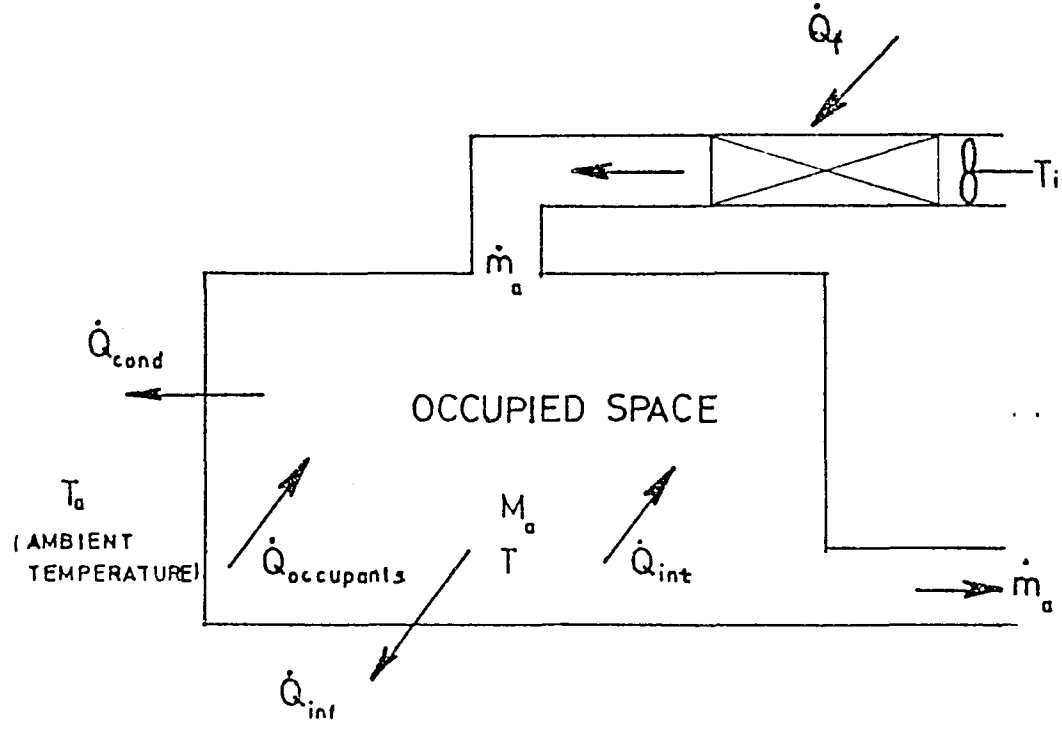

Figure 3.15. Thermal processes to describe heat transfers to an occupied space.

2. Storage effects of the structure are neglected due to their slow dynamic responses.
3. Changes in the stored energy of space air are assumed only due to changes in dry bulb temperatures and those due to humidity changes are considered negligible.
4. Heat transfer by radiation is not included in this analysis.
5. Uniform mixing of air in the occupied space is assumed.
6. Infiltration losses are assumed to be a function of supply air flow rate, occupant activity, internal heat sources, room temperature, and construction details in a given occupied space.

An energy balance on the occupied space of Figure 3.15 yields:

Rate of energy in = Rate of energy out + rate of change in stored energy

or

$$\dot{Q}_f + \dot{m}_a c_{pa} T_i + \dot{Q}_{occ} + \dot{Q}_{int} = \dot{m}_a c_{pa} T + \dot{Q}_{cond} + \dot{Q}_{inf} + M_a c_{pa} \frac{dT}{dt} \tag{3.15}$$

If we define

$$\dot{Q} = \dot{Q}_f + \dot{Q}_{occ} + \dot{Q}_{int} \tag{3.16}$$

and

$$\dot{Q}_{cond} = UA(T - T_a) \tag{3.17}$$

then we may rewrite equation (3.15) as

$$\frac{dT}{dt} = \frac{\dot{Q}}{M_a c_{pa}} + \frac{\dot{m}_a c_{pa}}{M_a c_{pa}} (T_i - T) - \frac{UA(T - T_a)}{M_a c_{pa}} - \frac{\dot{Q}_{inf}}{M_a c_{pa}} \tag{3.18}$$

For most applications, relatively small fluctuations in net heat gains and space temperature will be experienced within the occupied space. For this reason, only small perturbations about the operating or setpoint will be

considered. The operating point may be found by setting the time derivative contained in equation (3.18) to zero.

$$\frac{\bar{\dot{Q}}}{M_a c_{pa}} + \frac{\dot{m}_a c_{pa}}{M_a c_{pa}} (\bar{T}_i - \bar{T}) - \frac{UA(\bar{T} - \bar{T}_a)}{M_a c_{pa}} - \frac{\bar{\dot{Q}}_{inf}}{M_a c_{pa}} = 0 \tag{3.19}$$

Equations (3.18) and (3.19) may be combined to yield an equation in terms of perturbations about the operating point:

$$\frac{d(T-\bar{T})}{dt} = \frac{\dot{Q} - \bar{\dot{Q}}}{M_a c_{pa}} + \frac{\dot{m}_a c_{pa}}{M_a c_{pa}} [(T_i - \bar{T}_i) - (T - \bar{T})] - UA[(T - \bar{T}) - (T_a - \bar{T}_a)] - \frac{(\dot{Q}_{inf} - \bar{\dot{Q}}_{inf})}{M_a c_{pa}} \tag{3.20}$$

Equation (3.20) may be rewritten as

$$\frac{d\Delta T}{dt} = \frac{\Delta\dot{Q}}{M_a c_{pa}} + \frac{\dot{m}_a c_{pa}}{M_a c_{pa}} (\Delta T_i - \Delta T) - \frac{UA}{M_a c_{pa}} (\Delta T - \Delta T_a) - \frac{\Delta\dot{Q}_{inf}}{M_a c_{pa}} \tag{3.21}$$

From Assumption (4), we may write

$$\dot{Q}_{inf} = f(\dot{Q}, T) \tag{3.22}$$

Linearizing equation (3.22) about the operating point yields:

$$\Delta\dot{Q}_{inf} = K_1 \Delta\dot{Q} + K_2 \Delta T \tag{3.23}$$

The constants K_1 and K_2 are defined as follows and are evaluated at the operating point:

$$K_1 = \left.\frac{\partial\dot{Q}_{inf}}{\partial\dot{Q}}\right|_{T = \text{constant}} \tag{3.24}$$

$$K_2 = \left.\frac{\partial\dot{Q}_{inf}}{\partial T}\right|_{\dot{Q} = \text{constant}} \tag{3.25}$$

---

[1]Bar (-) notations indicate values at the operating point.

Substituting equation (3.23) into (3.21), taking the Laplace transform, and rearranging, we obtain for step inputs:

$$\Delta T(s) = \frac{K_{\dot{Q}} \Delta \dot{Q}(s)}{S(1 + \tau_{os}s)} + \frac{K_{T_i} \Delta T_i(s)}{S(1 + \tau_{os}s)} + \frac{K_{T_a} \Delta T_a(s)}{S(1 + \tau_{os}s)} \tag{3.26}$$

where

$$K_{\dot{Q}} = \frac{1 - K_1}{\dot{m}_a c_{pa} + UA + K_2} \tag{3.27}$$

$$K_{T_i} = \frac{\dot{m}_a c_{pa}}{\dot{m}_a c_{pa} + UA + K_2} \tag{3.28}$$

$$K_{T_a} = \frac{UA}{\dot{m}_a c_{pa} + UA + K_2} \tag{3.29}$$

$$\tau_{os} = \frac{M_a c_{pa}}{\dot{m}_a c_{pa} + UA + K_2} \tag{3.30}$$

A block diagram representation of equation (3.26) is shown in Figure 3.15. It may be noted that τ_{os}, the time constant of the occupied space, is a function of the enclosed mass of air, the mass flow rate of air, the envelope characteristics and infiltration. Equation (3.26) can be generalized to take into account more than one ambient temperature, as is the case with a floor or partition walls. Equation (3.26), represented by the block diagram of Figure 3.16, is in a form which can be coupled to the models of other elements in a control system to yield an overall transfer function for the building system. Once this overall transfer function is available for the building system, it should be possible to apply root locus, frequency response, sensitivity analysis, or other techniques of classical control theory to guide the designer of the system.

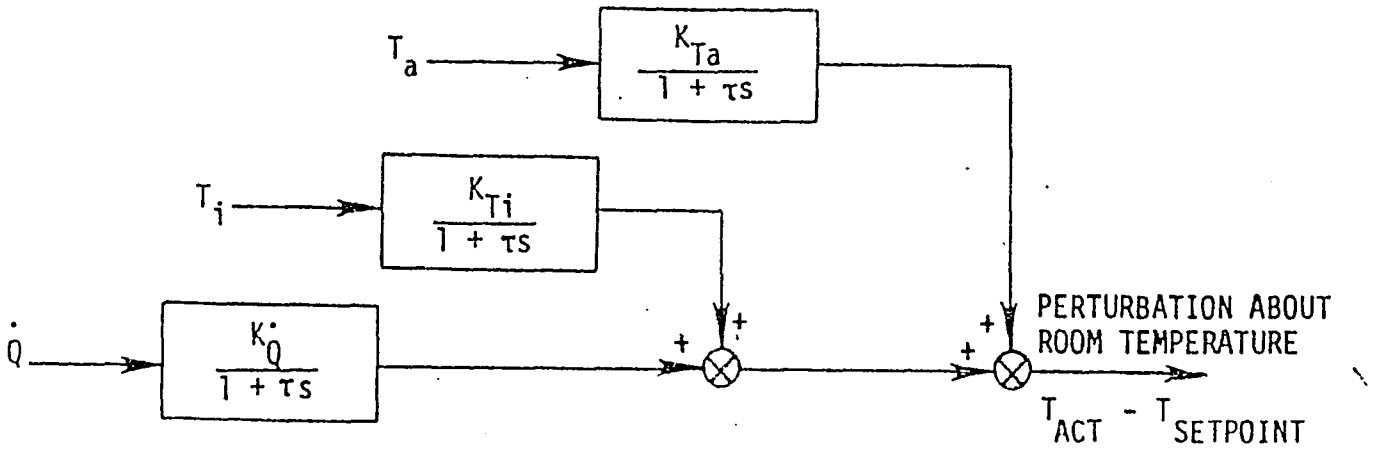

Figure 3.16. Block diagram presentation of mathematical model.

To conclude, the concepts of dynamic performance of a system as compared to the steady-state performance have been introduced in this chapter. Analytical models were derived for a commercial building from its transfer functions based on analog thermal circuits as reported in the literature. An open-loop model was used to predict dynamic performance of one zone in the commercial building and the results compared favorably with those of analog computer experiments found in the literature. A closed-loop model was derived from thermal analog circuits for one zone in a commercial building. The closed-loop model could not be applied to predict dynamics inside a zone of the commercial building firstly, because no closed-loop experimental data were available for the zone and secondly, because the model was too complex for analysis. Thus, a need to develop models of reduced complexity was identified. Recognizing this need a rational model of reduced complexity was derived from an energy balance on an occupied space.

4. MATHEMATICAL MODELS OF COMPONENTS FOR ENVIRONMENTAL CONTROL

The block diagram for the mathematical model of an occupied space, shown in Figure 3.15, can be coupled to mathematical models of other components for environmental control such as sensors, controllers, valves, actuators, heat exchangers and ducts. Mathematical models for these components will be developed in this chapter.

4.1 Terminology

Since many environmental control systems function as feedback control systems, terminology used in feedback control systems (101) is introduced in this section. Figure 4.1 shows a block-diagram representation of a feedback control system containing the basic elements. Terms shown in Figure 4.1 are defined in accordance with the ISA Standard (101).

4.1.1 Definitions: Variables in the system

The command (v) is the input which is established by some means external to and independent of the feedback control system.

The reference input (r) is derived from the command and is the actual signal input to the system.

The controlled variable (c) is the quantity that is directly measured and controlled. It is the output of the controlled system.

The primary feedback (b) is a signal which is a function of the controlled variable and which is compared with the reference input to obtain the actuating signal.

The actuating signal (e) is obtained from a comparison measuring device and is the reference input minus the primary feedback. This signal,

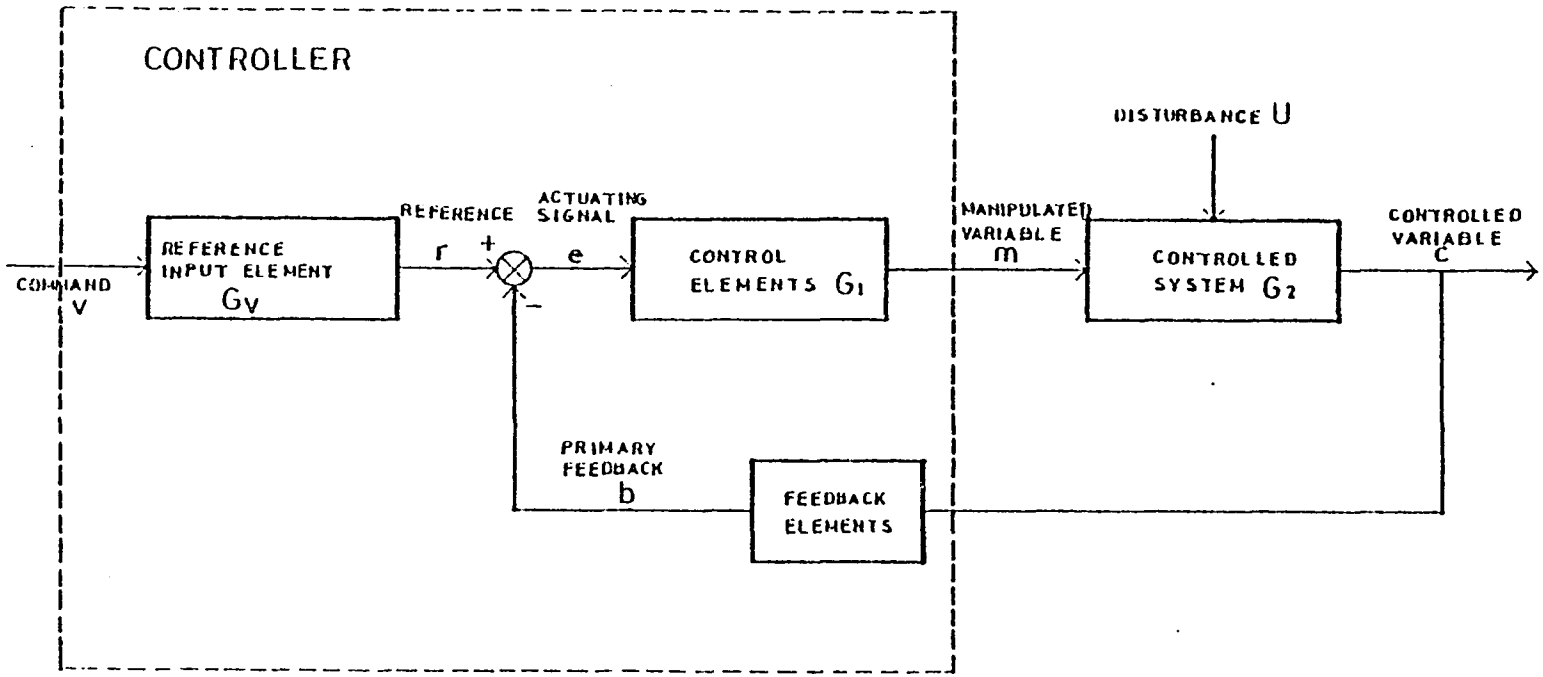

Figure 4.1. Block diagram of a feedback control system containing all basic elements.

usually at a low energy level, is the input to the control elements that produce the manipulated variable.

The manipulated variable (m) is that quantity obtained from the control elements which is applied to the controlled system. The manipulated variable is generally at a higher energy level than the actuating signal and may also be modified in form.

The disturbance (U) is the unwanted signal that tends to affect the controlled variable. The disturbance may be introduced into the system at many places.

4.1.2 Definitions: System components

The reference input elements (Gv) produce a signal proportional to the command.

The control elements (G_1) produce the manipulated variable from the actuating signal.[1]

The controlled system (G_2) is the device that is to be controlled. This is frequently a high-power element.[2]

The feedback elements (H) produce the primary feedback from the controlled variable. This is generally a proportionality device but may also modify the characteristics of the controlled variable.

---

[1] Control elements can include amplifiers, switches, actuators, valves, etc.

[2] A heat exchanger is an example of the controlled system.

4.2 Feedback Elements

In a control loop, the actions of the control are completely dependent on the static and dynamic responses of the sensor (feedback element). The ideal response of a sensor is a signal which is proportional to the controlled variable.

In the case of a thermal sensor, an element, at best, can only indicate its own temperature. This temperature is a function of the location of the sensor within the space, the thermal capacity of the sensor, and the surrounding heat transfer conditions.

4.2.1 Thermal sensor as a first order element

For a thermal sensing element at a uniform temperature, T_s, immersed in a fluid of temperature T, the internal energy of the sensor, Q_{int}, is a product of its mass, specific heat and temperature:

$$Q_{int} = (\frac{\pi d^2}{4} l\rho)cT_s \tag{4.1}$$

where the element is assumed to be cylindrical in shape and

d is the diameter

l is the length

ρ is the density

c is the specific heat

If T_s changes with time, the rate of change of stored energy is

$$\frac{\Delta Q_{int}}{t} = (\frac{\pi d^2}{4} l\rho)c \frac{dT_s}{dt} \tag{4.2}$$

From the law of conservation of energy, this change in stored energy must be equal to the amount of heat transferred to the surroundings

$$\frac{\Delta Q_{int}}{t} = h(\pi d)l(T - T_s) \tag{4.3}$$

where h is the heat transfer coefficient. Then combining (4.2) and (4.3)

$$(\frac{\pi d^2}{4} l\rho)c \frac{dT_s}{dt} = h(\pi d)l(T - T_s)$$

or

$$\frac{dT_s}{dt} = (\frac{4h}{\rho dc})(T - T_s) \tag{4.4}$$

Equation (4.4) is a first order differential equation and its solution gives the temperature of the sensor at time, t. An expression for the time constant of this sensor may be obtained by rearrangement of 4.4:

$$(\frac{\rho dc}{4h}) \frac{dT_s}{dt} + T_s = T$$

or

$$\tau_s \frac{dT_s}{dt} + T_s = T \tag{4.5}$$

where

$$\tau_s \text{ is the time constant} = \frac{\rho dc}{4h}^{1} \tag{4.6}$$

Taking Laplace Transform of equation (4.5)

$$\frac{T_s}{T} = \frac{1}{\tau_s s + 1} \tag{4.7}$$

For a small change in fluid temperature, ΔT, about an operating point, the change in the temperature of the sensor may be expressed as

---

[1]For any other shape where surface area is A, the time constant $\tau_s = \rho cV/hA$.

$$\frac{\Delta T_s}{\Delta T} = K_s(1 - e^{-t/\tau_s}) = H_s(s) \qquad (4.8)$$

Equation (4.8) expresses the transfer function of a sensor as a first approximation.

4.2.2 Factors affecting the response of thermal sensors

Temperature sensing elements such as expansion bulbs, thermocouples, and resistance elements possess appreciable lag because of the heat transfer characteristics of the surrounding medium and the heat capacity of the materials of construction. Thermal capacity of the sensor depends upon the mass and specific heat of the components. Heat is transferred to the thermal element by conduction, convection and radiation. Conduction is usually small compared to convection and radiation if the temperature of the sensor tends to be uniform.

A bare thermocouple or bare bulb installed in a rapidly moving fluid has almost first-order response. In this case, the element time constant can be calculated if all the material and fluid characteristics are known. The time constant was derived in equation (4.6) and expressed as $\rho cV/hA$. Therefore, a short time constant requires element characteristics of low mass, large surface area, and low specific heat.

The forced convection heat transfer coefficient can be calculated for a fluid flowing at right angles to a cylindrical thermal element.

$$Nu = n(Pr)^{0.3}(Re)^m \qquad (4.9)$$

where

Nu = Nusselt number = $h_c d/k_f$

h_c = convection coefficient

d = diameter of tube

k_f = thermal conductivity of fluid

m = a constant given below

n = a constant given below

Pr = Prandtl number = $c_f\mu/k_f$

C_f = specific heat of fluid

μ = absolute viscosity

ν = kinematic viscosity (μ/ρ_f)

ρ_f = fluid density

Re = Reynolds number ($V_f d/\nu$)

V_f = velocity of fluid

The constants in equation (4.9) depend upon Reynolds number as follows (102):

Re	n	m
40 - 4,000	0.68	0.47
4,000 - 40,000	0.19	0.62
40,000 - 400,000	0.026	0.80

The velocity of fluid flow V_f is a very important response factor. Equation (4.9) shows that the thermal-element time constant ($\tau_s = \rho dc/4h$) should vary inversely as the 0.62 power of velocity for Reynold Nos. 4,000 - 40,000.

The characteristics of the fluid surrounding the element are also important. Equation (4.9) indicates

$$h_c = \frac{k_f^{0.7} c_f^{0.3} \rho_f^{0.62}}{\mu^{0.32}} \qquad (4.10)$$

so that high thermal conductivity, high specific heat, high density, and

low viscosity of the fluid are necessary for fast response. For example, sensors immersed in air will have slow response than if immersed in water. In natural convection, the heat transfer coefficient will be governed by the expression $Nu=C(GrPr)^n$ and thus is influenced greatly by fluid properties.

For radiation heat trasnfer to a thermal element from a black body source, the heat flow q_r is given by (103)

$$q_r = \sigma\varepsilon A[(\frac{T_1}{100})^4 - (\frac{T_S}{100})^4] \tag{4.11}$$

where

σ = radiation constant

ε = emissivity of thermal element material

A = surface area of thermal element

T_1 = temperature of source

T_s = temperature of receiving element

This is a nonlinear equation and may be replaced by

$$q_r = h_r A(T_1 - T_s) \tag{4.12}$$

if the coefficient of radiation transfer h_r is defined by

$$h_r = \frac{1}{A}\frac{\partial q}{\partial T_1} = 4\sigma\varepsilon\theta^3 \tag{4.13}$$

where θ is the average of the source and element temperatures in deg R/100. When radiation is significant, the expression, h, in equations (4.3) through (4.6) must represent the combined heat transfer coefficient ($h_c + h_r$). The time constant for a thermal element responding to radiation heat transfer depends greatly upon the average operating temperature θ. As equation (4.13) indicates, the time constant should vary inversely as the

cube of the temperature. The emissivity of the thermal element material should also be large to decrease the time constant.

If the capillary tube connecting the sensor to the control elements is sufficiently long, heat transfers along the length of the tube can cause delay time and attenuation of the temperature. The mathematical model to predict the delay time and attenuation of temperature is developed in Section 4.7.1.

In an electric circuit consisting of a capacitance C and a resistance R, the time constant is RC. Similarly, in a thermal circuit, the time constant may be expressed as $R_f C_f$ where R_f is the thermal resistance to heat flow and C_f is the thermal capacity of the bulb of a thermal sensor.

From the expression for time constant

$$\tau_s = \frac{\rho c V}{hA} = \left(\frac{1}{hA}\right)(\rho c V) = R_f C_f \qquad (4.5)$$

where

$R_f = (1/hA)$

$C_f = \rho c V$

The variation in h has the most significant effect on the value of the time constant τ_s, since it is subject to the widest possible range of values, e.g., of the order of 5.68 $W/m^2°C$ for air, 56.78 $W/m^2°C$ for oil, up to 283.90 $W/m^2°C$ for water, and up to 5678.3 $W/m^2°C$ for boiling water. Thus, for the same sensor, the value of h, determined by heat transfer conditions between the sensor and the measured fluid, can cause τ_s to vary by a factor of 1,000.

4.2.3 Thermal sensor as a composite assembly

Dynamic responses of a sensor, when the sensor is a composite assembly of a well and a bulb (Figure 4.2), can be studied under the following two assumptions:

A. The capacitance of the well is small compared to that of the bulb.

B. The capacitance of the well is significant compared to that of the bulb.

If the capacitance of the well is small, the value of τ_s may be approximated by

$$\tau_s = (R_f + R_F)C_B$$

where

R_f is the thermal resistance between the fluid and well

R_F is the thermal resistance of the pocket between the well and the bulb

C_B is the thermal capacitance of the bulb

Therefore,

$$\tau_s = \left(\frac{1}{h\pi D_{well}} + \frac{\ln ID_{well}/D_{bulb}}{2\pi k_F}\right)\left(\frac{\pi D_{bulb}^2}{r}\right)c\rho \qquad (4.14)$$

where ID_{well} is the internal diameter of well and D_{bulb} is the diameter of the sensor.

As an example, if the bulb and the well are made of steel, and

$D_{bulb} = 0.0127$ m

$ID_{well} = 0.0190$ m

$OD_{well} = 0.0222$ m

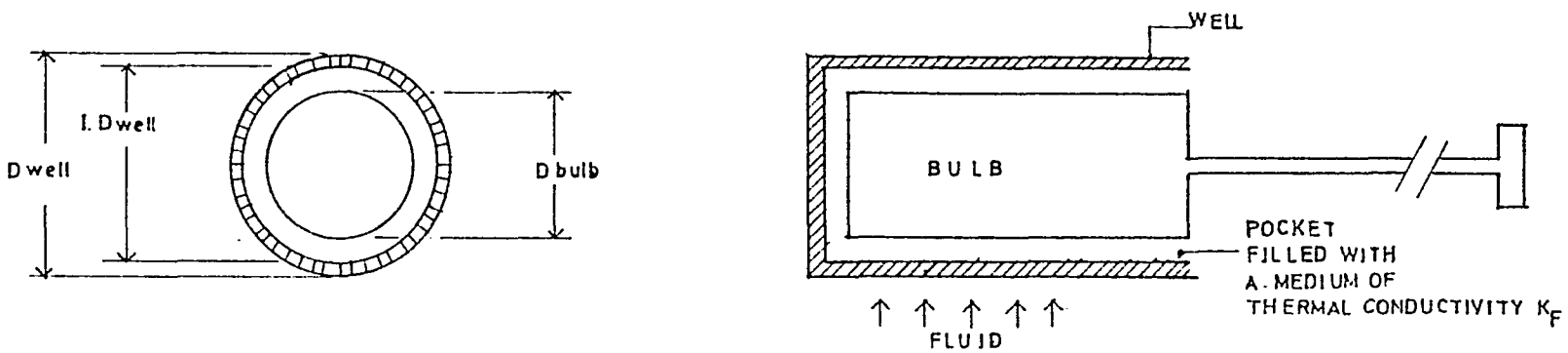

Figure 4.2. Thermal sensor as a composite assembly.

$h = 113.566\ W/m^2°C$

$c = 509.96\ J/Kg°C$

$\rho = 7848.79\ Kg/m^3$

For a sensor with the above data, the time constant is of the order of 21.84 minutes, 3.85 minutes, and 1 minute when the pocket is filled with air, oil or silicon jelly (G641, General Electric), respectively. So the resistance of the air space is the controlling resistance and must be reduced. A pocket filled with silicon jelly G641 represents a reduction of nearly 22 times in the value of the time constant, τ_s, when compared to the value of air in the pocket.

If the capacitance of the well is not negligible, the sensor can be modeled as a second order system (104).

$$\tau_w\tau_s \frac{d^2T_s}{dt^2} + (\tau_w + \tau_s) \frac{dT_s}{dt} + T_s = T \qquad (4.15)$$

where

τ_w = time constant of the well

τ_s = time constant of bulb (sensor)

T = temperature of fluid

A solution to equation (4.15) has been reported in reference (104)

$$\frac{T - T_s}{T - T_o} = \frac{\Delta T}{\Delta T_{max}} = \left(\frac{g}{g - 1}\right)e^{-t/g\tau_s} - \left(\frac{1}{g - 1}\right)e^{-t/\tau_s} \qquad (4.16)$$

where

ΔT = momentary difference between the indicated and actual temperatures

ΔT_{max} = difference between temperature of fluid and sensor temperature at t = 0

$$g = \tau_w/\tau_s$$

From equation (4.16), it can be seen that as the time constant of the well is increased, the overall lag is increased.

The time constant of the well depends upon the thermal capacity of the well and the thermal resistance between the fluid and the well. The time constant of the sensor depends upon the thermal capacity of the bulb and the thermal resistance of the pocket fluid. Therefore the sensor as a composite assembly will have a fast response when:

1. A close fit exists between the bulb and the well.
2. The pocket is filled with a fluid of high thermal conductivity.
3. The well material has a low specific heat.
4. The fluid flows past the well at high velocity.

4.3 Control Modes

A control element can provide the manipulated variable from the actuating signal in many modes. Mathematical models for the different control modes are developed in this section.

4.3.1 Two position control

Two-position control is a type of control action in which the manipulated variable is quickly changed to either a maximum or minimum value depending upon whether the controlled variable is greater or less than the set point. The minimum value of the manipulated variable is usually zero (off).

The equations for two-position control are

$m = M_1$ when $e > 0$

$$m = M_o \qquad \text{when } e < 0 \tag{4.17}$$

where

M_1 = maximum value of manipulated variable

M_0 = minimum value of manipulated variable

A differential or dead-band in two-position control causes the manipulated variable to maintain its previous value until the controlled variable has moved beyond the set point by a predetermined amount. In actual operation this action may be compared to hysteresis as shown in Figure 4.3.

A differential may be intentional as is common in domestic thermostats when employed for the purpose of preventing rapid operation of switches and solenoid valves and to enhance the life of the system.

Two position control is simple and inexpensive but it suffers from inherent drifts. Rapid changes of the controlled variable are possible with this type of control. Compared with other types of control actions, two position control can be more energy intensive. Some examples of applications of two position control include residential heating/cooling systems and roof top units in commercial buildings.

4.3.2 Proportional control

Proportional action is a type of control in which there is a continuous linear relation between values of the actuating signal and the manipulated variable. For purposes of flexibility, an adjustment of the control action is provided and is termed proportional sensitivity. Proportional control may be described as:

$$m = K_c e + M \tag{4.18}$$

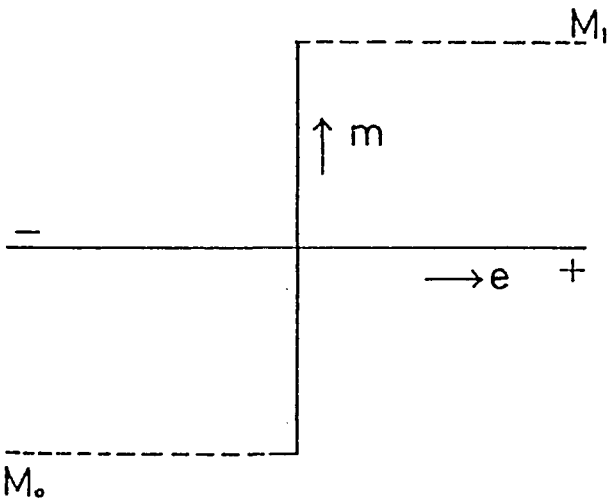

(a) Two position control action.

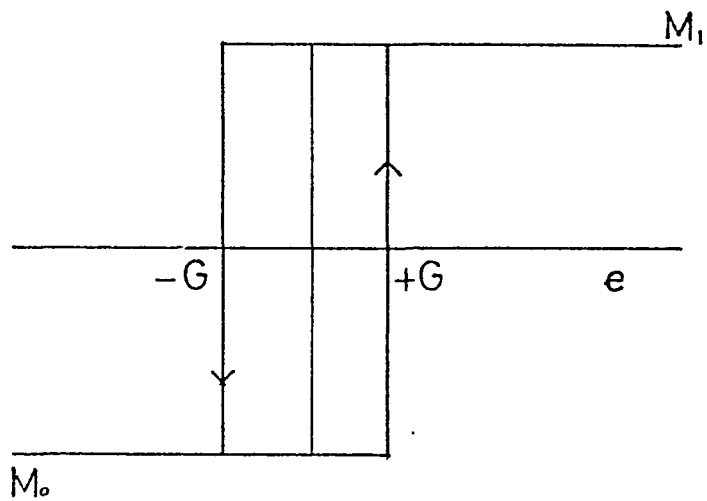

(b) Twc position control action with differential.

Figure 4.3. Two position control action.

where

K_c = proportional sensitivity

M = a constant

and other terms as defined previously.

The proportional sensitivity, K_c, is the change of output variable caused by a unit change of input variable.

The constant M in equation (4.18) may be termed as the calibration constant because the selection of a value for M determines the normal (zero actuating signal) value of the manipulated variable. The operation of proportional control action is illustrated in Figure 4.4.

For a unit step change in actuating signal

$$e = 0 \quad t < 0$$

$$e = E \quad t \geq 0 \tag{4.19}$$

where E is a constant; substituting in (4.18)

$$m - M = K_c E \tag{4.20}$$

The change in manipulated variable corresponds exactly to the change in deviation with a degree of amplification depending upon the setting of proportional sensitivity K_c. Thus, a proportional controller is simply an amplifier with adjustable gain.

Proportional control is more sensitive to the error signals compared to two position control and is capable of taking minor corrective actions. Proportion control is the least expensive out of continuous type controls but is more expensive compared to the two position control. Calibration procedures are more difficult for proportional control compared to the two

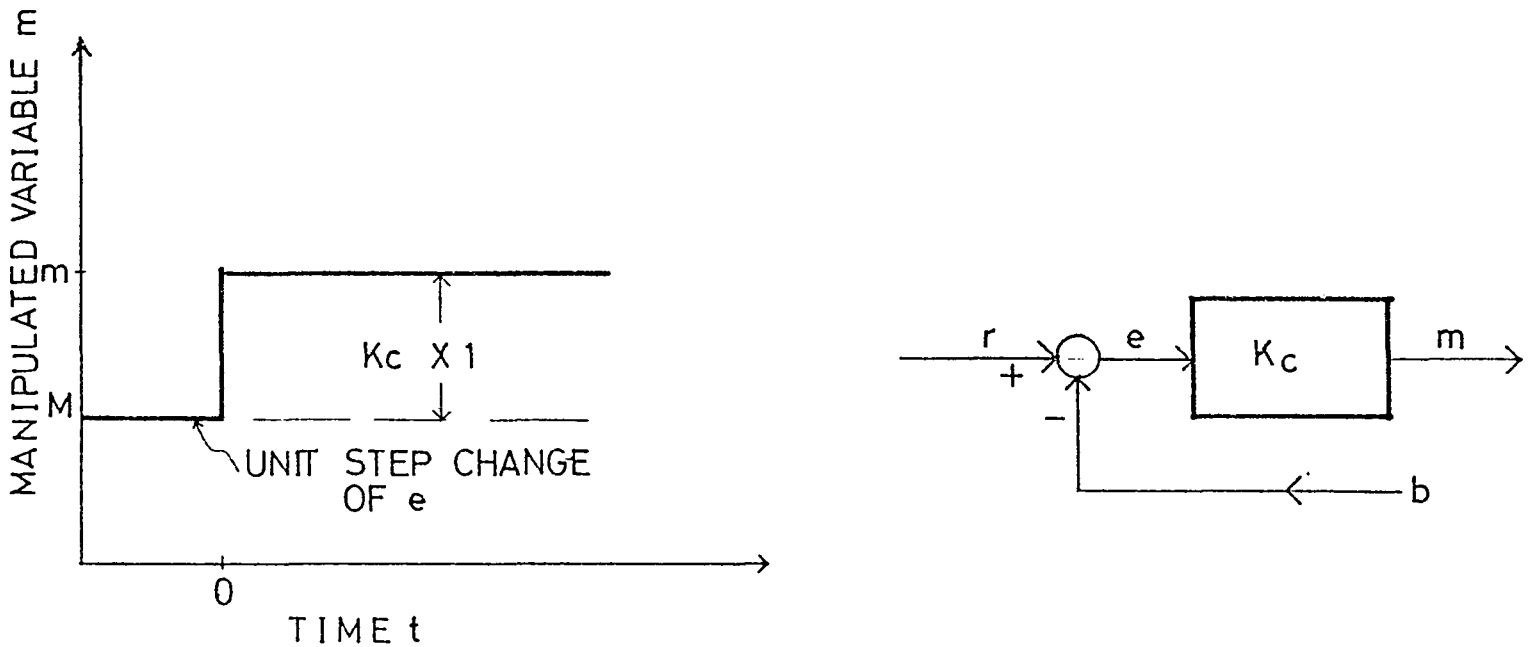

Figure 4.4. Proportional control action.

position control. Proportional control is used in air distribution systems, hydronic systems and in central systems for commercial buildings.

4.3.3 Integral control

Integral action is a type of control action in which the value of the manipulated variable m is changed at a rate proportional to the actuating signal. Thus, if the actuating signal is doubled over a previous value, the final control element is moved twice as fast. When the controlled variable is at the set point (zero actuating signal), the final control element remains stationary.

Mathematically integral control may be expressed as

$$\dot{m} = \frac{1}{t_{int}} e \tag{4.21}$$

or, in integrated form

$$m = \frac{1}{t_{int}} \int e \, dt + M \tag{4.22}$$

where

M = constant of integration

t_{int} = integral time (defined as the time of change of manipulated variable caused by a unit step change of e)

The operational form of the equation is

$$m = \frac{1}{t_{int} S} e \tag{4.23}$$

and is shown in Figure 4.5.

For a step change of actuating signal

$$e = 0 \qquad t < 0$$

$$e = E \qquad t \geq 0 \tag{4.24}$$

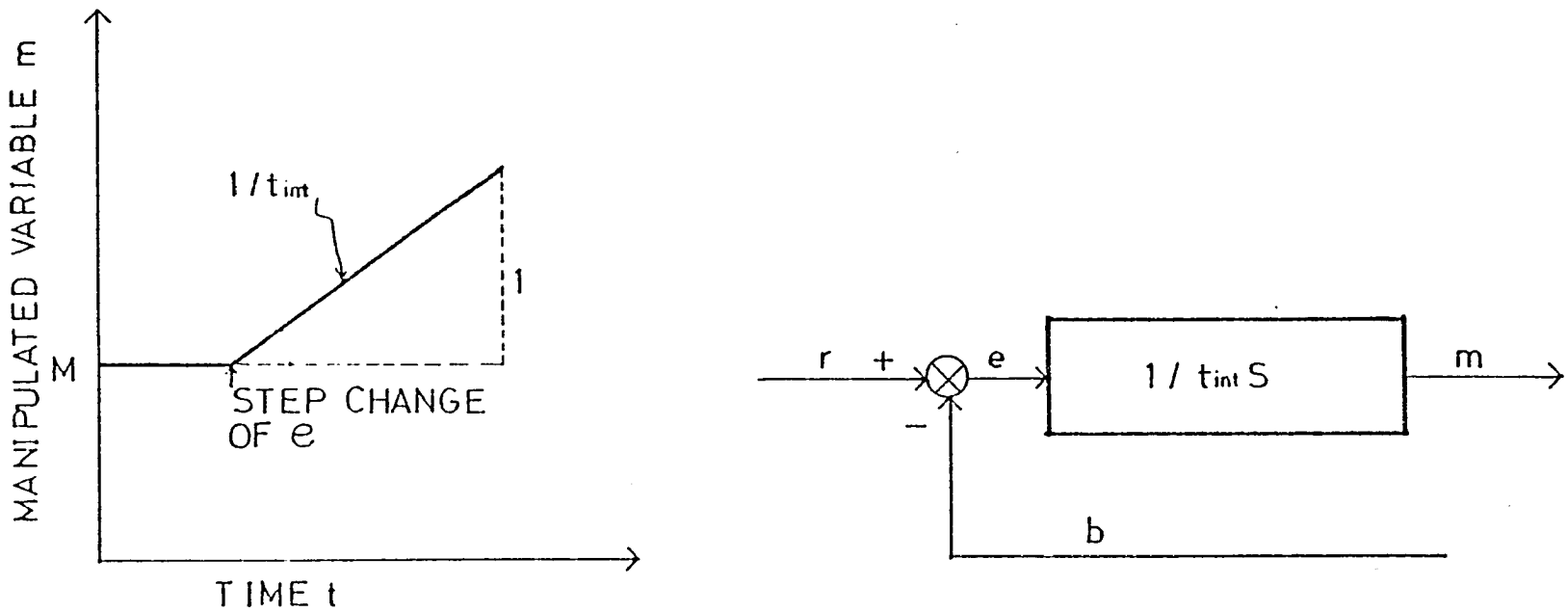

Figure 4.5. Operation of integral control action.

where E is a constant. Substituting in equation (4.22) and integrating

$$m - M = \frac{1}{t_{int}} Et \tag{4.25}$$

Thus, the manipulated variable changes linearly with time and "integrates" the area under the actuating signal function. For a unit step change of actuating signal (E = 1.0), the slope of the line is inverse of integral time (Figure 4.5).

Integral control has the advantage over proportional control that it tends to zero the offset, but it requires more expensive calibration procedures. Its maintenance is more difficult. Some applications of integral control include control of boilers, solar storage systems and meat processing plants.

4.3.4 Proportional-derivative control

Derivative control action may be defined as a control action in which the magnitude of the manipulated variable is proportional to the rate of change of actuating signal. This control mode has many synonyms such as "pre-set," "rate," "booster," and "anticipatory control" action. Derivative control response is always used in conjunction with the proportional mode. It is not satisfactory to use this response alone because of its inability to recognize a steady-state actuating signal.

Mathematically a proportional-derivative (PD) control action is defined by

$$m = \underbrace{K_c e}_{\text{proportional}} + \underbrace{K_c t_d \dot{e}}_{\text{derivative}} + M \tag{4.26}$$

where t_d = derivative time and other variables as described previously.

PD is the simple addition of proportional control and rate control action as shown by the operation equation

$$m = K_c(1 + t_d S)e$$

Proportional-derivative action is not adequately described by employing a step change of actuating signal because the time derivative of a step change is infinite at the time of change. Consequently, a linear (ramp) change of actuating signal must be used:

$$e = Et \tag{4.27}$$

where

E = a constant

t = time

Substituting equation (4.27) and its first time derivative into equation (4.26)

$$m - M = K_c E(t + t_d)$$

The actuating signal is defined at time t, whereas the manipulated variable is defined at $(t + t_d)$. The net effect is to shift the manipulated variable ahead by time t_d, the derivative time. As shown in Figure 4.6, the controller response leads the time change of actuating signal. Derivative time is defined as the amount of lead, expressed in units of time, that the control action is given. In other words, derivative time is the time interval by which the rate action advances the effect of proportional control action.

Proportional-derivative control has the advantage of a rapid response to the magnitude and to the rate of change in loads. However, PD control can become unstable easily because it has no zeroing capability. This

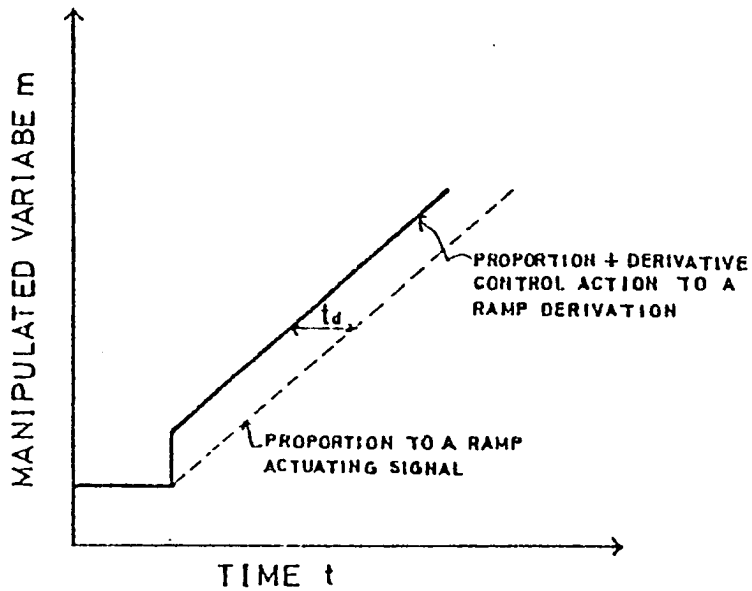

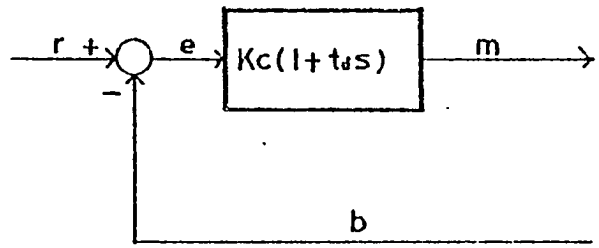

Figure 4.6. Proportional-derivative control action.

control is useful for controlling environments in buildings with large variations in occupancy.

4.3.5 Proportional-integral control

Integral control action is often combined additively with proportional control action. The combination is termed proportional-integral or proportional plus reset control and is used to obtain advantages of both control actions.

Proportional-integral control action is defined by the following differential equation

$$\frac{dm}{dt} = \frac{K_c}{t_{int}} e\Big|_{integral} + K_c \frac{de}{dt}\Big|_{proportional} \tag{4.28}$$

or, in integrated form

$$m = [\frac{K_c}{t_{int}} \int e\, dt]_{integral} + [K_c\, e + M]_{proportional} \tag{4.29}$$

where terms are as previously described. These equations illustrate the simple addition of proportional and integral control actions. In operational form:

$$m = K_c(\frac{1}{t_{int}S} + 1)\, e \tag{4.30}$$

where the system function $K_c/(t_{int}S)$ identifies the integral action and the system function K_c identifies the proportional action.

Proportional-integral (PI) control action has two adjustment parameters, the proportional sensitivity K_c and integral time t_{int}. The proportional sensitivity is defined the same as for the proportional control action. With the integral response turned off ($t_{int} \to \infty$), the proportional sensitivity is the number of units change in manipulated variable in

per unit change of actuating signal e. As clear from equation (4.30), the proportional sensitivity K_c affects both the proportional and integral parts of the action.

The integral action adjustment is achieved through integral time. For a step change of actuating signal e, the integral time, t_{int}, is the time required to add an increment of response equal to original step change of response as shown in Figure 4.7. Another term used with this type of control is reset rate, defined as the number of times per minute that the proportional part of response is replicated. Reset rate is therefore called "repeats per minute" and is the inverse of integral time.

For a step change of deviation

$$e = 0 \qquad t < 0$$

$$e = E \qquad t \geq 0 \tag{4.31}$$

Substituting in equation (4.28)

$$m - M = K_c E\left(\frac{t}{t_{int}} + 1\right) \tag{4.32}$$

This is the equation for a straight line. The first term, t/t_{int}, is the integral response, and the second term is the proportional response. The latter is indicated by dotted line of Figure 4.7.

PI control has the advantage that it can compensate for changes in input in addition to compensating the deviations in the controlled variable. High cost of maintenance is a disadvantage with this type of control.

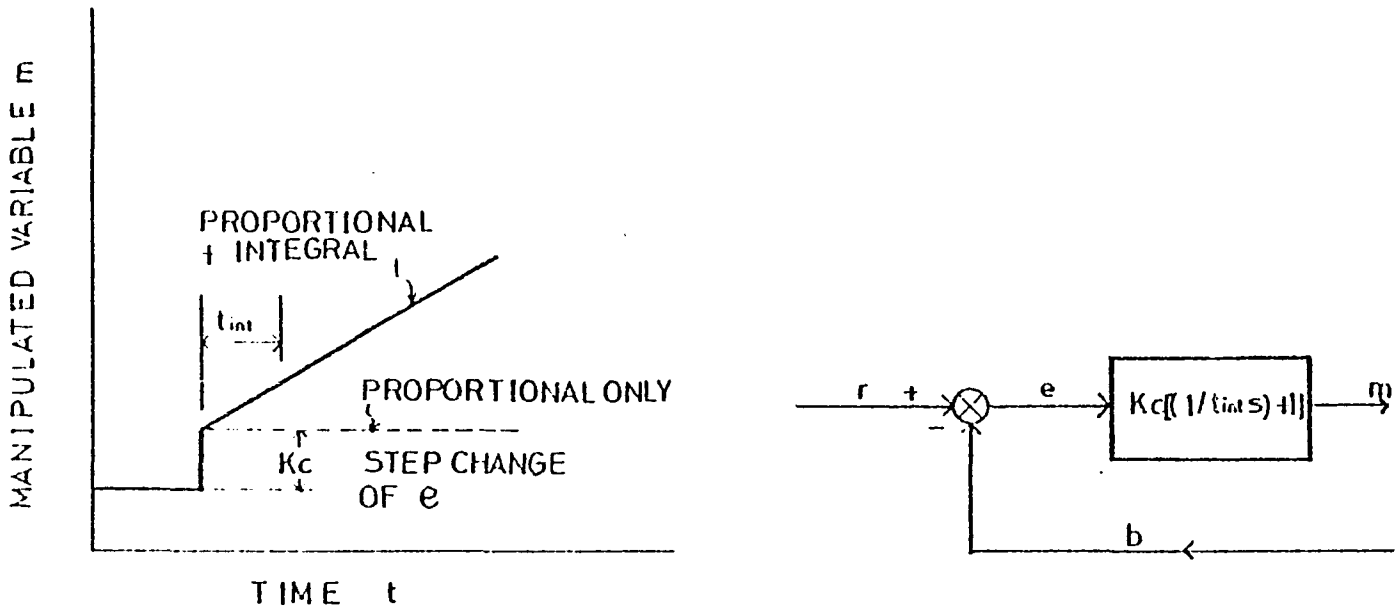

Figure 4.7. Operation of proportional-integral control.

4.3.6 Proportional-integral-derivative control

The additive combination of proportional action, integral action, and derivative action is termed proportional-integral-derivative action. It is described by the differential equation

$$\dot{m} = \frac{K_c}{t_{int}} e \Big|_{\text{integral}} + K_c \dot{e} \Big|_{\text{proportional}} + K_c t_d \ddot{e} \Big|_{\text{derivative}} \tag{4.33}$$

or

$$m = \frac{K_c}{t_{int}} \int e \, dt \Big|_{\text{integral}} + K_c e + M \Big|_{\text{proportional}} + K_c t_d \dot{e} \Big|_{\text{derivative}} \tag{4.34}$$

The operational equation is

$$m = K_c \left(\frac{1}{St_{int}} + 1 + t_d S\right) e \tag{4.35}$$

Proportional-integral-derivative (PID) control action is illustrated in Figure 4.8 in which the change of manipulated variable is shown for a ramp function of the actuating signal.

$$e = Et \tag{4.36}$$

Substituting this ramp function and its time derivative into equation (4.34):

$$m - M = K_c E \left(\frac{1}{t_{int}} \int t \, dt + t + t_d\right) \tag{4.37}$$

Integrating the first term

$$m - M = K_c E \left(\frac{t^2}{2t_{int}} + t + t_d\right) \tag{4.38}$$

The proportional part of the control action repeats the change of actuating signal (lower straight line) in Figure 4.8. The derivative part of

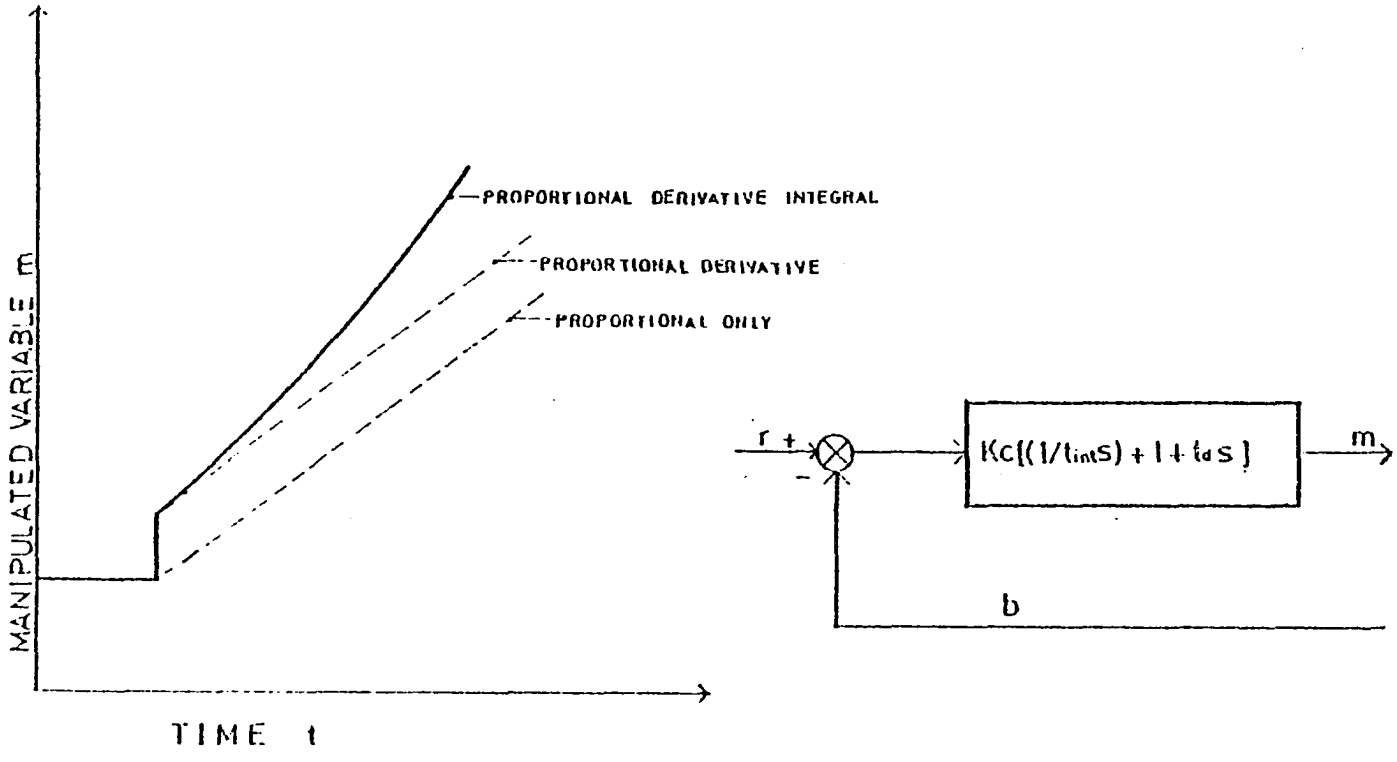

Figure 4.8. Operation of proportional-integral-derivative control.

the control action adds an increment of manipulated variable proportional to the area under the deviation line and as Figure 4.8 shows, the increment increases because the area increases at an increasing rate. The combination of proportional, integral, and derivative actions may be made in any sequence, because these actions are described by linear differential equations.

PID control action has many advantages. It can compensate for magnitude and rate of change in input. It zeroes the deviation in controlled variable and is the most energy efficient. However, it is the most expensive of all the controls and is difficult to calibrate. It is very hard to help PID control stable and requires frequent calibration checks. PID control is applied in environmental control chambers for scientific research, and in variable air volumne HVAC systems.

4.4 Actuators

An actuator is a device which converts the output of a control element into an input signal for the final control elements such as valves and dampers. In many cases an actuator incorporates an amplifier. The actuator must provide an accurate output position proportional to the input signal in spite of various forces acting on the output member. The most important forces are:

1. Inertia forces caused by the mass of moving parts.
2. Static friction forces during impending motion of two adjacent surfaces.
3. Thrust forces caused by weight and unbalanced fluid pressure.

Thus the actuator is often required to employ a power-amplifiying mechanism. The actuator may be powered by electric, pneumatic or hydraulic means.

4.4.1 Electrical actuators

Electrical actuators are commonly used in HVAC systems to control air flow. Mehta (105) has reported a mathematical model for an electrical actuator which can be used as a damper motor. Kirchhoff's laws were applied to model the electric motor. The shaft assembly was modeled as a mass and damper. The model reported can be expressed as

$$\frac{\Delta y(s)}{\Delta E(s)} = \frac{\pi BdN}{R(\tau_{mot}S + 1)(M_1S^2 + B_1S)} \tag{4.39}$$

where

Δy is the change in output (displacement)

ΔE is the change in input (voltage)

B is the flux density of the field of motor

d is the diameter of the moving motor coil

N is the number of turns in the motor coil

R is the resistance of the motor coil

τ_{motor} is the time constant for the motor

M_1 is the mass of the shaft

B_1 is the effective damping

4.4.2 Pneumatic actuators

A pneumatic actuator may be modeled as a spring-mass-damper combination. Forces applied to include the hysteresis and flow force on the item. The relation between the output (displacement) and the input (pressure) may be expressed as (106)

$$\frac{\Delta y(s)}{\Delta P(s)} = \frac{A}{(M_{act}S^2 + B_{act}S + K_{act})} + \frac{\Delta F_F(s) + \Delta F_H(s)}{\Delta P(s)(M_{act}S^2 + B_{act}S + K_{act})} \tag{4.40}$$

The second term on the right hand side of equation (4.40) adds a non-linear term and equation (4.40) can be used to describe the performance of the actuator for small changes in variables about an operating point. Details of symbols used in equation (4.40) are as follows:

Δy = small change in output (displacement)

ΔP = small change in input signal (pressure)

A = area of piston

M_{act} = mass of moving members

B_{act} = effective damping

K_{act} = effective spring action

ΔF_F = small change in frictional forces

ΔF_H = small change in hysteresis forces

4.4.3 Hydraulic actuators

Hydraulic actuators are used only when large power levels are needed. Mehta (105) has derived a mathematical model for an hydraulic actuator from pressure flow relations and force balance considerations. His model is reproduced below

$$\frac{\Delta C(s)}{\Delta Z(s)} = \frac{K_a S + K_b}{M_{act}K_c K_d S^4 + (K_c K_d B_{act} - M_{act}K_e K_d - K_f K_c M_{act})S^3}$$

$$+ (K_g + K_e K_d M_{act} - K_e K_d B_{act})S^2 + (K_e K_d B_{act} - K_h)S \tag{4.41}$$

The performance of the hydraulic actuator is also described by a nonlinear model and equation (4.41) is a linearized form valid for small changes about an operating point. Symbols used in equation (4.41) are as follows:

ΔC = small change in output (displacement)

ΔZ = small change in input (displacement from pre-amplifier)

M_{act} = mass of moving parts

B_{act} = effective damping

K = constants involving the physical dimensions of various parts

4.5 Final Control Elements

Final control elements convert the outputs of actuators (displacement) to manipulated variables, e.g., flow of a fluid. A control engineer has a variety of arrangements and characteristics of these devices from which to choose, with the choice dependent upon such items as fluctuations in pressure drop across the valve, the accuracy with which the device can be sized and the process characteristics. So the mathematical model for the control device will vary from one application to the other. As valves and dampers are the primary types of final control elements found in HVAC systems, basic characteristics of fluid flow through these devices are given here:

$$\dot{m}_w = C_d A\sqrt{2g(h_1 - h_2)} \tag{4.42}$$

where

$\dot{m}_f$ = fluid flow rate

C_d = coefficient of discharge

A = area open to flow

h_1 = upstream static head of flowing fluid

h_2 = downstream static head of flowing fluid

The area of port opening of the final control element will be assumed proportional to stem position so that

$$C_d A = K\Delta C \tag{4.43}$$

where

K = an overall coefficient

ΔC = change in stem portion or lift

Combining equations (4.42) and (4.43)

$$\Delta \dot{m}_w = [K\sqrt{2g(h_1 - h_2)}]\Delta C \tag{4.44}$$

This equation illustrates that the change in fluid flow rate $\Delta \dot{m}_f$ through the final control element, i.e., valve, is directly proportional to lift ΔC if (1) the differential head $(h_1 - h_2)$ is constant and (2) the overall coefficient K is constant. In practice these two conditions rarely prevail and it is necessary to modify the mathematical model for the control valve expressed by equation (4.44) according to the prevailing conditions.

These conditions should include the effect of series resistance which may result from the pipe line or duct work, orifices, hand valves, heat exchangers, or other equipment installed in series with the final element. For example, in practice the valve exists in a pipe line whose pressure drop varies with the flow according to the Darcy-Weisbach equation

$$h_L = F \frac{L}{D} \frac{v^2}{2g} \tag{4.45}$$

where

h_L = head loss of flowing fluid

F = friction coefficient (from Moody diagram)

L = equivalent length of pipe

D = inside diameter of pipe line

v = velocity of flow

The head loss therefore depends upon flow rate. Equation (4.45) may be written in terms of flow rate

$$\frac{hL}{L} = \frac{8}{\pi 2} \frac{F\dot{m}_f^2}{gD^5} \tag{4.46}$$

Modifying equation (4.44) due to pipe resistance

$$\Delta\dot{m}_w = [K\sqrt{2g(H_0 - H_2 - \Delta h_L)}]\Delta C \tag{4.47}$$

Equation (4.47) gives the modified mathematical model for a final control element which includes the head loss due to pipe or duct resistance.

Similarly, modifications to K in equation (4.44), depending upon the relationship between A and ΔC, should be incorporated. Relationship between A and ΔC will depend upon the type of valve (quick opening linear or equal percentage). These flow characteristics are often supplied by the manufacturers.

4.6 Controlled Devices

Over the past several years much work has been done on the dynamics of heat exchangers (31-37,39,41-43). These papers set forth a very complex method of analysis. Recently, a simple relationship for the dynamics of heat exchangers has been pursued (38,40,29). A simple model which

describes the dynamics of a heat exchanger is reported here which follows the development in reference (29).

The heat exchanger is modeled as a simple tube in crossflow (Figure 4.9). The coil tube is envisioned to be a block of metal (copper tube plus aluminum fins) that has a uniform temperature throughout, although this temperature changes with respect to time. The following symbols apply to the model:

t_{ai} = temperature of inlet air

t_{ao} = temperature of outlet air

t_{wi} = temperature of inlet water

t_{wo} = temperature of outlet water

t_w = mean water temperature $t_{wi} + t_w/2$

t_{ci} = temperature of coil at water inlet

t_{co} = temperature of coil at water outlet

t_c = mean temperature of coil = $t_{ci} + t_{co}/2$

$\dot{m}_w$ = flow rate of water

$\dot{m}_a$ = flow rate of air

C_{pw} = specific heat of water

C_{pa} = specific heat of air

Further specifications of the dynamic model of the coil includes the proposal that the rate of heat transfer from the water to the coil can be represented by the equation

$$\dot{Q}_{w-c} = A_w h_w (t_w - t_c) \tag{4.48}$$

where

$\dot{Q}_{w-c}$ = rate of heat transfer between water and coil

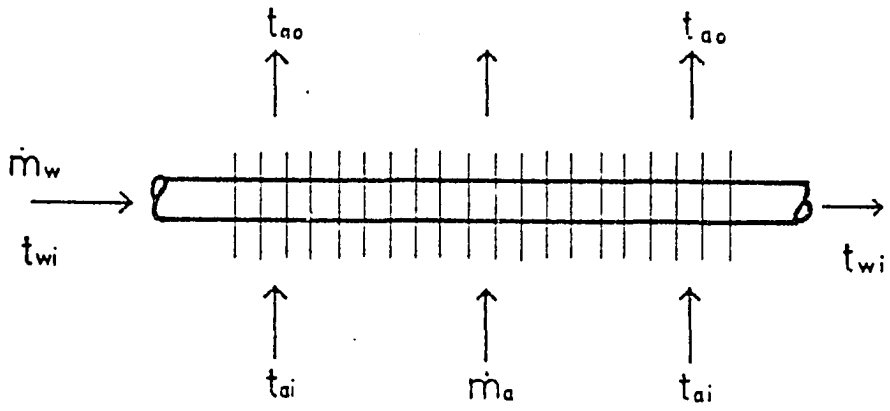

Figure 4.9. Model of a coil as a single tube in crossflow.

A_w = water side heat transfer area of coil

h_w = water side heat transfer coefficient

The potential for heat transfer assumed in equation (4.48) is the difference of the mean water temperature and the mean coil temperature. The equation for the heat-transfer rate from the coil to the air is

$$\dot{Q}_{c-a} = A_a h_a [t_c - (t_{ai} + t_{ao})/2] \tag{4.49}$$

where

$\dot{Q}_{c-a}$ = rate of heat transfer from the coil to the air

A_a = air side heat transfer area of coil

h_a = air ride heat transfer coefficient

The final three equations are energy balances on air, water, and coil, respectively.

Air: $$\dot{Q}_{c-a} = \dot{m}_a C_{pa}(t_{ao} - t_{ai}) \tag{4.50}$$

Water: $$\dot{m}_w C_{pw}(t_{wi} - t_{wo}) = \dot{Q}_{w-c} + M_w C_{pw} \frac{dt_w}{dt} \tag{4.51}$$

where

M_w = mass of water in coil

t = time

Coil: $$\dot{Q}_{w-c} - \dot{Q}_{c-a} = M_c C_c \frac{dt_c}{dt} \tag{4.52}$$

where

$M_c C_c$ = thermal capacity of coil

Substituting for $\dot{Q}_{w-c}$ and $\dot{Q}_{c-a}$ from equations (4.48) and (4.49) into equations (4.50), (4.51) and (4.52):

$$A_a h_a [t_c - (t_{ai} + t_{ao})/2] = \dot{m}_a C_{pa}(t_{ao} - t_{ai}) \tag{4.53}$$

$$\dot{m}_w C_{pw}(t_{wi} - t_{wo}) = A_w h_w (t_w - t_c) + M_w C_{pw} \frac{dt_w}{dt} \tag{4.54}$$

$$A_w h_w (t_w - t_c) - A_a h_a [t_c - (t_a + t_{ao})/2] = M_c C_c \frac{dt_c}{dt} \qquad (4.55)$$

Simultaneous solution of equations (4.53), (4.54) and (4.55) describes the dynamics of the heat exchanger.

Values of heat transfer coefficients in these equations (4.53-4.55) will be functions of the operating point. Moreover, it would seem necessary to specify whether A_a is prime or extended surface and also to incorporate the effect of fin efficiency. Information on products of heat transfer coefficients and areas of the coil at various operating points can be obtained experimentally by plotting Wilson's plots (107) for the coil. Once this information is available changes in air temperature at the outlet due to changes in water flow rate can be calculated from equations (4.53-4.55). Experimental studies reported in reference (29) show that the dynamics of a heat exchanger can be described by a first order system and the transfer function can be expressed as:

$$G_H(s) = \frac{K_H}{(1 + \tau_H S)} \qquad (4.56)$$

4.7 Distribution Components

Components used to transport fluids such as ducts, pipes, fans and pumps are modeled in this section.

4.7.1 Ducts and pipes

Ducts and pipes carrying fluids may be modeled as shown in Figure 4.10. Taking an energy balance for a control volume of the conduit of unit length with constant and uniform air temperature surrounding it (40), it can be written:

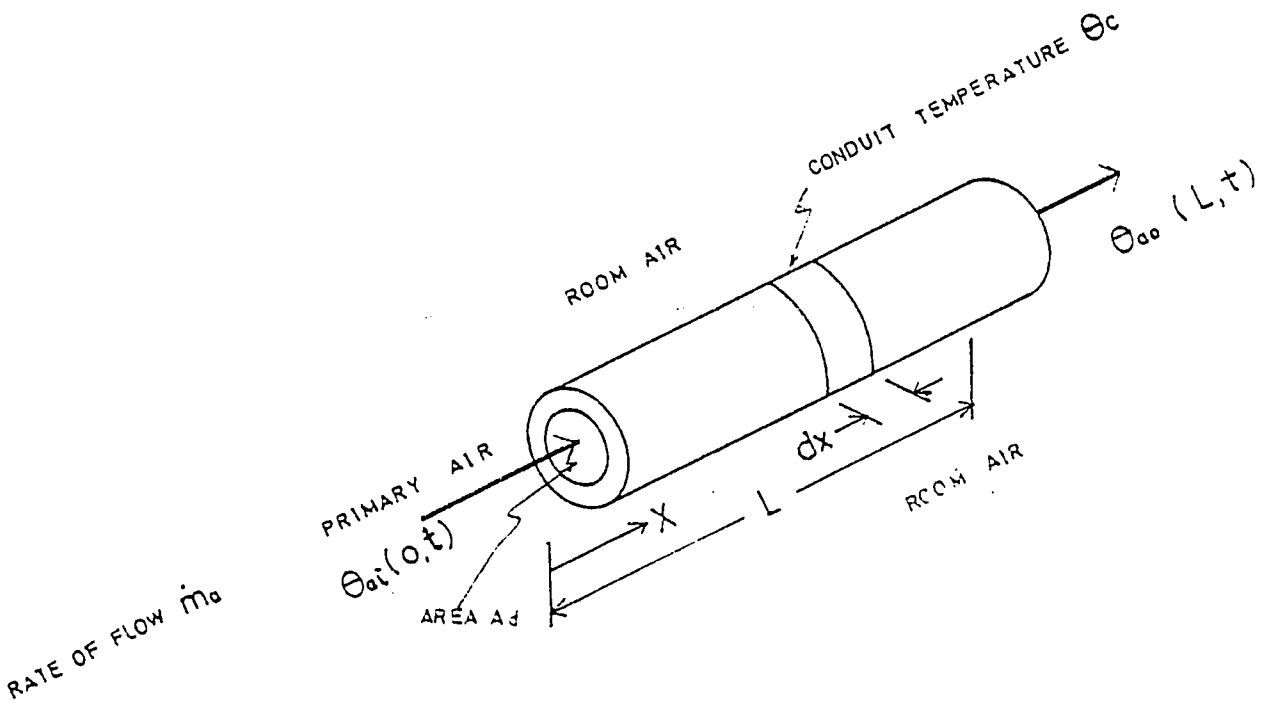

Figure 4.10. Model of a duct.

$$\rho_a A_c C_{pa} \frac{\partial \theta_a}{\partial t} + \dot{m}_a C_{pa} \frac{\partial \theta_a}{\partial x} + h_i(\theta_a - \theta_c) = 0 \tag{4.57}$$

$$w_c C_c \frac{\partial \theta_c}{\partial t} + h_o \theta_c - h_i \theta_a = 0 \tag{4.58}$$

where

ρ_a = density of supply air

A_c = area of cross section of conduit

C_{pa} = specific heat of supply air

θ_a = temperature of supply air above ambient

t = time

$\dot{m}_a$ = mass rate flow of supply air

h_i = conduit inside heat transfer coefficient

h_o = conduit outside heat transfer coefficient

θ_c = temperature of conduit above ambient

w_c = weight of conduit per unit length

C_c = specific heat of conduit material

Performance of interest is the response of temperature at any place in the conduit to changes of inlet temperature. The transfer function can be derived by taking Laplace Transform and solving for

$$G_D(s) = \frac{\theta_{ao}(s)}{\theta_{ai}(s)} = e(-\alpha L s) e(-\beta L) e(-\alpha L(\frac{\tau_c S}{\tau_c S+1}) \tag{4.59}$$

where

$\alpha = \rho_a A_c / \dot{m}_a$

$\beta = h_o h_i / [\dot{m}_a C_{pa}(h_o+h_i)]$

$\tau_c = W_c C_c / (h_0+h_i)$

L = length of duct

The first exponential term is the delay time, the second is the attenuation of the air temperature due to transfer of heat to the duct, and the third exponential function is a phase shift and attenuation due to transfer of heat from duct to the surrounding air. For short ducts as in residences, unity gain with zero delay and zero phase shift may be assumed (51).

4.7.2 Fans and pumps

Only a part of the electrical energy used by the motor of the fan (pump) is converted to useful shaft work and the rest of it is dissipated in the form of heat in the drive system. The efficiency of an electrical motor (η) used in a fan (pump) may be defined as the ratio of the energy delivered to the shaft to the total electrical energy input to the motor. The efficiency of the fan (pump), η_f, may be defined as the ratio of the energy imparted to the fluid to the energy delivered to the shaft. The energy imparted to the fluid is used in the following ways:

a. To impart kinetic energy to the fluid.

b. To increase static pressure.

c. To directly heat the fluid by friction and turbulence.

Static efficiency of the fan (pump), η_s, may be defined as the ratio of the energy used to increase the static pressure to the energy delivered to the shaft. Assuming kinetic energy to be small compared to other components, the temperature change of the fluid across the fan (pump) can be expressed as

$$\frac{\Delta T}{W} = \frac{\eta(\eta_f - \eta_s)}{\dot{m}_f C_f} \tag{4.60}$$

or for small changes in flow rates

$$\frac{\Delta \dot{m}_f(s)}{\Delta W(s)} = \frac{\eta(\eta_f - \eta_s)}{TC_f}(1 - e^{-st}) \qquad (4.60')$$

where

ΔT = the temperature increase of the fluid

W = the electrical energy input to fan (pump)

$\dot{m}_f$ = the maximum flow rate of fluid

C_f = the specific heat of the fluid

Values for the efficiency will vary with system loads and characteristic curves or experimental data will be required to solve 4.60 for dynamic conditions.

4.8 Occupant as a Control Loop Component

Mathematical models to predict the occupant's responses to a thermal environment were reviewed in Section 2.1 (Table 2.1). Simulating a building's thermal behavior can be given an added dimension if the occupant's thermal responses can be coupled to those of other components in a building system. To accomplish this coupling, the following two steps are required:

a. To identify those thermo-physical variables in comfort models which can be used as control signals for HVAC systems.

b. To identify a transfer function of the occupant.

4.8.1 Identification of thermo-physical variables

Variables in different comfort models were summarized in part (g) of Table 2.1. Variables in Fanger's model which can be used as control

signals to HVAC system are water vapor pressure at indoor environment conditions, indoor air dry bulb temperature, mean radiant temperature, convective heat transfer coefficient as a function of air velocity, and activity level as a function of CO_2 concentration levels in the occupied space while constant Clo values are assumed.

In Pierce Two Node Model, water vapor pressure at dew point, operative temperature and convection heat transfer coefficient are functions of room air dry bulb temperature, humidity, and air velocity. They can be used as control signals at constant clothing.

The KSU model predicts thermal sensation from changes in thermal conductance between core and skin in cool environments and from skin wettedness in warm environments. These two factors are functions of room air dry bulb temperature, humidity, mean radiant temperature, air velocity, metabolic activity and thermal properties of clothing. Again room air dry bulb temperature, humidity, air velocity and mean radiant temperature can be transduced to signals to control the operation of HVAC systems. Metabolic activity rate can be used as a control signal by sensing CO_2 concentrations in the occupied space at constant clothing.

4.8.2 Transfer function of the occupant

The mechanisms by which man and other homiotherms maintain a relatively uniform body temperature under varying environmental thermal loads have been under active study since 1884 (108). Over the years, a good deal of insight into temperature regulation by man has been gained by comparison of his responses with those of physical control systems used by engineers. Hardy (109) made an extensive literature search on control

systems in physiological temperature regulation and concluded that thermoregulatory control system can be modeled as a proportional-derivative controller. Input variables identified by them were: 1) level and rate of change in hypothelamic temperature, 2) level and rate of change in skin temperature, and 3) level and rate of change of deep sub-dermal temperatures. Three major outputs during regulation at constant environmental temperatures were: 1) increased metabolism (shivering and nonshivering heat production) in response to cold, 2) vasomotor responses to heat, and 3) sweating (panting) responses to heat.

If the occupant is considered as a control loop component in a HVAC system, he may desire to change the set point on the thermostat rather than a change in metabolic rate or vasomotor regulation. A modified diagram for the two position residential heating system of Figure 3.14 is shown in Figure 4.11 which includes the occupant as a second feedback element. The mathematical model for the second feedback element is (refer to equation (4.27))

$$\frac{\Delta V_r(s)}{\Delta T(s)} = K_{occ}(1 + t_d S) \tag{4.61}$$

where $\Delta V_r(s)$ is the desire to change reference temperature and ΔT is the change in space temperature.

In this chapter, mathematical models of various components in an environmental control system have been developed. The occupant has been treated as one of the components of the system. The mathematical models developed in this chapter can be coupled together to develop a mathematical model for a particular environmental control system. This procedure will be the subject of the next chapter.

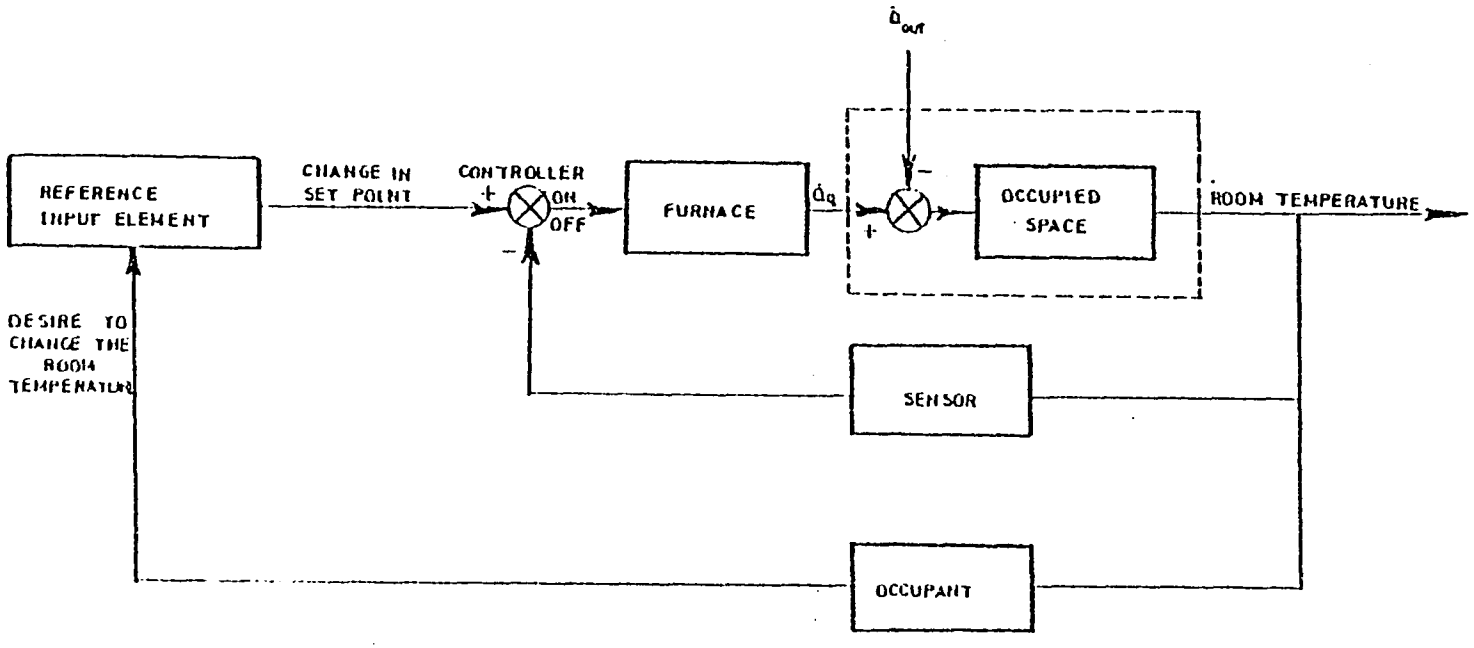

Figure 4.11. Block diagram for a two position residential heating system including the occupant.

5. MATHEMATICAL MODELS OF SYSTEMS FOR ENVIRONMENTAL CONTROL

Mathematical models developed for occupied spaces (Section 3.3) and for components for environmental control (Chapter 4) can be coupled to derive models for HVAC systems. To show the flexibility of the method, models have been developed for the following cases:

1. A forced air heating system for a single family residence.
2. A fan coil heating system for a class room.
3. A constant volume dual duct heating and cooling system for an office building.

5.1 A Heating System for a Single Family Residence

A schematic representation of a forced air heating system for a single family residence is shown in Figure 5.1. A block diagram representation of a heating system for a single family residence is shown in Figure 5.2. Transfer functions of the various blocks shown in Figure 5.2 are as follows:

Transfer function of the two position controller:

$K(s) = 0$ (off)

$K(s) = 1$ (on)

Transfer function of the occupied space for inputs from furnace, occupants and internal sources (see equation (3.26)):

$$G_1(s) = \frac{K_{\dot{Q}}}{(1 + \tau_{os}S)} = \frac{1 - K_1}{(\dot{m}_a C_{pa} + UA + K_2)} \quad \frac{1}{(1 + \tau_{os}S)}$$

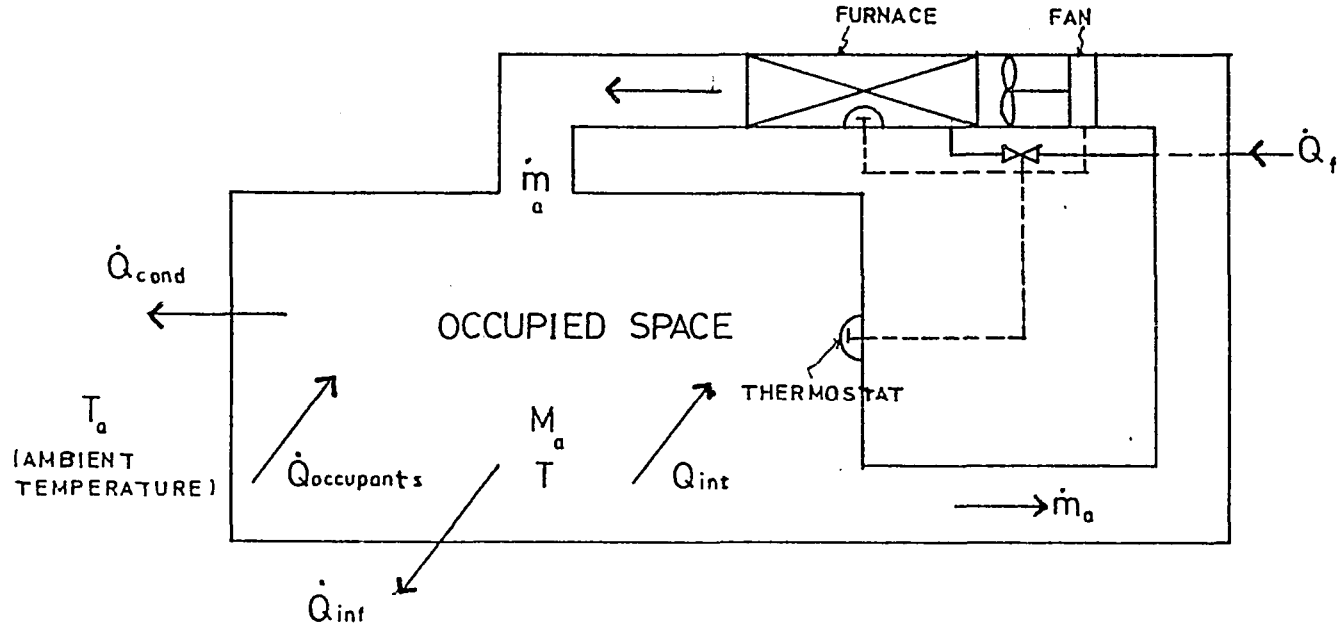

Figure 5.1. Schematic representation of a forced air heating system for a single family residence.

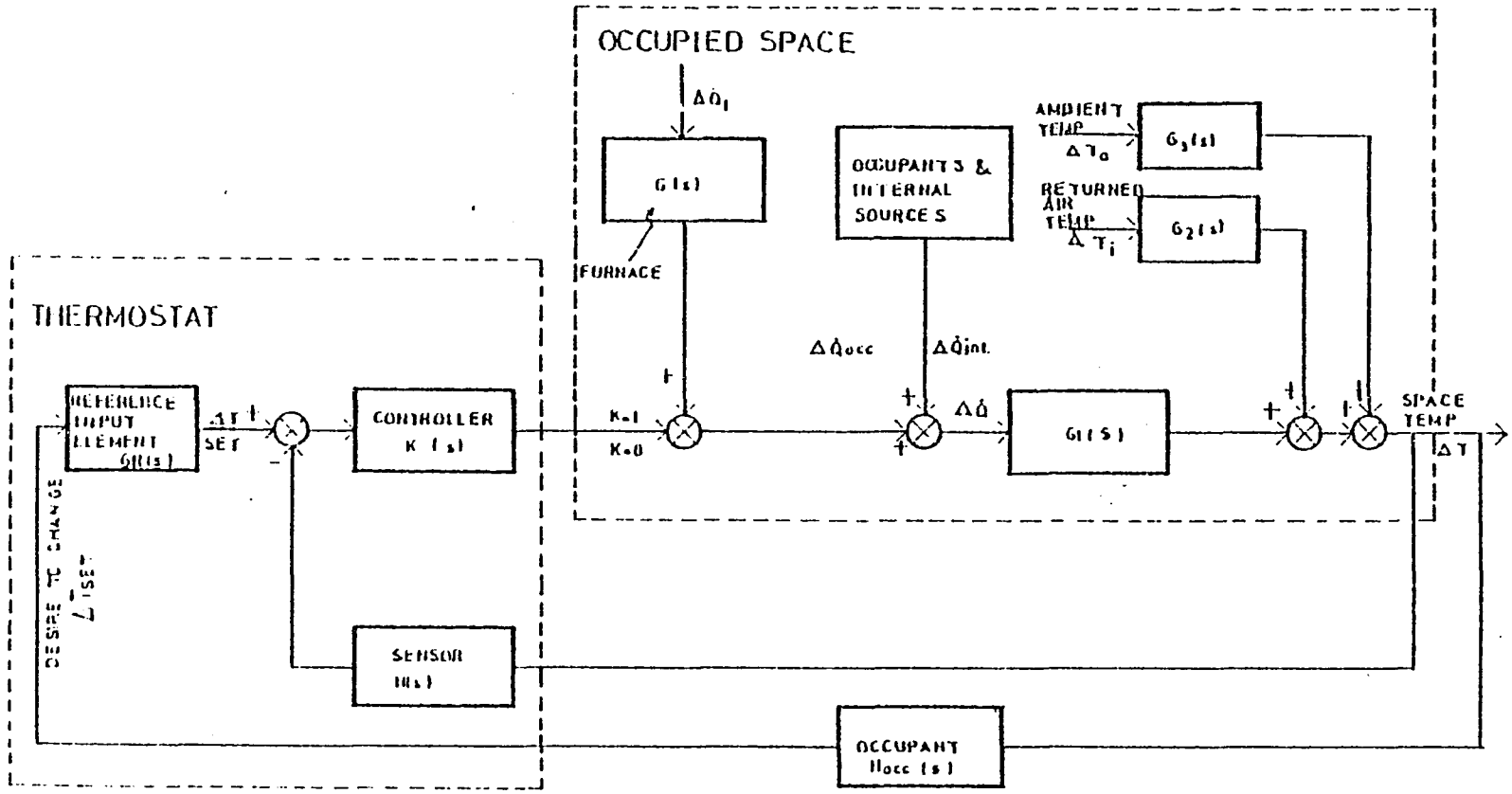

Figure 5.2. Block diagram of a heating system for a single family residence.

$$G_2(s) = \frac{K_{Ti}}{(1 + \tau_o s)} = \frac{\dot{m}_a C_{pa}}{(\dot{m}_a C_{pa} + UA + K_2)} \quad \frac{1}{(1 + \tau_{os} S)}$$

$$G_3(s) = \frac{K_{Ta}}{(1 + \tau_{os} S)} = \frac{UA}{(\dot{m}_a C_{pa} + UA + K_2)} \quad \frac{1}{(1 + \tau_{os} S)}$$

Transfer function of the feedback element

$$H_s(s) = \frac{K_s}{(1 + \tau_s S)}$$

Time constant of the occupied space (see equation (3.30))

$$\tau_{os} = \frac{M_a C_{pa}}{(\dot{m}_a C_{pa} + UA + K_2)}$$

In the transfer functions described above, K_1 and K_2 are described by equations (3.24) and (3.25), respectively:

$$K_1 = \left.\frac{\partial \dot{Q}_{inf}}{\partial \dot{Q}}\right|_{T=const}$$

$$K_2 = \left.\frac{\partial \dot{Q}_{inf}}{\partial T}\right|_{\dot{Q}=const}$$

Transfer function of the occupant as a feedback element

$$H_{occ}(s) = K_{occ}(1 + t_d S)$$

To derive the closed-loop transfer function, it can be written from Figure 5.2

$$\Delta T(s) = G_1(s)[(\Delta T_{set} - H_s(s)\Delta T)K(s) + \Delta \dot{Q}_f(s) + \Delta \dot{Q}_{occ}(s) + \Delta \dot{Q}_{inf}(s)]$$

$$+ G_2(s)\Delta T_i + G_3(s)\Delta T_a$$

Rearranging

$$\Delta T(s) = \frac{K(s)G_1(s)}{1 + K(s)G_1(s)H_s(s)} \Delta T_{set} + \frac{G_1(s)(\Delta \dot{Q}_f(s) + \Delta \dot{Q}_{occ}(s) + \Delta \dot{Q}_{int}(s))}{1 + K(s)G_1(s)H_s(s)}$$

$$+ G_2(s)\Delta T_i(s) + G_3(s)\Delta T_a(s) \tag{5.1}$$

To couple the occupant as a second feedback component, substitute in equation (5.1):

$$\Delta T_{set} = G_R(s)H_{occ}(s)\Delta T$$

$$\Delta T = \frac{K(s)G_1(s)G_R(s)H_{occ}(s)}{1 + K(s)G_1(s)H_s(s)}\ \Delta T + \frac{G_1(s)}{1 + K(s)G_1(s)H_s(s)}\ (\Delta\dot{Q}_f(s)$$

$$+ \Delta\dot{Q}_{occ}(s) + \Delta\dot{Q}_{int}(s)) + G_2(s)\Delta T_i(s) + G_3(s)\Delta T_a(s)$$

or rearranging:

$$\Delta T = \frac{G_1(s)[1+K(s)G_1(s)H_s(s)][\Delta\dot{Q}_f(s)+\Delta\dot{Q}_{occ}(s)+\Delta\dot{Q}_{int}(s)]}{[1+K(s)G_1(s)H_s(s)][1+K(s)G_1(s)H_s(s)-K(s)G_1(s)G_2(s)H_{occ}(s)]}$$

$$+ G_2(s)\Delta T_i(s) + G_3(s)\Delta T_a(s) \tag{5.2}$$

Equation (5.2) describes the closed-loop transfer function of a heating system for a single family residence which is coupled to the occupant. The derivation is relatively simple because the dynamics of the duct and supply fan have not been included. The exclusion is justified in the case of a residential facility since the duct lengths are not very long and rate of supply air is fairly constant. Absence of a mechanical air ventilation system has kept the derivation of the closed-loop transfer function relatively simple.

5.2 A Fan Coil System for a Class Room

A schematic representation of a fan coil system with mechanical ventilation for a class room is shown in Figure 5.3. A block diagram representation of the fan coil system is shown in Figure 5.4.

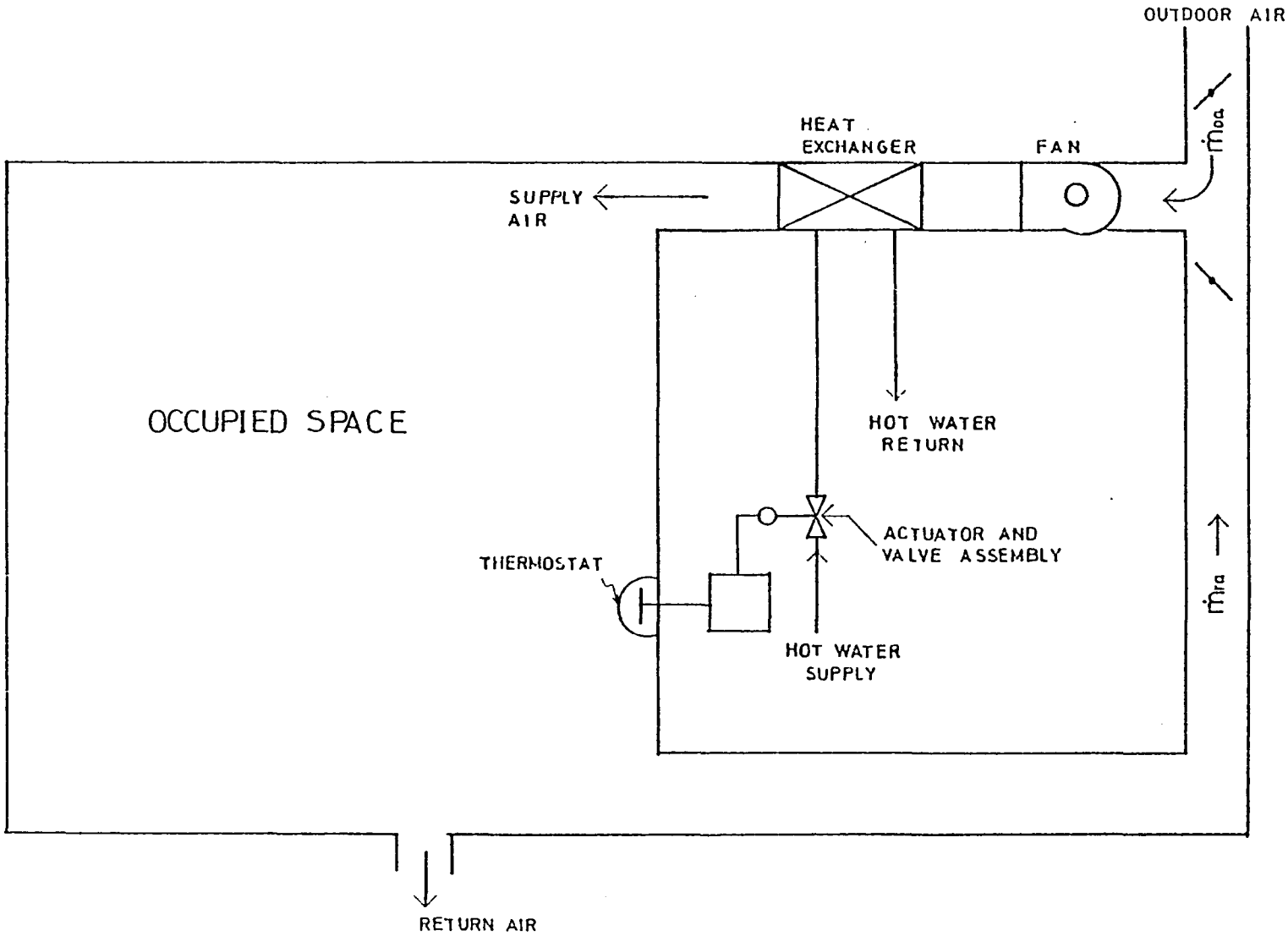

Figure 5.3. Schematic representation of a fan coil system for a class room.

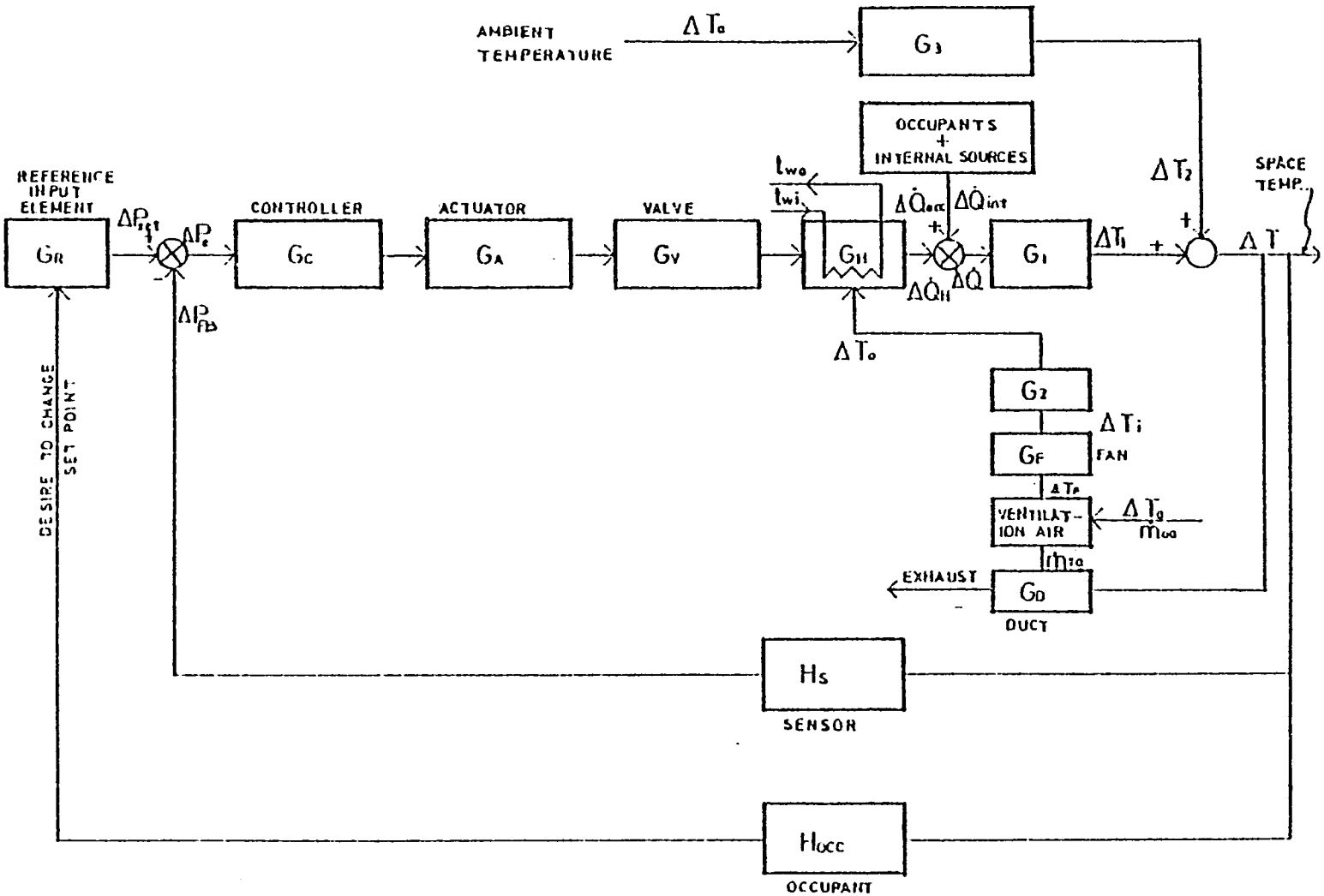

Figure 5.4. Block diagram of a fan coil system for a class room.

Transfer functions of the occupied space for heat exchanges from the heat exchanger, occupants and internal sources $G_1(s)$, for the mixed air temperature input $G_2(s)$, and for the ambient temperature inputs $G_3(s)$ are described by equation (3.26).

Transfer functions of the sensor $H_s(s)$, the occupant $H_{occ}(s)$, the controller $G_c(s)$, the actuator $G_a(s)$, the valve $G_v(s)$, the heat exchanger $G_H(s)$, the fan $G_F(s)$ and the duct G_D have been discussed in Chapter 4.

To derive the closed-loop transfer function, the basic equations associated with Figure 5.4 may be expressed as:

$$\Delta T(s) = \Delta T_1(s) + \Delta T_2(s) \tag{5.3}$$

$$\Delta T_2(s) = G_3(s)\Delta T_a(s) \tag{5.4}$$

$$\Delta T_1(s) = G_1(s)(\Delta \dot{Q}_H + \Delta \dot{Q}_{occ} + \Delta \dot{Q}_{int}) \tag{5.5}$$

Therefore

$$\Delta T(s) = G_1(s)(\Delta \dot{Q}_H + \Delta \dot{Q}_{occ} + \Delta \dot{Q}_{int}) + G_3(s)\Delta T_a(s) \tag{5.6}$$

$$\Delta \dot{Q}_H(s) = [\Delta \dot{m}_w C_{pw}(t_{wi} - t_{wo}) + \dot{m}_a C_{pa} \Delta T_o]G_H(s) \tag{5.7}$$

$$\Delta T_o(s) = G_2(s)\Delta T_i(s) \tag{5.8}$$

$$\Delta T_i(s) = G_F(s)\Delta T_F(s) = G_F(s)\left[\frac{\dot{m}_{oa}\Delta T_a + \dot{m}_{ra}\Delta T}{\dot{m}_a}\right] \tag{5.9}$$

Combining equations (5.8) and (5.9):

$$\Delta T_o(s) = G_2(s)G_F(s)\left[\frac{\dot{m}_{oa}\Delta T_a(s) + \dot{m}_{ra}\Delta T(s)}{\dot{m}_a}\right] \tag{5.10}$$

Also

$$\Delta \dot{m}_w = G_v(s)G_a(s)G_c(s)(\Delta p_{set}(s) - H_s(s)\Delta T(s)) \tag{5.11}$$

Substituting (5.10) and (5.11) in (5.7) and then substituting (5.7) in (5.6) and on rearrangement (see Appendix E for detailed calculations):

$$\Delta T(s) = \frac{G_1(s)G_H(s)G_v(s)G_a(s)G_c(s)C_{pw}(t_{wi} - t_{wo})}{X(s)} \Delta P_{set}(s)$$

$$+ \frac{G_1(s)}{X(s)} (\Delta \dot{Q}_{occ} + \Delta \dot{Q}_{int})$$

$$+ \frac{\dot{m}_a G_3(s) - G_1(s)G_H(s)G_2(s)G_F(s)\dot{m}_{oa}C_{pa}}{\dot{m}_a X(s)} \Delta T_a(s) \qquad (5.12)$$

where:

$$X(s) = [1 - (\frac{G_1(s)G_H(s)G_2(s)G_F(s)\dot{m}_{ra}C_{pa}}{\dot{m}_a} + G_1(s)G_H(s)G_v(s)G_a(s)$$

$$G_c(s)H_s(s)C_{pw}(t_{wi} - t_{wo})]$$

To couple the occupant as a second feedback component, substitute in equation (5.12)

$$\Delta P_{set}(s) = G_R(s)H_{occ}(s)\Delta T(s)$$

Rearranging (see Appendix E for detailed calculations):

$$\Delta T(s) = \frac{G_1}{X(s) - Y(s)} (\Delta \dot{Q}_{occ} + \Delta \dot{Q}_{int}) + \frac{\dot{m}_a G_3 - G_1 G_H G_2 G_F \dot{m}_{oa} C_{pa}}{X(s) - Y(s)} \Delta T_a \qquad (5.13)$$

where: G's are in Laplace Domain and,

$$Y(s) = G_1(s)G_H(s)G_v(s)G_a(s)G_c(s)C_{pw}(t_{wi} - t_{wo})G_R(s)G_{occ}(s)$$

Equation (5.12) describes the closed-loop transfer function of a fan coil heating system with mechanical ventilation for a classroom without occupants coupling. Equation (5.12) is similar to equation (5.1) derived for a forced air heating system for a residence. The derivation of equation (5.12) has been complicated due to the inclusion of the dynamics of

controller, actuator, valve, and heating coil. The mechanical ventilation loop has added to the complexities of the model. The effect of the mechanical ventilation subsystem can be seen by comparing the inputs in equations (5.1) and (5.12). The mixed air temperature, T_i, has been described in terms of space temperature T and ambient temperature T_a due to the mixing process. Equation (5.13) is the closed loop transfer function of the fan coil heating system to which the dynamics of the occupant have been coupled and is similar to equation (5.2). The increased degree of complexity discussed for equation (5.12) also applies to equation (5.13).

5.3 Constant Volume Dual Duct System for an Office Building

A schematic representation of a constant volume dual duct heating and cooling system is shown in Figure 5.5. A block diagram for the constant volume dual duct system is shown in Figure 5.6. Block numbers 1, 2, 3, 4, 5 and 6 represent room system, mixed air control system, steam humidifier system, hot deck system, cold deck system and mixing box system, respectively. Block numbers will be used as subscripts for various parameters in describing the system. The following notation is used for different transfer functions in Figure 5.6. The symbols in capital letters represent Laplace Transform domain, and the Laplace variable (s) is implied.

H: transfer function of a feedback element

G: transfer function of a controller

P: transfer function of a duct

R: transfer function of occupied space

C: transfer function of a coil

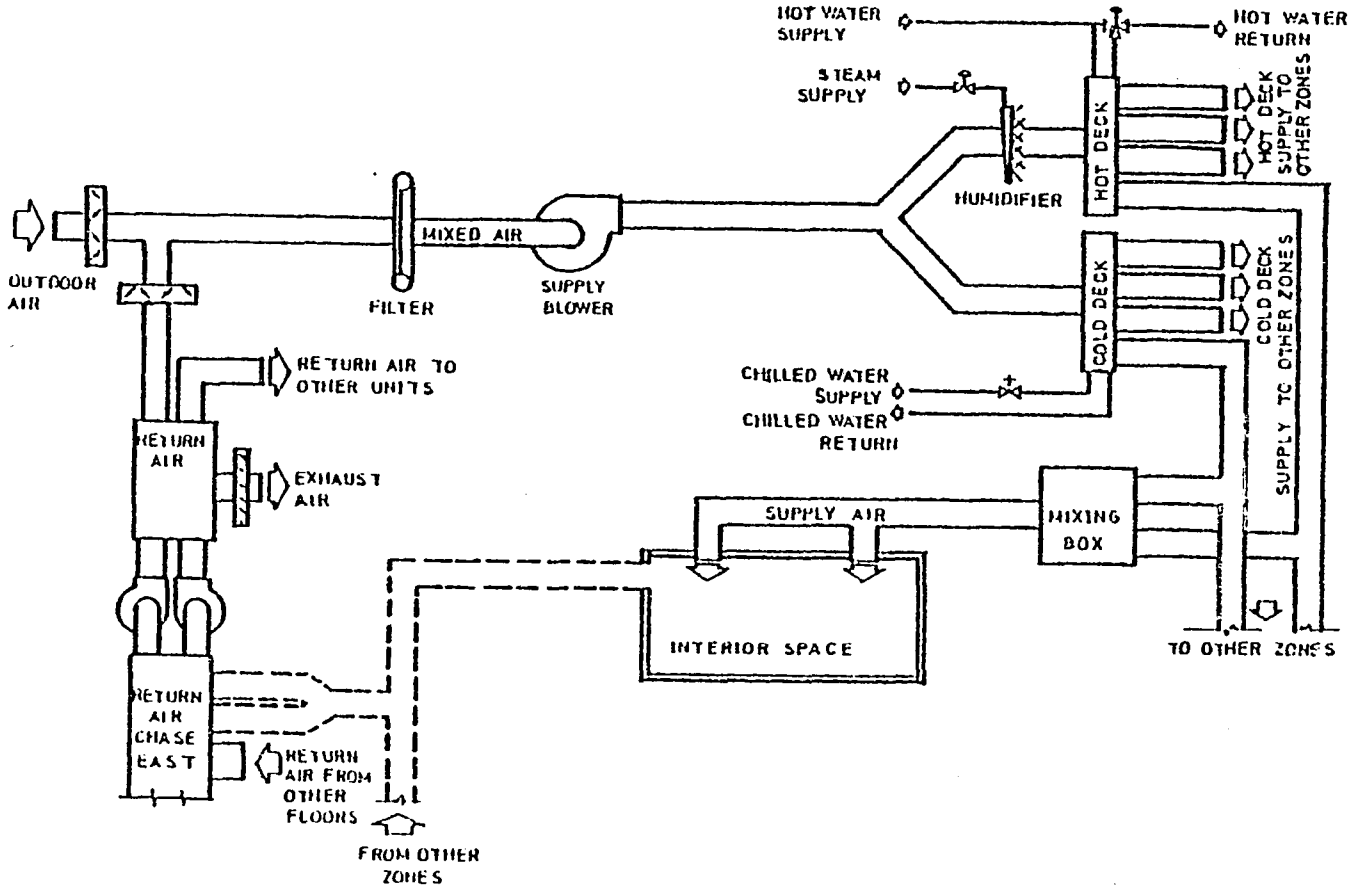

Figure 5.5. Schematic representation of a constant volume dual duct system for an office building.

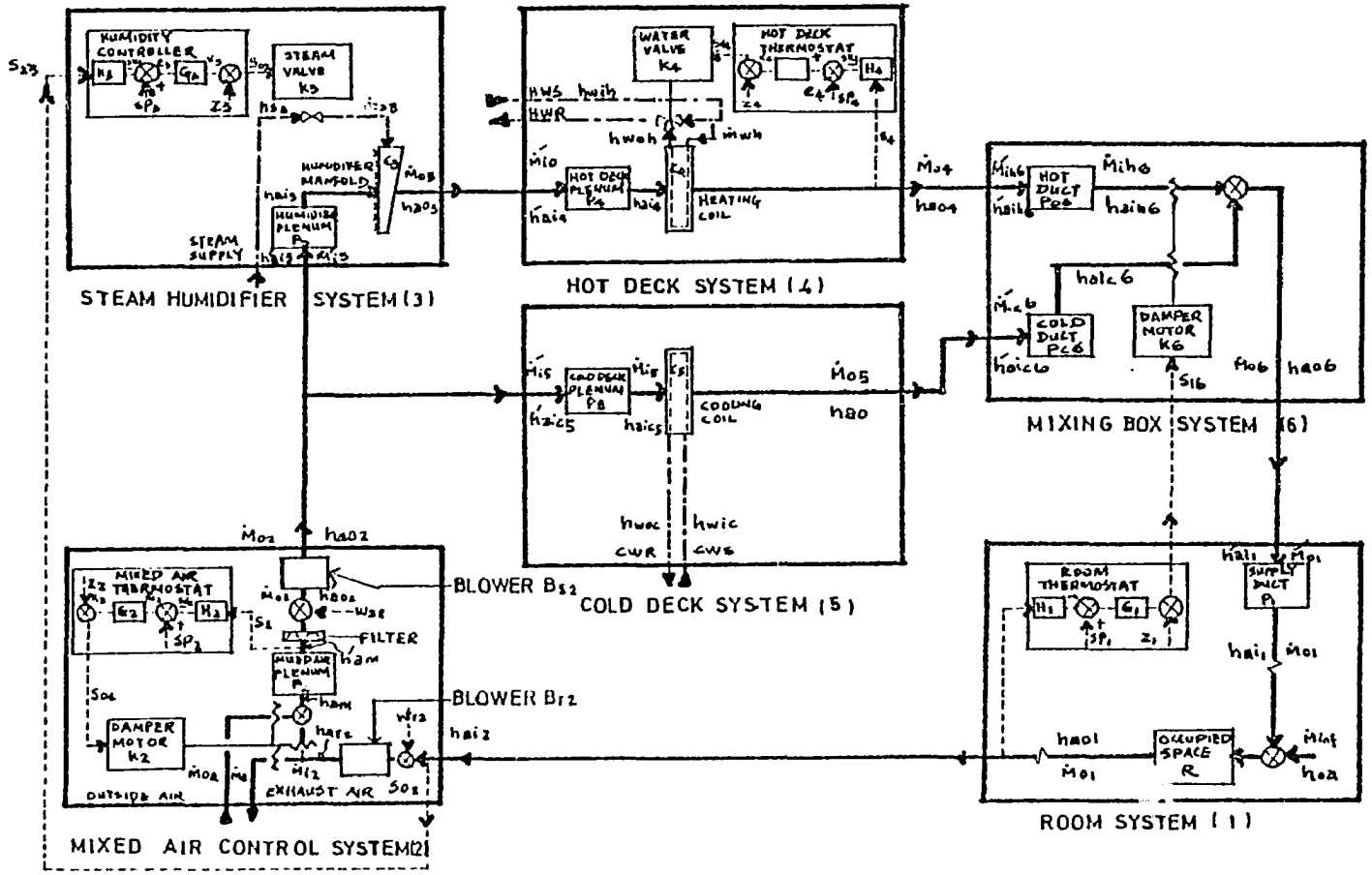

Figure 5.6. Block diagram of a constant volume dual duct system for an office building.

K: transfer function of an actuator, a damper motor or of a valve

B: transfer function of a fan

To derive the closed-loop transfer function, it is recognized that there are four feedback loops in the block diagram of Figure 5.6. The feedback loops are in blocks 1, 2, 3 and 4. The performance of any feedback loop is dependent upon the performance of other loops. Three typical equations are required to describe the coupling between subsystems, a mass balance, an energy balance and a control equation. This is in line with the technique used in deriving the transfer functions of a heating system for a single family residence and of a fan coil heating system. Fan coil heating system had one extra subsystem (mechanical ventilation system) compared to the residential heating system and the coupling of mechanical ventilation required a mass balance equation and an energy balance equation to derive equation (5.9). The coupling equations for the various subsystems in Figure 5.6 have been derived under the assumption that the infiltration rates in the room system do not change with time. Further, it is assumed that the mass flow rate of return air is constant with respect to time and is equal to the mass flow rate of supply air for the room.

For the coupling of room, mixing box and cold deck systems, the equations may be expressed as:

Mass balance:

$$\Delta\dot{M}_{ol} = \Delta\dot{M}_{ih6} + \Delta\dot{M}_{ic6} = 0 \qquad (5.14)$$

Energy balance:

$$\dot{M}_{o1}\Delta h_{ao1} + \dot{M}_{o1}(\Delta h'_{ai_1} - \Delta h_{ai_1}) = \dot{M}_{ainf}\Delta h_{ao} + \dot{M}_{o1}\Delta h'_{ai_1} + R[\Delta h_{oa} + \Delta\dot{Q}_{occ} + \Delta\dot{Q}_{int} + \dot{M}_{o1}(h_{ai_1} - h_{ao_1})] \tag{5.15}$$

$$\Delta M_{ic6}h_{aic6} = \Delta\dot{M}_{ic5}h_{aic5} + C_5\dot{m}_{wc}(h_{wci} - h_{wco}) \tag{5.16}$$

$$\Delta\dot{M}_{ih6}h_{aih6} + \Delta\dot{M}_{aic6}h_{aic6} = \dot{M}_{o6}\Delta h_{ao6} + \Delta\dot{M}_{ih6}(h'_{aih6} - h_{aih6}) + \Delta\dot{M}_{ic6}(h'_{aic6} - h_{aic6}) \tag{5.17}$$

Control equation:

$$\Delta\dot{M}_{ih6} = (\Delta SP_1 - \Delta h_{ao1}H_1)G_1K_6 \tag{5.18}$$

$$\Delta SP_1 = G_rH_{occ}\Delta h_{ao1} \tag{5.19}$$

For the coupling of room, mixed air control and humidifier subsystems, the equations may be expressed as:

Mass balance:

$$\dot{M}_{o1} = \dot{M}_{i3} = \dot{M}_{o2} \tag{5.20}$$

$$\dot{M}_{i3} = \dot{M}_{ra} + \dot{M}_{oa} \tag{5.21}$$

$$\dot{M}_{oa} = \dot{M}_{o1}(1 - X) \tag{5.22}$$

where

$$X = \dot{M}_{ra}/\dot{M}_{o1}$$

Energy balance:

$$\dot{M}_{o1}h_{ao1} + \dot{M}_{oa}h_{ao} + W_rB_{r2} + W_sB_{s2} = \dot{M}_{oa}h_{ao2} + \dot{M}_{o2}(h'_{ao2} - h_{ao2}) + \dot{M}_{oa}h_{ao1} + \dot{M}_{o2}(h_{am} - h'_{am}) \tag{5.23}$$

$$\Delta\dot{M}_{i3}h_{ao2} + \Delta\dot{m}_sh_sC_3 = \dot{M}_{o3}h_{ao3} \tag{5.24}$$

Control equations:

$$\Delta\dot{m}_s = (\Delta SP_3 - \Delta h_{ao1}H_3)G_3K_3 \tag{5.25}$$

$$\Delta X = (\Delta SP_2 - \Delta h'_{am}H_2)G_2K_2 \tag{5.26}$$

For the coupling of mixing box, hot deck and humidifier subsystems, the equations may be expressed as:

Mass balance:

$$\Delta\dot{M}_{ih6} = \Delta\dot{M}_{i3} + \Delta\dot{m}_s \tag{5.27}$$

$$\Delta\dot{M}_{o3} = \Delta\dot{M}_{i3} + \Delta\dot{m}_s \tag{5.28}$$

Energy balance:

$$\Delta\dot{M}_{io3}h_{ao3} + \Delta\dot{m}_{wh}(h_{wih} - h_{woh})C_4 = \Delta\dot{M}_{o4}h_{ao4} + \Delta\dot{M}_{io3}(h'_{ai4} - h_{ai4}) \tag{5.29}$$

Control equation:

$$\Delta\dot{m}_{wh} = (\Delta SP_4 - \Delta h_{ao4}H_4)G_4K_4 \tag{5.30}$$

Simultaneous solution of equations (5.14-5.30) describes the closed-loop performance of the constant volume dual duct heating/cooling system shown in Figure 5.6. It is observed that as the number of subsystems and control loops in HVAC systems increase, the analysis gets more and more complex. In a fan-coil heating only one additional subsystem (mechanical ventilation) was added compared with the residential heating whereas five additional subsystems and three additional control loops have been added for the constant volume dual duct system. The addition of subsystems and control systems requires more mass balance energy balance and control equations and, as such, a computer solution of the equations is more desirable. A computer program written to solve equations (5.14-5.30) can

also provide the flexibility of calculating outputs to one or more inputs at a time.

To conclude, modular models developed in Chapters 3 and 4 for the components of environmental control systems have been coupled for three different HVAC systems in this chapter. The basic approach of writing mass balance, energy balance and control equations has been stressed. The added complexities due to additional subsystems and control loops have been identified.

6. EXPERIMENTAL VALIDATION OF A SYSTEM FOR ENVIRONMENTAL CONTROL

Mathematical models to predict dynamic conditions inside an occupied space were developed in Chapter 3. Development from analog passive circuits was reported in Section 3.2. In Section 3.2.3 experimental data available from the work done by Magnussen (26) were used to validate the dynamic responses predicted from analog thermal circuits model. It was concluded there that models from analog thermal circuits can accurately predict dynamic conditions inside a building. However, it was shown there that the technique can lead to a very complex mathematical analysis, is limited in its applications and is expensive in terms of time and money. So a rational model to predict dynamic conditions inside a building was proposed in Section 3.3 and in reference (100). Experimental validation of the rational model is undertaken in this chapter using the Iowa State University Energy Research House (ERH) as an experimental facility.

6.1 Objectives

The objectives of the experimental efforts are to evaluate experimentally the validity of the rational model both in open loop and in closed loop mode to predict dynamic conditions inside a building.

6.2 Purpose

The purpose of this evaluation is to obtain a valid open-loop transfer function for occupied spaces and to test its coupling to the transfer

functions of other components in heating, ventilating and air-conditioning (HVAC) systems to carry out closed-loop analysis.

6.3 Open-Loop Mode

First, the rational model was tested in the open-loop mode.

6.3.1 Theory

The rational model for an occupied space derived from energy balance methods was described by equations (3.26)-(3.30) which are reproduced here in modified form for ready reference:

$$\Delta T(s) = \frac{K_Q^{\bullet}\Delta\dot{Q}(s)}{S(1 + \tau_{os}S)} + \frac{K_{Ti}\Delta T_i(s)}{S(1 + \tau_{os}S)} + \frac{K_{Ta}\Delta T_a(s)}{S(1 + \tau_{os}S)} \tag{6.1}$$

where

$$K_Q^{\bullet} = \frac{1 - K_1}{\dot{m}_a C_{pa} + \Sigma UA + K_2} \tag{6.2}$$

$$K_{Ti} = \frac{\dot{m}_a C_{pa}}{\dot{m}_a C_{pa} + \Sigma UA + K_2} \tag{6.3}$$

$$K_{Ta} = \frac{\Sigma UA}{\dot{m}_a C_{pa} + \Sigma UA + K_2} \tag{6.4}$$

$$\tau_{os} = \frac{M_a C_{pa} + \Sigma M_{Fur} C_{pf}}{\dot{m}_a C_{pa} + \Sigma UA + K_2} \tag{6.5}$$

In equations (6.2)-(6.5), the term UA has been replaced by ΣUA to account for the different types of construction for walls and roof of ERH as per details given in Appendix F. Similarly the term $\Sigma(M_{Fur}C_{pf})$ (sum of the products of mass and specific heat for various furniture items inside ERH) has been added to the numerator in equation (6.5) to account for the

changes in stored energy of furniture with variations in indoor air temperature as per details of furniture given in Appendix G.

In equations (6.2)-(6.5)

$$K_1 = \left.\frac{\partial \dot{Q}_{inf}}{\partial \dot{Q}}\right|_{T=\text{constant}} \qquad \text{(refer to equation 3.24)}$$

and

$$K_2 = \left.\frac{\partial \dot{Q}_{inf}}{\partial T}\right|_{\dot{Q}=\text{constant}} \qquad \text{(refer to equation 3.25)}$$

For open-loop conditions when no energy transfer takes place from the heat exchanger, no changes in number of occupants and no changes in internal heat gains, $\Delta\dot{Q} = 0$ and equation (6.1) can be written as

$$\Delta T(s) = \frac{K_{Ti}\Delta T_i(s)}{S(1 + \tau_{os}S)} + \frac{K_{Ta}\Delta T_a(s)}{S(1 + \tau_{os}S)} \qquad (6.6)$$

To validate equation (6.6) for the Iowa State University Energy Research House, the values of K_{Ti}, K_{Ta} and τ_{os} as per equations (6.3)-(6.5) need to be calculated. Parameters of the house envelope and furniture required to solve these equations can be taken from the calculations shown in Appendices F-G. Equations (6.3)-(6.5) are also expressed in terms of K_2 described by equation (3.25). To evaluate K_2, substitute in equation (3.25)

$$\dot{Q}_{inf} = \dot{m}_{ainf}C_{pa}(T - T_a) \qquad (6.7)$$

where

$\dot{m}_{ainf}$ = mass flow rate of infiltered air

T_a = outside air temperature

Therefore,

$$K_2 = \frac{d}{dT}\left[\dot{m}_{ainf} C_{pa} (T - T_a)\right]$$

or

$$K_2 = \dot{m}_{ainf} C_{pa} - \dot{m}_{ainf} C_{pa} \frac{dT_a}{dT} \qquad (6.8)$$

6.3.2 Procedures

Values of $\dot{m}_{ainf}$ and dT_a/dT to be used in equation (6.8) were determined experimentally. Details of procedures used are given in Sections 6.3.2.1 and 6.3.2.2.

6.3.2.1 Temperatures

1. Copper-Constantan thermocouples were manufactured using #24 gauge wire and one each was installed in the northwest bedroom, southwest bedroom, living room, greenhouse, soil (depth of 26", 80" and 134") and basement. Outputs from these thermocouples were calibrated using an ice bath. Thermocouples were protected from direct radiations using radiation shields. These thermocouples were located at least 2 feet above the floors and were equidistant from the walls. One of the special purpose stands built to install thermocouples is shown in Figure 6.1.
2. Temperatures at the locations of the thermocouples were scanned and recorded by a programmable data logger. Model 2240B data logger manufactured by John Fluke Mfg. Co. was used and is shown in Figure 6.2. Model 2240B data logger can scan and record data according to the programmed sequences and intervals.
3. Weather data were collected by connecting wind translator (P/N 1-0161-1), wind sensor (P/N100108), radiation translator (P/N100144), temperature dew point translator (P/N100483), temperature/dew point

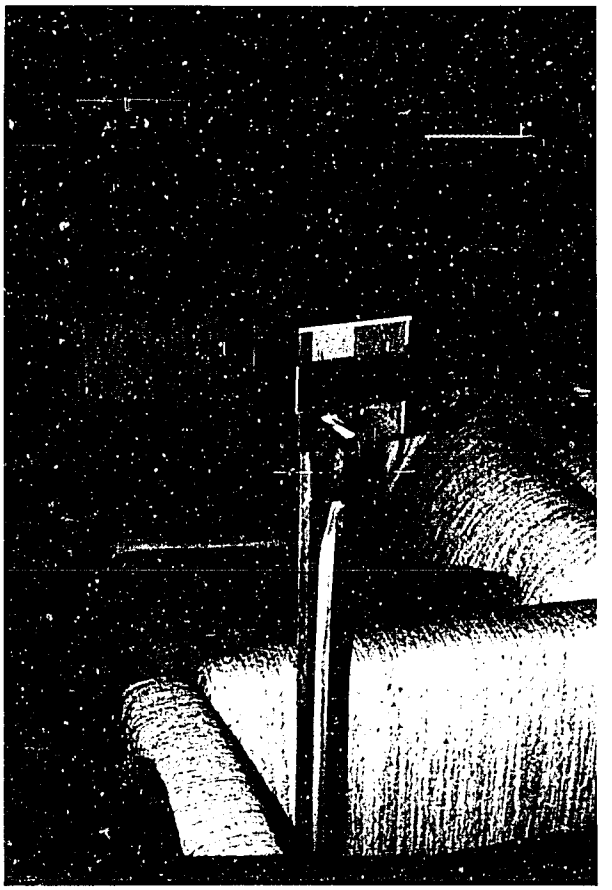

Figure 6.1. Photograph of a stand used to install thermocouples.

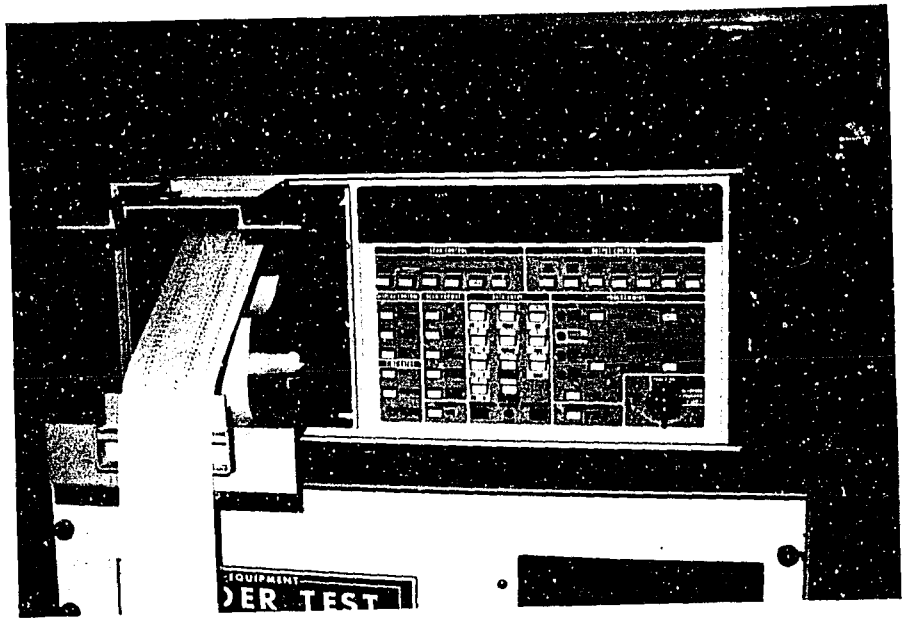

Figure 6.2. Photograph of a programmable data logger (Model 2240B, John Fluke Co.).

shield (P/N100325-1), temperature sensor (P/N100093), and dew point sensor (P/N100743) to the main frame (Model No. 100081) and power supply (Model No. 100074) unit of Modular Meteorological System supplied by Climatronics Corp., New York and shown in Figure 6.3. The sensors were located at the northwest corner of the roof of ERH. Outputs from the weather data transducers were scanned and recorded on Model 2240B data logger.

4. For open-loop validation, no heating/cooling system was operating at the time data were being taken.
5. To eliminate changes in the number of occupants, door openings, internal heat gains, etc. data were recorded during nights so that ERH was available to other researchers working on different projects during the day time.

6.3.2.2 Infiltration rates

1. A nondispersive infrared (NDIR) gas analyzer ANARAD Model was used to monitor the concentrations of methane to measure infiltration rates at ERH at the time data on temperatures were being recorded. The output of the gas analyzer was recorded on a Cole-Palmer Model 282/MM strip chart recorder. A picture of the set up is shown in Figure 6.4.
2. On every night of taking data, the gas analyzer and the strip chart recorder were turned on and allowed to warm up for about 20 minutes. After that the pump on the analyzer was switched on and zero gas (room air) was fed to the analyzer. With zero adjustment, digital meter reading was made to read zero ppm.

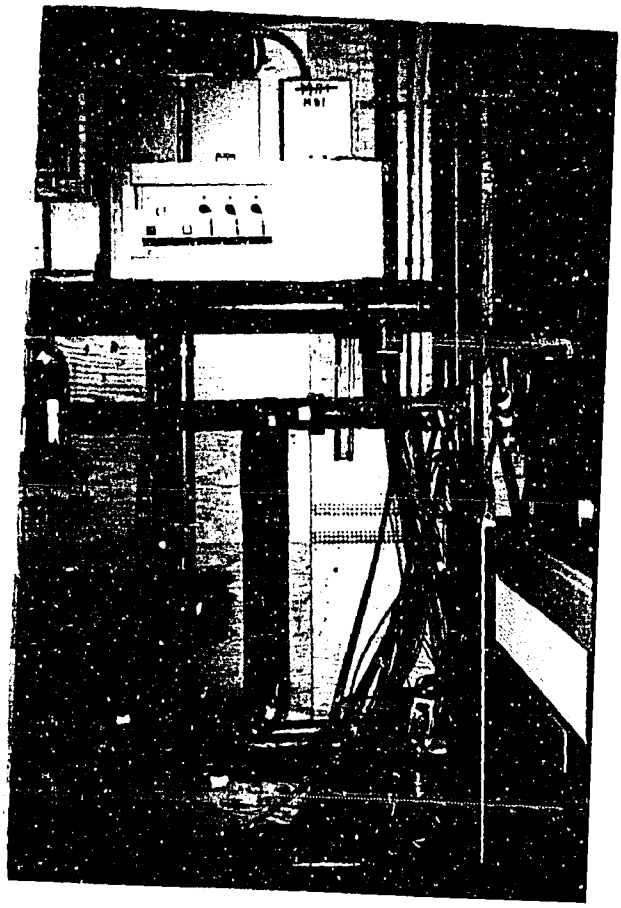

Figure 6.3. Photograph of a modular meteorological system (Climatronics Corp., New York).

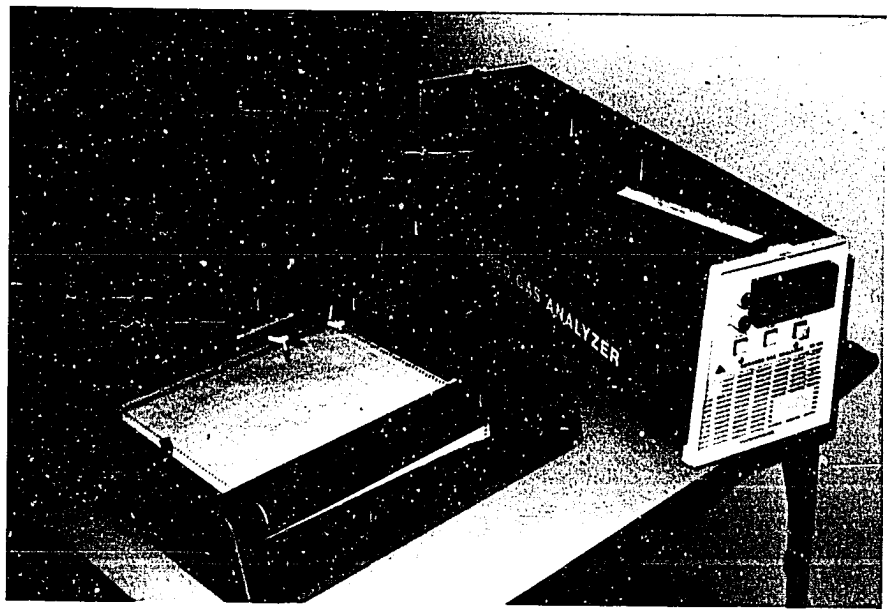

Figure 6.4. Photograph of ANARAD gas analyzer and Cole-Palmer strip chart recorder used in infiltration measurements at ERH.

3. Calibration switch was turned on and the digital meter was adjusted to read 1000 ppm with the adjustment of span control.
4. Calibration switch was turned off and again zero setting was checked. Zero and span adjustments were checked in turn until both readings were stabilized.
5. Flow rate of methane gas required to charge ERH with a concentration of 500 ppm of methane was calculated as follows:

   Inside volume of ERH = $480\ m^3$

   $$= \frac{480 \times (100)^3}{1{,}000} \text{ litres}$$

   Therefore, volume of methane gas to give concentration of 500 ppm

   $$= \frac{480(100)^3}{1{,}000} \times \frac{500}{10^6} \text{ litres}$$

   If flow of methane gas volume is to be accomplished in 15 minutes,

   rate of flow of methane gas per minute $= \frac{480 \times (100)^3}{1{,}000} \times \frac{500}{10^6} \times \frac{1}{15}$

   $= 16$ litres/minute
6. From calibration curve for methane gas flowmeter (Figure 6.5), it was found that the SS ball should be 44 divisions of scale on flowmeter.
7. Instrument grade (99.7%) methane gas was allowed to flow through the flowmeter (Figure 6.6) with SS ball adjusted to 44 divisions for 15 minutes into the discharge side of the main blower of HVAC system.
8. Return air from the duct was continuously pumped into the gas analyzer for recording concentrations of methane gas in ERH at different times.

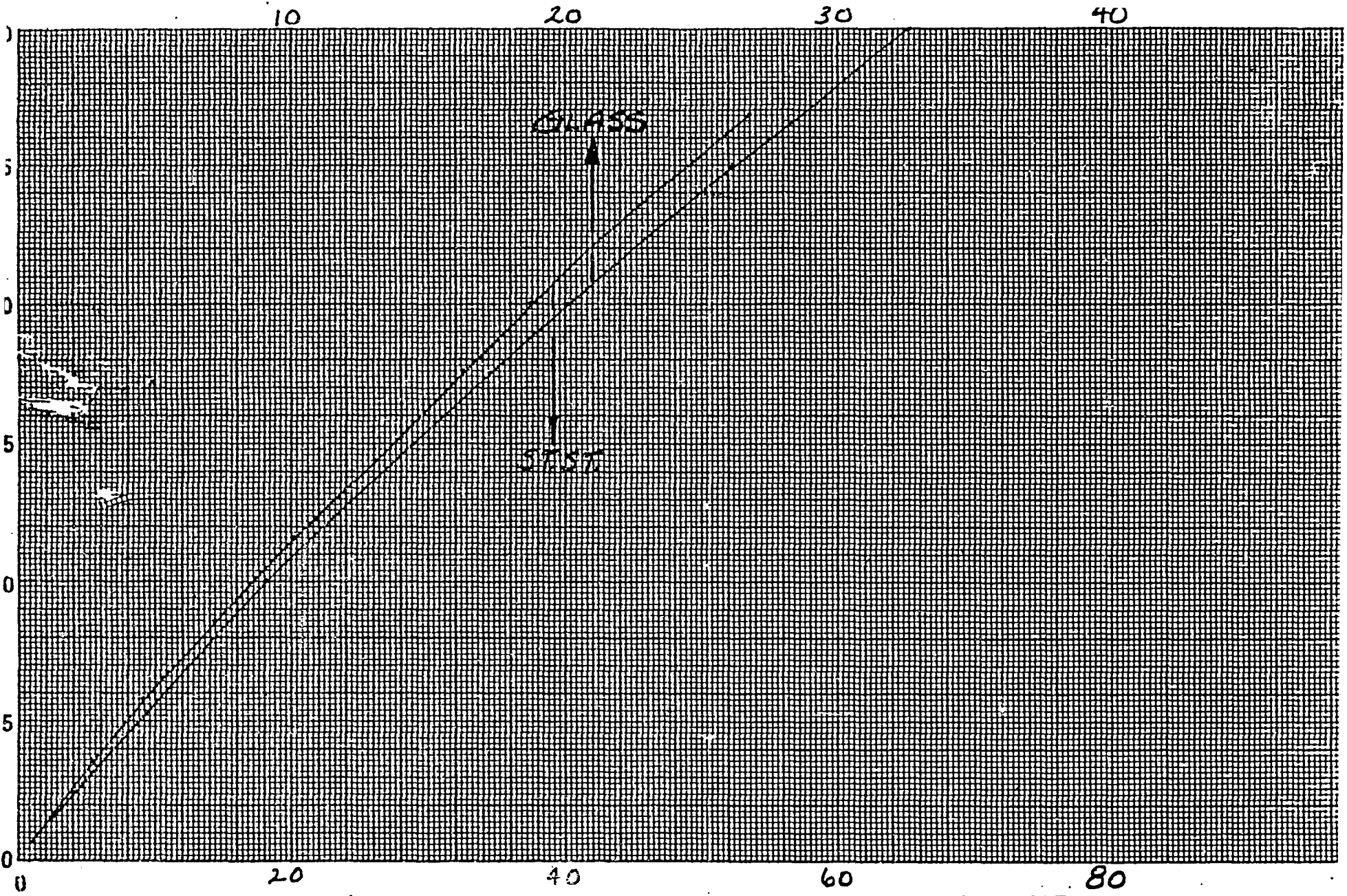

FLOW RATE LITERS /MIN. AT 760 mm. Hg. & 21°C. S.S. FLOAT

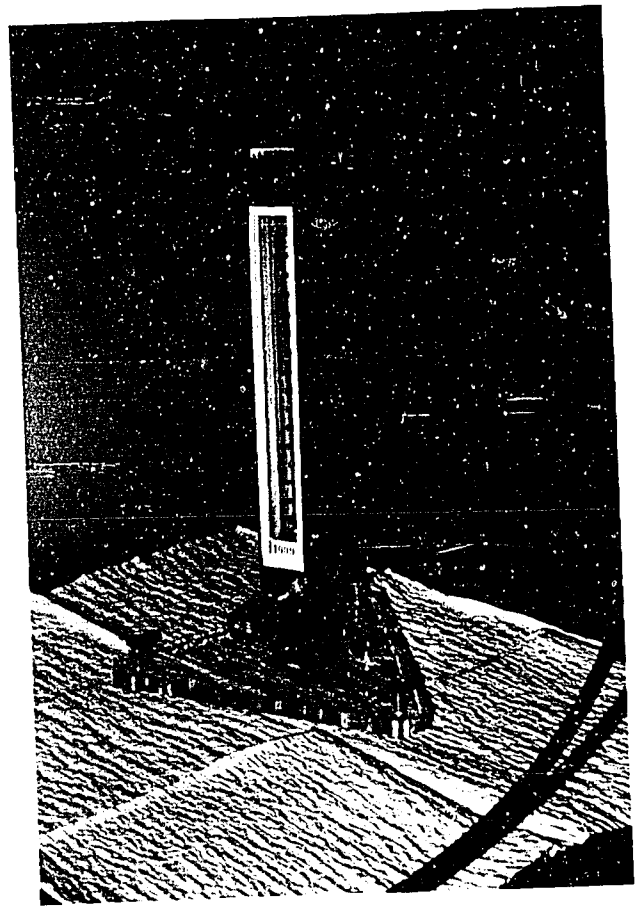

Figure 6.6. Photograph of flowmeter to monitor the rate of flow of instrument grade (99.7%) methane gas into ERH for infiltration studies.

9. Records of concentration of methane vs. time were obtained from the recordings on the strip chart recorder. One such record is shown in Figure 6.7.

6.3.3 Data analysis

Experimental data are analyzed for infiltration rates, temperatures and other parameters in the following sections.

6.3.3.1 Infiltration rates Using the methane leakage curve in Figure 6.7 data on methane concentration as a fraction of total charge are tabulated in Table 6.1. Same data are shown on a semi-log paper in Figure 6.8. We can write

$$\text{Concentration } C = e^{-t/\tau_{leak}} \tag{6.9}$$

where t is the time elapsed after charging and τ is the time constant of methane leakage process.

From equation (6.9)

$$\tau_{leak} = -t/\ln C = -\frac{t}{x} \tag{6.10}$$

Using the method of least squares for curve fitting, it can be written

$$\tau_{leak} = \frac{n\left(\sum_{i=1}^{n} x_i t_i\right) - \left(\sum_{i=1}^{n} x_i\right)\left(\sum_{i=1}^{n} t_i\right)}{n\left(\sum_{i=1}^{n} x_i^2\right) - \left(\sum_{i=1}^{n} x_i\right)^2} \tag{6.11}$$

where n is the total number of data points in Table 6.1.

$$\tau_{leak} = \frac{15(2697.30) - (18.38)(1800)}{15(26.37) - (18.38)^2}$$

$$= 127.76 \text{ minutes}$$

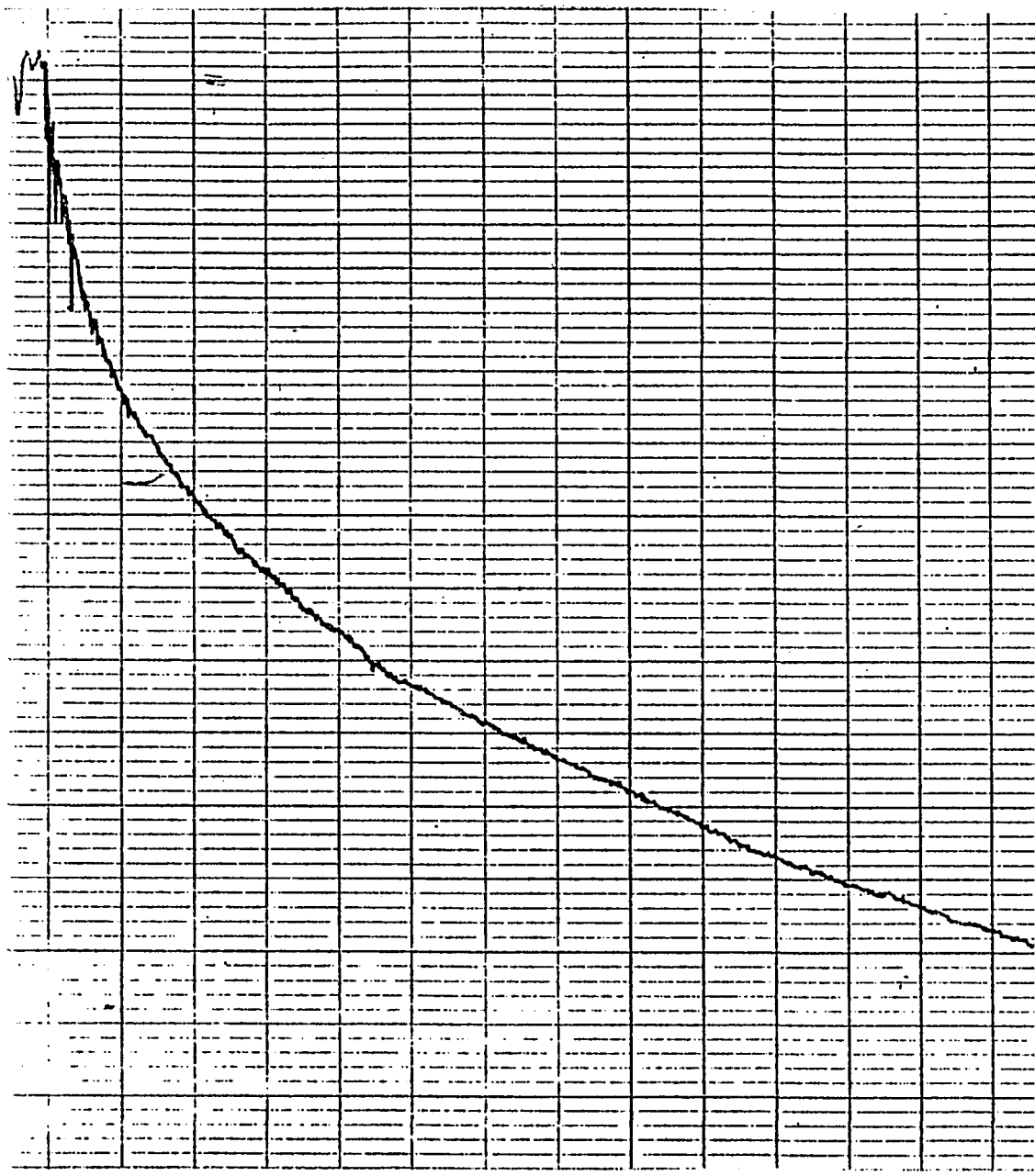

Figure 6.7. Strip chart recorder plot for methane leakage (night of July 26-27, 1979). Maximum charge: 500 ppm; chart speed: 4 cms/hour; status: fan on, open-loop mode tests.

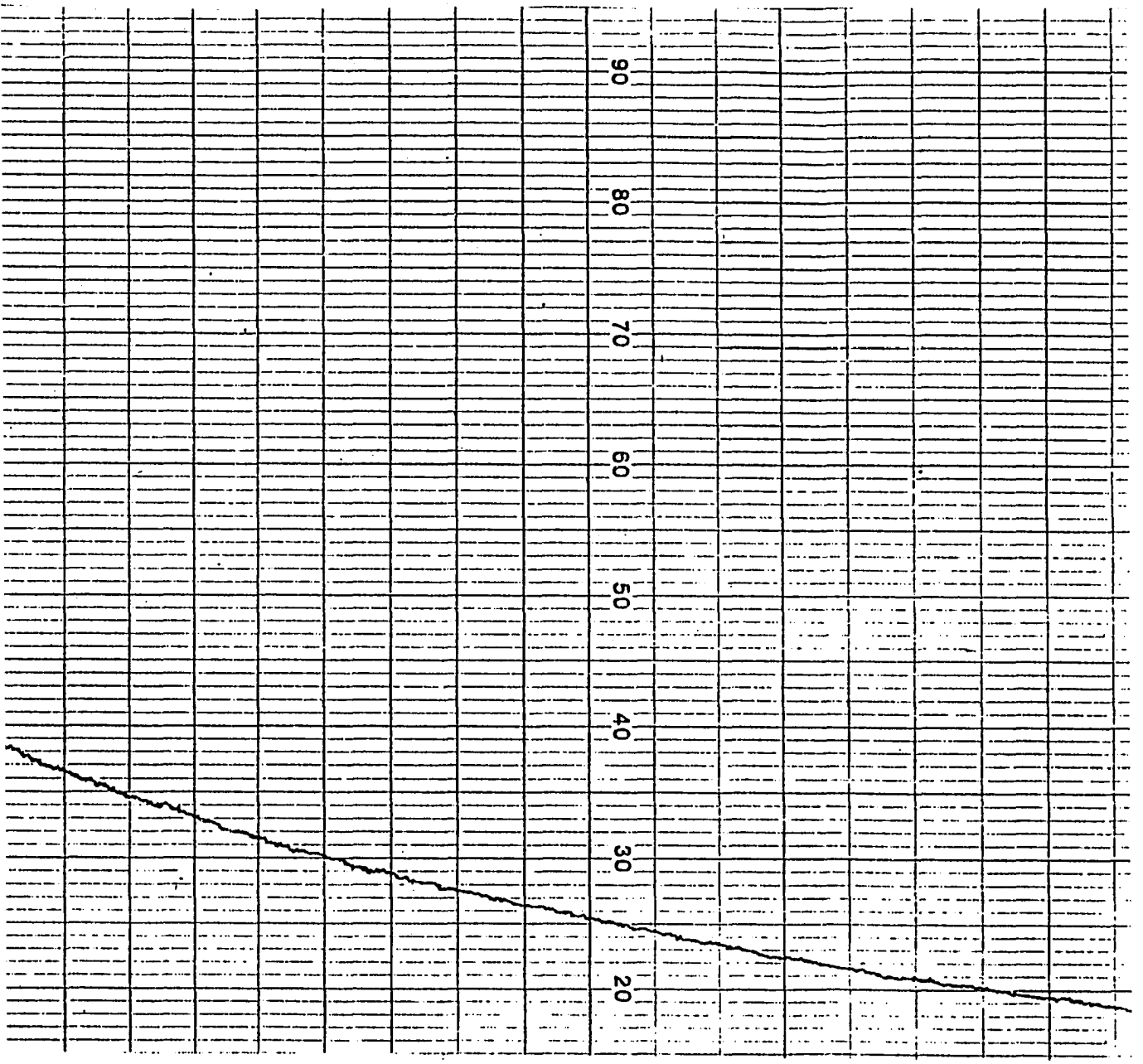

akage (night of July
chart speed: 4 cms/
sts.

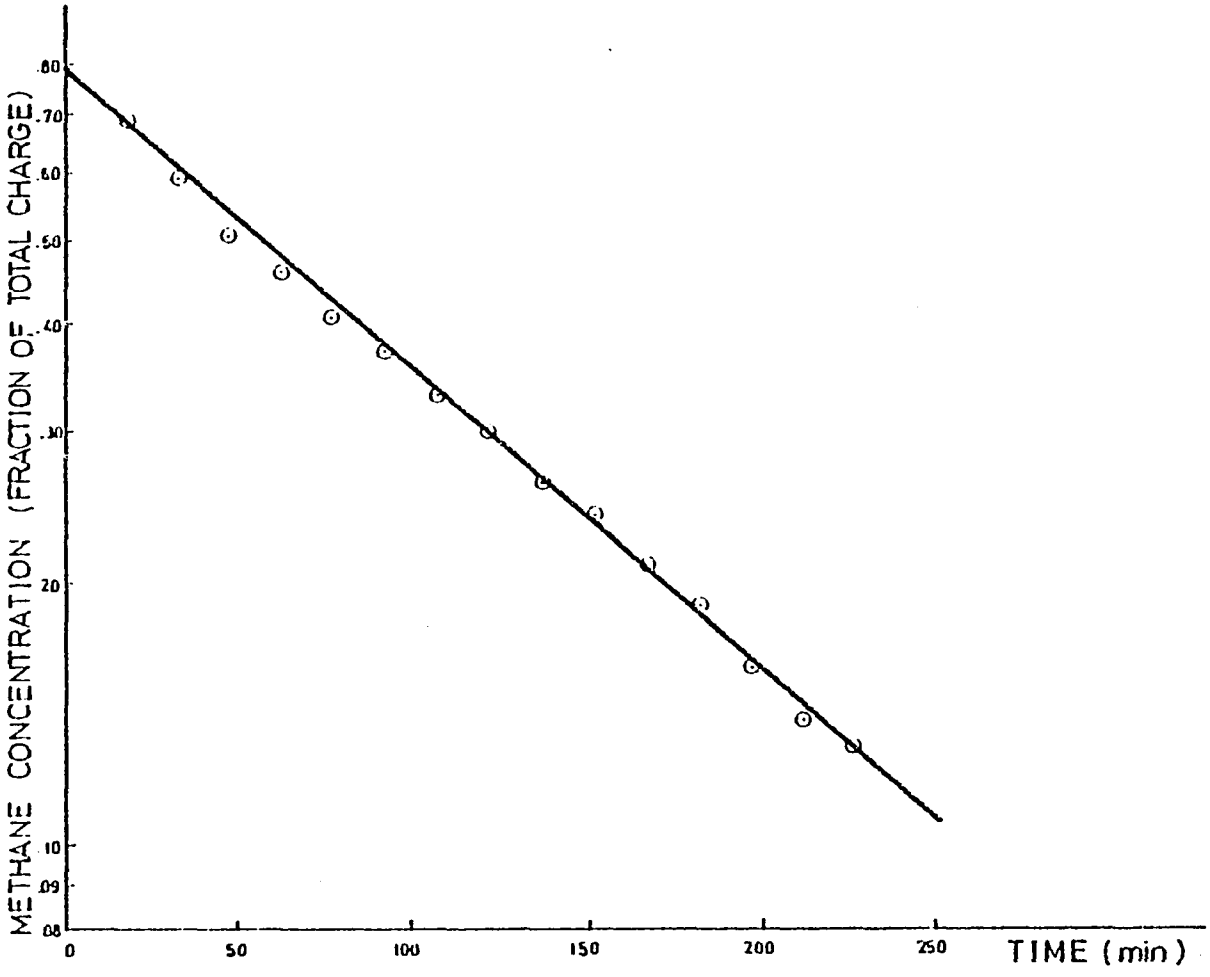

Figure 6.8. Methane concentration vs. time (July 26-27, 1979) at ERH.

Table 6.1. Methane concentration and time elapsed after charging (July 26-27, 1979)

S. No.	Methane concentration C (fraction of total charge)	ln C (x)	Time (minutes) t
1	0.69	-0.37	15
2	0.59	-0.53	30
3	0.51	-0.67	45
4	0.46	-0.78	60
5	0.41	-0.89	75
6	0.37	-0.99	90
7	0.33	-1.11	105
8	0.30	-1.20	120
9	0.26	-1.35	135
10	0.24	-1.43	150
11	0.21	-1.56	165
12	0.19	-1.66	180
13	0.16	-1.83	195
14	0.14	-1.97	210
15	0.13	-2.04	225

In 127.76 minutes, leakage = 0.632

In 60 minutes, leakage $= \frac{60 \times 0.632}{127.76}$

$= 0.30$

Hence infiltration rate = 0.30 air changes/ hour; therefore,

$$\dot{m}_{inf} = 16950 \times 0.30 \times 0.074$$

$$= 376.29 \text{ lbm/hour } (170.69 \text{ kg/hr}) \qquad (6.12)$$

6.3.3.2 Temperatures Data on inside temperatures and weather conditions obtained on the night of July 26-27, 1979 according to the

procedures described in Section 6.3.2.1 are given in Table 6.2. Measured average indoor air temperatures and measured average outdoor air temperatures are computed from the data in Table 6.2 and are shown in Table 6.3. From the data given in Table 6.3, we can calculate dT_a/dT by least squares method as

$$\frac{dT_a}{dT} = \frac{n\left(\sum_{i=1}^{n} T_i T_{ai}\right) - \left(\sum_{i=1}^{n} T_i\right)\left(\sum_{i=1}^{n} T_{ai}\right)}{n\left(\sum_{i=1}^{n} T_i^2\right) - \left(\sum_{i=1}^{n} T_i\right)^2}$$

where n is the total number of points in Table 6.3.

$$\frac{dT_a}{dT} = \frac{20(11766.97) - (567.98)(414.27)}{20(16130.54) - (567.98)^2}$$

$$= 4.4464 \qquad (6.13)$$

6.3.3.3 Other parameters Substituting the values of $\dot{m}_{ainf}$ from eauation (6.12) and of dT_a/dT from equation (6.13) into equation (6.8)

$$K_2 = -311.24 \qquad (6.14)$$

Using this value of K_2, and the data on ERH in Appendices F and G, we find from equations (6.3)-(6.5)

$$K_{T_i} = \frac{1704.96}{1704.96 + 480.01 - 311.24} = 0.91$$

$$K_{T_a} = \frac{480.01}{1704.96 + 480.01 - 311.24} = 0.26$$

$$\tau_{os} = \frac{1995.38}{1704.96 + 480.01 - 311.24} = 1.06 \text{ hrs}$$

Also from equation (6.6), we get by taking inverse Laplace Transform

$$\Delta T(t) = \frac{K_{T_a}\left(1 - e^{-t/\tau_{os}}\right)}{1 - K_{T_i}\left(1 - e^{-t/\tau_{os}}\right)} \Delta T_a(t) \qquad (6.15)$$

Table 6.2. Data sheet on experimental validation of rational model (open-loop mode); date, July 26-27, 1979; remarks, 1) fan on, 2) HVAC system off, 3) temperature in °C

Time	Soil temperatures °C			Wind velocity miles/hr	Outdoor air temp °C	Green-house temp °C	SW bed-room temp °C	NW bed-room temp °C	Living room temp °C	Base-ment temp °C
	26" deep	80" deep	134" deep							
01:00	19.7	21.7	24.7	6.550	22.5	23.4	29.3	28.8	28.3	27.9
01:15	19.7	21.7	24.7	6.476	21.7	23.1	29.2	28.8	28.4	28.0
01:30	19.7	21.7	24.7	6.470	21.1	23.2	29.2	28.8	28.4	28.0
01:45	19.7	21.7	24.7	6.396	20.6	22.6	29.2	28.8	28.4	28.0
02:00	19.7	21.7	24.7	6.338	20.2	22.3	28.2	28.8	28.4	28.0
02:15	19.7	21.7	24.7	6.319	19.8	21.9	29.2	28.8	28.3	27.9
02:30	19.7	21.7	24.7	6.341	19.6	21.7	29.1	28.8	28.4	28.0
02:45	19.7	21.7	24.7	6.292	19.4	21.6	29.0	28.8	28.3	27.9
03:00	19.7	21.7	24.7	6.248	19.1	21.2	29.0	28.8	28.2	27.9
03:15	19.7	21.7	24.7	6.277	18.9	21.1	28.9	28.7	28.2	28.0
03:30	19.7	21.7	24.7	6.267	18.7	21.0	28.9	28.7	28.1	27.9
03:45	19.7	21.6	24.7	6.271	18.5	21.8	28.8	28.7	28.1	27.9
04:00	19.7	21.8	24.7	6.187	18.3	20.5	28.6	28.7	28.1	27.9
04:15	19.7	21.7	24.7	6.221	18.2	20.5	28.7	28.6	28.1	27.9
04:30	19.7	21.7	24.7	6.181	18.3	20.7	28.7	28.6	28.1	27.8
04:45	19.7	21.7	24.7	6.169	18.1	20.6	28.6	28.5	28.1	27.8
05:00	19.7	21.7	24.7	6.194	17.8	20.4	28.6	28.6	28.0	27.8
05:15	19.7	21.7	24.7	6.180	17.6	20.3	28.6	28.5	28.0	27.8
05:30	19.7	21.7	24.7	6.154	17.5	20.2	28.5	28.5	28.0	27.7
05:45	19.7	21.7	24.7	6.146	17.4	20.0	28.5	28.5	27.9	27.8
06:00	19.7	21.7	24.8	6.138	17.4	20.0	28.5	28.5	27.9	27.7
06:15	19.7	21.7	24.8	6.130	17.5	18.9	28.4	28.4	27.9	27.7

Table 6.3. Comparison of predicted and measured indoor air temperatures as a function of ambient air temperature at ERH on July 26-27, 1979

Time	Average measured ambient temp T_a (°C)	$\Delta T_a = \frac{\Delta T_{GH} + \Delta T_{oA}}{2}$ (°C)	Calculated ΔT (°C)	Average measured indoor air temp T (°C)	Predicted indoor air temp (°C)
01:15	22.28	-0.25	-0.02	28.60	28.56
01:30	22.11	-0.55	-0.04	28.60	28.52
01:45	21.74	-0.35	-0.02	28.60	28.50
02:00	21.51	-0.40	-0.03	28.60	28.47
02:15	21.24	-0.20	-0.01	28.55	28.46
02:30	21.11	-0.15	-0.01	28.57	28.45
02:45	21.01	-0.35	-0.02	28.50	28.43
03:00	20.78	-0.15	-0.01	28.48	28.42
03:15	20.68	-0.15	-0.01	28.45	28.40
03:30	20.58	-0.20	-0.01	28.40	28.40
03:45	20.43	-0.25	-0.02	28.38	28.38
04:00	20.29	+0.10	+0.01	28.33	28.39
04:15	20.34	0.00	0.00	28.35	28.39
04:30	20.34	-0.15	-0.01	28.30	28.38
04:45	20.24	-0.25	-0.02	28.25	28.36
05:00	20.08	-0.15	-0.01	28.25	28.35
05:15	19.98	-0.10	-0.01	28.23	28.35
05:30	19.91	-0.15	-0.01	28.18	28.34
05:45	19.81	-0.00	-0.00	28.18	28.34
06:00	19.46	-1.10	-0.07	28.15	28.25

6.3.3.4 Results Using the values of K_{Ta}, K_{Ti}, τ_{os} and measured values of $\Delta T_a(t)$ in equation (6.15), predicted values of $\Delta T(t)$ and indoor air temperatures were calculated. These values are tabulated in Table 6.3 for July 26-27, 1979, and in Table 6.4 for August 1-2, 1979. Comparison of predicted and measured values of indoor air temperatures for these dates is shown in Figure 6.9. Sample calculations based on equation (6.15) are shown in Appendix H where the data for August 1-2, 1979 are also analyzed.

6.4 Closed-Loop Mode

Mathematical models to describe the closed-loop performance of systems for environmental control were derived in Chapter 5. Analysis of experimental data carried out in Section 6.3 has validated the rational model in open-loop mode with an accuracy of ±0.16°C. So work is pursued in this section to test the validity of the rational model in a closed-loop mode.

6.4.1 Theory

The mathematical model derived in Section 5.1 describes the dynamic performance of a heating system for a single family residence. Facilities available at the Iowa State University Energy Research House were used to validate the model of the heating system for a single family residence described by equation (5.1) which does not couple the responses of the occupant. Use of equation (5.1) is valid because no action was taken in response to the desired of the occupant to change set point. Equation (5.1) is reproduced below:

Table 6.4. Comparison of predicted and measured indoor air temperatures as a function of ambient air temperature at ERH on August 1-2, 1979

Time	Average measured ambient temp T_a (°C)	$\Delta T_a = \frac{\Delta T_{GH} + \Delta T_{oA}}{2}$ (°C)	Calculated ΔT (°C)	Average measured indoor air temp T (°C)	Predicted indoor air temp (°C)
23:30	21.53	-0.10	-0.01	27.43	27.39
23:45	21.47	-0.25	-0.02	27.43	27.38
00:00	21.30	-0.15	-0.01	27.43	27.37
00:15	21.20	-0.40	-0.03	27.43	27.34
00:30	20.93	-0.20	-0.01	27.40	27.33
00:45	20.79	-0.25	-0.02	27.38	27.31
01:00	20.63	-0.05	-0.01	27.35	27.31
01:15	20.60	-0.10	-0.01	27.35	27.30
01:30	20.53	-0.40	-0.03	27.35	27.27
01:45	20.40	-0.10	-0.01	27.30	27.27
02:00	20.37	-0.10	-0.01	27.33	27.27
02:15	20.30	-0.20	-0.01	27.25	27.25
02:30	20.17	-0.15	-0.01	27.23	27.24
02:45	20.07	-0.15	-0.01	27.25	27.23
03:00	19.97	-0.15	-0.01	27.18	27.22
03:15	19.87	-0.10	-0.01	27.15	27.22
03:30	19.83	-0.30	-0.02	27.13	27.20
03:45	19.63	-0.30	-0.02	27.10	27.18
04:00	19.43	-0.40	-0.03	27.10	27.15

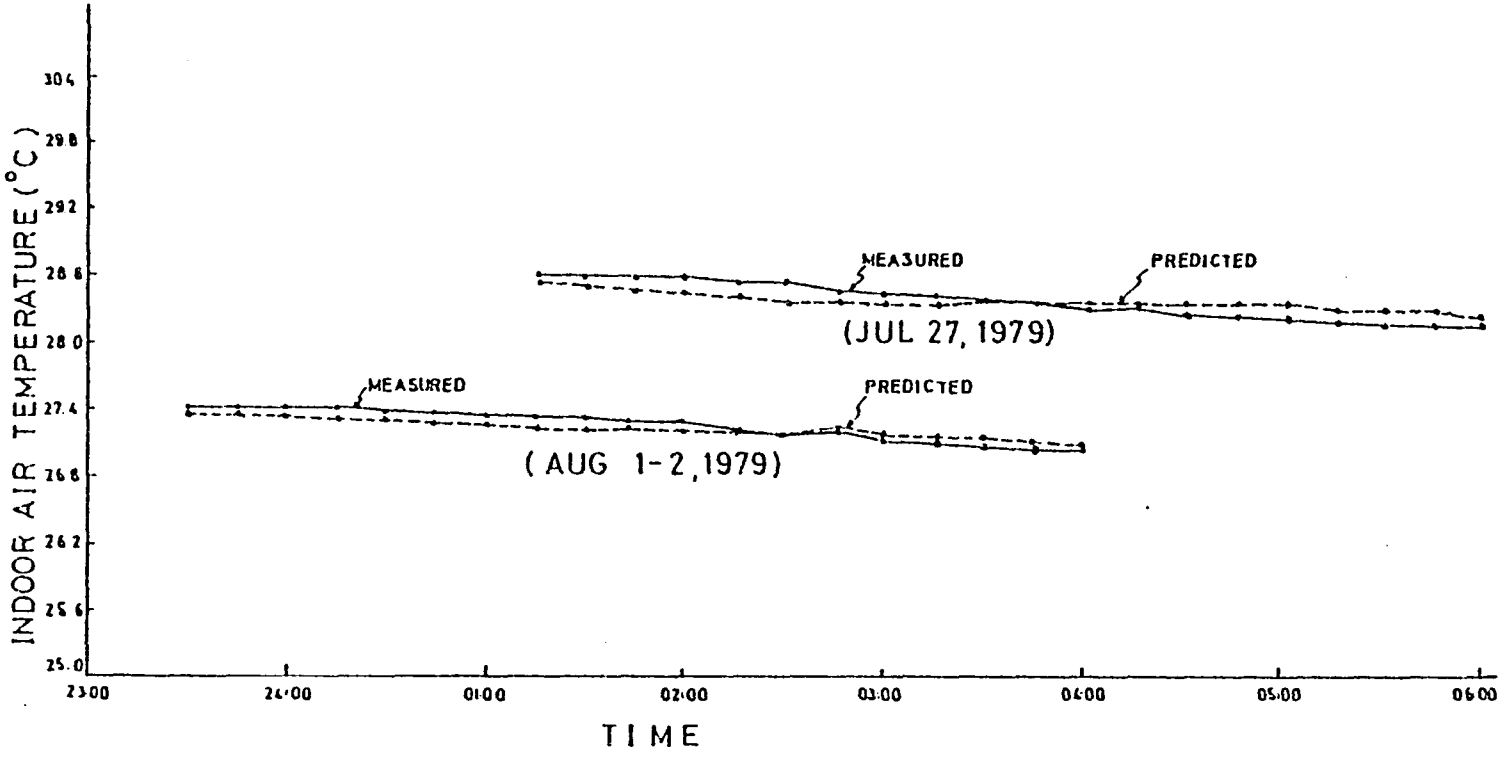

Figure 6.9. Predicted and measured indoor air temperatures under open-loop conditions at ERH.

$$\Delta T(s) = \frac{(KK_{\dot{Q}})(1 + \tau_s S)}{S[(1 + \tau_{os} S)(1 + \tau_s S) + KK_{\dot{Q}} K_s]} \Delta T_{set}(s)$$

$$+ \frac{K_{\dot{Q}}(1 + \tau_s S)}{S[(1 + \tau_{os} S)(1 + \tau_s S) + KK_{\dot{Q}} K_s]} (\Delta \dot{Q}_{occ} + \Delta \dot{Q}_f + \Delta \dot{Q}_{int})$$

$$+ \frac{K_{Ti}}{S(1 + \tau_{os} S)} \Delta T_i(s) + \frac{K_{Ta}}{S(1 + \tau_{os} S)} \Delta T_a(s) \qquad (5.1)$$

Under the conditions

$$\Delta T_{set}(s) = 0$$

$$\Delta \dot{Q}_{occ}(s) = 0$$

$$\Delta \dot{Q}_{int}(s) = 0$$

Equation (5.1) is reduced to

$$\Delta T(s) = \frac{K_{\dot{Q}}(1 + \tau_s S)}{S[(1 + \tau_{os} S)(1 + \tau_s S) + KK_{\dot{Q}} K_s]} \Delta \dot{Q}(s)$$

$$+ \frac{K_{Ti}}{S(1 + \tau_{os} S)} \Delta T_i(s) + \frac{K_{Ta}}{S(1 + \tau_{os} S)} \Delta T_a(s) \qquad (6.16)$$

Equation (6.16) is used to predict the dynamic responses of temperature inside ERH.

6.4.2 Procedures

1. Instrumentation and procedures used for measurements of inside temperatures and weather conditions were the same as used for open-loop validation and described in Section 6.3.2.1.
2. Instrumentation and procedures used for simultaneous measurements on infiltration rates were the same as used for open-loop validation and described in Section 6.3.2.2.

3. Experimental data were taken during night times for reasons mentioned in Section 6.3.2.1.

4. On the night of test, HVAC system of ERH was switched to the electric resistance heating mode and time was recorded when the electric heat was turned on.

5. Time was recorded when the space temperature was equal to the set point. After that the system was allowed to cycle automatically and a record was maintained of ON and OFF periods for the system. A record for the test on July 23-24, 1979 is shown in Table 6.5. The methane leakage curve for the same night is shown in Figure 6.10. During the ON-OFF cycling, temperatures were recorded every half a minute. Data on indoor air temperatures and weather conditions at every change of status of furnace during ON-OFF cycling are given in Table 6.6.

6.4.3 Data analysis

Experimental data are analyzed for infiltration rates, temperatures and other parameters in the following sections.

6.4.3.1 Infiltration rates Using the methane leakage curve in Figure 6.10, data on methane concentration as a fraction of total charge are tabulated in Table 6.7. Using the method of least squares, it can be written

$$\tau_{leak} = \frac{n\left(\sum_{i=1}^{n} x_i t_i\right) - \left(\sum_{i=1}^{n} x_i\right)\left(\sum_{i=1}^{n} t_i\right)}{n\left(\sum_{i=1}^{n} x_i^2\right) - \left(\sum_{i=1}^{n} x_i\right)^2} \qquad (6.17)$$

where n is the total number of points in Table 6.7.

Table 6.5. Record of status of furnace operation during cycling on July 23-24, 1979

	Time at which furnace turned ON	Time at which furnace turned OFF
1	01:39:30	01:46:30
2	01:59:00	02:03:30
3	02:17:00	02:23:00
4	02:35:00	02:41:30
5	02:54:00	02:59:30
6	03:11:30	03:19:00
7	03:31:30	03:38:30
8	03:51:30	03:57:00
9	04:11:30	04:17:00

$$\tau_{leak} = \frac{14(2241.78) - (16.34)(1533)}{14(23.12) - (16.34)^2}$$

$$= 111.78 \text{ minutes}$$

In 111.78 minutes, leakage = 0.632

in 60 minutes, leakage $= \frac{60 \times 0.632}{11.78}$

$$= 0.34$$

Hence infiltration rate = 0.34 air changes/hour

in $\dot{m}_{ainf}$ = 16950 x 0.34 x 0.074

= 426.46 lbm/hour (193.41 Kg/hour)

6.4.3.2 Temperatures Measured average indoor air temperatures and measured average outdoor air temperatures for the first ON cycle of the furnace were computed and are shown in Table 6.8. From the data given in Table 6.8, we can calculate dT_a/dT by the method of least squares as

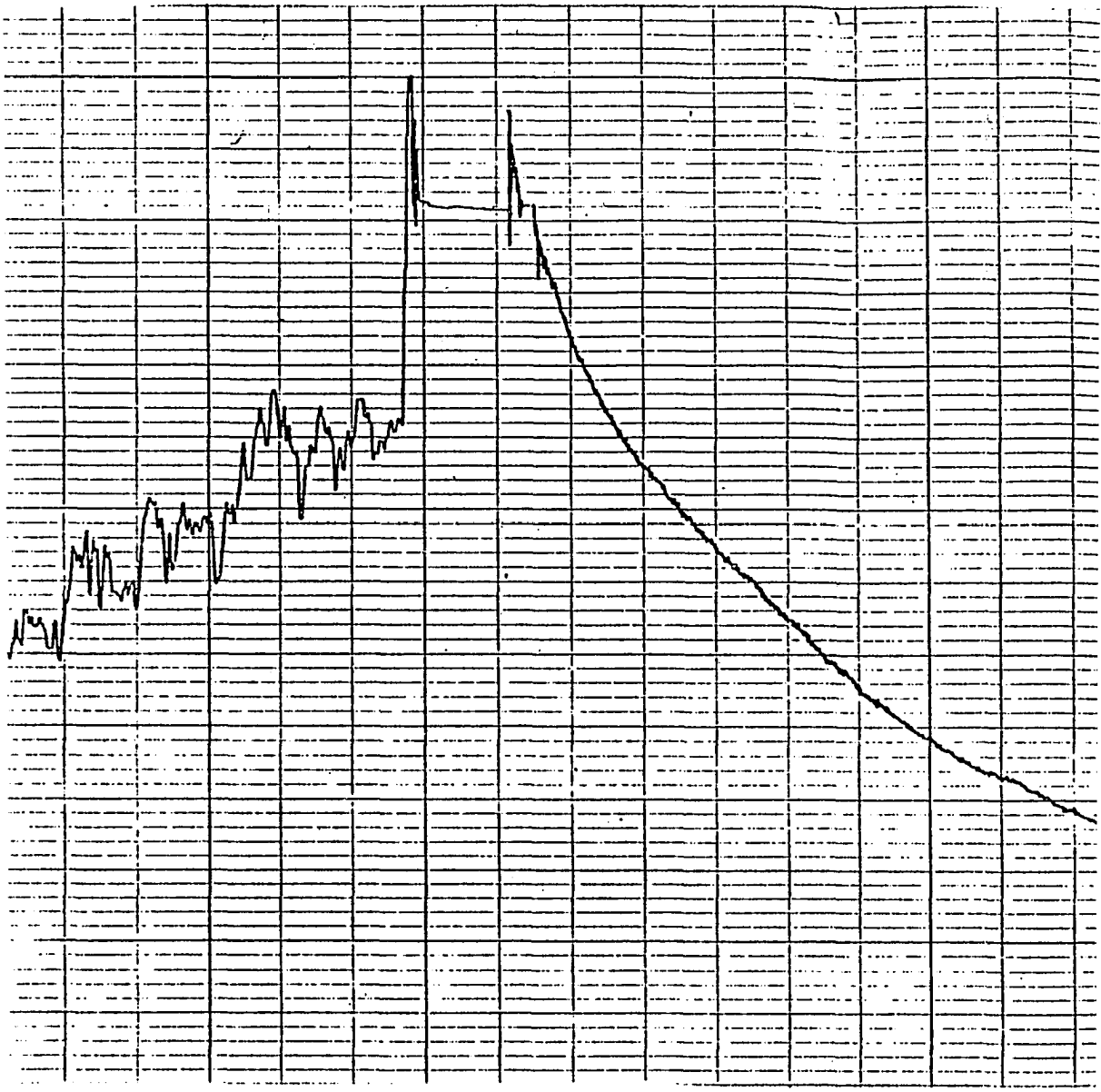

Figure 6.10. Strip chart recorder plot for methane leakage (night of July 23-24, 1979). Maximum charge: 500 ppm; chart speed: 4 cms/hour; status: closed-loop mode test.

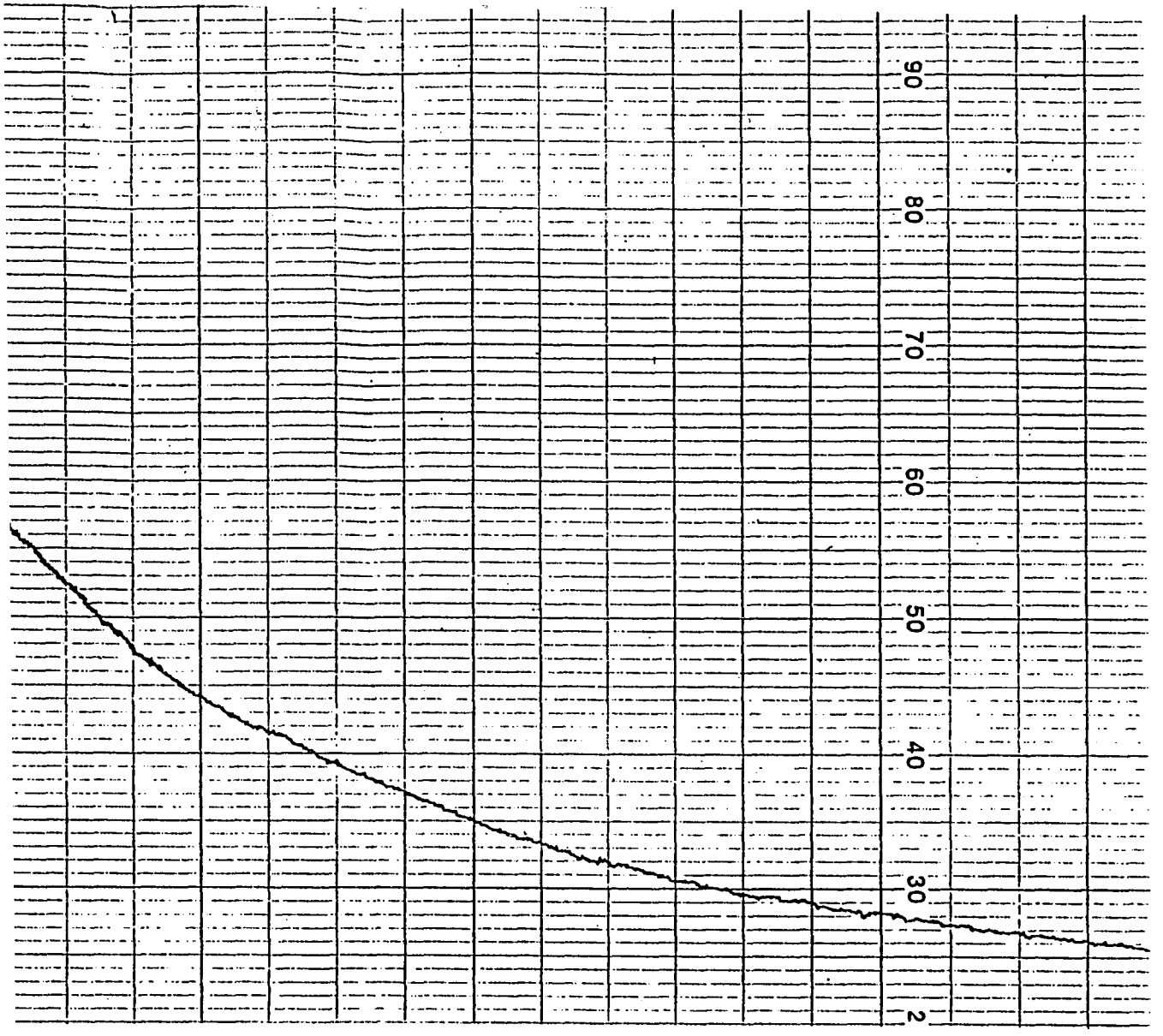

.eakage (night of July
1; chart speed: 4
it.

Table 6.6. Data sheet on experimental validation of rational model; date, July 23-24, 1979; remarks, 1) electric heat on, 2) automatic cycling of the furnace

Time	Soil temperatures °C			Wind velocity miles/hr	Outdoor air temp °C	Green-house temp °C	SW bed-room temp °C	NW bed-room temp °C	Living room temp °C	Base-ment temp °C
	26" deep	80" deep	134" deep							
01:39:30	19.3	21.3	24.4	6.591	23.6	24.3	30.2	30.1	30.9	29.2
01:46:30	19.3	21.3	24.4	6.601	23.5	24.6	31.1	30.5	32.1	29.9
01:59:00	19.3	21.3	24.4	6.594	23.4	24.5	30.2	30.1	31.0	29.4
02:03:30	19.3	21.3	24.4	6.592	23.5	24.4	31.0	30.5	32.0	29.8
02:17:00	19.3	21.3	24.4	6.596	23.4	24.5	30.3	30.2	30.9	29.3
02:23:00	19.3	21.3	24.4	6.595	23.3	24.2	31.2	30.6	32.1	29.9
02:35:00	19.3	21.3	24.4	6.579	23.2	24.3	30.2	30.2	30.9	29.4
02:41:30	19.3	21.3	24.4	6.573	23.3	24.3	31.1	30.7	32.1	30.5
02:54:00	19.3	21.3	24.4	6.544	23.2	24.2	30.3	30.2	30.9	29.5
02:59:30	19.3	21.3	24.4	6.535	23.2	24.1	31.2	30.7	32.1	29.9
03:11:30	19.3	21.3	24.4	6.469	23.0	24.0	30.3	30.3	30.8	29.5
03:19:00	19.3	21.3	24.4	6.431	23.0	24.1	31.2	30.7	32.1	30.5
03:31:30	19.3	21.3	24.4	6.458	23.0	24.1	30.3	30.3	30.8	29.6
03:38:30	19.3	21.3	24.4	6.458	22.9	24.1	31.0	30.7	32.0	30.3
03:51:30	19.3	21.3	24.4	6.455	22.1	23.4	30.3	30.4	30.9	29.6
03:57:00	19.4	21.3	24.4	6.445	22.0	24.1	31.2	30.9	32.3	30.4
04:11:30	19.3	21.3	24.4	6.416	21.8	23.8	30.3	30.4	30.9	29.6
04:17:00	19.3	21.3	24.4	6.424	21.8	23.7	31.2	30.9	32.1	30.3

Table 6.7. Methane concentration and time elapsed after charging (from Figure 6.10 for the night of July 23-24, 1979, closed-loop test)

Point No.	Methane concentration C (fraction of total charge)	ln C (x)	Time (minutes) t
1	0.88	-0.13	12
2	0.63	-0.46	27
3	0.56	-0.58	42
4	0.48	-0.73	57
5	0.41	-0.89	72
6	0.35	-1.05	87
7	0.32	-1.14	102
8	0.28	-1.27	117
9	0.25	-1.39	132
10	0.22	-1.51	147
11	0.20	-1.61	162
12	0.18	-1.71	177
13	0.15	-1.90	192
14	0.14	-1.97	207

$$\frac{dT_a}{dT} = \frac{n\left(\sum_{i=1}^{n} T_i T_{ai}\right) - \left(\sum_{i=1}^{n} T_i\right)\left(\sum_{i=1}^{n} T_{ai}\right)}{n\left(\sum_{i=1}^{n} T_i^2\right) - \left(\sum_{i=1}^{n} T_i\right)^2}$$

$$= \frac{12(8335.71) - (342.75)(292.06)}{12(9820.26) - (342.75)^2}$$

$$= -0.2053 \qquad (6.18)$$

6.4.3.3 Other parameters Substituting the value of $\dot{m}_{ainf}$ from equation (6.17) and of dT_a/dT from equation (6.18) into equation (6.8):

$$K_2 = 123.36 \qquad (6.19)$$

Table 6.8. Measured ambient and indoor air temperature during the first ON cycle of furnace at ERH on July 23-24, 1979

Time	Average measured ambient temperature T_a (°C)	Average measured indoor air temperature T (°C)
21:30:00	24.96	25.08
21:45:00	24.86	26.55
22:00:00	24.56	27.30
22:15:00	24.49	27.80
22:30:00	24.36	28.25
22:45:00	24.40	28.53
23:00:00	24.33	29.05
23:15:00	24.22	29.45
23:30:00	24.10	29.73
00:00:00	24.03	30.03
00:15:00	23.89	30.35
	23.86	30.63

From Table 6.5 it can be seen that for the period 01:39:30 to 04:17:00 (2.63 hours), furnace was on for 0.92 hours. Therefore, from equation (3.24)

$$K_1 = \frac{\dot{dQ}_{inf}}{\dot{dQ}} = \frac{2.63 \times 102.35(87.10 - 73.10)}{0.92 \times 43102.5}$$

$$= 0.09 \qquad (6.20$$

Using the values of K_1, K_2 and the data on ERH in Appendices F and G, and from equations (6.2)-(6.5)

$$K_{\dot{Q}} = \frac{1 - .091}{1704.96 + 480.01 + 123.36} = 0.0003$$

$$K_{Ti} = \frac{1704.96}{1704.96 + 480.01 + 123.36} = \frac{1704.96}{23.08.33} = 0.79$$

$$K_{Ta} = \frac{480.01}{1704.96 + 480.01 + 123.36} = \frac{480.01}{2308.33} = 0.21$$

$$\tau_{os} = \frac{1995.35}{1704.96 + 480.01 + 123.36} = \frac{1995.35}{2308.33} = 0.87 \text{ hours} \qquad (6.21)$$

and K = 1 for furnace ON.

6.4.3.4 Results Predicted values of ΔT calculated from equation (6.16) using the parameters of equation (6.21) at the end of 9 different ON cycles of the furance are tabulated in Table 6.9. Actual measured indoor air temperatures and predicted indoor air temperatures at the end of each ON cycle are plotted in Figure 6.11. Comparison of measured and predicted values of indoor air temperatures reveals that the mathematical model can predict the dynamic conditions of indoor air temperature within ±0.1°C. Average measured indoor air temperatures fluctuated between 30.10°C to 31.20°C while the predicted values of indoor air temperature fluctuated between 30.10°C to 31.13°C. Thus, the mathematical model can predict the peaks and excursions of indoor air temperatures within ±0.07°C. The capability of the model to accurately predict the peaks and excursions of indoor air temperatures accurately can be used to predict the differential and the cycling patterns of a residential heating system.

To conclude, the rational model was validated both in the open loop and closed loop modes in this chapter. It was shown that for the ISU Energy Research, the rational model can predict space temperatures with a maximum deviation of ±0.16°C. Conversely, if the propagation of uncertainties in the parameters used to calculate space temperatures are considered as shown in Appendix H, the predicted space temperatures can have ±10% uncertainty in their values. Thus, for the ERH, predicted space temperatures should be within 0.35°C of the measured values for acceptability.

Table 6.9. Comparison of predicted and measured indoor air temperatures as a function of ambient air temperature at ERH at the end of 9 ON cycles in closed-loop operation on July 23-24, 1979

Furnace status	Time	Average measured ambient temperature T_a (°C)	ΔT_a (°C)	Calculated ΔT (°C)	Average measured indoor temperature T (°C)	Predicted indoor air temperature T (°C)
ON	01:39:30	23.19	-0.07		30.10	
OFF	01:46:30	23.15	-0.04	+0.89	30.90	30.99
ON	01:59:00	23.19	+0.04		30.18	
OFF	02:03:30	23.19	0.00	+0.56	30.83	30.74
ON	02:17:00	23.19	0.00		30.18	
OFF	02:23:00	23.06	-0.10	+0.75	30.95	30.93
ON	02:35:00	23.06	0.00		30.18	
OFF	02:41:30	23.09	+0.03	+0.83	31.10	31.01
ON	02:54:00	23.01	-0.08		30.23	
OFF	02:59:30	22.99	-0.02	+0.70	30.98	30.93
ON	03:11:30	23.56	+0.57		30.23	
OFF	03:19:00	22.92	+0.36	+1.00	31.13	31.23
ON	03:31:00	22.92	0.00		30.25	
OFF	03:38:30	22.89	-0.03	+0.85	31.00	31.10
ON	03:51:30	22.39	-0.50		30.30	
OFF	03:57:00	22.59	+0.20	+0.83	31.20	31.13
ON	04:11:30	22.42	-0.17		30.30	
OFF	04:17:00	22.39	-0.03	+0.83	31.13	31.13

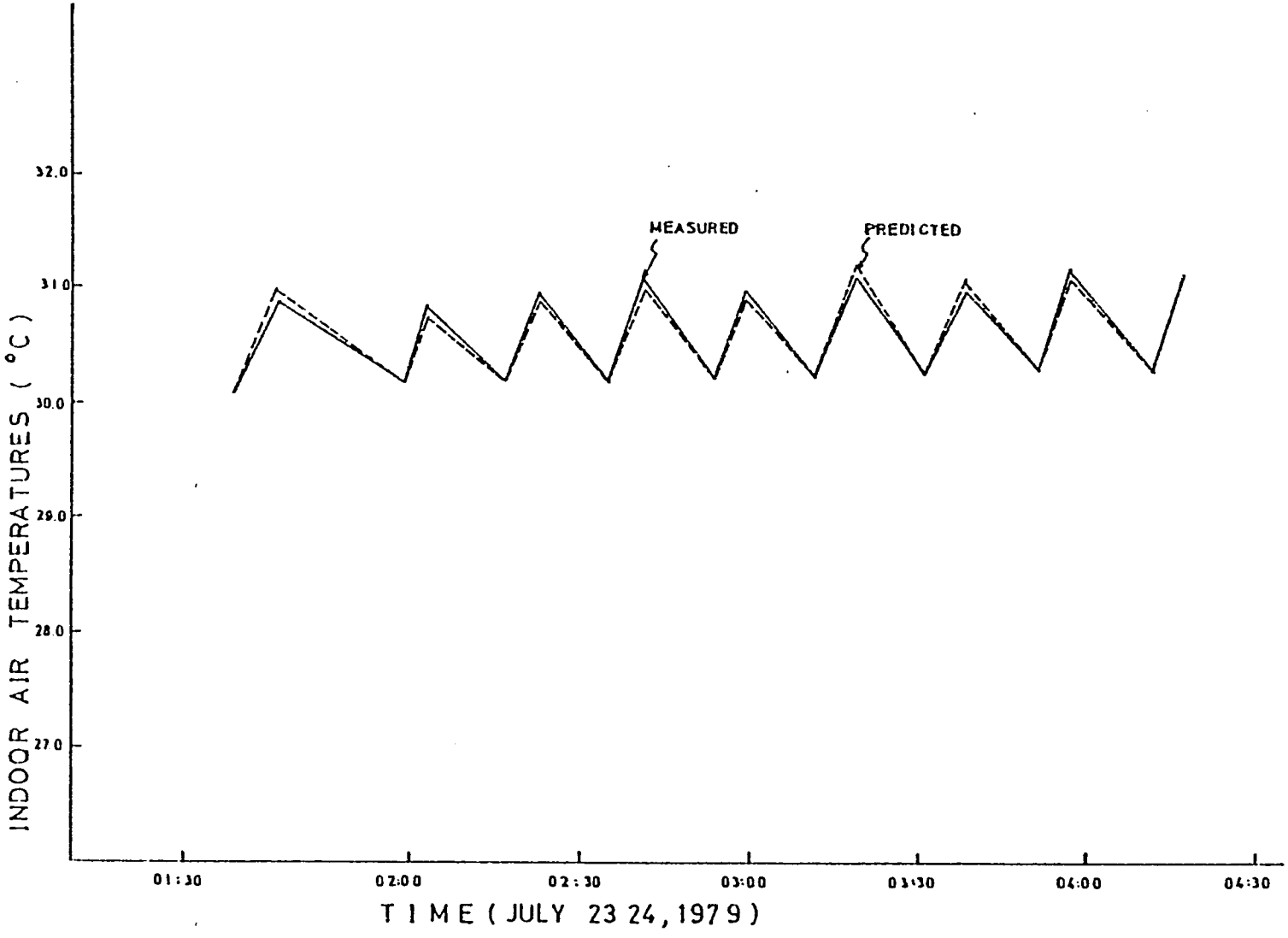

Figure 6.11. Predicted and measured indoor air temperatures in closed-loop mode (July 23-24, 1979).

7. BUILDING SYSTEMS PERFORMANCE ANALYSIS

Rational model to predict dynamic conditions was proposed in Section 3.3 and the experimental validation of a rational model was presented in Chapter 6. The experimental validation showed that the model can predict dynamic conditions inside ERH within ±0.16°C. Some applications of the model to analyze building systems performance have been discussed in this chapter.

7.1 Effects of Control Dynamics on Energy Consumption

The rational model, developed in Section 3.3, has been used in this section to determine the effects of control system dynamics on energy consumption in buildings. The residential heating system shown in Figure 3.14 and Figure 7.1 was analyzed using the following assumptions:

1. The control mode was two position. As the boundary of the occupied space in Figure 7.1 is drawn across the furnace, the dynamics of the safety switches were considered to be included as a part of two position controller.
2. Energy was transferred to the occupied space only by the furnace, $\dot{Q}_f$.
3. Heat was transferred from the occupied space to the surroundings through the envelope. Solar radiations, infiltration and internal loads generated by occupants and lights were all considered as modifiers to a net heat load term, $\dot{Q}_{out}$
4. Changes in stored energy were only due to changes in the dry bulb temperature of occupied space.

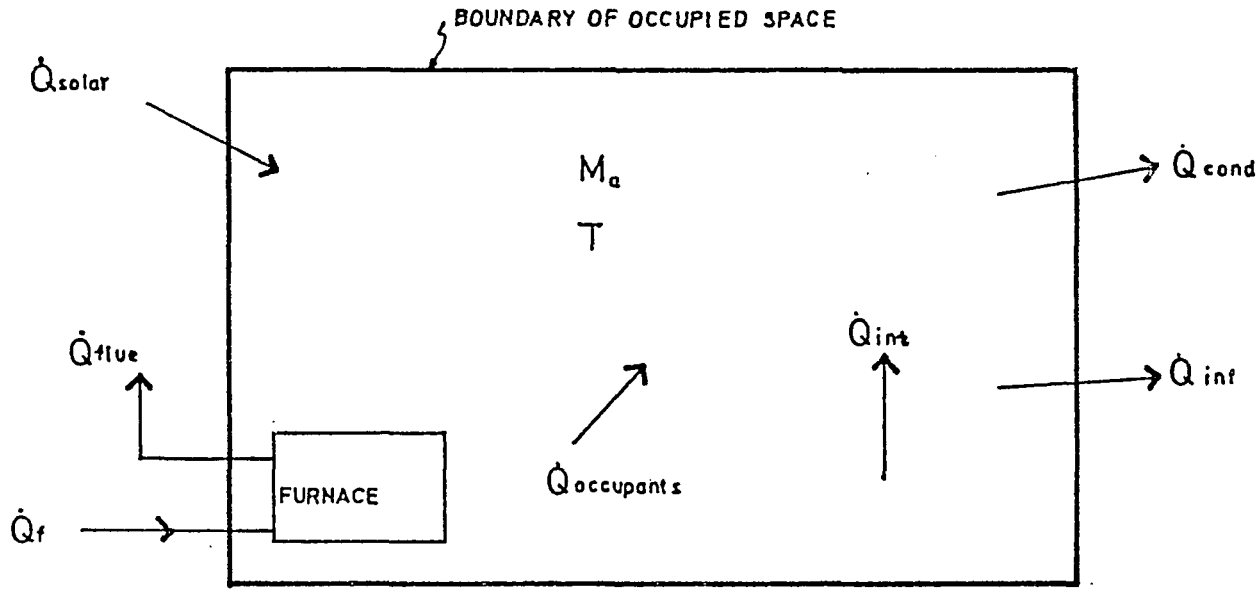

$$\dot{Q}_{out} = \left|(\dot{Q}_{occupants} + \dot{Q}_{int} + \dot{Q}_{solar}) - (\dot{Q}_{cond} + \dot{Q}_{inf} + \dot{Q}_{flue})\right|$$

$$\text{when } (\dot{Q}_{cond} + \dot{Q}_{inf} + \dot{Q}_{flue}) > (\dot{Q}_{occupant} + \dot{Q}_{int} + \dot{Q}_{solar})$$

$$\dot{Q}_{out} = -[(\dot{Q}_{occupants} + \dot{Q}_{int} + \dot{Q}_{solar}) - (\dot{Q}_{cond} + \dot{Q}_{inf} + \dot{Q}_{flue})]$$

$$\text{when } (\dot{Q}_{occupants} + \dot{Q}_{int} + \dot{Q}_{solar}) > (\dot{Q}_{cond} + \dot{Q}_{inf} + \dot{Q}_{flue})$$

Figure 7.1. Thermal processes to describe heat transfers in equation (7.1).

5. Storage effects of structure were neglected due to their slow dynamic responses.
6. Storage effects of furniture were considered to be a part of changes in stored energy of the air mass in an occupied space.

From the above assumptions, equation (3.15) may be simplified:

$$\dot{Q}_f = \dot{Q}_{out} + M_a c_{pa} \frac{dT}{dt} \tag{7.1}$$

or

$$\left(\frac{dT}{dt}\right)_{\substack{\text{Furnace}\\ \text{ON}}} = \frac{\dot{Q}_f - \dot{Q}_{out}}{M_a c_{pa}} \tag{7.2}$$

$$\left(\frac{dT}{dt}\right)_{\substack{\text{Furnace}\\ \text{OFF}}} = \frac{-\dot{Q}_{out}}{M_a c_{pa}} \tag{7.3}$$

So, for a given thermostat differential, the rate of increase or decrease of indoor air temperature depends on the heating load, $\dot{Q}_{out}$, which varies throughout the heating season. Results are shown in Table 7.1 and Figure 7.2 for an average dwelling of floor area 139.2 m^2, using two different thermostat differentials (2.22°C and 3.33°C); two heating loads, one at the design temperature (-23.33°C) and the other at 50% of the maximum heating load; and three different furnace capabilities (38.0 MJ/hr, 26.4 MJ/hr, and 21.1 MJ/hr). Results include total ON period, total OFF period and the cycles per day of the system. A sample calculation is shown in Appendix I.

7.1.1 Effects of over-capacity and part load operation on cycling and energy consumption

For a thermostat differential of 2.22°C, it can be seen from Figure 7.2 that with a furnace capacity of 21.1 MJ/hr (25% over-capacity), the

Table 7.1. A sensitivity analysis derived from a simple dynamic model

Differential ΔT_h	Furnace capacity $\dot{Q}_f$(J/hr)	Heating load $\dot{Q}_{out}$(J/hr)	Minutes on per cycle	Minutes off per cycle	Time period minutes	Hours on per day	Hours off per day	Cycles per day
2.22°C	3.80×10^7	1.690×10^7	2.58	3.23	5.81	10.66	13.34	248
		0.845×10^7	1.84	6.45	8.29	5.33	18.67	174
	2.64×10^7	1.690×10^7	5.73	3.69	9.42	14.66	9.40	152
		0.845×10^7	3.04	6.45	9.50	7.68	16.33	152
	2.11×10^7	1.690×10^7	12.91	3.23	16.16	19.17	4.83	90
		0.845×10^7	4.30	6.45	10.75	9.60	14.40	134
3.33°C	3.80×10^7	1.690×10^7	3.87	4.84	8.71	10.66	13.34	165
		0.845×10^7	2.77	9.68	12.45	5.34	18.66	116
	2.64×10^7	1.690×10^7	8.61	5.54	14.15	14.64	9.36	102
		0.845×10^7	4.56	9.68	14.25	7.68	16.32	101
	2.11×10^7	1.690×10^7	19.36	4.84	24.20	19.20	4.80	60
		0.845×10^7	6.45	9.68	16.13	9.60	14.40	80

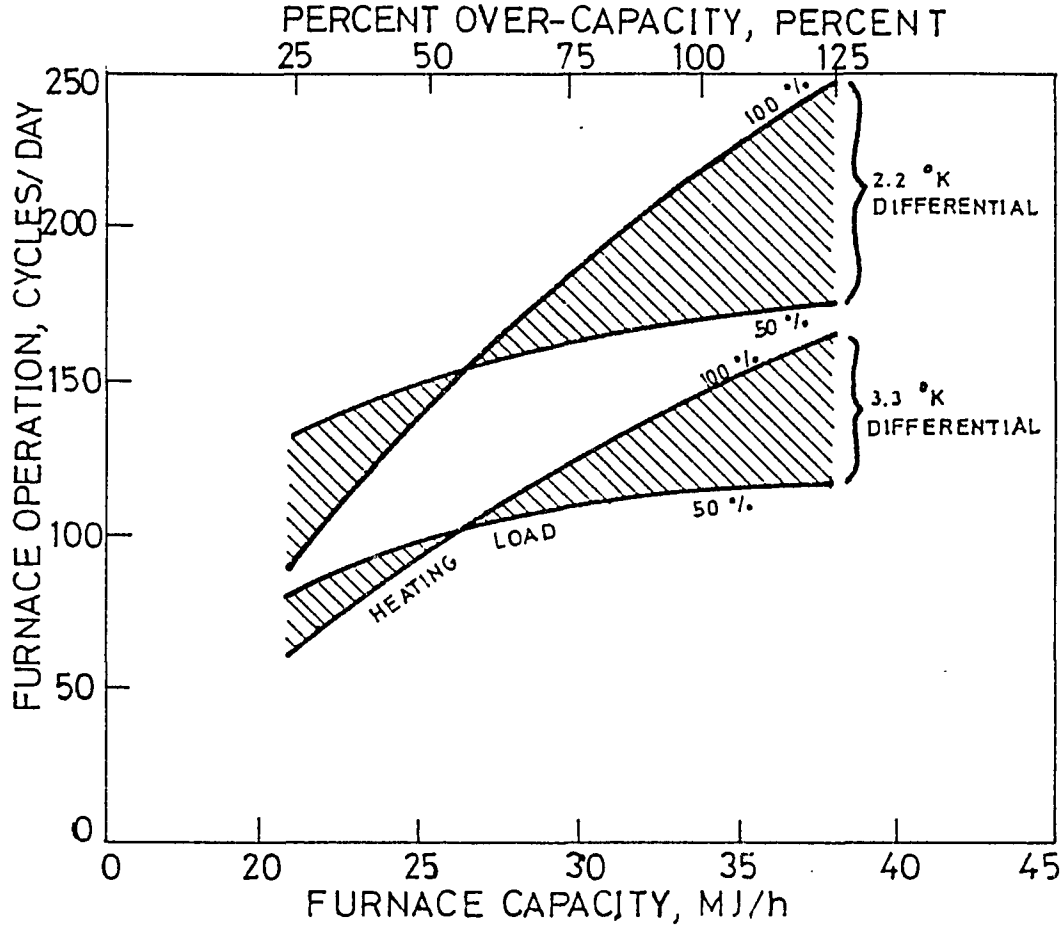

Figure 7.2. Furnace cycles per day as a function of heating load, furnace capacity and thermostat differential.

number of cycles increases from 90 cycles/day to 134 cycles/day when the heating load is reduced to 50% of the design value. Increased cycling at part load operation due to lower installed capacity (25% over-capacity) has been considered by the designers (25) to be detrimental to the system and the practice is to install a furnace with higher over-capacity (100%-200%) so that cycling reduces at part load operation. Certain "rules of thumb" have been devised to size furnaces with over-capacity to reduce cycling at part load operation.

One rule of thumb used by contractors in the midwest is to use about 0.113 MJ/hr m^3 for above ground space and 0.09 MJ/hr m^3 for basement space. Using this rule, the installed furnace capacity for the example shown in Table 7.1 should be 38.0 MJ/hr (125% over-capacity). At this capacity (125% over-capacity), the cycling rate reduces from 248 cycles/day at 100% load to 174 cycles/day at 50% load. However, with 25% over-capacity the actual number of cycles at 50% load would have been 134 cycles/day instead of 174 cycles/day. Thus, the current design practice fails to achieve the real objective of having fewer cycles/day at part load operation.

Bonne et al. (110) have reported that the seasonal efficiency of a residential combustion heating system is dependent upon the cycling patterns. Based upon their model HFLAME, they have reported an efficiency for a residential furnace of 60.97% at 72 cycles/day and only 58.42% at 240 cycles/day. Thus, a properly sized furnace (having over-capacity to the left side of the crossover in Figure 7.2) can result in lower cycles/day (compared to the over-capacity to the right side of the crossover in

Figure 7.2) which means higher seasonal efficiency and lower energy consumption.

7.1.2 Effects of thermostat differential on cycling and energy consumption

For a furnace with over-capacity to the left side of the crossover in Figure 7.2, the number of cycles/day increases at part load operation. Thus, the seasonal efficiency will be expected to reduce at part load operation though it is still higher than a furnace with over-capacity to the right of the crossover. It can be seen from Figure 7.2 that for a given over-capacity, on the left side of the crossover, the percent increase in cycles/day at part load operation reduces if the thermostat differential is increased from 2.2°K to 3.3°K. Thus, a reduction in part load efficiency on the left side of the crossover can be compensated to save fuel by increasing the differential of the thermostat. However, fuel saving strategies based on variations of thermostat differential or changes in number of cycles/hour must include considerations of the occupant's dynamic responses which were discussed in Section 2.1.2.

7.2 New Control Strategies for Energy Conservation

In Section 7.1 it has been shown that the dynamics of a control system have a significant influence on the efficiency and hence the energy consumption of a residential heating system. For the two-position control system, it was shown that for certain conditions increasing the differential of the thermostat can be used to advantage to reduce cycles per day and to increase the efficiency of a residential heating system. Review of

different studies on the effects of thermal transients in Section 2.1.2 indicates that wide variations in dry bulb temperatures, relative humidities, and their respective rates of change are acceptable factors to occupants at normal levels of activity and clothing. The studies reviewed in Section 2.1.2 do not include any information on the dynamics of occupant as a feedback component as identified in Section 4.8. Moreover, no information is available on the influences of clothing or activity level on the dynamics of the occupants. So it is suggested that future research efforts should be directed in the area. The limited information available from reviews in Section 2.1.2 can be used at present as a basis from which specific energy management program can be developed. In particular, the following control strategies may be derived from the discussions in Sections 2.1.2 and 7.1.

7.2.1 Thermal strategies

Thermal strategies to be derived from the discussions in Sections 2.1.2 and 7.1 may be divided into a) active control strategies and b) passive control strategies.

7.2.1.1 Active control strategies For energy efficient design of new residential heating systems, the following procedures are suggested:

1. Calculate the design heat load and for the maximum acceptable temperature fluctuations (4.5 K - a conclusion drawn from the studies by Giffiths and McIntyre (81) Table 2.2), determine the crossover point as in Figure 7.2.
2. Size the furnace capacity with over-capacity less than the crossover point.

3. A furnace selected on the criteria of steps 1 and 2 will have increased cycling at part load operation and thus will tend to be less efficient at part load operation than at full load operation. However, the part load efficiency resulting from a selection based on steps 1 and 2 would still be more efficient at part load operation compared to one with over-capacity greater than the cross-over point.
4. To compensate for the loss of efficiency in part load operation as discussed in step 3, redesign the anticipator heater in the thermostat so that at increased cycling due to part load operation, the differential of the thermostat is automatically increased up to 4.5°K. Alternatively, thermostats with adjustable differentials may be marketable.

For existing residential heating systems, the following procedures are suggested:

1. Calculate the design heat load, and for a differential of 4.5°K, determine the crossover point for over-capacity as in Figure 7.2.
2. If the installed furnace capacity is greater than the crossover point, replace the existing burner with one sized to have over-capacity lower than the crossover point.
3. Install a thermostat with a wider differential (up to 4.5°K).

7.2.1.2 Passive control strategies The parameter K_2 as described by equation (3.25) can be applied to develop criteria to evaluate energy consumption characteristics of envelopes within a given category of buildings. For example, a number of single family residences with equal floor areas can be compared to study the influence of different types of

structures, shapes, infiltration characteristics and life styles of the occupants on energy consumption. Such studies can be used to derive passive control strategies for energy conservation. To illustrate this application, it may be recalled that

$$K_2 = \left.\frac{\partial \dot{Q}_{inf}}{\partial T}\right|_{\dot{Q} = \text{Const.}} \tag{3.25}$$

$$\dot{Q}_{inf} = \dot{m}_{ainf} C_{pa} (T - T_a) \tag{6.7}$$

Under the conditions when heating or cooling is not required:

$$K_2 = \dot{m}_{ainf} C_{pa} - \dot{m}_{ainf} C_{pa} \left(\frac{dT_a}{dT}\right) \tag{6.8}$$

Therefore, the value of K_2 depends upon the mass flow rate of infiltration air $\dot{m}_{ainf}$ and the factor (dT_a/dT). Factor dT_a/dT depends upon the the type of construction of the house (heat transfer and infiltration characteristics) and under passive conditions can have a value anywhere from (+1) to (+∞) as shown in Figure 7.3. A value of (+1) for dT_a/dT means a very loose construction from infiltration point of view or no resistance to heat transfer across the envelope. Substitution of these two extreme values of (dT_a/dT) in equation (6.8) reveals that K_2 can vary from 0 (no envelope) to $-\infty$ (perfect envelope) for a building with passive control. The numerical value of K_2 is one single parameter which combines the elements of infiltration and heat transfer characteristics of a structure. If the infiltration losses can be defined to include losses due to door openings or window openings the numerical value of K_2 becomes a parameter which can be used to compare life styles. To use K_2 as a

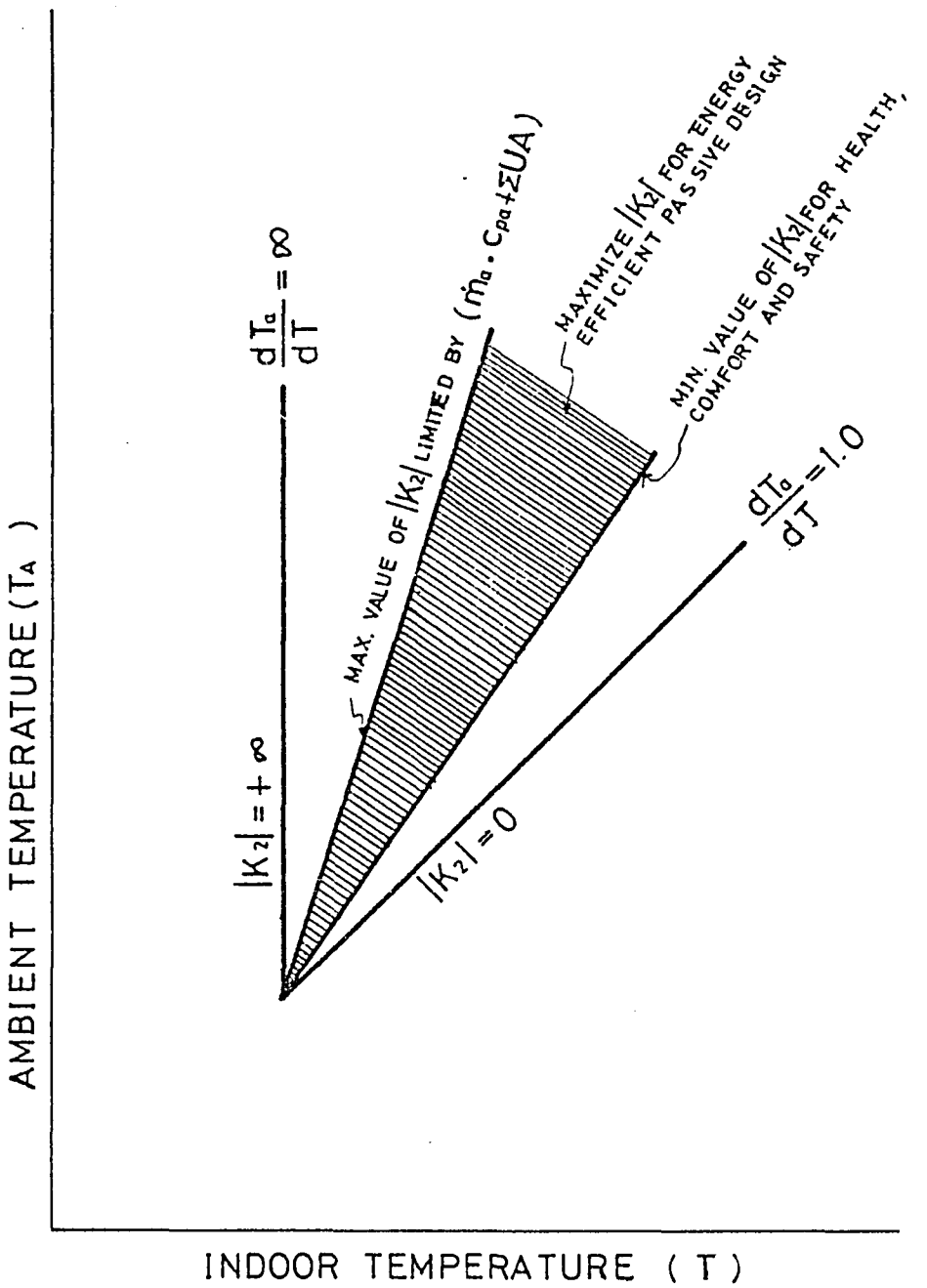

Figure 7.3. Relationships between ambient and indoor temperatures for passive design.

criterion to evaluate energy consumption characteristics of envelopes with a category of buildings, the following procedures are suggested.

7.2.1.2.1 Procedures for existing buildings

1. Select buildings within the same category on equal floor area basis.
2. During spring or fall when heating or cooling is not needed, record hourly indoor temperatures and outdoor air temperatures.
3. Measure infiltration rates at the time the temperatures are being measured using procedures described in Section 6.3.2.2.
4. Calculate the values of $|K_2|$ using procedures described in Section 6.3.3.
5. Structures within the same category designed to provide equal floor areas and which have equal number of air changes per hour will be more energy intensive as the value of $|K_2|$ decreases. Occupants in structures with equal floor areas, identical envelope characteristics and designed for same number of air changes per hour will be identified as having more energy intensive life styles as the value of $|K_2|$ decreases. In structures with equal floor areas but with different number of air changes per hour, the one will be more energy intensive as the value of (dT_a/dT) decreases. Some corrective steps to control energy intensive passive buildings are suggested in the discussion on use of $|K_2|$ for energy efficient passive design for new buildings.

7.2.1.2.2 Procedures for energy efficient passive design It was shown in Section 7.2.1.2.1 that for energy efficient passive design,

$|K_2|$ should be as large as possible. In the limit $|K_2|$ has to be less than $(\dot{m}_a C_{pa} + \Sigma UA)$ because a value of $|K_2|$ equal to $(\dot{m}_a C_{pa} + \Sigma UA)$ yields an infinite value of the time constant for the occupied space (equation (3.30)). Physically an infinite time constant of an occupied space to inputs from weather, internal sources or from heat exchanger has no meaning and hence a limit on the maximum value of $|K_2|$ is shown in Figure 7.3. Thus, codes should be developed to specify maximum and minimum value of $|K_2|$ for health, comfort and safety, and energy considerations. The following procedures are suggested to maximize the value of $|K_2|$ within the limits shown in Figure 7.3.

1. Increase the thermal mass of the structure. The results will be shown by increased values of (dT_a/dT) and of $|K_2|$.
2. Reduce over-capacity of the heating source.
3. Use space temperature reset whenever possible to reduce the temperature difference between indoor and outdoor temperatures. The result will be shown by increased values of (dT_a/dT) and $|K_2|$.
4. Reduce infiltration losses by incorporating self-closing doors and tight fitting windows.
5. Increase air supply rates at constant values of (ΣUA). This results in increased value of $(\dot{m}_a C_{pa})$ and hence an increase in $|K_2|$. However, increased air supply rates should take into considerations the points discussed in the next section.

7.2.2 Air movement strategies

It has been suggested in Section 7.2.1.2.2 (paragraph 5) that increases in air supply rates can improve the energy consumption character-

istics of the envelope. Woods (111) has shown that an increase in whole-body air movement must be accompanied by an increase in SET* to keep constant comfort levels. Calculations in reference (111) indicate that, for air movement in the range of 0.2 to 1.0 m/sec, a shift of 1°C is required for an increase of 0.38 m/sec to keep the same comfort level. However, when air movement is less than 0.2 m/sec (i.e., still air), the calculated shift is significantly greater: 1°C for an increase of 0.04 m/sec. So a very low velocity of air should be aimed at for winter conditions to provide comfort at lower space temperatures to save energy. Alternatively, high air velocities in summer can permit higher space temperatures resulting in reduced air conditioning loads and energy savings. Thus, air movement strategies derived from comfort considerations are in agreement with those derived from energy efficient passive design considerations for summer conditions whereas they conflict for winter conditions. Figure 7.4 has been constructed using equations (6.3)-(6.5) and can aid the designer to seek an optimum solution. The following steps are suggested:

1. For a certain design load and a desired space temperature, T, select the supply air temperature, T_s, so that $\dot{m}_a$ calculated from the following equation:

$$\dot{Q}_L = \dot{m}_a C_{pa}(T_s - T) \tag{7.4}$$

lies to the right of line XY in Figure 7.4. This step will ensure that a very high value of K_{Ta} is not picked up which means an optimum combination of ΣUA, $\dot{m}_a$ and K_2.

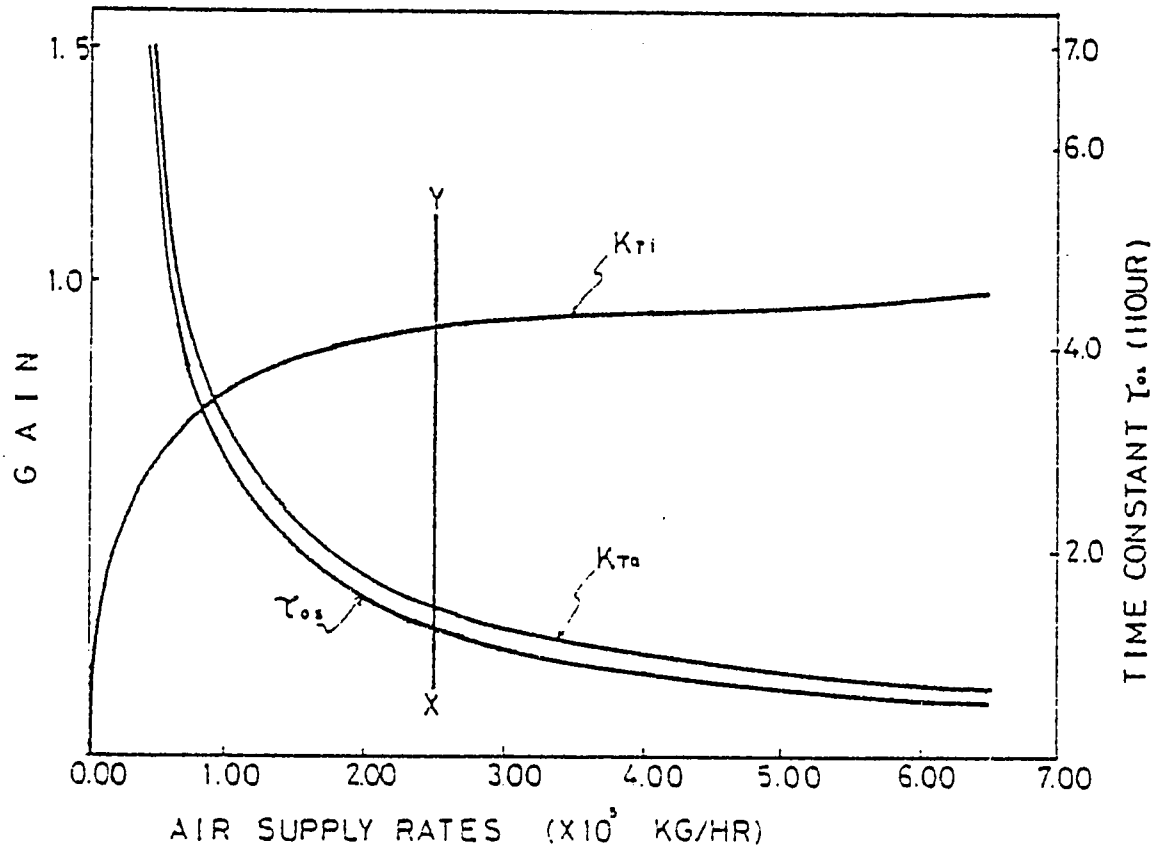

Figure 7.4. Calculated effects of air supply rates on the dynamics of occupied space.

2. Find out the outlet air velocity for the proposed diffuser from the equation

$$\dot{m}_a = A_e V_o \rho \tag{7.5}$$

where A_e = effective area of the outlet.

3. Calculate the local velocity at the location of the occupants, V_x, in the occupied space from (97)

$$\frac{x}{\sqrt{A_e}} = K \frac{V_o}{V_x} \tag{7.6}$$

where

x = distance of the location of the occupants from the outlet

K = constant of proportionality

4. Calculate the effective draft temperature, θ_d, from the equations:

$$\theta_d = (T - T_s) - 7.66(V_x - 0.15) \tag{7.7}$$

$$\theta_d = (T - T_s) - 0.07(V_x - 30) \tag{7.8}$$

depending upon the units of velocity V_x

a) equation (7.7) to be used for m/sec

b) equation (7.8) to be used for ft/mt

5. Values of θ_d should be between (-1.67) to (+1.11) when velocities are m/sec and temperature in °K and between (-3) to (+2) for velocities in ft/minute and temperature (°F).

6. If the calculated values in step 4 do not fall within the limits in step 5, choose a new effective area for the diffuser and repeat steps 1-5.

A design criteria based on steps 1-6 should coordinate load criteria, dynamic performance criteria and air diffusion performance index (ADPI) criteria which is the number of points in the occupied space at which the draft temperatures satisfy the comfort criteria expressed as a percentage of the total points measured.

7.3 Stability of Control Loops in HVAC Systems

Dynamic analysis of physical systems seeks information about the response of the system to some inputs. The response characteristics of interest are expressed in terms of its time behavior. One parameter of response evaluation is the magnitude from output variable after a long period of time has elapsed since the application of input. If the system achieves a finite output, it is said to be stable. Dynamic analysis is generally thought to be useful for stable systems, whereas the responses of unstable systems are thought to be of no practical value. In reality, unstable building systems do exist sometimes and stability analysis can be used to improve their stability.

Stability of a building system depends upon the dynamic responses of individual components viz. occupied space, sensors, controllers, valves, actuators, heat exchangers, ducts and occupants. Mathematical models for these components have been developed and reported in Chapters 3 and 4. These models can be used to derive open-loop or closed-loop transfer functions for the system. Techniques of control theory viz. Routh's criteria, Root Locus Methods, Bode's Plots, etc., can be applied to these transfer functions to test stability of the system (112). Applications of

these techniques can aid the designer in finding the limiting overall gain which provides stable system while achieving minimum steady-state deviation of the controlled variable. In building systems, however, an increase in the gain of the controller can reduce the energy requirements in some HVAC systems such as dual duct and terminal reheat systems (28). In other HVAC systems where proportional controllers are used, applications of control theory for stability analysis can be helpful in designing limited-stable systems where the controlled variable is allowed to oscillate within predetermined bandwidths.

To illustrate the application of control theory to the transfer functions derived from mathematical models developed in Chapters 3 and 4, a closed-loop transfer was derived for the electric heating mode of the Iowa State University ERH. This transfer function was described by equation (5.2) and is reproduced here for analysis of inputs from the furnace:

$$\Delta T(s) = \frac{K_Q^{\bullet}(1 + \tau_s S)\cdot\Delta\dot{Q}_f(s)}{S[(1 + \tau_{os}S)(1 + \tau_s S) + KK_Q^{\bullet}K_s]} + \frac{K_{Ti}}{S(1 + \tau_{os}S)}\,\Delta T(s)$$

or

$$\frac{\Delta T(s)}{\Delta\dot{Q}_f(s)} = \frac{K_Q^{\bullet}(1 + \tau_{os}S)(1 + \tau_s S)}{[(1 + \tau_{os}S)(1 + \tau_s S) + KK_Q^{\bullet}K_s][S(1 + \tau_{os}S) - K_{Ti}]} \qquad (7.9)$$

Substituting the values of various parameters from equation (6.21):

$$\frac{\Delta T(s)}{\Delta\dot{Q}_f(s)} = \frac{0.0003(1 + .0083S)(1 + 0.8644S)}{[(1 + 0.8644S)(1 + .0083S) + 0.0003 \times 0.00134]}$$

$$\times\ [S(1 + 0.8644S) - 0.7386] \qquad (7.10)$$

From equation (7.10), the Characteristic Equation can be written as:

$[(1 + 0.8644S)(1 + 0.0083S) + 4 \times 10^{-7}] \times [(0.8644S^2 + S) - 0.7386] = 0$

or $0.0062S^4 + 0.8480S^3 + 1.8318S^2 + 0.2816S - 0.7386 = 0$

or $S^4 + 136.77S^3 + 295.45S^2 + 45.42S - 119.13 = 0$ (7.11)

From the Characteristic Equation (7.11), the Routhian array can be written as

S^4	1	295.45 -199.13
S^3	136.77	45.42
S^2	295.12	-119.13
S^1	100.63	-119.13
S^0	230.25	

Since there is no change of sign in the first column of the Routhian array, it can be concluded that there are no roots with positive real parts and hence the system is stable. Had there been any sign change in the first column indicating roots with positive real parts, Root Locus methods could have been applied to detect the gain value marking the borderline of stability and instability, Pole-Zero diagram analysis could also have been used to compensate the system by adding more dominant roots.

7.4 Sensitivity Analysis

The design and selection of an optimal HVAC system must include consideration of the interplay among a large number of parameters which describe the thermal responses of the building. An important feature of any technique or model used in design is its ability to predict the effect of variations in the parameters on the response of the building system. These predictions can then be used to draw conclusions about the design, selection, and operation of HVAC systems. Examples of the use of analog

computers in parametric studies for buildings appear in the literature (25-26).

However, it was shown in Section 3.2 that analog computer experiments can be very expensive in terms of money and time. As a result, mathematical models for the components of building systems have been developed in Chapters 3 and 4. The mathematical models have been validated experimentally as reported in Chapter 6. In Section 7.3 it has been shown that the mathematical models can be used to apply the techniques of control theory to yield information on the stability of a proposed system. The intent of the present section is to examine the suitability of the mathematical model as a basis for sensitivity analysis.

7.4.1 The sensitivity equation

To develop the sensitivity equation, the mathematical model described by equation (3.15) may be expressed as

$$F(\dot{T},T,t,q_o) = 0 \tag{7.12}$$

where q_o may be any parameter of interest for sensitivity analysis such as $\dot{Q}$, M_a, $\dot{m}_a$ or U.

The general solution of differential equation (7.12) may be expressed as

$$T = T(t,q_o) \tag{7.13}$$

If the parameter of interest q_o is varied by a small amount, Δq_o, equation (7.12) can be rewritten as:

$$F(\dot{T},T,t,q_o + \Delta q_o) = 0 \tag{7.14}$$

and its solution as

$$T = T(t, q_o + \Delta q_o) \tag{7.15}$$

Using equations (7.13) and (7.15), a measure of sensitivity can be obtained:

$$\Delta u \equiv \frac{T(t, q_o + \Delta q_o) - T(t, q_o)}{\Delta q_o} \tag{7.16}$$

If identity (7.16) has a limiting value as Δq_o approaches zero,

$$\lim_{\Delta q_o \to 0} = \frac{T(t, q_o + \Delta q_o) - T(t, q_o)}{\Delta q_o} = \frac{\partial T(t, q_o)}{\partial q_o} \tag{7.17}$$

and

$$\frac{\partial T(t, q_o)}{\partial q_o} \equiv u(t, q_o) \tag{7.18}$$

The function $u(t, q_o)$ is called the sensitivity coefficient of the dynamic system (113).

The partial derivative of equation (7.12) is:

$$\frac{\partial F}{\partial \dot{T}} \frac{\partial \dot{T}}{\partial q_c} + \frac{\partial F}{\partial T} \frac{\partial T}{\partial q_o} + \frac{\partial F}{\partial q_o} = 0 \tag{7.19}$$

Substitution of equality:

$$\frac{\partial \dot{T}}{\partial q_o} = \frac{\partial}{\partial t} \left(\frac{\partial T}{\partial q_o}\right) = \dot{u}$$

into equation (7.19) results in equation (7.20):

$$\frac{\partial F}{\partial \dot{T}} \dot{u} + \frac{\partial F}{\partial T} u = \frac{-\partial F}{\partial q_o} \tag{7.20}$$

Equation (7.20) is a differential equation with u as a dependent variable and is the required sensitivity equation. Thus, the solution of this equation should lead to a method of expressing u as a function of time.

7.4.2 Solving the sensitivity equation

In order to solve equation (7.20), it is recognized that

1. Equation (7.20) is a linear differential equation with constant coefficients, or $\partial F/\partial \dot{T}$ and $\partial F/\partial T$ are not functions of u.
2. In deriving equation (7.20), we assume that the solutions of equation (7.12) are analytically dependent on the parameters. Insofar as Δq_o represents parametric variations which do not change the order of equation (7.12), the condition for analytical dependence holds.
3. In deriving the sensitivity equation (7.20), no reference has been made to the initial conditions. So let us consider the following two cases.

Case A: If the initial conditions of equations (7.12) and (7.14) are identical, then at t = 0, there is no deviation between the two systems and all the initial conditions for equation (3.15) are zero.

$$u(0) = 0$$

$$\dot{u}(0) = 0 \qquad (7.21)$$

Case B: If initial conditions of equations (7.12) and (7.14) are different, then the differences for T(0) are not zero. Say

$T(0) = a$ for equation (7.12)

$T(0) = a + \Delta a$ for equation (7.14)

The integral of equation (7.12) can be written as

$$T(t) = a + \int_o^t F\ (\dot{T}, t, q_o)\ dt \qquad (7.22)$$

so that equation (7.22) fulfills the desired initial condition for equation (7.12), i.e., when t = 0, T(0) = a.

Differentiating equation (7.22) with respect to a

$$\frac{\partial T(t)}{\partial a} = 1 \tag{7.23}$$

Therefore, initial conditions for equation (7.20) are:

$$u(0) = 1$$

$$\dot{u}(0) = 0 \tag{7.24}$$

If some other initial condition plays the role of a variable parameter for $t = 0$, then by analogy its derivative will also be equal to 1.

When more than one parameter is to be considered, mixed derivatives of the type $\partial^2 T/\partial q_1 \partial q_2$ will be required. In order to calculate the derivatives of higher order, equation (7.20) may be differentiated:

$$\frac{\partial^2 F}{\partial \dot{T} \partial q_o} \dot{u} + \frac{\partial F}{\partial T} \frac{\partial u}{\partial q_o} + \frac{\partial^2 F}{\partial T \partial q_o} u + \frac{\partial F}{\partial T} \frac{\partial u}{\partial q_o} = - \frac{\partial^2 F}{\partial q_o^2} \tag{7.25}$$

Substituting

$$\frac{\partial u}{\partial q_o} + \frac{\partial}{\partial t} \left(\frac{\partial u}{\partial q_o}\right) = \dot{V} \tag{7.26}$$

where

$$\frac{\partial u}{\partial q_o} \equiv V$$

$$\frac{\partial F}{\partial T} \dot{V} + \frac{\partial F}{\partial T} V = - \frac{\partial^2 F}{\partial q_o^2} - \frac{\partial^2 F}{\partial \dot{T} \partial q_o} \dot{u} - \frac{\partial^2 F}{\partial T \partial q_o} u = -X \tag{7.27}$$

Comparing equations (7.20) and (7.27), we find that the homogeneous parts are identical.

So, the partial or mixed derivatives of arbitrary order with respect to a parameter q_o of the dynamic system have the same homogeneous part as equation (7.20). Since the nonhomogeneous terms in equation (7.27)

contain derivatives of lower order, a solution of the sensitivity equation (7.20) exists under all initial conditions of Case A and Case B. Therefore, the mathematical model as expressed by equation (7.20) is suitable for sensitivity analysis.

7.4.3 Procedures for sensitivity analysis

It was shown in Section 7.4.1 that a sensitivity equation can be set up for a physical system from its mathematical model. It was proved in Section 7.4.2 that a solution does exist for the sensitivity equation. Procedures have been described below to perform the sensitivity analysis for a mathematical model.

Step 1. Identify the inputs and the outputs of interest for sensitivity analysis. For example, the output variable of interest in the mathematical model of the occupied space (equation (3.15)) could be space temperature, T, and its sensitivity to inputs like $\dot{Q}_{occ}$, $\dot{Q}_{f}$, T_{i}, $\dot{m}_{a}$, M_{a}, $\dot{Q}_{inf}$, C_{pa}, $\dot{Q}_{cond}$ and $\dot{Q}_{int}$ may be desired.

Step 2. Find the sensitivity coefficient (equation (7.18)) for each one of the input variables. For example, the sensitivity coefficient of the mathematical model of equation (3.15) with respect to $\dot{Q}_{occ}$ will be

$$\left.\frac{\partial T}{\partial \dot{Q}_{occ}}\right| = M_a C_{pa} \frac{\partial^2 T}{\partial t \partial \dot{Q}_{occ}} + \dot{m}_a C_{pa} \frac{\partial T}{\partial \dot{Q}_{occ}}$$

$\dot{Q}_f$=const
T_i=const
$\dot{m}_a$=const
M_a=const
$\dot{Q}_{inf}$=const
C_{pa}=const
$\dot{Q}_{cond}$=const (7.28)

Determine equations similar to equation (7.28) for the other seven inputs.

Step 3. Derive other terms required to set up the sensitivity equations (7.20), one each for every input variable to which sensitivity of the output is desired. For example, the sensitivity equation of the space temperature T in equation (3.15) to an input from occupants has been derived to be:

$$(2M_a^2 C_{pa}^2 + M_a \dot{m}_a C_{pa}^2) \frac{\partial^3 T}{\partial t^2 \partial \dot{Q}_{occ}} + (3M_a \dot{m}_a C_{pa} + \dot{m}_a^2 C_{pa}^2) \frac{\partial^2 T}{\partial t \partial \dot{Q}_{occ}}$$

$$+ \dot{m}_a C_{pa}^2 \frac{\partial T}{\partial \dot{Q}_{occ}} = 1 \qquad (7.29)$$

Determine equations similar to equation (7.29) for the other seven sensitivity coefficients.

Step 4. Find the boundary conditions for each of the eight sensitivity equations derived in step 3. For example, boundary conditions for the input from occupants may be

$t = t_o$, $T = T_o$ and $\dot{Q}_{occ} = \dot{Q}_o$

$t = t_1$, $T = T_1$ and $\dot{Q}_{occ} = \dot{Q}_1$

Step 5. Solve all the eight sensitivity equations derived in step 3 with their respective boundary conditions for sensitivity analysis.

To conclude, some applications of the mathematical models of building systems performance analysis have been described in this chapter. The rational model has been applied to study the effects of environmental control dynamics on energy consumption and to derive some new control strategies. The new control strategies have been identified as thermal and air movement strategies. The closed-loop transfer function derived for a heating system for a single family residence has been subjected to Routh's Stability Criteria and was shown to be stable. It has been shown that mathematical models for dynamic analysis of buildings can be used to formulate sensitivity equation. Procedures to perform sensitivity analysis have been described.

8. BUILDING SYSTEMS ECONOMIC ANALYSIS

The mathematical models of the building systems developed in Chapters 3, 4 and 5 can be used to apply the techniques of control theory as demonstrated in Chapter 7 for improved designs. Once a proposed design meets comfort, functional and technical criteria and is technically feasible, it must stand alone on its financial merits to the owner of the building system. The purpose of the present chapter is to identify those methods of economic analysis which are suitable to compare the financial merits of alternative designs.

8.1 Economic Criteria

In general, economic analysis of alternatives involving engineering considerations may be based on one or more of the following criteria:

a. Benefit/cost ratio

b. Pay back period

c. Life cycle cost analysis

Benefit/cost ratio is useful in analyzing governmental expenditure for different purposes such as control of natural resources, providing economic services, protection to citizens and cultural development. Pay back period is used in practice in making a large percentage of business decisions. However, Smith (114) recommends that the use of pay back period should be restricted to a supplementary, special purpose criteria and should be avoided for final acceptance-rejection decisions due to the following reasons.

1. Cash flows beyond the pay back year are neglected, thus the criteria fails to give weight to cash flows that occur after the date of payout.
2. The timing of cash flows within the payback period is neglected.
3. The "test" is not a uniform one; it discriminates against long-lived projects.
4. Users tend to use shorter and shorter payoff requirements until few investments, if any, can pass the test.
5. Payback method assumes an interest rate of zero.
6. Payback does not provide for return on debt or equity capital.
7. Payback ignores the time value of money.
8. The method does not provide for income taxes or investment credits.
9. Payback ignores inflation and elements of cost that escalate at a rate greater than the rate of inflation.

8.2 Life Cycle Cost Analysis

Life cycle cost analysis for building systems can be used to determine whether a particular alternative affords an economic incentive. The following major steps constitute a life cycle cost analysis.

1. Specification of economic objectives and constraints.
2. Identification of alternate technical solutions.
3. For each alternative, identification of relevant cost variables and their values over time.

4. Adjustment of cash flows to an equivalent basis.
5. Calculation of life-cycle costs and comparison of costs for alternatives.

Because investments in building systems involve expenses and savings that spread over the life of the system, it is important to use an evaluation method, such as life-cycle costing, which incorporates all important cash flows over the life period. To calculate an owner's life-cycle costs for an alternative, the following variables are relevant and their evaluation demands a conscientious effort on the part of those supplying data for an economic analysis.

A. Economic life: Life of a property is the number of years of service over which the prudent user expects to retain the property in use for its stated purpose (114). Care should be taken while using any available data (115) on physical lives for building system components for an input to an economic model. Economic life is that which will produce minimum cost and it can be less than the physical life. Moreover, income tax considerations in an economic analysis somewhat reduce the impact of errors in the estimation of economic life, especially when the life involved is more than 14 years and these considerations can change the percentiles reported in reference (115). Considerations of interest rates can change the optimal service interval for equipment. An increase in interest rate means an increase in economic life. The prospect of inflation either can accelerate or can retard replacement. Moreover, economic considerations may not favor the purchase/installation of brand new equip-

ment and thus the data on economic lives in an economic model should be based on optimal service interval rather than on physical lives.

B. Acquisition costs: These costs are incurred in identifying and designing the system, in purchasing, delivering, and installing the system, and in modifying the building to receive it.

C. Maintenance costs: These costs include system repair costs, insurance premiums and routine maintenance costs.

D. Operating costs: These costs include those for fuel, property taxes, and other operating requirements.

E. Salvage values: The net salvage value is the gross resale value less such costs as those required for restoration, removal, selling commissions, delivery charges, or demolition.

In assessing costs it is also important to take into account the impact of property and income taxes as well as the effect of any state or federal government incentive programs such as business energy credits. When financing of an energy saving measure is in part by borrowing, the tax sheltered after-tax rate of return, i_a, should be calculated. Depreciation is the allocation of (first cost-salvage) over the life of the asset, as determined for income tax purposes. A suitable method such as straight-line, sum-of-the-years or short-life write-off method should be used to account for depreciation. Finally, anticipated inflation rates may be different from the rate of future change in the cost of the various fuels and as such may be treated separately. Since fuel cost savings will be the main source of reduction in operating costs among the building

system alternatives analyzed, the economic analysis should be sensitive to fuel prices and projected fuel price increases.

Literature review reveals that the theme with various researchers has been to report life cycle cost analysis models for special applications (116-117). The intent of the present chapter is not to develop or report an economic analysis model under particular specifications and constraints. Instead, fundamental relationships between operating revenues and return on debt and equity (114) are reported which can be used for life cycle cost analysis under different specifications and constraints. These relationships are described by the following equations:

$$PEC = PEM + [B - V(p/f)_n^{ia} - t(PED)]/(1 - t) \tag{8.1}$$

$$AEC = AEM + [B(a/p)_n^{ia} - V(a/f)_n^{ia} - t(AED)]/(1 - t) \tag{8.2}$$

$$PEX = (PER - PEM)(1 - t) - B + V(p/f)_n^{ia} + t(PED) \tag{8.3}$$

$$AEX = (AER - AEM)(1 - t) - B(a/p)_n^{ia} + V(a/f)_n^{ia} + t(AED) \tag{8.4}$$

$$i_c = r_d i_d + (1 - r_d) i_e \tag{8.5}$$

$$i_a = i_c - t r_d i_d = (1 - t) r_d i_d + (1 - r_d) i_e \tag{8.6}$$

$$i_b = BTRR = r_d i_d + (1 - r_d) i_e/(1 - t) = i_a/(1 - t) \tag{8.7}$$

The following definitions apply to these equations:

PEC = present equivalent cost

PEM = present equivalent cash operating costs

B = first costs

V = salvage value

$(p/f)^{ia}_n$ = single payment present worth factor

t = effective combined federal and state income tax rate

PED = present equivalent tax depreciation allocations

AEC = annual equivalent cost

AEM = annual equivalent cash operating cost

$(a/p)^{ia}_n$ = capital recovery factor

$(a/f)^{ia}_n$ = sinking fund factor

AED = annual equivalent tax depreciation allocations

PEX = present equivalent excess of revenues minus costs

AEX = annual equivalent excess of revenues minus costs

i_c = composite cost of capital

i_d = rate of return required on debt capital

i_e = annual effective after tax rate of return required on equity capital

i_a = tax-sheltered after-tax rate of return

i_b = effective annual before-tax rate of return

r_d = debt ratio = debt/(debt + equity)

8.3 Decision Procedures in Life Cycle Cost Analysis

Several methods are available in which the same economic results can be displayed. Each method has its own set of advantages and disadvantages. The methods include:

a. Annual equivalent cost comparisons of different alternatives (comparison of outputs of equation (8.2)).

b. Present equivalent cost comparisons of different alternatives (comparison of outputs of equation (8.1)).

c. Rate of return comparisons of different alternatives. Rates of return are calculated by equating equation (8.3) or (8.4) to zero to calculate i_a. If only one compound interest factor is involved, the problem can be solved directly. When two or more factors are involved, the method of solution is one of trial and error.

For the economic analysis of building systems, the rate of return method offers some advantages over the annual equivalent cost and present equivalent cost methods. Rate of return method gives an accurate ranking of independent alternatives if the objective is to maximize rate of return. In AEC and PEC analysis, savings are maximized at a stipulated rate of return. Although AEC and PEC methods of analysis are appropriate for mutually exclusive alternatives, the correct choice will not always be evident for independent alternatives. The investor runs the risk of choosing the alternative with a lower rate of return even though savings appear to be maximized.

After the rate of return is calculated from equations (8.3) or (8.4) for the various alternatives, the optimum choice must be made among them. Procedures for optimum choice vary depending on whether the rates of return refer to independent measures over present conditions, to mutually exclusive alternatives, or a combination of the two.

The decision procedure for independent measures over present conditions is as follows:

1. Rank projects in descending order of prospective rate of return.
2. Approve projects according to rank until funds are exhausted or the rate of return is less than the minimum acceptable rate of return (MARR).

Network diagrams and choice tables are very helpful in making decisions on mutually exclusive alternatives. These methods are cited in reference (114).

8.4 Dynamics of the Economic Model

A review of the list of relevant costs/terms described in Section 8.2 reveals that each category is subject to time variation and uncertainty. This is the case in almost every investment decision. However, it is worthwhile to point out the problem areas and some examples of sources of information as related to building systems.

The rate of future annual increases in fuel costs is the dominant component in life-cycle cost calculations. Estimating this rate involves reliance on fuel industry projections, uncertain national and international government policies, and possible costs of newly developing technologies in the energy field. The uncertain pace of development of new technologies creates difficulties in choosing a suitable period of economic life. The pace of developing technologies also leaves uncertain that proportion of the building's energy load which can be reduced. Future maintenance costs depend on the reliability of the products as well as estimates of cost increases for parts and labor. Finally, the investor

must decide upon a realistic, acceptable rate of return to use in deciding whether the given project is worth undertaking.

One method of dealing with such uncertainties is the use of Sensitivity Analysis similar to that discussed in Section 7.4. This procedure allows the analyst to determine how the economic outcome will vary as a function of one or more factors while all others are held constant. For example, an energy saving technique will be economically attractive if it results in a sufficient reduction in fuel costs. Thus, it might be appropriate to compare the results when the size of the annual fuel cost increase is varied while all other data remain unchanged. The investor can then determine whether he considers the percent increase which makes the investment worthwhile to be a realistic estimate. Sensitivity analysis indicates relationships such as follows (114) for a more costly energy conserving technique.

1. A longer period of economic life produces larger net benefits.
2. Lower costs of acquisition and maintenance bring about greater net benefits.
3. Under some circumstances the cost penalty of a parameter being x units less than its expected value is different from the cost penalty caused by it being x units greater than expected value.
4. Variability can be treated implicitly if MARR used is greater than the required ROR. The difference takes care of the uncertainty (variability) of parameters.
5. Variability can be treated explicitly if statistical expected values of the parameters are employed with equal cost penalty or

an unlikely but possible serious outcome is insured and its cost is explicitly treated in the economic model

6. Simultaneous variation of more than one parameter sometimes offers several advantages as follows:
   a. This approach is more realistic than varying one parameter at a time.
   b. This approach may signal the possibility of a disastrous outcome when input variations have a multiplicative rather than compensating effect.

The disadvantages in simultaneous variation of more than one parameter are of course too many calculations. For example, if two parameters are trivalued, nine sets of calculations in the application of an economic model (equation (8.3) or (8.4)) are needed. Under such circumstances, use of computers or special techniques such as Monte Carlo Simulation (114) can be used for sensitivity analysis.

To conclude, it is recommended that Sensitivity Analysis using simple economic models such as equation (8.3) or (8.4) should be undertaken as a future research project to identify the most significant economic parameters. This information can lead to identifying areas of technical research where the future stress should be to generate data on energy savings in buildings.

9. GENERAL APPLICATIONS, CONCLUSIONS AND RECOMMENDATIONS FOR FUTURE WORK

9.1 General Applications

Institutional mechanisms which will use the results of the research work reported in this dissertation are identified in Figure 9.1 which is a chart showing the principal paths by which technology moves from concept to construction practices. Blocks A to F of Figure 9.1 illustrate the flow of technology from the concept stage to incorporation of test methods and performance requirements into specifications, codes and regulations. Blocks G to J of Figure 9.1 illustrate the use of the research results in modeling, product and system development, construction practice and design practice.

Research reported in this dissertation fits Blocks A, B, C, G and H of Figure 9.1. One contribution of this research is that the problem of predicting dynamic behavior of building systems has been reduced to manageability. Analytical models developed and reported are simple, modular, accurate and powerful. The power of the mathematical models to yield useful information to the designer has been demonstrated in Sections 7.1 and 7.2 where they have been very successfully applied to study the effects of environmental control dynamics on energy consumption and to derive some new control strategies for energy conservation. It has been shown in Sections 7.1 and 7.2 that a design criterion based upon dynamic considerations can easily be coordinated with comfort criteria, load criteria and air diffusion dynamics (ADPD) criteria.

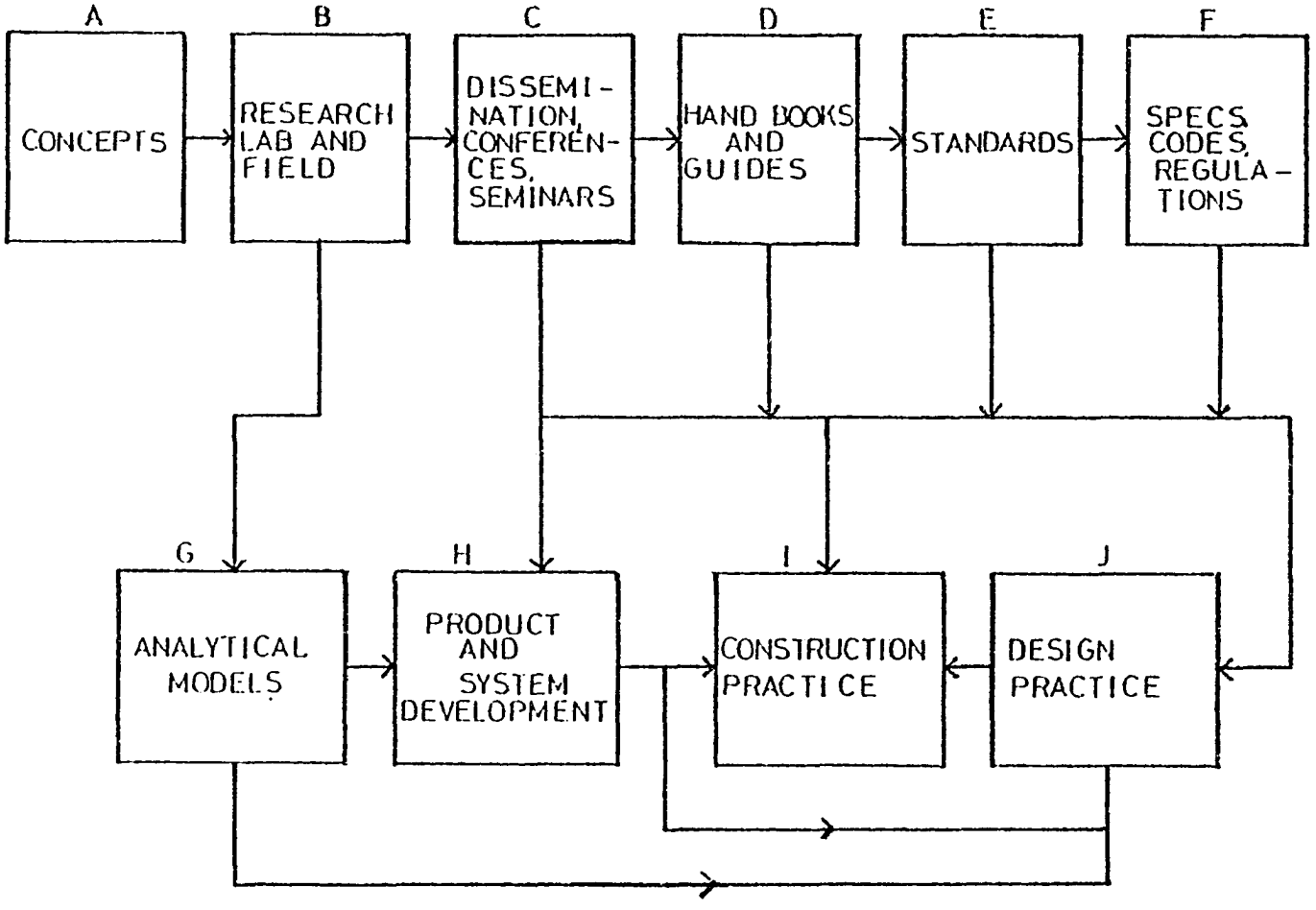

Figure 9.1. Flow of technology from concept to application.

It has been shown in Chapter 5 that the reported analytical models can be coupled to each other to derive overall closed-loop transfer functions for different types of HVAC systems. These transfer functions can also be used by the designer to obtain useful information. For example, it has been shown in Sections 7.3 and 7.4 that the transfer functions derived from the analytical models of Chapters 3 and 4 can be subjected to the techniques of control theory. Such methods are rather powerful because digital computers can conveniently be applied to include even nonlinearities in the light of Popav stability techniques (118). Thus, all the developments in modern control theory have been put at the disposal of the designer for optimal design of HVAC systems.

9.2 Conclusions

From the literature review it has been found that the dynamic characteristics and interactions of different components in a building system (envelope, HVAC system and equipment) have not been investigated in detail in the past. The emphasis on steady state has been reflected in the determination of occupant comfort conditions also. However, primarily because of the present and expected future cost of energy used by building environmental control systems, an urgent need to understand the dynamic responses of building systems has been identified. ASHRAE is currently in the process of formulating a multi-million dollar research program to meet this need in the coming five years. This dissertation is a timely effort through which cost effective mathematical models have been developed and validated to predict dynamic performance of building systems.

To achieve the first two objectives as stated in Chapter 1, mathematical models to predict dynamic conditions inside an occupied space were developed both from analog thermal circuits and energy balance methods. Applications of the models derived from analog thermal circuits were shown to be complex and expensive in terms of time and money. A rational model derived from energy balance has proved to be simple, accurate and was shown to be less complex, yet accurate and powerful in its applications. The rational model rendered itself in a form to which the analytical models of the other control systems elements and of controlled systems can be coupled. The rational model was used to develop three models of environmental control systems: a heating system for a single family residence, a fan-coil system for a classroom and a constant volume dual duct system for an office building.

To accomplish the third objective, the concept of the rational model was subjected to experimental validation, in the Iowa State University Energy Research House, both in the open-loop and closed-loop modes. For the open-loop mode, the results predicted by the mathematical model were within ±0.16°C of the measured value. For the closed-loop mode, the mathematical model predicted nine cycles of furnace operation with an accuracy of ±0.13°C for space temperatures.

To achieve the fourth objective, the rational model was applied to study the effects of environmental control dynamics on energy consumption and to derive some new control strategies for energy conservation. The new control strategies were identified as thermal strategies and air movement strategies. Thermal strategies included both active control strategies and passive control strategies. Finally for the fifth objective of

this dissertation, derivation of thermal strategies led to the identification of a single parameter which can be used to compare the energy characteristics of building envelopes in a given category and to improve passive designs for energy efficient buildings. Derivation of air movement strategies showed that a design criteria based upon dynamic considerations can easily be coordinated with comfort criteria, load criteria and air diffusion dynamics (ADPI) criteria.

The closed-loop transfer function derived for a heating system for a single family residence was subjected to Routh's stability criteria and was found to be stable. It was shown that mathematical models for dynamic analysis of buildings can be used to formulate sensitivity equations for sensitivity analysis and the techniques of modern control theory can be applied to optimize design.

Techniques of life cycle cost analysis were reviewed which may be used to evaluate those design alternatives which meet the comfort criteria and are technically feasible. Potential problems in economic analysis of building systems were identified. Institutional mechanisms which will use the results of the research reported in this dissertation were identified and their relationship to other mechanisms, needed to move the research concepts to construction practices, were shown.

9.3 Recommendations for Future Work

The objectives of the present research project to develop cost effective mathematical models to predict dynamic performance of building systems have been met. However, many more research projects will have to be carried out before the building systems technology can move from the con-

cepts and results of the research presented in this dissertation to the construction practices. All the tasks indicated in the Blocks C to F and H to J of Figure 9.1 will have to be accomplished. Different obstacles on the feed-forward and feed-back paths connecting the blocks of Figure 9.1 will have to be overcome. To be specific, accomplishment of the tasks of Blocks A, B, C and G (subject matter of this dissertation) can be further strengthened through the following future research projects.

1. A research project should be undertaken to validate the mathematical models reported in this dissertation to perform the sensitivity analysis on an existing facility like the Iowa State University Energy Research House. All the sensitivity equations as outlined in Section 7.4.3 should be derived. A computer program should be developed to solve the sensitivity equations. Experimental data will be needed to establish some boundary conditions for the sensitivity equations and that is the reason that work on an existing facility is recommended. Computer solutions of the sensitivity equations should be made available in graphical and tabular form. The potential use of the solutions of the sensitivity equations in the graphical or tabular form by the designers should be examined to optimize the building design.
2. Some research efforts should be directed to apply the theoretical techniques of modern control theory such as frequency response methods to examine the possibility of predicting seasonal performance of HVAC systems without using hour by hour data as required for analysis in time domain. Mathematical models developed in this dissertation have been described in Laplace Transform variables and can be readily adopted for frequency response methods.

3. Experimental research efforts should be pursued to calibrate the models for more environmental control systems. Setting up of an inexpensive experimental facility may be a laboratory model, for a fan-coil heating system is recommended to accomplish this goal.
4. Experimental work should be undertaken to verify the effects of furnace over-capacity and its part load operation on cycling patterns as predicted by the rational model in section 7.7.1. It is recommended that some existing facility should be used for this purpose. This project should include studies on the effects of thermostat differential on cycling and energy consumption to test the validity of new control strategies as recommended in this dissertation. Studies of the effects of changes in differential on the occupant's acceptability should be a part of the project. Work should be pursued to determine the gain and time constants of the occupant when used as a feedback component.
5. A data base should be developed on different parameters used in economic analysis of building systems. Techniques should be developed to specify the confidence with which the building owners, design engineers, contractors and manufacturers can use these data.

9.4 Closure

An effort has been made to add a new dimension to the concept of design practice for building systems. The message is that future design practices for building systems should include dynamics criteria if they are to make use of various available energy saving strategies. Dynamic

considerations can also help to create new energy saving strategies. Projected depletion rates of nonreplenishable fossil fuels demand that we direct our talents and efforts to reduce energy use and this dissertation is an effort made in that direction with a life long commitment to continue the effort.

10. REFERENCES

1. Stanford Research Institute. Patterns of Energy Consumption in the United States. Prepared for the Office of Science and Technology, Washington, D.C. Stanford, Ca: Stanford Research Institute, 1972.

2. U.S. Department of Commerce. Technical Options for Energy Conservation in Buildings. NBS Technical Note 789, July, 1973.

3. Shavit, G. "Energy Savings through Computer Control of Fan Systems with Floating Space Temperature." ASHRAE Trans. 83(1977): 374.

4. Fullarton, S. R. "Energy Characteristics of Buildings in Iowa." Unpublished M.S. thesis, Iowa State University, 1978.

5. Fanger, P. O. Thermal Comfort Analysis and Applications in Environmental Engineering. New York: McGraw Hill Book Company, 1973.

6. Gagge, A. P.; Stolwijk, J. A. J.; and Nishi, Y. "An Effective Temperature Scale Based on a Simple Model of Human Physiological Regulatory Response." ASHRAE Trans. 77(1971): 247.

7. Hamilton, D. C.; Leonard, R. G.; and Pearson, J. T. "Dynamic Response Characteristics of a Discharge Air Temperature Control System at Near Full and Part Heating Load." ASHRAE Trans. 80(1974): 181.

8. Fourier, J. B. Theorie Analytique de la Choleur. Paris: Gauthier Villars, 1822.

9. Mackey, C. O.; and Wright, L. T. "Periodic Heat Flow-Homogeneous Walls or Roofs." ASHVE Trans. 50(1944): 293.

10. Mackey, C. O.; and Wright, L. T. "Periodic Heat Flow-Composite Walls or Roofs." ASHVE Trans. 52(1946): 283.

11. Pipes, L. A. "Matrix Analysis of Heat Transfer Problems." Franklin Institute Journal 263(1957): 195.

12. Hill, I. R. A Method of Computing the Transient Temperature of Thick Walls from Arbitrary Variation of Adiabatic-Wall Temperature and Heat Transfer Coefficient. National Advisory Committee for Acronautics, Tech. Note 4105, 1957.

13. Muncey, R. W. "Thermal Response of a Building to Sudden Change of Temperature or Heat Flow." Australian Journal of Applied Science 14 (1963): 123.

14. Mitalas, G. P.; and Stephenson, D. G. "Room Thermal Response Factors." ASHRAE Trans. 73(1967): III-2.1.

15. Stephenson, D. G.; and Mitalas, G. P. "Cooling Load Calculations by Thermal Response Factor Method." ASHRAE Trans. 73(1967): III-1.1.

16. Kusuda, T. "Thermal Response Factors for Multi-Layer Structures of Various Heat Conduction Systems." ASHRAE Trans. 75(1969): 246.

17. Stephenson, D. G.; and Mitalas, G. P. "Calculation of Heat Conduction Transfer Functions for Multi-Layer Slabs." ASHRAE Trans. 77 (1971): 130.

18. Stoecker, W. F. Procedures for Simulating the Performance of Components and Systems for Energy Calculations. Compiled and published by the Task Group on Energy Requirements for Heating and Cooling of Buildings. New York: ASHRAE, 1975.

19. Paschkis, V. "Periodic Heat Flow in Building Walls Determined by Electrical Analog Method." ASHVE Trans. 48(1942): 75.

20. Willcox, T. N.; Dergel, C. T.; Reque, S. G.; Toelaer, C. M.; and Brisken, W. R. "Analog Computer Analysis of Residential Cooling Loads." ASHVE Trans. 60(1954): 505.

21. Nottage, H. B.; and Parmelee, G. V. "Circuit Analysis Applied to Load Estimating." ASHVE Trans. 60(1954): 59.

22. Nottage, H. B.; and Parmelee, G. V. "Circuit Analysis Applied to Load Estimating." ASHAE Trans. 61(1955): 125.

23. Buchberg, H. "Electric Analogue Prediction of the Thermal Behavior of an Inhabitable Enclosure." ASHAE Trans. 61(1955): 339.

24. Buchberg, H. "Electric Analogue Studies of Single Walls." ASHAE Trans. 62(1956): 177.

25. Nelson, L. W. "The Analog Computer as a Product Design Tool." ASHRAE Journal 3(1965): 37.

26. Magnussen, J. L. Analog Computer Simulation of an Air Conditioning System in a Commercial Building Incorporating Yearly Weather Data. Presented at First Symposium on the Use of Computers for Environmental Engineering Related to Buildings (supported by ASHRAE and NBS), November 30-December 2, 1970.

27. Kaya, A. "Analytical Techniques for Controller Design." ASHRAE Journal 18 (April, 1976): 35.

28. Zelenski, R. E.; Lund, R. A.; Harrison, H. L.; and Sowls, R. E. "An Investigation of a Closed-Loop System for Duct Air Temperature Control." ASHRAE Trans. 75(1968): VI-1.1.

29. Stoecker, W. F.; Rosario, L. A.; Hadenreich, M. E.; and Phelan, I. R. "Stability of an Air-Temperature Control Loop. ASHRAE Trans. 84 (1978): 35.

30. Stenger, J. B.; Leonard, R. G.; and Pearson, J. T. Case Studies Exploring the Behavior of a Discharge Air Temperature Control System. Final Report on Research Project RP-143. Report No. HL75-37. Ray W. Herrick Laboratories, Purdue University, 1975.

31. Cohen, W. C.; and Johnson, E. F. "Dynamic Characteristics of Double Pipe Heat Exchangers." Industrial and Engineering Chemistry 48 (June 1956): 1031.

32. Masubuchi, M. "Dynamic Response and Control of Multipass Heat Exchangers." Journal of Basic Engineering Trans. ASME, Series D, 82 (March 1960): 51.

33. Larsen, H. T. "Dynamics of Heat Exchangers and their Models." Journal of Basic Engineering, Trans. ASME, Series D (June 1960): 489.

34. Hampel, A. "On the Dynamics of Steam-Liquid Heat Exchangers." Journal of Basic Engineering, Trans. ASME, Series D, 82(June 1961): 245.

35. Gartner, J. R.; and Harrison, H. L. "Frequency Response Transfer Functions for a Tube in Cross-Flow." ASHRAE Trans. 69(1963): 323.

36. Gartner, J. R.; and Harrison, H. L. "Dynamic Characteristics of Water-To-Air Crossflow Heat Exchangers." ASHRAE Trans. 71(1965): 212.

37. Gartner, J. R.; and Daane, L. E. "Dynamic Response Relations for a Serpentine Crossflow Heat Exchanger with Water Velocity Disturbance." ASHRAE Trans. 75(1969): 53.

38. Gartner, J. R. "Simplified Dynamic Relations for Finned-Coil Heat Exchangers." ASHRAE Trans. 78(1972): 163.

39. Pearson, J. T.; and Leonard, R. G. "Gain and Time Constants for Finned Serpentine Crossflow Heat Exchangers." ASHRAE Trans. 80 (1974): 255.

40. Tobias, J. R. "Simplified Transfer Function for Temperature Response of Fluids Flowing through Coils, Pipes, or Ducts." ASHRAE Trans. 79 (1973): 19.

41. Bhargave, S. C.; McQuiston, F. D.; and Zirkle, L. D. "Transfer Functions for Crossflow Multirow Heat Exchangers." ASHRAE Trans. 81(1975): 294.

42. Pearson, J. T.; Leonard, R. G.; and Frost, J. L. "An Improved Dynamic Response Model for Finned Serpentine Cross-Flow Heat Exchangers." ASHRAE Trans. 83(1977): 218.

43. Goodman, W. "Performance of Coils for Dehumidifying Air." Heating, Piping and Air-Conditioning 11(1939): 158.

44. Elmahdy, A. H. "Analytical and Experimental Multi-row Finned-Tube Heat Exchanger Performance During Cooling and Dehumidifying Processes." Ph.D. Thesis, Carleton University, Ottawa, Canada, 1975.

45. Elmahdy, A. H.; and Mittalas, G. P. Fortran IV Program to Simulate Cooling and Dehumidify Finned Tube Multi-Row Heat Exchangers." Division of Building Research Computer Program No. 43, National Research Council of Canada, 1977.

46. Elmahdy, A. H.; and Mittalas, G. P. "A Simple Model for Cooling and Dehumidifying Coils for Use in Calculating Energy Requirements for Buildings." ASHRAE Trans. 83(1977): 103.

47. Hamilton, D. C.; Leonard, R. G.; and Pearson, J. T. "Dynamic Response Characteristics of a Discharge Air Temperature Control System at Near Full and Part Heating Load." ASHRAE Trans. 80(1974): 181.

48. Zermuehlen, R. O.; and Harrison, H. L. "Room Temperature Response to a Sudden Heat Disturbance Input." ASHRAE Journal 7(March 1965): 25.

49. Zelenski, R. E.; and Harrison, H. L. "Room Temperature Response to Heat Disturbance Inputs." ASHRAE Trans. 72(1966): II2.1.

50. Harrison, H. L.; Hansen, W. S.; and Zelenski, R. E. "Development of a Room Transfer Function Model for Use in the Study of Short Term Transient Response." ASHRAE Trans. 75(1968): 198.

51. Thompson, J. G.; and Chen, Paul N. T. "Digital Simulation of the Effect of Room and Control System Dynamics on Energy Consumption." ASHRAE Trans. 85, Part 2(1979): to be published.

52. Chapman, W. P. "Research Needs in the Field of Dynamic Response of Environmental Control Processes in Buildings." ASHRAE Letter to T. C. and T. G. Chairmen. New York, July 9, 1979.

53. Cuba, J. F. Bibliography on Available Computer Programs in the General Area of Heating, Refrigerating, Air-Conditioning and Ventilating. ASHPRE Research Project GRP-153, October 1975.

54. ASHRAE. Handbook of Fundamentals. New York: American Society of Heating, Refrigerating and Air Conditioning Engineers, 1977.

55. Houghten, F. C.; and Yaglou, C. P. "Determining Lines of Equal Comfort." ASHVE Trans. 29(1923): 163.

56. Ellis, F. P. "Tolerable and Desirable Levels of Warmth in Warm Climates, with Special Reference to Requirements of Men in Royal Navy. Ann. of the Royal College of Surg. of England 13(1953): 369.

57. Lind, A. R. "Effect of Individual Variation on Upper Limit of Prescriptive Zone of Climates. J. Appl. Physiol. 28(1970): 307.

58. Koch, W.; Jennings, B. H.; and Humphreys, C. M. "Environmental Study II - Sensation Responses to Temperature and Humidity under Still Air Conditions in the Comfort Range." ASHRAE Trans. 66(1960): 264.

59. Nevins, R. G.; Rholes, F. H.; Springer, W. E.; and Feyerherm, A. M. "Temperature-Humidity Chart for Thermal Comfort of Seated Persons." ASHRAE Trans. 72(1966): 283.

60. Webb, Paul: Bioastronautics Data Book. NASA, 1964.

61. Inouye, T.; Hick, F. K.; Telser, S. E.; and Keeton, R. W. "Effect of Relative Humidity on Heat Loss of Men Exposed to Environments of 80, 76, and 72 F. ASHVE Trans. 59(1953): 329.

62. Asmussen, E.; and Nielsen, M. "Studies on the Regulation of Respiration in Heavy Work. Acta Physiol. Scand. 12(1946): 171.

63. McCutchan, J. W.; and Taylor, C. L. "Respiratory Heat Exchange with Varying Temperatures and Humidity of Inspired Air. J. Appl. Physiol. 4(1951): 121.

64. McNall, Jr., P. E.; Jaax, J.; Rholes, F. H.; Nevins, R. G.; and Springer, W. "Thermal Comfort (Thermally Neutral) Conditions for Three Levels of Activity." ASHRAE Trans. 73(1967): I.

65. Nielsen, M.; and Pedersen, L. "Studies on the Heat Loss by Radiation and Convection from the Clothed Human Body. Acta Physiol. Scand. 27 (1952): 272.

66. Winslow, C. E.; Gagge, A. P.; and Herrington, L. P. "The Influence of Air Movement upon Heat Losses from the Clothed Human Body. J. Physiol. 127(1939): 505.

67. Gagge, A. P.; Stolwijk, J. A. J.; and Nishi, Y. "The Prediction of Thermal Comfort when Thermal Equilibrium is Maintained by Sweating." ASHRAE Trans. 75(1969): 108.

68. Ibamato, K; and Nishi, Y. Thermal Sensation Analyzer and its Application to Air Conditioning. Bulletin #46, Faculty of Engineering, Hakkaido University, Japan, 1968.

69. Nishi, Y; and Gagge, A. P. "Moisture Permeation of Clothing - A Factor Governing Thermal Equilibrium and Comfort." ASHRAE Trans. 76(1970): I.

70. Brebner, D. F.; Kersleke, D. M.; and Waddell, J. L. "The Diffusion of Water Vapor through Human Skin." J. Physiol. 132(1956): 225.

71. Bullard, R. W.; Banerjee, M. R.; Chen, F.; Elizondo, R.; and MacIntyre, B. A. "Skin Temperature and Thermoregulatory Sweating: A Control System Approach." In Physiological and Behavioral Temperature Regulation. Edited by J. D. Hardy et al. Springfield, Ill.: Charles C. Thomas, 1970.

72. Gagge, A. P.; Burton, A. C.; and Bazett, H. C. "A Practical System of Units for the Description of the Heat Exchange of Man with his Environment." Science 94(1941): 428.

73. Gagge, A. P. "A New Physiological Variable Associated with Sensible and Insensible Perspiration." American J. Physiol. 120(1937): 277.

74. Fanger, P. O. Thermal Comfort Analysis and Applications in Environmental Engineering. New York: McGraw Hill Book Company, 1973.

75. Gagge, A. P.; Stolwijk, J. A. J.; and Nishi, Y. "An Effective Temperature Scale Based on a Simple Model of Human Physiological Regulatory Response." ASHRAE Trans. 77(1971): 247.

76. Sprague, C. H.; Jai, R. B.; Nevins, R. G.; and Azer, N. Z. "The Prediction of Thermal Sensation for Man in Moderate Thermal Environments via a Simple Thermogulatory Model." ASHRAE Trans. 80(1974): 130.

77. Azer, N. Z.; and Hsu, S. "The Prediction of Thermal Sensation from a Simple Model of Human Physiological Regulatory Response." ASHRAE Trans. 83(1977): 88.

78. Gagge, A. P.; Stolwijk, J. A. J.; and Harely, J. D. "Comfort and Thermal Sensations and Associated Physiological Responses at Various Ambient Temperatures. Environ. Res. 1(1967): 1.

79. Sprague, C. H.; and McNall, P. E. "The Effects of Fluctuating Temperature and Relative Humidity on Thermal Sensation (Thermal Comfort) of Sedentary Subjects." ASHRAE Trans. 76(1970): 34.

80. Wyon, D. P.; Anderson, I.; and Lundquist, G. R. "Spontaneous Magnitude Estimation of Thermal Discomfort During Changes in Ambient Temperature." J. Hygiene (Cambridge) 70(1972): 203-221.

81. Griffiths, I. D.; and McIntyre, D. A. "Sensitivity to Temporal Conditions." Ergonomics 17(1974): 499-507.

82. Nevins, R. G.; Gonzales, R. R.; Nishi, Y.; and Gagge, A. P. "Effect of Changes in Ambient Temperature and Level of Humidity on Comfort and Thermal Sensations." ASHRAE Trans. 81(1975): 169-182.

83. Wyon, D. P.; Asgeirsdottir, Th.; Kjerulf-Jensen, P.; and Fanger, P. O. "The Effect of Ambient Temperature Swings on Comfort, Performance and Behavior. Arch. Sci. Physiol. 27(1973): 441-458.

84. ASHRAE. Thermal Environmental Conditions for Human Occupancy. ASHRAE Standard 55-74, 1974.

85. Berglund, L. G.; and Gonzalez, R. R. "Application of Acceptable Temperature Drifts to Built Environments as a Mode of Energy Conservation." ASHRAE Trans. 84(1978): 110.

86. Nishi, Y.; Gonzalez, R. R.; Nevins, R. G.; and Gagge, A. P. "Field Measurement of Clothing Thermal Insulation." ASHRAE Trans. 82(1976): 248.

87. Wyon, D. P.; Brum, N. O.; Olesen, S.; Kjerulf-Jensen, P.; and Fanger, P. O. Factors Affecting the Subjective Tolerance of Ambient Temperature Swings. 5th International Congress Heating Ventilating and Air Conditioning, Copenhagen, 1971.

88. McIntyre, D. A.; and Gonzalez, R. R. "Man's Thermal Sensitivity During Temperature Changes at Two Levels of Clothing Insulation and Activity." ASHRAE Trans. 82(1976): 219.

89. Gonzalez, R. R.; and Berglund, L. G. "Efficacy of Temperature and Humidity Ramps in Energy Conservation. ASHRAE Journal 21(1979): 34.

90. Griffiths, I. D.; and McIntyre, D. A. "Subjective Responses to Relative Humidity at Two Air Temperatures. Arch. Sci. Physiol. 27 (1973): 459.

91. Gonzalez, R. R. Experimental Analysis of Thermal Acceptability. Proceedings of Symposium on Thermal Analysis - Human Comfort - Indoor Environments. NBS, Gaitherburg, Maryland. NBS SP491, 1977.

92. Gagge, A. P.; and Nevins, R. G. Effect of Energy Conservation Guidelines on Comfort, Acceptability and Health. Final Report of Contract # CO-04-51891-00 of Federal Energy Administration, March 1976.

93. Nevins, R. G.; Rholes, F. H.; Springer, W.; and Feyerherm, A. M. "A Temperature Humidity Chart for Thermal Comfort of Seated Persons." ASHRAE Trans. 72(1966): 283.

94. ASHRAE. Standards for Natural and Mechanical Ventilation. ASHRAE Standard 62-73, 1973.

95. General Radio. Instruments for Industrial Noise Measurement. Concord, Massachusetts: General Radio, 1978.

96. Beranek, L. L. "Revised Criteria for Noise in Buildings." Noise Control 1(1957): 19.

97. Nevins, R. G. Air Diffusion Dynamics. Birmingham, MI: Business News Publishing Co., 1976.

98. IES. Lighting Handbook. New York: Illuminating Engineering Society, 1972.

99. Shaviv, E.; and Shaviv, G. "Modelling the Thermal Performance of Buildings." Buildings and Environment 13(1978): 95.

100. Mehta, D. Paul; Woods, J. E.; and Brueck, D. M. A Rational Model for Thermodynamic Analysis of Occupied Spaces. Proceedings of Energy Management Conference, Iowa State University, Oct. 28-30, 1978.

101. ISA. Standard C85.1 Terminology for Automatic Control. ISA, 1963.

102. Holman, J. P. Heat Transfer. New York: McGraw Hill Book Co., 1972.

103. Siegel, R.; and Howell, J. P. Thermal Radiation Heat Transfer. New York: McGraw Hill Book Co., 1972.

104. Beckwith, T. G.; and Buck, N. L. Mechanical Measurements. Reading, Massachusetts: Addison-Wesley Publishing Co., 1973.

105. Mehta, D. Paul. "An Analysis of an Electro-Hydraulic Actuator." Unpublished M.S. thesis, Kansas State University, 1967.

106. Blackburn, J. F.; Reethof, G.; and Shearer, J. L. Fluid Power Control. New York: John Wiley and Sons, Inc., 1960.

107. Wilson, E. E. "A Basis for Rational Design of Heat Transfer Apparatus." ASME Trans. 37(1915): 47.

108. Ott, I. "Heat Center in the Brain." J. Nerv. and Mental Dis. 14 (1887): 152.

109. Hardy, J. D. Temperature - Its Measurement and Control in Science and Industry. Vol. 3. New York: Reinhold Publishing Corp., 1963.

110. Bonne, U.; Janssen, J. E.; Nelson, L. W.; and Torborg, R. H. Control of Overall Thermal Efficiency of Combustion Heating Systems. Proceedings of 16th International Symposium on Combustion, MIT, Cambridge, Mass., August 1976.

111. Woods, J. E. "Thermal and Non-thermal Human Responses to Air Movement and Relative Humidity." ASHRAE Trans. 84(1978): 75.

112. D'Azzo, J. J.; and Houpis, C. H. Feedback Control System Analysis and Synthesis. New York: McGraw Hill Book Co., 1966.

113. Tomovic, R.; and Vukobratovic, M. General Sensitivity Theory. New York: American Elsevier Publishing Co., 1972.

114. Smith, G. W. Engineering Economy. 2nd ed. Ames, Iowa: Iowa State University Press, 1975.

115. Akalin, M. T. "Equipment Life and Maintenance Cost Survey. ASHRAE Journal 20(1978): 40.

116. Ruegg, R. T. "Life-Cycle Costs and Solar Energy." ASHRAE Journal 18(1976): 22.

117. Montag, G. M. "A Commercial Building Ownership Energy Conservation Cost Analysis Model. ASHRAE Journal 20(1979): 49.

118. Hsu, J. C.; and Meyer, A. U. Modern Control Principles and Applications. New York: McGraw Hill Book Co., 1968.

119. Holman, J. P. Experimental Methods for Engineers. New York: McGraw Hill Book Co., 1966.

120. Grimsrud, D. T.; Sherman, M. H.; Diamond, R. C.; and Sonderegger, R. C. Air Leakage, Surface Pressures and Infiltration Rates in Houses. Proceedings of the Second CIB Symposium on Energy Conservation in Built-Environment. Copenhagen, May 1979.

11. APPENDIX A: CLOSED-LOOP TRANSFER FUNCTION FOR THE SYSTEM SHOWN IN FIGURE 3.10

$$T(s) = \{R - [\frac{0.813(.167S+1)}{(2.86S+1)} I_R + \frac{0.025(.12S+1)}{(31.25S+1)(3.125S+1)^2(.526S+1)} I_F$$

$$+ \frac{0.596}{(.555S+1)(.0286S+1)} I_w + \frac{0.126(.152S+1)}{(0.455S+1)(2.632S+1)} T_I$$

$$+ \frac{0.025(0.1S+1)}{(1.25S+1)(.333S+1)} T_G + \frac{10^{-5}(0.562)(0.2S+1)}{(285.7S+1)^2(1.389S+1)} T_o]$$

$$x \frac{\frac{0.567(.823S+1)}{(.909S+1)(20S+1)}}{1 + \frac{.135(.192S+1)}{(.909S+1)}}\} x (\frac{30,000}{4S+1})(\frac{0.8(1.35S+1)}{(2.8S+1)})(\frac{.0013}{(.45S+1)})$$

$$+ \{[\frac{0.0045}{(6.67S+1)} T_o + \frac{10^{-6}}{(303S+1)^2} T_G + \frac{0.02}{(.714S+1)(.028S+1)} T_I$$

$$+ \frac{0.02}{(3.85S+1)} I_w + \frac{0.005}{(6.25S+1)^3} I_R + \frac{.158(2S+1)}{(.67S+1)} I_F]$$

$$x \frac{7,700}{(\frac{30,000}{4S+1})[\frac{.8(1.35S+1)}{2.8S+1}} x (\frac{30,000}{4S+1})(\frac{.8(1.35S+1)}{(2.8S+1)})(\frac{.0013}{.45S+1})\}[1 +$$

$$\frac{K_1}{(\tau_1 S+1)}]$$

$$1 + \frac{K_1}{(\tau_1 S+1)} - \frac{0.567(.823S+1)}{(0.909S+1)(20S+1)} x (\frac{30,000}{4S+1})(\frac{.8(1.35S+1)}{(2.8S+1)})(\frac{.0013}{(.45S+1)})$$

12. APPENDIX B: PARTIAL FRACTIONS OF THE COEFFICIENT OF T_G

$$F(s) = \frac{1}{S(S+2.2222)(S+.0033)^2}$$

$$F(s) = \frac{A}{S} + \frac{B}{(S+2.2222)} + \frac{C}{(S+.0033)^2} + \frac{D}{(S+.0033)}$$

$$A = [SF(s)]_{S=0} = \frac{1}{(2.2222)(.0033)^2} = 41322.7272$$

$$B = [(S+2.2222)F(s)]_{S=-2.2222}$$

$$= \left.\frac{1}{S(S+.0033)^2}\right|_{S=-2.2222}$$

$$= \frac{1}{(-2.2222)(4.9235)} = -0.0914$$

$$C = [(S+.0033)^2F(s)]_{S=-.0033}$$

$$= \left.\frac{1}{S(S+2.2222)}\right|_{S=-.0033} = \frac{1}{(-.0033)(2.2222 - .0033)}$$

$$= -136.5679$$

$$D = \frac{d}{dS}\,[(S+.0033)^2F(s)]_{S=-.0033}$$

$$= \frac{d}{dS}\left[\frac{1}{S(S+2.2222)}\right]_{S=-.0033}$$

$$= 0_x \left.\frac{(2S+2.2222)}{(S^2+2.2222S)^2}\right|_{S=-.0033}$$

$$= \frac{-2.2156}{(0.00005362)}$$

$$= -41322.6358$$

$$F(s) = \frac{41322.7272}{S} - \frac{0.0914}{(S+2.2222)} - \frac{136.5679}{(S+.0033)^2} - \frac{41322.6358}{(S+.0033)}$$

Therefore:

$$2.4229 \times 10^{-10} T_G F(s)$$

$$= TG \times 10^{-10}\left[\frac{100120.8357}{S} - \frac{0.2215}{(S+2.2222)} - \frac{330.8904}{(S+.0033)^2} - \frac{100120.6145}{(S+.0033)}\right]$$

$$= T_G\left[\frac{10^{-5}}{S} - \frac{2.215\times10^{-11}}{(S+2.2222)} - \frac{3.3089\times10^{-8}}{(S+.0033)^2} - \frac{10^{-5}}{(S+.0033)}\right]$$

13. APPENDIX C: PARTIAL FRACTIONS OF THE COEFFICIENT OF T_I

$$F(s) = \frac{1}{S(S+2.2222)(S+1.4006)(S+35.7143)}$$

$$= \frac{A}{S} + \frac{B}{(S+2.2222)} + \frac{C}{(S+1.4006)} + \frac{D}{(S+35.7143)}$$

$$A = SF(s)\Big|_{S=0} = \frac{1}{(2.2222)(1.4006)(35.7143)} = 0.0089$$

$$B = (S+2.2222)(F(s)\Big|_{S=-2.2222} = \frac{1}{(-2.2222)(-2.2222+1.4006)(-2.2222+35.7143)}$$

$$= 0.016354$$

$$C = (S+1.4006)F(s)\Big|_{S=-1.4006} = \frac{1}{(-1.4006)(2.2222-1.4006)(35.7143-1.4006)}$$

$$= -0.025325$$

$$D = (S+35.7143F(s)\Big|_{S=-35.7143} = \frac{1}{(-35.7143)(2.2222-35.7143)(1.4006-35.7143)}$$

$$= -2.4363 \times 10^{-5}$$

$$F(s) = \frac{0.0089}{S} + \frac{0.01635}{(S+2.2222)} - \frac{0.025325}{(S+1.4006)} - \frac{2.4363\times10^{-5}}{(S+35.7143)}$$

Or:

$$22.2533\ T_I F(s) = \frac{0.1980T_i}{S} + \frac{0.3638T_I}{(S+2.2222)} - \frac{0.563454T_I}{(S+1.4006)} - \frac{54.2157\times10^{-5}}{(S+35.7143)}$$

14. APPENDIX D: PARTIAL FRACTIONS OF THE COEFFICIENT OF I_R

$$F(s) = \frac{1}{S(S+2.2222)(S+0.016)^3}$$

$$= \frac{A}{S} + \frac{B}{(S+2.2222)} + \frac{C}{(S+0.16)^3} + \frac{D}{(S+0.16)^2} + \frac{E}{(S+0.16)}$$

$$A = SF(s)\Big|_{S=0} = \frac{1}{(2.2222)(.16)^3} = 109.8643$$

$$B = (S+2.2222)F(s)\Big|_{S=-2.2222} = \frac{1}{(-2.2222)(0.16-2.2222)^3} = 0.0513$$

$$C = (S+0.16)^3F(s)\Big|_{S=-.16} = \frac{1}{(-0.16)(2.0622)} = -3.0307$$

$$D = \frac{d}{dS}[(S+.16)^3F(s)]_{S=-.16} = \frac{-(2S+2.2222)}{(S^2+2.222S)^2}\Big|_{S=-0.16}$$

$$= \frac{-(-0.32+2.2222)}{(.16^2-2.2222x0.16)^2}$$

$$= \frac{-1.9022}{(.0256-0.3555)^2} = \frac{-1.9022}{0.1088}$$

$$= -17.4779$$

$$E = \frac{1}{2}\frac{d^2}{dS^2}[(S+0.16)^3F(s)]_{S=-0.16}$$

$$= \frac{1}{2}\frac{d}{dS}\left[\frac{-(2S+2.2222)}{(S^2+2.222S)^2}\right]_{S=-0.16}$$

$$= \frac{1}{2}\left[\frac{-(S^2+2.222S)2 + (2S+2.2222)(2)(S^2+2.222S)(2S+2.222)}{(S^2+2.222S)^4}\right]_{S=-0.16}$$

$$= \frac{1}{2}\left[\frac{-2+2(2S+2.2222)^2}{(S^2+2.2222S)^3}\right]_{S=-0.16}$$

$$= \left[\frac{(2S+2.2222)^2-1}{(S^2+2.2222S)^3}\right]_{S=-0.16}$$

$$= \frac{(2.2222-0.32)^2-1}{(.16^2-2.2222\times 0.16)^3}$$

$$= -106.72$$

$$F(s) = \frac{109.8643}{S} + \frac{0.0513}{(S+2.2222)} - \frac{3.030}{(S+0.16)^3} - \frac{17.4779}{(S+0.16)^2} - \frac{106.72}{(S+0.16)}$$

Or:

$$0.000SI_R F(s)$$

$$= I_R \left[\frac{0.0549}{S} + \frac{2.5650\times 10^{-5}}{(S+2.2222)} - \frac{0.0015}{(S+0.16)^3} - \frac{0.-087}{(S+0.16)^2} - \frac{0.05336}{(S+0.16)}\right]$$

$$= I_R \left[\frac{5490\times 10^{-5}}{S} + \frac{2.5650\times 10^{-5}}{(S+2.2222)} - \frac{150\times 10^{-5}}{(S+0.16)^3} - \frac{870\times 10^{-5}}{(S+0.16)^2} - \frac{5336\times 10^{-5}}{(S+0.16)}\right]$$

15. APPENDIX E: DERIVATIONS FOR FAN COIL HEATING SYSTEM

All transfer functions are in Laplace Transform. Substituting equations (5.10) and (5.11) into (5.7):

$$\Delta\dot{Q}_H = [G_v G_a G_c(\Delta P_{set} - H_s\Delta T)C_{pw}(t_{wi} - t_{wo}) + \dot{m}_a C_{pa} G_2 G_F(\frac{\dot{m}_{oa}\Delta T_a + \dot{m}_{ra}\Delta T}{\dot{m}_a})]G_H$$

Substituting $\Delta\dot{Q}_H$ in equation (5.5)

$$\Delta T_1 = G_1\{[G_v G_a G_c(\Delta P_{set} - H_s\Delta T)C_{pw}(t_{wi} - t_{wo}) + \dot{m}_a C_{pa} G_2 G_F(\frac{\dot{m}_{oa}\Delta T_a + \dot{m}_{ra}\Delta T}{\dot{m}_a})]G_H + \Delta\dot{Q}_{occ} + \Delta\dot{Q}_{int}\}$$

Substituting for ΔT_1 and ΔT_2 (equation (5.4)) in equation (5.3):

$$\Delta T = G_1 G_H G_v G_a G_c \Delta P_{set} C_{pw}(t_{wi} - t_{wo}) - G_1 G_H G_v G_a G_c H_s \Delta T C_{pw}(t_{wi} - t_{wo}) + \frac{G_1 G_H C_{pa} G_2 G_F \dot{m}_{oa}\Delta T_a}{\dot{m}_a} + \frac{G_1 G_H C_{pa} G_2 G_F \dot{m}_{ra}}{\dot{m}_a}\Delta T + G_1(\Delta\dot{Q}_{occ} + \Delta\dot{Q}_{int}) + G_3\Delta T_a$$

Rearranging:

$$\Delta T[1 - \frac{G_1 G_H G_2 G_F \dot{m}_{ra} C_{pa}}{\dot{m}_a} - G_1 G_H G_v G_a G_c H_s C_{pw}(t_{wi} - t_{wo})] = G_1 G_H G_v G_a G_c C_{pw}(t_{wi} - t_{wo})\Delta P_{set} + G_1(\Delta\dot{Q}_{occ} + \Delta\dot{Q}_{int}) + (\frac{\dot{m}_a G_3 - G_1 G_H G_2 G_F \dot{m}_{oa} C_{pa}}{\dot{m}_a})\Delta T_a$$

or

$$\Delta T = \frac{G_1 G_H G_v G_a G_c C_{pw}(t_{wi} - t_{wo})}{\{1 - [\frac{G_1 G_H G_2 G_F \dot{m}_{ra} C_{pa}}{\dot{m}_a} + G_1 G_H G_v G_a G_c H_s C_{pw}(t_{wi} - t_{wo})]\}} \Delta P_{set}$$

$$+ \frac{G_1(\Delta\dot{Q}_{occ} + \Delta\dot{Q}_{int})}{\{1 - [\frac{G_1 G_H G_2 G_F \dot{m}_{ra} C_{pa}}{\dot{m}_{re}} + G_1 G_H G_v G_a G_c H_s C_{pw}(t_{wi} - t_{wo})]\}}$$

$$+ \frac{(\dot{m}_a G_3 - G_1 G_H G_2 G_F \dot{m}_{oa} C_{pa})\Delta T_a}{\dot{m}_a\{1 - [\frac{G_1 G_H G_2 G_F \dot{m}_{ra} C_{pa}}{\dot{m}_a} + G_1 G_H G_v G_a G_c H_s C_{pw}(t_{wi} - t_{wo})]\}} \qquad (15.1)$$

To couple the occupant to the system, substitute in (15.1)

$$\Delta P_{set} = G_R G_{occ} \Delta T$$

$$\Delta T\,[1 - \frac{G_1 G_H G_v G_a G_c C_{pw}(t_{wi}\ 0\ t_{wo}) G_R G_{occ}}{X(s)}]$$

$$= \frac{G_1}{X(s)}(\Delta\dot{Q}_{occ} + \Delta\dot{Q}_{int}) + \frac{\dot{m}_a G_3 - G_1 G_H G_2 G_F \dot{m}_{oa} C_{pa}}{X(s)} \Delta T_a$$

where

$$X(s) = \{1 - [\frac{G_1 G_H G_2 G_F \dot{m}_{ra} C_{pa}}{\dot{m}_a} + G_1 G_H G_v G_a H_s C_{pw}(t_{wi} - t_{wo})]\}$$

or

$$\Delta T = \frac{G_1}{X(s) - G_1 G_H G_v G_a G_c C_{pw}(t_{wi} - t_{wo}) G_R G_{occ}}(\Delta\dot{Q}_{occ} + \Delta\dot{Q}_{int})$$

$$+ \frac{\dot{m}_a G_3 - G_1 G_H G_2 G_F \dot{m}_{oa} C_{pa}}{X(s) - G_1 G_H G_v G_a G_c C_{pw}(t_{wi} - t_{wo}) G_R G_{occ}} \Delta T_a \qquad (15.2)$$

or

$$\Delta T = \frac{G_1}{X(s) - Y(s)}(\Delta\dot{Q}_{occ} + \Delta\dot{Q}_{int})$$

$$+ \frac{\dot{m}_a G_3 - G_1 G_H G_2 G_F \dot{m}_{oa} C_{pa}}{X(s) - Y(x)} \Delta T_a \qquad (15.3)$$

where:

$$Y(s) = G_1 G_H G_v G_a G_c C_{pw} (t_{wi} - t_{wo}) G_R G_{occ}$$

16. APPENDIX F: DATA ON THE ISU ENERGY RESEARCH HOUSE

The data reported in this appendix were taken from the record files maintained at ERH. Data on the sensor were received from GTE.

1. Volume of air enclosed = 16950 ft^3 (480 m^3)
2. Total floor area = 2385 ft^2 (221.6 m^2)
3. Below grade areas
   a. Floor area = 730 ft^2 @ U = 0.063 B/hr $ft^2°F$
   b. West wall = 378 ft^2 @ U = 0.047 B/hr $ft^2°F$
   c. North wall (156 + 162) = 318 ft^2 @ U = 0.047 B/hr $ft^2°F$
   d. East wall (i) = 127 ft^2 @ U = 0.047 B/hr $ft^2°F$

$$U_{BG} = \frac{730 \times .063 + 378 \times .047 + 318 \times .047 + 127 \times .047}{730 + 378 + 318 + 127} = 0.0545 \text{ B/hr ft}^2°\text{F}$$

A_{BG} = 1553 ft^2

$U_{BG}A_{BG}$ = 84.67 B/hr°F

U_{BG} = 0.0545 B/hr $ft^2°F$

4. Above grade areas
   a. Roof area = 730 ft^2 @ U = 0.029 B/hr $ft^2°F$
   b. West wall = 405 ft^2 @ U = 0.048 B/hr $ft^2°F$
   c. North wall = 450 ft^2 @ U = 0.048 B/hr $ft^2°F$
   d. East wall (i) = 500 ft^2 @ U = 0.048 B/hr $ft^2°F$
      (ii) = 168 ft^2 @ U = 0.35 B/hr $ft^2°F$

$$U_{AG} = \frac{730 \times .029 + 405 \times .048 + 450 \times .048 + 500 \times .048 + 168 \times .35}{730 + 405 + 405 + 500 + 168}$$

A_{AG} = 2253 ft^2 U_{AG} = 0.0644 B/hr $ft^2°F$

A_{AGG} = 120 ft^2 U_{AGG} = 0.35 B/hr $ft^2°F$

$\Sigma A_{AG}U_{AG}$ = 187.09 B/hr°F

5. Partition wall

   $A_{PW} = 535\ ft^2$ @ $U_{PW} = 0.35$ B/hr $ft^2°F$

   $A_{PW} = 350\ ft^2$ @ $U_{PW} = 0.06$ B/hr $ft^2°F$

   $\Sigma A_{PW}U_{PW} = 208.25$ B/hr°F

6. $\dot{m}_a C_{pa} = 1704.96$ Btu/hr°F

7. $\Sigma UA = 480.01$ B/hr°F

8. $M_a C_p = 301.03$ B/°F

9. Time constant of sensor = 30 secs

10. Gain of sensor = 0.00134/°F (source--correspondence with GTE Sylvania Inc., Metal Laminates Div., 1704 Barnes Street, Reidsville, NC 27320

17. APPENDIX G: DETAILS OF FURNITURE ITEMS IN THE ISU ENERGY RESEARCH HOUSE AND THEIR THERMAL CAPACITIES

Item	Units	Total mass (lbm)	Materials	Specific heats (B/lbm°F)	Thermal capacity (B/°F)
1. Basement chairs	4	160	steel (140), wicker (8) leather (12)	0.17, 0.3, 0.3	29.80
2. Table (36"x36"x29")	1	80	oak(80)	0.3	24.00
3. Easy chair	1	120	steel (105), wicker (6), urethane foam (9)	0.17, 0.3, 0.17	21.20
4. Table (27"x27"x16")	1	20	steel (15), glass (5)	0.17, 0.2	5.50
5. Sofas	2	400	leather (30), wood (120), urethane (250)	0.33, 0.33, 0.17	92.00
6. Table (22"x22"x17")	2	80	oak (80)	0.30	24.00
7. Wall cabinet (35"x 76"x18")	3	675	oak (675)	0.30	202.50
8. Table (17"x59"x27")	1	100	oak (100)	0.30	30.00
9. Chair	1	30	steel (10) + wood (20)	0.17, 0.33	8.30
10. Ladder	1	30	wood (30)	0.33	9.90
11. Cylinder base	1	150	steel (150)	0.17	25.50
12. Cylinder	1	150	steel (150)	0.17	25.50
13. Maytag washer	1	240	steel (240)	0.17	40.80
14. Maytag dryer	1	180	steel (180)	0.17	30.60
15. Dining table	1	150	glass (50), steel (100)	0.2, 0.17	27.00
16. Chairs	4	160	steel (140), wicker (8), leather (12)	0.17, 0.3, 0.3	29.80
17. Sofa set (3 pieces)	1 set	475	cotton (375), wood (100)	0.31, 0.33	149.25
18. Table (18"x18"x16")	2	40	glass (20, brass (20)	0.20, 0.09	5.80
19. Table (25"x25"x20")	1	50	steel (40, glass (10)	0.17, 0.20	8.80
20. Stove Tappan	1	160	steel (160)	0.17	27.20
21. Refrigerator Amana	1	300	steel (300)	0.17	51.00
22. Dishwasher Maytag	1	150	steel (150)	0.17	25.50
23. Cooking range Amana	1	100	steel (100)	0.17	17.00
24. Kitchen cabinets	7	1750	wood (1750)	0.33	577.50
25. NW bedroom bed	1	250	steel (200), cortex (50)	0.17, 0.3	49.00

Item	Units	Total mass (lbm)	Materials	Specific heats (B/lbm°F)	Thermal capacity (B/°F)
26. Chart	2	240	glass (120), wood (120)	0.2, 0.33	63.60
27. SW bedroom bed	1	125	wood (80) + cortex (40) + urethane (5)	0.33, 0.31, 0.17	39.65
28. Table	1	100	Formica (50), wood (50)	0.28, 0.33	30.50
29. SE bedroom bed	1	125	wood (80), cortex (40), urethane (5)	0.33, 0.31, 0.17	39.65
				TOTAL	1545.85

18. APPENDIX H: CALCULATIONS, DATA ANALYSIS FOR EXPERIMENTAL VALIDATION AND PROPAGATION OF UNCERTAINTIES

18.1 Infiltration rate

Using the methane leakage curve in Figure 18.1 data on methane concentration as a fraction of total charge are tabulated in Table 18.1. From the data in Table 18.1, using least squares method

$$\tau_{leak} = \frac{n\left(\sum_{i=1}^{n} x_i t_i\right) - \left(\sum_{i=1}^{n} x_i\right)\left(\sum_{i=1}^{n} t_i\right)}{n\left(\sum_{i=1}^{n} x_i^2\right) - \left(\sum_{i=1}^{n} x_i\right)^2} \qquad (18.1)$$

where n is the total number of data points in Table 18.1.

$$\tau_{leak} = \frac{10(1167.24) - (12.29)(735.00)}{10(18.89) - (12.29)^2}$$

$$= 88.34 \text{ minutes}$$

In 88.34 minutes, leakage = 0.632

In 60.00 minutes, leakage will be $\frac{60 \times 0.632}{88.34} = 0.43$

Hence infiltration rate = 0.43 air changes/hour

$$\dot{m}_{ainf} = 16950 \times 0.43 \times 0.074$$

$$= 539.35 \text{ lbm/hour } (244.60 \text{ Kg/hour}) \qquad (18.2)$$

18.2 Temperatures

Data on inside temperatures and weather conditions obtained on the night of August 1-2, 1979 according to the procedure described in Section 6.3.2 is given in Tables 18.2 and 6.4. Using the method of least squares

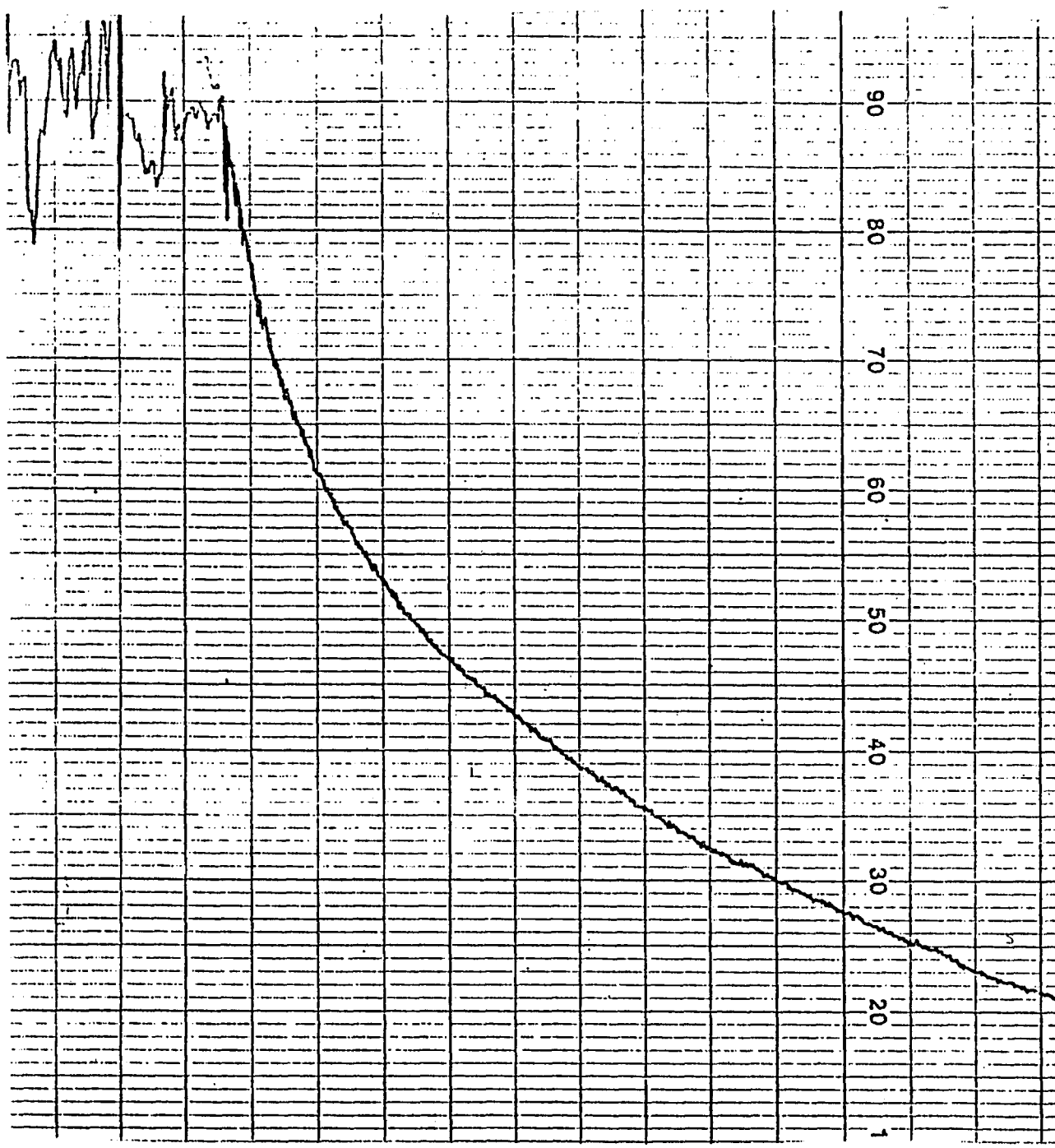

Figure 18.1. Strip chart recorder plot for methane leakage (August 1-2, 1979). Maximum charge: 500 ppm; chart speed: 4 cms/hour; Open-loop test; fan on.

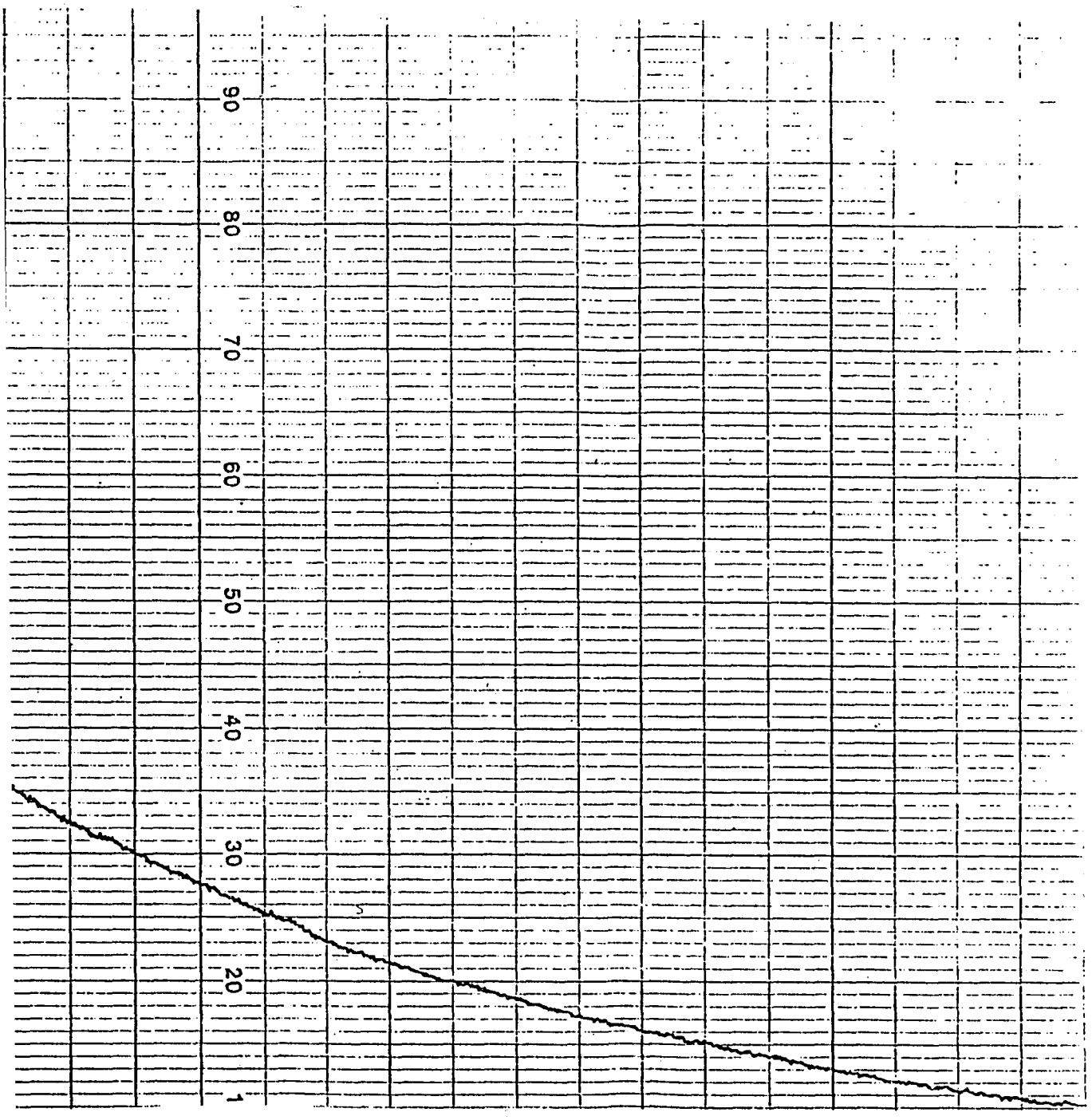

ıane leakage (August 1-2,
chart speed: 4 cms/hour;

Table 18.1. Methane concentration and time elapsed after charging (August 1-2, 1979)

S. No.	Methane concentration C (fraction of total charge)	ln C (X)	Time (minutes) t
1	0.86	-0.15	6
2	0.59	-0.53	21
3	0.46	-0.78	36
4	0.39	-0.94	51
5	0.32	-1.14	66
6	0.26	-1.35	81
7	0.22	-1.51	96
8	0.18	-1.71	111
9	0.14	-1.97	126
10	0.11	-2.21	141

$$\frac{dT_a}{dT} = \frac{n\left(\sum_{i=1}^{n} t_i t_{ai}\right) - \left(\sum_{i=1}^{n} t_i\right)\left(\sum_{i=1}^{n} t_{ai}\right)}{n\left(\sum_{i=1}^{n} t_i^2\right) - \left(\sum_{i=1}^{n} t_i\right)^2} \tag{18.3}$$

where n is the total number of points in Table 5.4.

$$\frac{dT_a}{dT} = \frac{19(10618.01) - (518.57)(388.99)}{19(14153.66) - (518.57)^2} = 5.04 \tag{18.4}$$

18.3 Other parameters

Substituting the values of $\dot{m}_{ainf}$ from equation 18.2 and of dT_a/dT from equation (18.4) into equation (6.8), we get

$$K_2 = -522.95 \tag{18.5}$$

Using this value of K_2, and the data on ERH in Appendices F and G, we find from equations 5.1.3.3-5.1.3.5

Table 18.2. Data sheet on experimental validation of rational model; date August 1-2, 1979; remarks, 1) Fan on, 2) HVAC system off, 3) temperatures in °C

Time	Soil temperatures °C 26" deep	80" deep	134" deep	Wind velocity miles/hr	Outdoor air temp °C	Green-house temp °C	SW bed-room temp °C	NW bed-room temp °C	Living room temp °C	Base-ment temp °C
23:30:00	20.2	22.3	24.7	06.399	20.8	21.4	28.3	27.7	27.0	26.7
23:45:00	20.2	22.3	24.7	06.609	20.5	21.5	28.3	27.7	27.0	26.7
00:00:00	20.2	22.3	24.7	06.558	20.2	21.3	28.3	27.7	27.0	26.7
00:15:00	20.2	22.3	24.7	06.565	19.8	21.4	28.2	27.8	27.0	26.7
00:30:00	20.2	22.3	24.7	06.386	19.4	21.0	28.2	27.7	27.0	26.7
00:45:00	20.2	22.2	24.7	06.460	19.1	20.9	28.1	27.7	27.0	26.7
01:00:00	20.2	22.3	24.7	06.451	18.9	20.6	28.0	27.7	27.0	26.7
01:15:00	20.2	22.3	24.7	06.429	18.7	20.7	28.0	27.7	27.0	26.7
01:30:00	20.2	22.3	24.7	06.397	18.6	20.6	28.0	27.7	27.0	26.7
01:45:00	20.2	22.3	24.7	06.370	18.2	20.6	27.9	27.7	26.9	26.7
02:00:00	20.2	22.3	24.7	06.326	18.2	20.5	27.9	27.7	27.0	26.7
02:15:00	20.2	22.3	24.7	05.905	18.1	20.4	27.8	27.6	28.9	26.7
02:30:00	20.2	22.3	24.7	05.907	17.8	20.3	27.7	27.6	26.9	26.7
02:45:00	20.2	22.3	24.7	05.985	17.7	20.1	27.8	27.6	26.9	26.7
03:00:00	20.2	22.3	24.7	05.961	17.3	20.2	27.7	27.5	26.8	26.7
03:15:00	20.2	22.3	24.7	05.946	17.1	20.1	27.6	27.5	26.8	26.7
03:30:00	20.2	22.3	24.7	05.934	17.0	20.1	27.5	27.5	26.8	26.7
03:45:00	20.2	22.3	24.7	05.864	16.8	19.7	27.5	27.5	26.8	26.6
04:00:00	20.3	22.3	24.7	05.815	16.5	19.4	27.5	27.5	26.8	26.6

$$K_{Ti} = \frac{1704.96}{1704.96 + 480.01 - 522.95} = 1.03$$

$$K_{Ta} = \frac{480.01}{1704.96 + 480.01 - 522.95} = 0.29$$

$$\tau_{os} = \frac{1995.38}{1704.96 + 480.01 - 522.95} = 1.20 \text{ hours}$$

Using these values of K_{Ti}, K_{Ta}, τ_{os} and equation (6.15), predicted values are calculated as follows:

For row (2) of Table 6.4 (Time = 23:45)

$$\Delta T_a = -0.25°C$$

Therefore, from equation (6.15):

$$\Delta T = \frac{0.29(1 - e^{-0.25/1.20})}{1 - 1.03(1 - e^{-0.25/1.20})} (-0.25) \ °C$$

$$= \frac{0.29 \times 0.19}{1 - 1.03 \times 0.19} (-0.25) = -0.02°C$$

Adding $\Delta T = -0.02°C$ to the indoor air temperature predicted at 23:30 hours (27.40°C), predicted indoor air temperature at 23:45 hours is 27.38°C as shown in Table 6.4. These calculations are repeated at intervals of 0.25 hours to tabulate predicted indoor air temperatures in Table 6.4. The predicted indoor air temperatures tabulated in Table 6.3 for July 26-27, 1979 were also calculated the same way.

18.4 Sample calculations for Table 6.9

Substituting equation (6.21) into equation (6.16) and taking inverse Laplace Transform:

$$\Delta T(t) = \frac{0.000259(1 - e^{-t/\tau_{os}})}{[1 - K_{T_i}(1 - e^{-t/\tau_{os}})]} \dot{\Delta Q}(t)$$

$$+ \frac{K_{T_a}(1 - e^{-t/\tau_{os}})}{[1 - K_{T_i}(1 - e^{-t/\tau_{os}})]} \Delta T_a(t) \qquad (18.6)$$

For the first ON cycle in Table 6.9, substituting t = 7 minutes; ΔT_a = -0.07°C (-0.13°F); $\Delta\dot{Q}(t)$ = 43102.50 B/hr, and K_{T_i}, K_{T_a}, τ_{os} from equation (6.21): ΔT = +0.89°C, which was added to the operating point of 30.10°C to calculate the predicted space temperature of 30.99°C shown in Table 6.9. These calculations were repeated for 9 cycles shown in Table 6.9.

18.5 Uncertainty analysis for predicted space temperatures

Predicted space temperatures were calculated from:

$$\Delta T(t) = \frac{K_{T_a}(1 - e^{-t/\tau_{os}})}{1 - K_{T_i}(1 - e^{-t/\tau_{os}})} \Delta T_a(t) \qquad (6.15)$$

The parameters K_{T_a}, K_{T_i}, τ_{os} and T_a included uncertainties (errors) in their values and these errors were propagated in the calculated values of space temperatures. For an analysis of the propagation of uncertainties, the propagation-of-error equation can be expressed as (119):

$$W_R^2 = [\frac{\partial R}{\partial x_1}]^2 W_{x_1}^2 + [\frac{\partial R}{\partial x_2}]^2 W_{x_2}^2 + \ldots + [\frac{\partial R}{\partial x_n}]^2 W_{x_n}^2 \qquad (18.7)$$

In equation (18.7), R represents the calculated quantity and x_1, x_2, ... x_n represent the independent parameters used to calculate the quantity R so that $R = f(x_1, x_2, \ldots x_n)$. The uncertainty W can be the percent error or any other precision index can be used as long as the same type of precision index is used in each term.

Equation (18.7) was applied to equations (3.28-3.30) and to equation (6.7) to determine the uncertainties propagated in K_2, K_{T_a}, K_{T_i} and τ_{os} with the error values shown in Table 18.3.

Table 18.3. Errors in the parameters

Parameter	Error (percent)	Source
U	±7.5%	Determined from the data given in reference (54).
$\dot{m}_a$	±0.5%	Determined from the values of accuracies given for the different types of flowmeters in reference (104).
$\dot{m}_{ainf}$	±20%	Determined from the data reported in reference (120).
T	±1%	Determined from the values of accuracies given for the different types of thermocouples in reference (104).

As a sample calculation, application of equation (18.7) to equation (6.7) yields:

$$W_{K_2}^2 = [C_{pa}(T - T_a)]^2(.2)^2 + [\dot{m}_{ainf}C_{pa}(1 - \frac{dT_a}{dT})]^2(.01)^2$$

$$+ [\dot{m}_{ainf}C_{pa}(\frac{dT}{dT_a} - 1)^2]](.01)^2 \qquad (18.8)$$

Solution of equation (18.8) yielded $W_{K_2}^2 = 28.09$. Similarly, it was found that $W_{\tau_{os}}^2 = 0.0032$, $W_{K_{T_a}}^2 = .0051$, $W_{K_{T_i}}^2 = .0181$. Using the values of W_{K_2}, $W_{K_{T_a}}$, $W_{\tau_{os}}$, $W_{K_{T_i}}$ and applying equation (18.7) to equation (6.15), $W_{\Delta T}^2$ was calculated to be 0.0105 or $W_{\Delta T} = \pm 0.10$.

19. APPENDIX I: SAMPLE CALCULATION FOR TABLE 7.1

Consider an average dwelling 15.25 m x 9.14 x 2.44 m at a location where the outside design temperature is -23°C. The inside temperature is 21°C.

Sample Calculations:

1. Heating Load: For an energy efficient house, assume that the design heat loss is 0.121 MJ/hr per m^2 floor area (i.e., 10.7 Btu/hr ft^2). Then the design heating load is

$$\dot{Q}_{out} = (0.121 \frac{MJ}{hrm^2}) (9.14 \text{ m x } 15.23 \text{ m}) = 16.9 \text{ MJ/hr}$$

2. Net Heat Transfer to the Room Air $\dot{Q}_{net}$:

$$\dot{Q}_{net} = \dot{Q}_f - \dot{Q}_{out}$$

$$= (15.23 \text{ x } 9.14 \text{ x } 2.44)m^3 (0.113 \frac{MJ}{m^3}) - 16.9 \text{ MJ/hr}$$

$$= 21.1 \text{ MJ/hr}$$

3. On and OFF lines for the furnace:

For furnace ON period $\frac{dT}{dt} = \frac{Q_{net}}{M_a c_{pa}} = +51.67$ °C/hr

For furnace OFF period $\frac{dT}{dt} = \frac{-Q_{out}}{M_a c_{pa}} = -41.32$ °C/hr

For a thermostat differential $\Delta T_h = 2.22$°C

Furnace ON time = $\frac{2.22}{51.67}$ °C/hr = 2.58 min.

Furnace OFF time = $\frac{2.22}{41.32}$ hr = 3.23 min.

Time period for one cycle = 5.81 min.

$$\text{Cycles/day} = \frac{1}{5.81} \times 60 \times 24 = 248 \text{ cycles/day}$$

These calculations are repeated for two loads, three different furnace capacities, two different thermostat differentials. The results have been tabulated in Table 7.1.